

Molecular Determinants of Microglial Inflammatory Responses to Intermittent Hypoxia

By

Stephanie M.C. Smith

A dissertation submitted in partial fulfillment of
the requirements for the degree of

Doctor of Philosophy
(Comparative Biomedical Sciences)

at the

UNIVERSITY OF WISCONSIN-MADISON

2014

Date of final oral examination: 04/10/14

The dissertation is approved by the following members of the Final Oral Committee:

Dr. Jyoti Watters, Associate Professor, Comparative Biosciences
Dr. Gordon Mitchell, Professor, Comparative Biosciences
Dr. Linda Schuler, Professor, Comparative Biosciences
Dr. Tracy Baker-Herman, Assistant Professor, Comparative Biosciences
Dr. Loren Denlinger, Associate Professor, Medicine

ACKNOWLEDGEMENTS

I am incredibly grateful to my mentor, Dr. Jyoti Watters, for providing me the opportunity to conduct research in her laboratory, for exposing me to all facets of research, for her scientific and career guidance, and for being a truly outstanding mentor. You are truly an inspiration to me both professionally and personally. Thank you for your continued guidance throughout my graduate research while for fostering my independence that aided in my development as a researcher and as a person. Thanks to all the past and current members of the Watters lab for your friendship and intellectual insight that has made many of these studies possible. I specifically want to thank Dr. Maria Nikodemova, Dr. Scott Friedle, Alex Wessel, Thomas Dietz, Rebecca Kimyon, Scott Ray, and Alissa Small who were instrumental both technically and intellectually in many of these studies. Thank you to all of members of the Mitchell, Baker-Herman, Johnson, and Suresh laboratories for your friendship which has made the years working on my Ph.D. truly enjoyable. I specifically want to mention thank Dr. Adrienne Huxtable and Dr. Brendan Dougherty for their work on collaborative projects and for our many discussions on science and life. Thanks also to the members of my research committee, Dr. Gordon Mitchell, Dr. Linda Shuler, Dr. Tracy Baker-Herman, and Dr. Loren Denlinger for your helpful suggestions, guidance, and encouragement throughout the completion of my thesis. A special thank you to Dr. Gordon Mitchell for your continued mentorship throughout my studies and for the many discussions on science, careers, and life. Thank you to my amazing family and friends who have been a constant source of love, encouragement, and laughter. I specifically want to thank my parents, Mike and Mary, for their unwavering love and support. I also want to thank my wonderful husband and best friend, Ryan, for being my rock and for always forgiving the late nights and weekends spent in the lab. I would like to thank

those who were instrumental early on in guiding to science as a career path. I specifically want to thank Dr. Edward Elko for seeing the scientist in me well before I could; if not for your early guidance, I may have never considered a career in science. I also want to thank Dr. Dusty Sarazan and Dr. Andrea Mitchell for their mentorship and encouraging me to pursue a graduate degree.

TABLE OF CONTENTS

Abstract	ix
Chapter 1	1
Introduction & Literature Review	1
Introduction	2
Obstructive Sleep Apnea (OSA)	3
Obstructive Sleep Apnea and CNS Dysfunction	5
Neurological Consequences of OSA	6
Neurodegenerative diseases and Traumatic/Ischemic injury	7
Obstructive sleep apnea: an inflammatory disorder?	8
Systemic Immune Response	9
Consequences of Inflammation	9
IH and Neuropathology: Findings from Animal Models	11
IH-induced Neurotoxicity	12
Role of Oxidative Stress and Inflammation in IH-induced Neuronal Death	13
Differential Cellular Responses to Intermittent Hypoxia	14
Neurons	16
Astrocytes	17
Oligodendrocytes	18
Microglia	19
Intermittent Hypoxia and CNS Inflammation	20
Microglia	20
Potential Mechanisms of IH-induced Microglial Activation	22
Systemic Inflammation	22
Indirect Activation of Microglia by DAMPs Released from Stressed/Injured Cells	24
Direct Activation of Microglia by IH	32
Common Signal Transduction Pathways Mediating Microglial Inflammation: Relevance to IH-induced Microglial Activation	34
Inflammasome	34
Mitogen-Activated Protein Kinases (MAPKs)	36
Transcription Factor Activation	38
Secreted Molecules Produced by Microglia	41
Microglial Responses to IH: Friend of Foe?	43

Concluding Remarks.....	45
Figure 1	46
Figure 1 Legend.....	47
Figure 2.....	48
Figure 2 Legend.....	49
References.....	50
Chapter 2.....	71
Hypoxia Attenuates Purinergic P2X Receptor-Induced Inflammatory Gene Expression in Brainstem Microglia.....	71
Abstract.....	72
Introduction.....	74
Materials and Methods.....	76
Results.....	80
Discussion.....	84
Acknowledgements:.....	91
Figure 1	92
Figure Legend 1	93
Figure 2	94
Figure Legend 2.....	95
Figure 3	96
Figure Legend 3	97
Figure 4.....	98
Figure Legend 4.....	99
References.....	100
Chapter 3.....	107
Cell-Type Specific Jumonji Histone Demethylase Gene Expression in the Healthy Rat CNS: Detection By A Novel Flow Cytometry Method.....	107
Abstract.....	108
Introduction.....	109
Materials and Methods.....	112
Results.....	118
Discussion.....	124
Acknowledgements.....	131

Figure 1	132
Figure Legend 1	133
Figure 2	134
Figure Legend 2	135
Figure 3	136
Figure Legend 3	137
Figure 4	138
Figure Legend 4	139
Figure 5	140
Figure Legend 5	141
Figure 6	142
Figure Legend 6	143
Table 1	144
Table Legend 1	146
Table 2	147
Table Legend 2	147
References.....	148
Chapter 4.....	153
Chronic intermittent hypoxia exerts CNS region-specific effects on rat microglial inflammatory and TLR4 gene expression	153
Abstract.....	154
Introduction.....	155
Materials and Methods.....	158
Results.....	161
Discussion.....	164
Acknowledgements.....	170
Figure 1	171
Figure Legend 1	172
Figure 2	173
Figure Legend 2	174
Figure 3	175
Figure Legend 3:	176
Figure 4	177

Figure Legend 4	178
Table 1	179
References.....	180
Chapter 5.....	186
Microglial Inflammatory Responses to Chronic Intermittent Hypoxia are Mediated in Part Through TLR4 Activation	186
Abstract.....	187
Introduction.....	189
Methods	193
Results:.....	200
Discussion:.....	209
Acknowledgements.....	214
Figure 1	215
Figure Legend 1	216
Figure 2	217
Figure legend 2	218
Figure 3	219
Figure Legend 3	220
Figure 4	221
Figure Legend 4.....	222
Figure 5	223
Figure Legend 5	224
Figure 6.....	225
Figure Legend 6.....	226
Figure 7	227
Figure Legend 7	228
Figure 8.....	229
Figure Legend 8.....	230
Figure 9	231
Figure Legend 9	232
Figure 10.....	233
Figure Legend 10.....	234
Table 1	235

Supplementary Figure 1	236
Supplementary Figure Legend 1	237
Supplementary Figure 2	238
Supplementary Figure Legend 2	239
Supplementary Figure 3	240
Supplementary Figure Legend 3	241
Supplementary Figure 4	242
Supplementary Figure Legend 4	243
Supplementary Figure 5	244
Supplementary Figure Legend 5	245
Supplementary Figure 6	246
Supplementary Figure Legend 6	247
Supplementary Figure 7	248
Supplementary Figure Legend 7	249
Supplementary Figure 8	250
Supplementary Figure Legend 8	251
Supplementary Figure 9	252
Supplementary Figure Legend 9	253
Supplementary Figure 10	254
Supplementary Figure Legend 10	255
Supplementary Figure 11	256
Supplementary Figure Legend 11	257
Supplementary Figure 12	258
Supplementary Figure Legend 12	259
References	260
Chapter 6	267
Microglial Inflammatory Responses to Chronic Intermittent Hypoxia are Subject to Epigenetic Modification Through JMJD3 Activity	267
Abstract	268
Introduction	269
Methods	271
Results	276
Discussion	279

Acknowledgements.....	282
Figure 1.....	283
Figure Legend 1.....	284
Figure 2.....	285
Figure Legend 2.....	286
Figure 3.....	287
Figure Legend 3.....	288
Figure 4.....	289
Figure Legend 4.....	290
Figure 5.....	291
Figure Legend 5.....	292
Table 1.....	293
References.....	294
Chapter 7.....	298
Discussion and Conclusions.....	298
Introduction.....	299
Summary of Findings.....	299
Integrative Model for IH-induced Microglial Activation.....	304
Clinical Implications.....	307
Future Directions.....	311
Figure 1.....	314
Figure Legend 1.....	315
Figure 2.....	316
Figure Legend 2.....	317
References.....	318
Appendix 1.....	327
Appendix 2.....	366
Appendix 3.....	407

ABSTRACT

Microglia are the only resident immune cells in the CNS, and they are major producers of inflammatory molecules. The overarching hypothesis guiding this thesis is that microglia are activated by pathologic forms of hypoxia, to induce the expression of pro-inflammatory/neurotoxic molecules and contribute to neuropathology. Experiments utilize both animal and cell culture models as well as immuno-magnetic microglia isolation from fresh CNS tissue and a newly developed flow cytometry method to directly examine the impact of hypoxia on microglial function and investigate the mechanisms regulating these responses. Our initial studies demonstrated that a single sustained hypoxia/reoxygenation (HRO) event was sufficient to induce pro-inflammatory gene expression in microglia of rats exposed 2 hours of sustained hypoxia (10% O₂) followed by a return to room air for 22 hours. In addition, the HRO event modulated P2X4 and P2X7 purinergic receptor signaling pathways, such that the P2X receptor agonist BzATP, promoted inflammation under normoxic conditions and had protective/anti-inflammatory effects following HRO, suggesting that microglia are activated by a single hypoxic event and that purinergic receptors play an important modulatory role. We next investigated the effects of multiple, brief HRO events (intermittent hypoxia), on microglial inflammatory activities. Intermittent hypoxia (IH), is a hallmark feature of sleep disordered breathing, and it causes significant neurological deficits. Oxidative stress and inflammatory pathways play a central role in IH-induced neuropathology, however, the cellular source(s) and mechanisms underlying IH-induced inflammation are poorly understood. This thesis explores the role of microglia in IH-induced neuroinflammation, and identifies key pathways modulating these responses. We found that IH up-regulated microglial pro-inflammatory genes/proteins in rodent models of IH, effects that are region-specific, with a time course correlating with neuron death.

Importantly, toll-like receptor 4 (TLR4) expression was also increased in microglia exposed to IH (both *in vivo* and *in vitro*) with a time course corresponding with pro-inflammatory gene expression acutely. However, TLR4 up-regulation persisted even after inflammation returned to baseline, suggesting it may not be exerting pro-inflammatory effects chronically. *In vitro*, we found that the microglial inflammatory response to IH is attenuated in primary cells derived from TLR4 deficient mice, suggesting that TLR4 is a key receptor mediating IH-induced microglial inflammatory activation. *In vitro*, upregulated microglial TLR4 exacerbated their inflammatory response to a TLR4 agonist, lipopolysaccharide (LPS), suggesting that IH may prime microglia to become more pro-inflammatory. To test if this was true *in vivo*, systemic inflammation was induced by intraperitoneal LPS injection in mice exposed to 14 days of IH. Surprisingly, microglial inflammatory responses to LPS were attenuated, whereas the expression of anti-inflammatory cytokines and trophic factors such as interferon- β , interleukin-10, and brain derived neurotrophic factor were increased by IH. These findings suggest that chronic IH may shift the TLR4 signaling pathway from a primarily pro-inflammatory (MYD88-dominant) to an anti-inflammatory (TRIF-dominant) signaling pathway, perhaps as a mechanism of compensation to provide neuroprotection against the chronically injurious IH stimulus. To better understand the gene regulatory effects of IH on microglia, we investigated the ability of chronic IH exposure to induce epigenetic changes known to regulate microglial inflammatory responses. We focused on a class of Jmj-C domain containing histone demethylases (Jumonjiss) whose expression is up-regulated by hypoxia but also require molecular oxygen for catalytic activity. We found JMJD3 and JMJD5 to be enriched in microglia compared to other CNS cell types using the newly developed flow cytometry method. We also found JMJD3 expression to be increased by IH *in vitro* and in microglia isolated from rats exposed to IH in a time frame

correlating with peak inflammatory gene expression. Moreover, IH-induced inflammation in cultured microglia was attenuated in the presence of the JMJD3 inhibitor, GSK-J4. These findings suggest that JMJD3 is an important mediator of IH-induced pro-inflammatory gene transcription in microglia. Overall, this research provides fundamental information into the biological responses of microglia following exposure to IH, and has identified 3 pathways whereby IH-induces microglial inflammation. These studies lay the foundation for future work exploring the manipulation of microglial inflammatory and neurotrophic phenotypes by IH. In addition, they also provide insight into cell regulatory mechanisms that may be therapeutically targeted in microglia to reduce their activation in sleep apnea and other diseases associated with microglial inflammatory activities and hypoxia.

CHAPTER 1

INTRODUCTION & LITERATURE REVIEW

Stephanie M.C. Smith

Portions of this chapter are in preparation for publication

INTRODUCTION

Sleep-disordered breathing, most commonly experienced as obstructive sleep apnea (OSA), affects millions of people worldwide and has gained recognition over the past few decades as an important and growing global health concern. By current estimates, ~6% of women and 13% of men between the ages of 30-70 experience moderate to severe SDB¹, representing a 43% and 48% increase in the prevalence of SDB over the past 2 decades^{1,2}. Perhaps even more alarming than the sheer prevalence of OSA is the overwhelming body of research linking OSA to an increased risk of developing and/or exacerbating cardiovascular diseases, metabolic disorders, and cognitive deficits²⁻⁶. The most common treatment for OSA is continuous positive airway pressure (CPAP) which is applied via a nasal device throughout the night, but despite the devastating consequences of OSA, the cumbersome nature of this treatment along with other factors including poor education on the risks associated with OSA results in low patient compliance⁷. As such, increased research efforts have sought to understand the biological consequences of OSA in order to develop new pharmacologic/therapeutic treatment options for OSA. A link between all of these OSA-associated co-morbidities is inflammation which is known to play an important role in the initiation, progression, and/or severity of each condition⁸⁻¹⁰. The pathological consequences of OSA-induced inflammation have been best-studied in the context of cardiovascular disease and are the subject of several recent reviews¹¹⁻¹³. While the relationship between the neurological consequences of OSA and inflammation are less clear, the central nervous system (CNS) is highly vulnerable to increases in inflammation, as many of inflammatory molecules are neurotoxic, and inflammation has been linked to exacerbation of both traumatic and degenerative neuropathologies^{14,15}. Evidence from animal models exposed to intermittent hypoxia (IH), a hallmark feature of OSA, suggest inflammation

underlies OSA-induced neuronal injury and cognitive impairment, and is therefore a promising target for therapeutic intervention^{16,17}. However, the cellular sources and mechanisms regulating this inflammation are poorly understood.

This chapter will be divided into 3 main sections. The first section will provide background information on OSA, the neurological consequences of OSA and the evidence implicating IH-induced oxidative stress inflammation in this pathology. The second section will focus on data from animal and cell culture models discussing molecular mechanisms mediating IH-induced CNS injury. In the third section we will discuss our hypothesis that microglia, the only resident immune cell in the CNS, play a crucial role in IH-induced inflammatory processes and the potential mechanisms underlying microglial responses to IH. We focus on what is known about microglial inflammation, and introduce new concepts that have yet to be explored.

OBSTRUCTIVE SLEEP APNEA (OSA)

Sleep-disordered breathing is defined as intermittent and cyclical cessations in breathing (apneas) or reductions in airflow (hypopneas) that are: specific to the sleep state, significant enough to cause hypoxemia and hypercapnea, and often result in arousal from the sleep state¹⁸. Thus, sleep-disordered breathing has two primary hallmark features: intermittent hypoxemia and sleep fragmentation¹⁸. Sleep apnea is the most common form of sleep-disordered breathing and occurs due to: 1) a collapsing or “obstruction” of the upper airway (OSA); 2) a “central” event or cessation of brainstem respiratory motor output (central sleep apnea; CSA); or 3) a combination of the two¹⁸.

OSA is the most common (~90% of all cases) and the best studied form of sleep-disordered breathing⁶, and will be the primary focus of this review. The severity of OSA is defined by the apnea/hypopnea index (AHI) where the combined number of apnea and hypopnea

events is divided by the number of hours asleep. OSA severity is classified as mild (AHI $5 < 15$), moderate (AHI $15 < 25$), or severe (AHI > 25)¹⁸. Approximately 1 in 5 adults have an AHI < 5 . The prevalence and severity of OSA is significantly increased in obese patients¹⁹. While obesity is the largest risk factor for developing OSA, additional risk factors include: male sex, age, ethnicity, menopause, and craniofacial abnormalities^{2,19,20}. Obesity and aging are two prominent risk factors for developing OSA^{2,19}, and as such, the prevalence of OSA is likely to increase as the incidence of obesity and life expectancy continue to rise¹⁹. This is particularly concerning as OSA increases the risk of developing and/or exacerbating existing cardiovascular disease, metabolic disorders, and cognitive deficits^{3-5,21,22}. CPAP is the most common and effective treatment for OSA²³, and regular use of CPAP can reverse many of the adverse side effects of OSA^{24,25}. While CPAP is particularly effective in improving cardiovascular and metabolic outcomes for OSA patients, CPAP is less effective in reversing OSA-induced cognitive deficits²⁵⁻²⁷, suggesting that OSA can cause permanent CNS damage. Thus, alternative mechanisms to treat the neuropathological consequences of OSA are of particular interest.

In addition to affecting adults, OSA is experienced by at least 2-3% of school-aged children, and 10-20% of children who are habitual snorers¹⁹. Risk factors for children include obesity and enlarged adenoid tissue that constricts the upper airway¹⁹. In children, OSA caused by enlarged adenoid glands can be surgically corrected by removal of the excess tissue²⁸⁻³⁰. Left untreated, the condition often improves over the course of development as the upper airway widens, but long-lasting cardiovascular and cognitive consequences last into adulthood^{19,31,32}. While there are many similarities in the pathology of OSA between adults and children including: disruptions to the cardiovascular system, metabolism, cognitive processing and increased inflammatory processes, the overall effect of OSA on these systems are different

during development and the adult³³. Because age-dependent differences in the pathophysiology of OSA and its associated co-morbidities are beyond the scope of this research in this thesis, we focus here on the effects of OSA in adults, but will draw inference from studies in children when necessary. For a review on the pathophysiology of OSA in children refer to^{34,35}.

OBSTRUCTIVE SLEEP APNEA AND CNS DYSFUNCTION

Adults with untreated OSA self-report increased excessive daytime sleepiness (EDS)³⁶, difficulty with concentration, mood instability, depression, and cognitive problems that significantly impact quality of life³⁷. Clinical studies investigating the effects of OSA on cognition have yielded mixed results that have made it difficult to discern the direct impact of OSA on specific cognitive processes^{38,39}. These inconsistencies are likely due at least in part to differences in sample population criteria, and differing batteries of the neurocognitive tests used. However, the interpretation of these studies is also complicated by the fact that many patients with OSA also have co-morbidities that are associated in their own right with neurocognitive decline including diabetes, hypertension, and cerebrovascular disease²¹. In addition, the neuropathology of OSA is likely to progress with time, and OSA is often diagnosed years after symptom onset, making it difficult if not impossible to normalize for time since disease onset⁴⁰. Regardless, the overwhelming number of studies reporting cognitive deficits in OSA patients is telling and highly suggestive that OSA negatively impacts cognition. More recently, imaging studies have demonstrated that OSA patients have neuroanatomical and metabolic abnormalities that are consistent with studies indicating cognitive decline⁴¹⁻⁵⁰. In addition, neural injury and cognitive impairment are present in animal models designed to mimic the intermittent hypoxia aspect of OSA^{51,52}. Taken together, these studies exemplify the negative impact of OSA on

neural function. Below we will briefly discuss the major findings and recent advances arising from clinical, neuroimaging, and animal studies on the effects of OSA on the CNS.

Neurological Consequences of OSA

Clinical studies in adult patients with OSA show a relationship between OSA and cognitive impairments which present as attention deficits, memory loss, and decreased executive functioning. For a comprehensive review on the neurological consequences of OSA, refer to reference 53. A large population-based study into the effect of OSA on attention found that OSA patients have reduced coordination of fine motor skills during sustained attention and concentration that is not explained by fatigue or daytime sleepiness⁵⁴. Additionally, studies revealed increases in involuntary attention switching in OSA patients that correlated with both sleep fragmentation and hypoxemia⁵⁵. Combined, these studies indicate that OSA causes significant deficits in attentive behavior.

Memory is a complex function that can be divided into two main classifications: short-term and long-term. Memory impairment is a common complaint in OSA patients⁵³. A large collection of studies have been performed investigating the effects of OSA on memory, and some degree of impairment is clear. However, a consensus on the type of memory affected by OSA remains unclear⁵³. Studies controlling for vigilance report verbal episodic memory is the most affected by sleep apnea^{56,57}. Overall, these findings suggest OSA has a negative impact on memory, however the effects may be small and variable.

Executive function is a term that broadly refers to the management and control of cognition and includes: working memory, reasoning, planning, multi-tasking, and problem solving. Several studies have reported deficits in various aspects of executive functioning in untreated OSA patients^{57,58}, and these impairments have been associated with decreased

activation of the prefrontal cortex⁵⁹. Possibly, the most notable and intriguing data implicating OSA in the impairment of executive function come from studies investigating the impact of OSA on incidence of automobile accidents. People with OSA are 2-7 times more likely to be involved in automobile accidents^{19,58,60}. The complex act of driving integrates executive functioning with attention and vigilance, all of which are negatively affected by OSA. The increased incidence of automobile accidents likely represents a tangible and potentially devastating manifestation of the combined negative consequences of OSA on cognition.

To correlate cognitive impairments observed in OSA to changes in the underlying neuroanatomical structure, a growing body of studies has taken advantage of MRI technology and new highly sensitive analytical techniques to measure gray matter in patients with OSA compared to controls. For a comprehensive review of these findings refer to reference 43. The areas the area most affected by OSA are regions associated with memory, attention, and higher cognition. Significantly reduced gray matter has been reported in the hippocampus and temporal cortices in patients with OSA. In addition to affecting regions of higher cognition, several studies have found decreased gray matter in regions of the cerebellum associated with motor regulation of the upper airway as well as cognitive processing

Neurodegenerative diseases and Traumatic/Ischemic injury

In addition to the negative effects of OSA on normal cognition, OSA is highly correlated with other major neurological problems. Indeed, over 50% of patients with ischemic (e.g. stroke), traumatic (e.g. spinal or brain injury), neurodegenerative (e.g. Alzheimer's disease⁶¹, Parkinson's disease^{62,63}, Amyotrophic Lateral Sclerosis, Multiple Sclerosis), and genetic neural disorders (e.g. Down's syndrome, Fragile X) experience sleep disordered breathing/OSA⁶⁴. Of these, the association between OSA and ischemic injury/stroke has been the best studied. The

percentage of stroke patients with sleep apnea is strikingly high and has been reported to be anywhere from 45% to 95% of patients⁶⁵. Untreated OSA increases the risk factor for having a stroke by >2.5 fold in men⁶⁶, and stroke patients with preceding OSA have more functional deficits than those without OSA and spend more time in the hospital following the ischemic event⁶⁵. In addition, if the OSA remains untreated, stroke patients have increased morbidity/mortality rates, and they are at a heightened risk for having a subsequent stroke.

The impact of OSA on the progression of neurodegenerative and genetic disorders is less understood. However, a recent study in a small population of Alzheimer's patients with OSA found that CPAP improved cognitive scores in the fields of memory and attention⁶⁷ suggesting that some of the cognitive deficits exhibited in these patients could be slowed or reversed by treating the OSA. However, these studies need to be repeated on a larger cohort of patients.

OBSTRUCTIVE SLEEP APNEA: AN INFLAMMATORY DISORDER?

Inflammation is a complex, programmed biological process that is initiated in response to infection or injury. It is the body's natural mechanism designed to remove/heal the insult and return the system to homeostasis. However, when this process goes unchecked or becomes dysregulated, it has deleterious effects on health and can often cause or exacerbate disease. Over the past several years, numerous studies have reported that patients with OSA have higher levels of circulating inflammatory molecules compared to matched control subjects without OSA⁶⁸⁻⁷⁰. While the biological consequences of OSA-induced inflammation are not well understood, it is hypothesized to play a role in the development and progression of OSA-associated co-morbidities^{69,71,72}.

Systemic Immune Response

The connection between OSA and inflammation is best documented in the periphery, where both children and adults with OSA are reported to have higher levels of circulating inflammatory molecules. Increased levels of the pro-inflammatory cytokine, tumor necrosis factor (TNF)- α in OSA patients is perhaps the most consistent evidence to support the notion that OSA can directly activate inflammatory pathways^{69,73}. In addition to TNF α , other molecules indicative of inflammation are reportedly increased in OSA patients including the pro-inflammatory cytokines interleukins (IL)-1 α , -6, -8, and -18, and cell adhesion molecules (CAMs)^{68,74,75}. Additionally, circulating levels of the anti-inflammatory cytokine IL-10 are decreased in OSA patients^{13,68}. T-cells, monocytes, and neutrophils are reported to be major producers of inflammatory molecules in response to OSA⁷⁶. Many of these molecules decrease to normal levels after surgery or treatment of OSA with CPAP⁶⁹, suggesting that the increased inflammation is a direct consequence of OSA.

Consequences of inflammation

Inflammation is known to increase the risk of developing and/or exacerbating cardiovascular disease, metabolic syndrome, mood disorders, and neurodegenerative diseases^{9,15,77,78}. Therefore, OSA-induced inflammation may be one mechanism underlying the pathological consequences of OSA. Here we will explore this concept more fully, as well as what is known about inflammation in the progression of cardiovascular, metabolic, and cognitive disorders.

Cardiovascular Disease

The causative link between inflammation and cardiovascular disease is becoming increasingly appreciated, and the role of OSA in this paradigm has been the subject of several recent reviews^{68,69}.

Inflammation has been implicated in all phases of atherosclerosis development¹⁰. It is understood that immune cells, primarily monocytes, adhere to the vasculature in response injury, lipid peroxidation, or even infection, and produce inflammatory molecules such as cytokines, chemokines, and adhesion molecules that facilitate the recruitment of foam cells, ultimately resulting in vascular plaque formation¹⁰.

Several of the pro-inflammatory molecules reported to be increased in OSA patients including TNF α , IL-8, and CAMs independently increase the risk for developing atherosclerosis and other cardiovascular diseases. Cardiovascular disease and particularly atherosclerosis, is associated with cognitive decline^{79,80}. While all of the factors discussed above can contribute to heart disease, they are also predictors of CNS dysfunction⁷⁷. The brain is a highly metabolic organ, utilizing up to 20% of total oxygen consumption⁸¹. Plaque formation and narrowing of the cerebrovasculature reduces blood flow to the CNS resulting in inefficient oxygen delivery and waste removal. This can ultimately result in the development of a form of dementia known as vascular dementia⁷⁹. In addition, increased inflammation within the cerebrovasculature can cause endothelial cell dysfunction and disruption of the blood brain barrier, thus increasing diffusion of inflammatory molecules and enabling peripheral immune cell infiltration into the CNS¹⁰.

Cognitive deficits

While it is unknown if OSA-induced systemic inflammation plays a definitive, causal role in the associated cognitive impairments, there is some evidence in support of this idea. As

previously discussed, there is an increased incidence of mood disorders including mood instability, depression, and cognitive problems that significantly impact quality of life among patients with OSA^{37,82}. While the root of these problems is unknown, chronic systemic and central inflammation are believed to be a contributing factor to the development of major depressive disorder⁸³ supporting the idea that OSA-induced inflammation may underlie some of these mood disturbances experienced by OSA patients⁷². Many of the inflammatory molecules increased in patients with OSA are among the molecules identified to regulate depressive disorders including: TNF α , IL-6, CAMs, and various chemokines⁷². Although this is an intriguing prospect, there have been no studies yet that have directly examined the correlation between OSA, inflammation, and mood disruption.

To our knowledge, only two studies have directly investigated the relationship between OSA-induced inflammation and cognitive impairments. The first study found that increased blood concentrations of the soluble TNF-receptor 1 (sTNF-R1) correlated with diminished cognitive performance⁷². The second found that OSA patients with metabolic syndrome are at an increased risk of developing cognitive deficits compared to those without metabolic syndrome⁷⁷. But interestingly, after stratifying for inflammation, only those with metabolic disorder coupled with a high level of inflammation were at risk for developing cognitive deficits⁷⁷. These results indicate that inflammation may be a more robust predictor of the risk for developing OSA-induced cognitive decline. Failure to account for this may explain some of the discrepancies between studies investigating the impact of OSA on cognition.

IH AND NEUROPATHOLOGY: FINDINGS FROM ANIMAL MODELS

IH is only one component OSA. OSA patients also experience sleep fragmentation and airway obstructions which cause increased intratracheal pressure⁶. In addition, OSA patients

often have confounding variables such as obesity and existing cardiovascular disease. While the consequences of OSA are likely to be combinatorial, with all of these factors contributing to pathology, animal models mimicking the IH aspect of OSA have become useful research tools to study the pathophysiology of OSA since they develop cardiovascular, metabolic, and cognitive disorders^{51,84-86} that are similar to presentations in OSA patients. The role of oxidative stress and inflammation in the progression of IH-induced neural injury are among the exciting findings emerging from this body of research.

Intermittent hypoxia is a broad term used to describe repeated exposures of hypoxia followed by reoxygenation. It is important to note that not all IH protocols are made equal, and they can have widely disparate effects on the system depending on hypoxia severity, duration, and number of the hypoxic events⁸⁷. Indeed, mild to moderate IH protocols can have beneficial effects and can be used therapeutically⁸⁸⁻⁹⁰, while severe and chronic IH protocols (as in the sleep apnea animal model) cause deleterious and pathologic effects⁵¹. In this chapter, we focus on the pathologic paradigms of IH as those induce neuroinflammation, promote cognitive and memory impairments, and promote neuronal loss in rodent models.

IH-induced neurotoxicity

Whereas insights from clinical studies have yielded useful information into the neuropathology associated with OSA, the mechanisms underlying OSA-induced cognitive deficits and neural injury are not easily studied in humans. Animal models mimicking the IH component of OSA exhibit cognitive deficits and neuronal injury strikingly similar to what is observed in OSA patients. In a seminal paper by Gozal et al., they reported increased neuronal apoptosis in cortical and hippocampal regions in rats exposed to intermittent hypoxia, and this neuronal loss correlated with spatial learning deficits⁹¹. This was the first study to report neuro-

cognitive deficits in an animal model of IH and it has since sparked intense research efforts into the neuropathological consequences and molecular mechanisms underlying IH-induced CNS injury.

Consistent with the MRI information from OSA patients, animal models also exhibit regional susceptibility of IH-induced damage. In both mouse and rat animal models, regions associated with memory and cognition are the best studied. Numerous studies using both rodent models have reported that neurons in the cortex^{17,91–93} and hippocampus^{91,93} are particularly susceptible to IH-induced apoptosis, and this apoptosis is associated with decreased performance on cognitive tests^{91,93}. Surprisingly, there is differential susceptibility of neurons within the hippocampus to the damaging effects of IH; significant neuronal apoptosis is observed in the CA1 region, while the CA3 region is somehow protected from these effects^{91,94}. Additional studies in animal models have provided evidence of IH-induced neural injury to cerebellar Purkinje cells and apoptosis of fastigial nuclei neurons, both of which are important for cardiovascular and respiratory patterning and control⁴⁷. Interestingly, in several cases, neuronal death and cognitive impairments were prevented or reversed with the administration of compounds that interfere with oxidative stress and inflammatory pathways^{16,17,95–99}. These findings suggest that oxidative stress and inflammation may underlie IH-induced neural injury.

Role of oxidative stress and inflammation in IH-induced neuronal death

Oxidative stress and inflammation are highly interrelated, and both are known to cause neuronal death. Repeated exposure of hypoxia and reoxygenation can induce cellular oxidative stress, or a shift in the energy balance within a cell resulting in increased production of reactive oxygen species (ROS) or reactive nitrogen species (RNS) that supersede the antioxidant capabilities of the cell¹⁰⁰. Animal models of IH exhibit signs of oxidative stress within the CNS

as evidenced by the presence of lipid peroxidation⁹³, and increased levels of ROS- producing enzymes^{97,99}, all of which correlate with neuronal death and cognitive impairments. In addition, antioxidant treatment^{95,96} or inhibition of ROS producing enzymes⁹⁶ can reverse these effects, further signifying the importance of oxidative stress in the progression of IH-induced neuronal injury.

Oxidative stress is an upstream mediator of inflammatory processes¹⁰¹, and of particular note, has been shown to regulate the expression of the pro-inflammatory enzymes inducible nitric oxide synthase (iNOS) and cyclooxygenase-2 (COX-2), both of which have been implicated in the progression of IH-induced neuronal injury^{14,101,102}. In animal models, IH induces the expression of iNOS and COX-2 in neuronal cells, and inhibition of either molecule has protective effects against neuronal apoptosis and cognitive deficits^{16,98}. Taken together, these studies implicate oxidative stress and inflammation as key mechanisms whereby IH induces neuronal death. Oxidative stress may be an upstream mechanism by which IH induces inflammation within the CNS.

DIFFERENTIAL CELLULAR RESPONSES TO INTERMITTENT HYPOXIA

Animal models of IH provide useful information regarding the effects of IH in the CNS. However, the complexity of the intact system makes it difficult to ascertain the direct effects of IH on specific CNS cell types. While animal models are more physiologically relevant, cell culture systems are useful tools for the study of specific cell populations, and *in vitro* systems provide unique insights into the differential cellular responsiveness to a given stimuli.

Approximately 10^{11} - 10^{12} neurons comprise the adult CNS, and they are supported by possibly 2 times that many glial cells including astrocytes, oligodendrocytes, and microglia. Before discussing the cellular susceptibility to intermittent hypoxia it is important to note the

heterogeneity that exists within of CNS cell populations. For example, hundreds of distinct neuronal cells have been classified based on function, morphology, neurotransmitter production, and localization within the CNS. As such, it is reasonable to presume that there will be at least some heterogeneity in the cellular responses of neurons and the surrounding glial cells to IH due to differences in cellular functions and the microenvironments in which the cells reside. This is particularly important to consider when interpreting tissue culture studies which utilize either immortalized neuronal cell lines or primary cells cultured from embryonic tissues that are grown in vastly different environments compared to the native, intact system. Here we will discuss what is known about the molecular mechanisms mediating differential cellular susceptibility and responses of CNS cells to oxidative stress and inflammation, and how these findings relate to IH-induced neuropathology.

Thus far, few studies have looked at the effects of IH on CNS cells in culture. However, numerous studies have investigated the impact of a single sustained hypoxic event followed by reoxygenation. This paradigm of hypoxia/reoxygenation (HRO) is commonly utilized to study one aspect of ischemia/reperfusion injury, with other features being nutrient (glucose) deprivation and mechanical injury caused by reperfusion of the tissue. Because of the relevance of HRO to ischemic injury, its cellular and neuropathologic effects have been widely studied, and may provide useful insights into the mechanisms underlying IH-induced injury. Importantly, in HRO models, cells are exposed to a single sustained hypoxic episode followed by a single reoxygenation event, while IH consists of repeated, shorter episodes of hypoxia and reoxygenation. Thus, the HRO model may provide insights into the general cellular responses to hypoxia and reoxygenation, although the pattern and duration of HRO as experienced in IH, are certain to impact cellular responses. Nevertheless, with so few studies investigating IH in

culture, we will draw on the HRO literature when necessary to piece together what is known about the cellular responses to hypoxia, and combine this with data from animal studies to speculate about the differential effects of IH on CNS cells.

Neurons

Neurons form the core component of the CNS and facilitate all sensory, motor, and cognitive functions. Although there is evidence for neuro-regeneration in the hippocampus and olfactory bulbs, neurons are primarily post-mitotic cells that differentiate from stem cells early during development; this differentiation ceases into adulthood¹⁰³. This inability for neuronal cells to regenerate may explain why CPAP therapy is less effective in restoring OSA-induced cognitive impairments. Thus, the mechanisms underlying neuronal death/dysfunction are of particular interest for the development of new therapeutic interventions.

Neurons are by far the best studied CNS cell in the context of IH. As expected, IH affects various neuronal populations differently. As previously discussed, IH causes neuronal injury and death in cortico-hippocampal regions while other regions including the brainstem and spinal cord neurons undergo physiological adaptations that are believed to be neuroprotective to preserve the cardio-respiratory system⁵¹. Such differences are difficult to recapitulate *in vitro*, likely due to the difficult nature of culturing certain populations of neurons as well as an inability to accurately recapitulate the proper microenvironment. To our knowledge, no studies have investigated the impact of IH on neuronal cultures. However, several studies have investigated HRO, in hippocampal and cortical neurons. Exposure of these neurons to HRO in culture promotes apoptotic cell death as a result of increased ROS and RNS which induce glutamate release from neurons. Glutamate binds NMDA receptors, enhancing excitability, and causes cell

death due to excitotoxicity¹⁰⁴. Neuronal survival in response to HRO is increased in the presence of antioxidants and/or ROS/RNS inhibitors^{100,104,105}.

Astrocytes

Astrocytes are the most numerous glial cell type in the CNS. They provide metabolic support to neurons, uptake neurotransmitters, regulate ion homeostasis, maintain the blood-brain barrier, and mediate scar formation/tissue repair in response to injury¹⁰⁶. Astrocytes have long been appreciated for their ability to produce neurotrophic factors that support neuron health¹⁰⁶, but very little is known about their response to IH.

To date, only one study has specifically looked at the astrocytic response to IH. In a rat model of IH, there was significant astroglial hyperplasia and hypertrophy in the cortex and hippocampus that persisted even after neuronal apoptosis had ceased¹⁰⁷. In addition, they observed increased branching and restructuring of neuronal circuits despite the presence of reactive gliosis. Thus, astrocytes may be neuroprotective and promote survival under conditions of chronic exposure to IH. This is consistent with a previous study where astrocytes exposed to HRO in culture increased IL-6 production in a ROS-dependent manner, and this IL-6 protected PC-12 neurons from HRO-induced death¹⁰⁸.

Astrocytic processes line the vasculature in the CNS and help maintain the integrity of the blood-brain barrier¹⁰⁹. IH increases angiogenesis and vascularization of the CNS¹¹⁰, but thus far, no studies have examined whether IH alters the integrity of the vasculature within the CNS. If IH does alter the integrity of the vasculature within the CNS, it could result in the breakdown of the blood-brain barrier and increase leakage of proteins and water into the CNS promoting brain damage¹¹¹. Results from studies investigating astrocyte/blood-brain barrier function in response to HRO have yielded mixed results¹¹¹.

Oligodendrocytes

Oligodendrocytes are the myelinating cells in the CNS. They undergo a complex proliferation and differentiation process culminating the insulation axon sheath¹¹². Disruption of myelination during development results in cognitive deficits and neuro-structural abnormalities¹¹². In the adult CNS, demyelination causes reduced signal transduction, axon damage and neuron death. To date, no study has directly examined the effects of IH on oligodendrocytes in the adult CNS, but adults with OSA have reduced white matter in multiple CNS regions, which suggests there may be demyelination, shrinkage of axons, and/or axonal loss¹¹³. One study investigating the effects of IH on the developing CNS found that IH causes significant damage to immature oligodendrocytes while mature oligodendrocytes are less affected¹¹⁴. Interestingly, there are regional differences in the effects of IH on oligodendrocytes, as there was decreased myelination in the corpus callosum, striatum, fornix, and cerebellum whereas the pons and spinal cord retained normal myelination¹¹⁴. In addition, IH decreased the expression of several proteins associated with myelination in the affected CNS regions, indicating that changes in the process of myelination and possibly arrested oligodendrocyte maturation correlate with observed decreases in neurofilament synthesis, stunted axonogenesis, and synaptogenesis¹¹⁴. A second study investigating the effects of IH on the developing brain also showed that IH caused significant decreases in the myelination of the corpus callosum, and that these effects were irreversible and more severe in IH-treated animals compared to those treated with sustained hypoxia¹¹⁰. These findings may explain the long-lasting cognitive deficits exhibited by children with OSA and young animals exposed to IH. However, the mechanisms underlying IH-mediated injury of oligodendrocytes remain unclear.

Microglia

Microglial cells are similar to macrophages and are the only resident immune cell in the CNS. In the healthy brain, microglia exhibit a ramified morphology with highly dynamic processes that continuously survey the brain, monitor synaptic health, and facilitate synaptic pruning/remodeling¹¹⁵. When disturbances in cellular homeostasis are detected, they undergo a complex activation process enabling them to migrate to the site of injury, proliferate, phagocytose cells or cellular debris, and produce large quantities of neurotoxic and/or neuroprotective molecules¹¹⁵. Microglial activation and production of inflammatory molecules contributes to neurotoxicity in almost all known neurodegenerative, traumatic and ischemic injuries. The involvement of microglia in the contribution to IH-induced neuropathology has been widely speculated, but no studies except our own (Chapters 4, 5, and 6) have directly investigated the impact of IH on any microglial activity.

Although no studies have directly investigated the role of microglia in OSA or IH-induced neural injury, these cells are a likely source of inflammation in the CNS. We know that a single episode of hypoxia/reoxygenation is sufficient to activate cultured microglia and promote an inflammatory state¹¹⁶. Many molecules have been shown to regulate the microglial inflammatory response to HRO including oxidative enzymes, mitogen-activated protein kinases (MAPKs), and transcription factors ultimately resulting in production of pro-inflammatory molecules¹¹⁷⁻¹²³. These molecules and their potential role in IH-induced inflammation will be further discussed. In addition, IH causes oxidative stress and neuronal damage, both of which are signals of cellular distress that induce the release of molecules known to activate microglia¹²⁴. Microglial production of inflammatory molecules in response to inflammatory stimuli likely exacerbates the already injured CNS and further promotes neuronal injury. In the following

sections, we will explore the possible role of microglia in IH-induced inflammation and neuropathology in greater detail.

INTERMITTENT HYPOXIA AND CNS INFLAMMATION

Thus far, we have provided a literature review on neuropathological consequences of OSA as well as evidence for inflammation as an important factor in the development of OSA associated co-morbidities. Studies in animal and cell culture models have revealed the extensive mechanistic and regional heterogeneity in the cellular responses to IH and HRO. Additionally, animal models identify oxidative stress and inflammation in the CNS as the cause of cortico-hippocampal neurotoxicity and cognitive deficits following exposure to IH. These studies have provided significant advances into the mechanisms underlying the neuropathological consequences of IH and OSA. However, the cellular source(s) of IH-induced neuroinflammation and the molecular underpinnings of this inflammation are not well understood.

The CNS was once believed to be an immune privileged organ. It is now well-established that the CNS has a specialized population of resident innate immune cells known as microglia that act as the first line of defense against infection or injury, and that are often a major source of inflammatory molecules within the CNS¹¹⁵. However, despite their fundamental role in neuroinflammation, microglia have never been studied in the context of IH or OSA. In the following sections, we focus on microglial cells, present possible mechanisms whereby IH can activate microglia, and discuss their potential contributions to IH-induced neuropathology.

MICROGLIA

Microglia are derived from myeloid progenitor cells that migrate into the brain parenchyma during embryonic development where after they become trapped when the blood brain barrier forms. They then differentiate into a self-renewing population of mature microglial

cells¹¹⁵. Following this window of CNS infiltration, there is little to no exchange between the blood and brain parenchyma, and thus, microglia exist as a stable cell population that inhabits the brain, spinal cord, eye, and optic nerve.

While microglia are often compared to macrophages due to their etiologic and phenotypic similarities, microglia are a specialized immune population with functional characteristics which are especially suited for monitoring and responding to changes within the CNS¹²⁵. In the healthy CNS, microglial cells have a ramified morphology with extensive processes that continuously survey the environment. Microglial activities are essential for the development and maintenance of the healthy CNS, as they unremittingly monitor synaptic activity, produce neurotrophic factors, and facilitate synaptic pruning/remodeling¹¹⁵. When disturbances in CNS homeostasis are detected due to altered neuronal activity, infection, trauma, or neurodegeneration, microglia rapidly alter their phenotype in a programmed response to the given stimuli. These responses can include increased motility, proliferation, phagocytic activity, and the production of pro/anti-inflammatory and/or immunomodulatory molecules. As previously discussed, the CNS is a highly complex organ with extensive regional and cellular heterogeneity which results in vastly different microenvironments. As such, microglial cells are not a homogeneous population, and they have extensive regional differences in their basal activities¹²⁶⁻¹²⁸ as well as in their responses to pathologic stimuli¹²⁹. Indeed, differential microglial responses may underlie some of the regional heterogeneity in neurotoxicity in the context of IH.

Microglia are a major source of pro-inflammatory molecules within the CNS. Many of these inflammatory molecules are transcriptionally regulated and are very lowly expressed in the healthy CNS, but they can be rapidly transcribed and produced in large quantities in response to pathologic stimuli^{130,131}. Many of the pro-inflammatory molecules produced during pathology

are neurotoxic, and thus, if this system goes unchecked, it can cause severe neurological damage. Dysregulation of microglial inflammatory pathways are believed to contribute to the progression of neurodegenerative pathologies¹⁰².

POTENTIAL MECHANISMS OF IH-INDUCED MICROGLIAL ACTIVATION

Very little is known regarding the mechanisms mediating IH-induced CNS inflammation. In this section we will discuss three potential methods by which IH can activate microglia: 1) Systemic inflammation cross-talk with the CNS, 2) Indirect activation of microglia by damage-associated molecular patterns (DAMPs) released from surrounding cells that have been injured by IH, and 3) Direct activation of microglia by IH. While we will be discussing these possibilities separately and in more detail below, they are highly interconnected and share many common signaling molecules and inflammatory cascades. See Figure 1 for our working schematic for how these 3 pathways are activated by IH and integrate to promote neuroinflammation/pathology.

Systemic Inflammation

While increased systemic inflammation in OSA and animal models of IH is well established, it is unclear whether it is sufficient to induce inflammation in the CNS. While the CNS is to some extent protected from peripheral immune responses, there is ample evidence in support of peripheral involvement in the induction of central immune responses despite the presence of the blood brain barrier. These mechanisms will be discussed below. (Fig.1, A & B)

Direct communication between peripheral and central inflammation

Circulating inflammatory molecules can gain entry into the CNS via active transport mechanisms as has been described for IL-1, TNF α , and IL-1ra¹³². Alternatively, it is possible that these molecules gain direct entry into the brain parenchyma through the circumventricular

regions such as the organum vasculosum lateralis terminalis (OVLT), where the BBB is lacking¹³³. Both of these methods would facilitate direct microglial activation by circulating inflammatory molecules.

Blood brain barrier disruption

The BBB is a highly selective barrier that is formed by tight junctions between cerebrovascular endothelial cells, a thick basement membrane, and a layer of astrocytes that separates the blood from the cerebral spinal fluid¹¹¹. Despite the protective nature of the BBB, circulating cytokines can directly bind to the endothelial cells in the brain and induce endothelial production of inflammatory molecules that readily cross the BBB such as nitric oxide (NO) and prostaglandins that can directly activate microglia and cause damage to surrounding neurons and astrocytes. In addition, both of these molecules are known to cause breakdown of the BBB¹³⁴, thus permitting direct entry of cytokines/chemokines as well as peripheral immune cells into the otherwise restricted CNS parenchyma. An additional mechanism by which the BBB may become compromised in the context of IH is through negative effects of IH directly on the endothelial cells and astrocytes that comprise the BBB¹¹¹. However, while BBB disruption is possible, this mechanism is unlikely to occur in response to IH as peripheral immune cells have not been reported to accumulate in the CNS and we have not observed measurable lymphocytes or monocytes in our studies (data not shown).

Vagal nerve transmission

Although it is not fully understood, there is evidence that stimulation of peripheral vagal neural afferents by inflammatory cytokines can directly induce production of pro-inflammatory cytokines in the CNS. This was best demonstrated with peripheral administration of the pro-inflammatory cytokine, IL-1¹³⁵, or lipopolysaccharide (LPS)¹³⁶, a component of the gram-

negative bacterial cell wall and a potent immune activator. However, this response was abolished in vagotomized animals^{135,136}, which suggests that peripheral inflammatory signals can be perpetuated in the CNS via the vagal nerve.

Indirect activation of microglia by DAMPs released from stressed/injured cells

Microglia are master surveyors of their environment. While the mechanisms by which microglia sense their environment are not fully understood, it is well established that they possess receptors that are activated by molecules released from stressed/dying cells^{124,129}. Upon activation of these receptors, microglial inflammatory, phagocytic, and/or migratory activities can be initiated¹¹⁵. In animal models of IH, these damage associated molecules may be released from injured or stressed neurons and glia resulting in microglial activation (Fig. 1, D). In the following sections, we will discuss potential receptor families and molecules mediating this response.

Damage-Associated Molecular Patterns (DAMPs)

Cell culture and animal models reveal that cortical and hippocampal neurons are highly susceptible to H₂O₂-induced oxidative stress and cell death. Injured/stressed neurons and glia release stress molecules (collectively known as DAMPs, damage-associated molecular patterns) into the extracellular space that function as ‘alarmins’ or danger signals to microglia¹²⁴. Many DAMPs are endogenous ligands for pattern recognition receptors (PRRs) or scavenger receptors expressed on microglia, and as a result, they are capable of initiating a sterile immune response.

PRRs are best known for their ability to bind highly conserved motifs expressed by microbial cells, known as pathogen-associated molecular patterns (PAMPs)¹³⁷. Four families of PRRs have been identified: Toll-like receptors (TLRs), NOD-like receptors (NLRs), C-type lectin receptors (CLRs), and Retinoic acid-inducible gene (RIG)-I-like receptors (RLRs). Within

the CNS, these receptors are primarily expressed on microglial cells, but they can also be found to varying degrees on neurons, astrocytes, and cerebrovascular endothelial cells¹³⁸. We will discuss the potential role of these PRRs and DAMPs in IH-induced CNS inflammation with a particular emphasis on the TLRs and NLRs (see inflammasome).

Toll-like Receptors (TLRs)

The TLR family is arguably the best studied of the PRRs. They consist of a single transmembrane domain with an extracellular N-terminal domain comprised of leucine-rich repeats (LRRs) and a cytoplasmic tail with a conserved region known as the Toll/IL-1 receptor domain (TIR)¹³⁹. Ten human and at least 12 rodent TLR receptors have been identified, and are distinguished based on their associated ligand affinity and signaling pathways. Upon ligand binding, TLRs homo- or hetero- dimerize resulting in activation of complex intracellular signaling cascades that ultimately lead to the expression of a wide array of genes involved in inflammatory responses¹⁴⁰; and this transcriptional profile differs among cell types and the specific TLR activated¹⁴¹. TLR signaling cascades can be roughly divided into two distinct pathways based on the major adaptor molecules utilized for signal transduction. With the exception of TLR3, the most prominent TLR signaling cascade involves the recruitment of an adaptor protein, Myeloid differentiation factor-88 (MyD88), which initiates a cascade of events ultimately leading to MAPK activation and transcription factor activation including: nuclear factor kappa-light-chain-enhancer of activated B cells (NFκB), activating protein (AP)-1, and hypoxia inducible factor (HIF)-1α¹⁴²⁻¹⁴⁵. Alternatively, TLR3 recruits a different adaptor protein known as TIR domain containing adaptor inducing IFNβ (TRIF) which again, through a multi-step process ultimately results in the activation of the transcription factor, interferon responsive factor (IRF)- 3 and 7 which translocate to the nucleus to directly induce (or indirectly through

activation of STAT1) to induce type-I interferons and interferon related genes^{145,146}.

Importantly, TLR4 is also capable of activating the TRIF pathway. See Figure 2 for a model depicting the TLR4-mediated MYD88- and TRIF- dependent signaling cascades.. For a complete review of TLR receptors and their signaling pathways see reference 147.

TLR Signaling in the CNS

Within the CNS, microglia are the primary cells expressing TLRs. Microglia express TLRs 1-9¹⁴⁸ and these receptors are potent regulators of microglial immune responses. In addition to microglia, astrocytes, oligodendrocytes, and neurons have all been reported to express TLRs under certain conditions¹³⁸. However, the functional relevance of TLRs in these cells is not well understood and therefore, will not be further discussed here. Activation of microglial TLRs has been best studied in the context of PAMPS, and they result in the production of a host of cytokines, chemokines, and enzymes that promote neurotoxicity. TLR-mediated inflammation has long been recognized to induce neurotoxicity in response to infections including: bacterial, viral, fungal, and prion¹⁴⁹. However, the activation of TLRs by endogenous ligands to induce sterile inflammation during neuropathology is not as well understood¹⁴⁹. The role of TLRs in IH-mediated microglial activation and neuronal injury has yet to be investigated. In the following sections, we will review evidence for TLR involvement in OSA-mediated systemic inflammation and present information to support TLR-mediated responses in the CNS.

Evidence for TLR involvement in OSA-induced inflammation

A recent study demonstrated that monocytes isolated from patients with OSA have increased expression of TLR2 and TLR4 compared to non-OSA controls. The increased expression of TLR2 and TLR4 was associated with elevated production of cytokines, suggesting

that the increased expression of these receptors may prime the cells to be more pro-inflammatory. The increased expression of TLR2, TLR4, and pro-inflammatory cytokines were reversed with CPAP treatment, indicating that IH and/or sleep disruption promotes the upregulation of these molecules¹⁵⁰. Consistent with these data, TLR4¹⁵¹ and TLR2/6¹⁵² have been reported to be upregulated by hypoxia in cultured macrophages through a HIF-1 α -dependent pathway, potentiating LPS-induced inflammation in hypoxia¹⁵¹. In addition to increased TLR expression, patients with OSA have increased circulating levels of several known DAMPs which are ligands for TLR2 and TLR4 (Fig. 2).

High-mobility group box 1 (HMGB1), a TLR2 and TLR4 ligand, is increased in the serum of children and adults with OSA^{153,154}. In addition, the circulating levels of the TLR4 ligand monocyte responsive protein (MRP)-8/14 (S100A8/S100A9, or calprotectin) is increased in both children and adults with OSA^{32,155} and is proposed to be a potential biomarker for disease severity and predicting risk of long-term morbidity. In addition to HMGB1 and MRP8/14 other known TLR4 ligands are reported to be increased in adults with OSA including HSP70, fibrinogen, and oxidized LDL¹⁵⁶⁻¹⁶¹. HSP70 expression is increased in monocytes of OSA patients¹⁶¹. Fibrinogen has been reported by numerous groups as being increased in patients with OSA and is used as a biomarker for determining the risk of developing cardiovascular disease¹⁵⁶⁻¹⁵⁹. Oxidized LDL, a marker of oxidative stress, is increased in the plasma of OSA patients¹⁶⁰. Oxidized LDL activates a TLR4/TLR2/CD36 complex on macrophages to induce formation of foam cells that can cause arterial plaques¹⁶². While the cellular source(s) of these circulating DAMPs are unknown, they are all potential mediators of peripheral inflammation in OSA patients, and many of them have been shown to mediate sterile inflammation within the CNS.

However, whether these DAMPs are also increased extracellularly in the CNS of IH-exposed animals or OSA patients is not yet known.

TLR involvement in IH-induced inflammation and neural injury

TLR-mediated microglial inflammation has been linked with increased neurotoxicity in almost all neurodegenerative, infectious, traumatic, and ischemic pathologies^{138,149,163}. During sterile inflammation, the prevailing hypothesis is that DAMPs released from damaged or stressed cells activate microglia through TLRs (or other PRR and scavenger receptors) to induce inflammation (Fig. 1D). In turn, this inflammation is neurotoxic and promotes further cellular stress/death in the surrounding cells, thus creating a ‘vicious cycle’ of inflammation and cell death¹⁶⁴⁻¹⁶⁷ (Fig. 1C), . HSP60, HMGB1, and MRP8/14 are the primary DAMPs that have been identified in inducing microglial inflammation within the CNS¹⁶⁶⁻¹⁶⁸.

IH-induced hippocampal neuronal death is confined to the CA1 region of the hippocampus, while neurons in the CA3 and dentate gyrus are protected from the effects of IH⁹¹. A proteomic analysis comparing the CA1 and CA3 regions immediately following a 6 hour exposure to IH was performed⁹⁴, and HSP60 and α -synuclein, two known DAMPs and TLR4 ligands⁹⁴, were identified as being selectively increased by IH in the CA1 region. Although it is unknown if these increases truly reflect an increase in extracellular DAMPs in the CA1 region since extracellular protein concentrations were not determined in these studies, IH does induce oxidative stress and cell death in this region, both of which are known to induce HSP60 release from cells *in vitro*¹⁶⁶. The mechanisms regulating extracellular levels of α -synuclein are less well understood but are associated with increased microglial inflammation in Parkinson’s disease¹⁵. The IH-induced CA1-specific increase in DAMPs may contribute to the enhanced

susceptibility of the CA1 region to IH-induced neuronal death if these molecules are released into the extracellular space.

Additionally, HMGB1 and MRP8/14 are two other potential molecules mediating IH-induced inflammation, as they are both increased in the serum of patients with OSA and they are known to have inflammatory effects within the CNS¹⁵. HMGB1 is a nuclear protein, but it is rapidly released into the extracellular space in response to cellular stress and inflammasome activation¹⁶⁹. In response to oxidative stress, neurons rapidly translocate HMGB1 from the nucleus to the cytosol, where it is subsequently secreted from the cell¹⁷⁰ (Faraco, 2011). HMGB1 acts on microglia via interactions with TLR2, TLR4, and/or the scavenger receptor MAC-1 (CD11b) to induce inflammation^{168,171}. HMGB1 has also been shown to be released from macrophages in response to stress and it acts in an autocrine/paracrine fashion to enhance inflammation^{169,172}. Similarly, MRP8/14 is also released from microglia and can act as an autoregulator. MRP8/14 is released from activated phagocytes to enhance TLR4 signaling in response to LPS¹⁷³, and increased expression of MRP8/14 in the CNS is an indicator of neuroinflammation^{167,173}. In addition, HMGB1 and MRP8/14 have been identified as key DAMPs inducing TLR4-mediated inflammation following ischemic injury^{167,169,170,173}. Interestingly, oxidization of MRP8/14 causes it to be less pro-inflammatory, and may be one mechanism regulating the extent of microglial inflammation during IH¹⁷⁴.

Hypoxia may independently enhance TLR4 signaling pathways resulting in increased production of inflammatory molecules in response to DAMPs. HRO increases the effects of LPS in cultured microglia and potentiates the expression of iNOS, TNF α , and NF- κ B¹⁷⁵, suggesting that TLR4-mediated inflammation may be primed by the HRO event. Whereas, 48 hours of sustained hypoxia increases TLR4 expression in cultured microglial cells, and this

paradigm of hypoxia reportedly shifts TLR4 signaling away from the MyD88 pathway to a TRIF dominant pathway¹⁷⁶. While the role of TLR4 in IH-mediated neuroinflammation remains to be studied, IH may enhance TLR-mediated inflammation by causing a release of endogenous TLR ligands into the extracellular space, and by strengthening TLR signaling pathways to promote increased inflammatory microglial gene expression.

Extracellular ATP and Purinergic Receptor Activation

Extracellular ATP is an essential neurotransmitter and a potent regulator of microglial processes through purinergic P2 receptor activation. The concentration of extracellular ATP is determined by the release rate relative to the rate of enzymatic degradation and cellular uptake. Under normal conditions, the concentration of extracellular ATP is low and localized primarily at the synapse, where it is less likely to activate purinergic receptors on microglia¹⁷⁷. However many pathologic stimuli including: traumatic and/or metabolic stress resulting from hypoxic/hypoglycemic/ischemic injury, inflammatory stimuli including LPS and IL-1 β , and cytolysis can cause a potent increase in extracellular nucleotide concentration¹⁷⁸ that is sufficient to activate purinergic receptors on microglial cells¹⁷⁸. As ATP is ubiquitously produced, all cells within the proximity of microglia are potential sources of extracellular ATP including: neurons, astrocytes, oligodendrocytes, endothelial cells, and even other microglia. To our knowledge, with the exception of our own studies¹⁷⁹ microglial purinergic signaling has not been studied in the context of HRO or IH. However, ATP is released from primary cortical neurons exposed to HRO in a severity-dependent manner to regulate microglial responses¹⁸⁰. Thus, IH is likely to increase extracellular concentrations of ATP that can modulate several microglial responses.

Purinergic receptors can regulate many microglial processes including: migration, phagocytosis, inflammation, proliferation, and trophic factor production¹⁸¹. ATP and its

metabolite ADP are potent purinergic P2 receptor agonists, while AMP and adenosine are specifically recognized by adenosine (P1) receptors. P2 receptors are divided into two classes: ligand-gated, ionotropic P2X receptors and the G-protein coupled, metabotropic P2Y receptors¹⁷⁷. There are seven known P2X receptors (P2X₁₋₇) and nine P2Y receptors (P2Y_{1-2,4-6,8-14}). Our lab has recently shown that all P2 receptors (with the exception of P2Y11 which is not present in the rodent genome), are expressed in murine microglia to varying degrees, the expression profiles of which differ based on age and sex¹²⁸. These findings suggest that microglial responses to purines may differ between males and females and during development/aging.

P2Y1, P2Y6, and P2Y12 are highly expressed in microglia. P2Y1 and P2Y12 regulate chemotaxis/migration^{128,182,183}. P2Y6 regulates phagocytosis and is important for clearing cellular debris when activated by UDP that is released from injured cells¹⁸⁴. In addition P2Y1, and P2Y2 have been shown to suppress inflammatory responses in microglia^{185,186}.

By far the most well studied P2 receptors in microglia are P2X4 and P2X7. P2X4 is best known for its role in chronic pain. Chronic upregulation and activation of P2X4 in dorsal spinal cord microglia induces the production of BDNF¹⁸⁷ which enhances a form of neuroplasticity that results in chronic neuropathic pain. In addition, P2X4 is reported to regulate microglial inflammatory responses and chemotaxis¹⁸⁸. P2X7 is highly expressed on myeloid cells and is best known for its regulatory role of inflammatory pathways through the inflammasome¹⁸⁹ (discussed in further detail below). On macrophages, P2X7 activation enhances LPS-induced inflammation^{190,191}, and its activity is indeed necessary for LPS-induced inflammation¹⁹⁰. Upon activation of TLR4 by LPS, intracellular stores of ATP are released from the cell and act P2X7 to facilitate inflammasome activation¹⁹¹. While this process has been well

described in cultured macrophage cells, P2X7 may have immune-suppressive effects on microglia. Our lab has previously shown that P2X7 activation downregulates LPS-induced microglial inflammation through activation of the transcription factor receptors (EGRs)¹⁹². Several labs have since found similar P2X7-mediated effects in microglial responses to inflammation. Interestingly, P2X4 and P2X7 have been hypothesized to work together to mediate inflammatory processes^{188,193}. P2X4 is rapidly trafficked to the cell surface from intracellular stores in response to LPS in microglia, but not macrophages¹⁸⁸. Additionally, selective inhibition of P2X7 blocks LPS-induced trafficking of P2X4 to the microglial cell membrane¹⁹⁴. P2X4 and P2X7 prefer to assemble as homotrimers¹⁹⁵, but they can also form functional hetertrimers¹⁹⁶. However, the functional significance of P2X4 and P2X7 complexing is currently unknown.

Direct Activation of Microglia by IH

Aside from peripheral inflammatory molecule involvement in microglial activation, and indirect microglial activation through DAMPs, IH may also have direct physiological consequences in microglial cells through activation of oxidative stress pathways (Fig.1-3). As previously discussed, ROS are the product of normal cellular metabolism and are produced primarily during aerobic mitochondrial respiratory metabolism¹⁹⁷. The biological reduction of molecular oxygen produces normal byproducts such as superoxide anion, hydrogen peroxide, hydroxyl radical, and organic peroxides that are collectively referred to as ROS¹⁹⁷. These are essential cell signaling molecules, but at high levels, they can also cause cellular damage including lipid and protein oxidation and DNA damage. As such, there are critical cellular mechanisms available to prevent ROS accumulation, including the production of endogenous antioxidants enzymes and ROS scavengers that keep the levels of ROS within the cell in

check¹⁰⁰. Oxidative stress occurs when the balance between the production of ROS and its elimination by antioxidants shifts, resulting in an increased concentration of ROS. In microglia HRO results in the activation of NADPH oxidase on the cell membrane Hypoxia followed by reoxygenation causes changes in the cellular membrane potential, oxidant generating systems, and antioxidant defenses that culminate as oxidative stress or an increase in ROS production¹⁰⁰. ROS can be formed by a number of mitochondrial and extra-mitochondrial enzymes, both of which are important for induction of inflammatory pathways. While ROS production by microglia has not been studied in the context of IH, several studies have found that HRO-induced ROS is sufficient to induce microglial inflammation and their production of pro-inflammatory cytokines^{117,119,198}.

NADPH Oxidase, ROS and Inflammation

NADPH oxidase is the primary source of microglia-generated extracellular ROS¹⁹⁸. Under normal conditions, this membrane-bound enzyme is inactive, but in response to a wide array of stimuli, including HRO, NADPH oxidase is activated and rapidly catalyzes the production of superoxide (O_2^-) from oxygen¹⁹⁷. Extracellular superoxide is a key mediator of neurotoxicity and acts synergistically with pro-inflammatory cytokines to enhance neurotoxic effects¹⁰². In addition to the role of NADPH oxidase in the production of extracellular ROS, it may also contribute to the generation of intracellular ROS formation which are important second messengers regulating inflammatory cascades. ROS have a particularly important role in the regulation of inflammation. Indeed, the induction of ROS is hypothesized to be common pathway induced by all forms of inflammatory stimuli and its production is essential for microglia to mount an inflammatory response¹⁹⁹.

In microglia, sustained hypoxia causes an accumulation of extracellular K^+ , and with reoxygenation, there is an influx of calcium through voltage-gated potassium/calcium channels which induces NADPH oxidase activation and ROS formation¹¹⁹. ROS accumulation is an indicator of cellular stress and they activate inflammatory signal transduction pathways including the inflammasome, MAPKs, and transcription factors such as HIF-1, NF- κ B, and AP-1¹⁹⁷. (Further discussed the following sections). In animal models, IH-induced ROS formation contributes to neuronal death and cognitive impairments^{92,93,95-97}, and ROS are hypothesized to mediate induction of inflammatory pathways in glial cells^{95,200}. Administration of the superoxide dismutase mimetic manganese tetrakis, or flavanoids with broad spectrum antioxidant capabilities, has neuro-protective effects in IH-treated animals and blocks IH-induced neuron death and cognitive impairments^{92,95-97,99}.

COMMON SIGNAL TRANSDUCTION PATHWAYS MEDIATING MICROGLIAL INFLAMMATION: RELEVANCE TO IH-INDUCED MICROGLIAL ACTIVATION

Thus far, we have proposed several potential mechanisms by which IH can induce microglial activation. In reality, the impact of sleep apnea on microglial activities is multifaceted and likely involves a combination of some or all of the mechanisms presented, as well as some that have yet to be identified. Regardless, many of these pathways intersect on common downstream signaling molecules and induce similar patterns of gene expression. Here we will discuss these pathways and the evidence for their involvement in IH and OSA-mediated CNS injury.

Inflammasome

The inflammasome is a high molecular weight, multi-protein complex that is a core component of the innate immune system. The inflammasome complex activates caspase-1 which causes cleavage of pro-IL-1 β and IL-18 into their mature forms, subsequently enabling

their release from the cell through a non-canonical secretory pathway²⁰¹. In addition, the inflammasome also facilitates release of the DAMP, HMGB1, from immune cells^{202,203}. There are 4 well-defined inflammasome complexes and that are distinguished based on the main core receptors making up the complex; NLRP1, NLRP3, or NLRP4 from in the NLR family of PRRs, or AIM2 from the HIN protein family²⁰¹. The NLRP3 inflammasome is the most widely activated and best studied inflammasome, and will be the primary focus here.

The NLRP3 inflammasome is activated by a wide variety of stimuli including pathogenic stimuli including bacterial, fungal, viral, and components (PAMPs), endogenous danger molecules including extracellular ATP and DAMPs, elevated levels of extracellular glucose, prion proteins, and synthetic particles such as silica and asbestos^{201,204}. NLRP3 activation by TLRs is hypothesized to occur through a two step process where TLR activation primes the NLRP3 inflammasome by 1) increasing transcription and translation of IL-1 β , IL-18, and NLRP3, and 2) ATP and/or ROS release into the extracellular space acts as a secondary activator to induce P2X7 mediated pore formation or ROS-dependent assembly of the inflammasome complex. The mechanisms regulating inflammasome activation have been widely debated. Four pathways for inflammasome activation have been proposed (for a comprehensive review see references 199 and 201): 1) the lysosome rupture and release of cathepsin B into the cytosol, 2) extracellular ATP binding to P2X7 and inducing pore formation allowing NLRP3 ligands to enter the cell, 3) ROS-dependent activation, and 4) TLR-IRAK-1 mediated direct activation of NLRP3. Inflammasome activation is associated with many neuropathologies including: infectious diseases (encephalomyelitis and meningitis), injury (ischemia/stroke, spinal cord injury, and traumatic brain injury), and chronic neurodegenerative

diseases (demyelinating diseases, amyotrophic lateral sclerosis, Parkinson's disease, Alzheimer's disease, and prion disease) (comprehensively reviewed in reference 163).

Inflammasome involvement in IH-induced neuropathology has not been investigated. However, it is a key pathway mediating microglial inflammatory responses, and many of the mechanisms previously discussed for IH-induced microglial activation converge on the inflammasome, as it is activated by TLRs, DAMPs, extracellular ATP, and ROS¹⁹⁹. In addition to increased production of inflammasome activators, hypoxia alone increases inflammasome activation in microglial cells in culture through the up-regulation of caspase-11 which in turn activates caspase-1 and subsequent IL-1 β processing¹²¹. HRO induced expression of caspase-1 and IL-1 β in the amygdala impairs new memory formation²⁰⁵, providing one mechanism whereby IH-induced inflammation and memory deficits can occur. Evidence for IH-induced inflammasome activation also comes from studies in OSA patients and IH animal models that have evaluated peripheral immune responses. The inflammasome-mediated molecules IL-18, IL-1 β , and HMGB1 are increased in the serum of patients with OSA^{154,206–208}.

Mitogen-Activated Protein Kinases (MAPKs)

External cellular stimuli trigger intracellular signaling cascades that are transmitted and propagated via coordinated kinase and phosphatase activity that ultimately translates the original stimulus into a cellular response that often involves alterations in gene expression. In inflammatory cells, one of the most prominent kinase families is the mitogen-activated protein kinases (MAPKs). There are four subfamilies of MAPKs including: (1) extracellular signal-regulated kinases (ERK1/2 or p44/p42 MAPK), (2) p38 MAPKs, (3) c-jun N-terminal kinases (JNKs), and (4) ERK5/big MAP kinase 1 (BMK1). In microglia, p38 and ERK1/2 have been best studied for their role in the induction of inflammatory gene expression, and both have been

shown to regulate microglial activities in response to inflammatory stimuli (Reviewed in reference 209). p38 activation is associated with induction of pro-inflammatory gene expression through activation of transcription factors such as NF- κ B and AP-1²⁰⁹. ERK1/2 is traditionally associated with cell survival pathways, but it has also been shown to mediate microglial production of inflammatory molecules under certain conditions²⁰⁹.

p38 is a cytosolic serine threonine kinase that is activated when dually phosphorylated at both Tyr and Thr residues by the MAPK kinases (MAPKKs), MEK3 or MEK6. In microglia, p38 phosphorylation is triggered by a variety of stimuli including: oxidative stress, HRO, ATP, glutamate, PAMPs, DAMPs, and inflammatory molecules^{186,209-213}. In cultured microglia, HRO induces p38 activation but not ERK or JNK, and mediates expression of NO and TNF α as well as iNOS²¹³. Inhibition of p38 blocked the induction of NO and iNOS by hypoxia²¹³. In addition, HRO-induced p38 MAPK increases expression of caspase-11, causing activation of caspase-1, and secretion of IL-1 β and IL-18¹²¹. Consistent with these results, HRO-induced production of NO, TNF α , IL-1 β , and iNOS is blocked by a p38 inhibitor¹²³. Similarly, monocytes exposed to IH in culture increased p38 MAPK and subsequent NF- κ B activity²¹⁴.

Like p38, ERK1 and ERK2 are also serine threonine kinases that are localized to the cytosol until activation by the MAPKKs, MEK1 or MEK2. When activated, ERK1/2 can phosphorylate both cytosolic and nuclear proteins after nuclear translocation²⁰⁹. While ERK1/2 activation can regulate microglial inflammatory gene induction through activation of the transcription factor AP-1, it can also promote anti-apoptotic, proliferative, and trophic pathways through the activation of the transcription factor CREB²¹⁰. We have previously shown that microglia increase p38 and ERK1/2 in response to oxidative stress, but pre-treatment with ATP decreases ERK1/2, possibly via effects on P2Y1 receptor activation, while having no effect on

p38²¹⁰. These data suggest that during oxidative stress, activation of microglia by ATP may increase inflammatory gene expression by preferentially activating the pro-inflammatory MAPK p38 and suppressing the repressive activities of ERK1/2.

Transcription Factor Activation

Transcription factors are proteins that bind conserved domains of DNA in a gene promoter region, recruit transcriptional machinery, and promote gene transcription. All of the previously discussed pathways converge on downstream transcription factors that facilitate microglial gene transcription. Although there are many hypoxia-sensitive transcription factors, we will discuss those we hypothesize to regulate microglial inflammatory gene expression in response to IH.

HIF-1 α

HIF-1 α is the prototypical hypoxia responsive transcription factor. Under normoxia, HIF-1 α is hydroxylated by prolyl hydroxylases (PHDs) which targets HIF-1 α for poly-ubiquitination, thus keeping cytosolic HIF-1 α protein levels low (Reviewed in references 142 and 215). However, during hypoxia, these PHDs are inhibited, thus enabling accumulation of HIF-1 α protein where it translocates to the nucleus to induce gene transcription. Many HIF-1 α target genes regulate cell survival and angiogenesis, and are increased as both adaptive measures to protect cells from hypoxic injury and to increase vascularization and tissue oxygenation. Additionally, HIF-1 α plays an important role in inflammatory processes under both hypoxic and normoxic conditions. HIF-1 α increases TLR4 expression in cultured microglia exposed to hypoxia and in animal models of neonatal hypoxic injury^{176,216}. In addition, HIF-1 α has recently been found to play an important role in the innate immune system, as it is necessary for proper inflammasome function, NF- κ B activation and inflammatory gene expression (Reviewed in

reference 217). HIF-1 α can be activated under normoxic conditions in macrophages through activation of TLR4, and mediates transcriptional upregulation of iNOS and COX-2, two known mediators of IH-induced neuronal death in animal models²¹⁸.

NF- κ B

The transcription factor NF- κ B is the central regulator of inflammatory gene expression in innate immune cells. NF- κ B is rapidly activated in microglia in response to inflammatory stimuli and promotes pro- and anti-inflammatory gene transcription. NF- κ B activation is induced by inflammatory stimuli including PRR activation and via cytokines including TNF α and IL-1 β . NF- κ B is sequestered in the cytosol by I κ B. Activated I κ B kinase-beta (IKK β) phosphorylates I κ B and induces its degradation, freeing NF- κ B to translocate into the nucleus where it influences the expression of many inflammatory genes (Reviewed in reference 219). IKK β can be activated downstream of p38 or through MYD88-dependent TLR activation of TAK1¹⁴⁴. NF- κ B has long been known to be activated by hypoxia, although it was only recently that the link between hypoxia and NF- κ B was identified²²⁰. As PHDs negatively regulate HIF-1 α , they also negatively regulate IKK β targeting it for degradation. During hypoxia, when PHDs are inhibited, IKK β becomes activated and ultimately induces NF- κ B activation²²⁰. In addition, NF- κ B is necessary for the HIF-1 α protein to accumulate during hypoxia²²⁰, although the mechanisms involved in this are not fully understood. Thus, NF- κ B plays a central role in the hypoxic response, and indeed, without IKK β , HIF-1 α protein failed to accumulate in the cytosol in response to hypoxia and in bacterial-infected macrophages²²⁰.

NF- κ B is a common downstream regulator of microglial inflammatory gene expression induced by a number of stimuli¹⁰², and in cells where multiple hypoxia-sensitive transcription factors are expressed, NF- κ B can be preferentially activated, and the pattern of hypoxic exposure

is an important determinant in this. For example, in response to IH, NF- κ B is preferentially activated over HIF-1 α in vasculature^{221,222}, whereas sustained hypoxia increased HIF-1 α . In addition, cultured monocytes from OSA patients exhibit increased NF- κ B activity and pro-inflammatory gene expression^{221,223}, but not HIF-1 α . Lastly, there are also cell type-specific responses with regard to NF- κ B activation. HRO preferentially increases NF- κ B activities in microglia over astrocytes¹⁷⁵. Together, these studies suggest that IH-induced inflammatory gene expression is at least in part regulated by NF- κ B.

CREB

cAMP response element-binding proteins (CREB) are a family of transcription factors that bind DNA at cAMP response elements (CRE). CREB proteins localize to the nucleus and they become activated by phosphorylation by many serine threonine kinases including MAPKs^{186,209,224}. Activated CREB proteins associate with the transcriptional co-activator proteins CBP (CREB-binding protein) and p300 to promote gene transcription. During hypoxia, MAPK-dependent CREB activation occurs, although the mechanisms are not well defined. However, activation of CREB is associated with the increased transcription of cell-survival genes, and its activation promotes neuron survival during hypoxic/ischemic injury²²⁵. In microglia, CREB activation induces cell survival and anti-inflammatory pathways¹⁸⁶. CREB activation is downstream of many inflammatory cascades that induce ERK1/2 and/or JNK activation. In addition, P2Y1 receptor activation by ATP will induce phosphorylation of CREB, and our lab has previously shown that P2Y1 activation in microglia will down-regulate LPS-induced inflammation through a CREB-mediated pathway^{115,186,210}. CREB-mediated anti-inflammatory activity is hypothesized to occur through competitive inhibition of NF- κ B¹⁴⁹. Both the RelA subunit of NF- κ B and CREB require the co-activator CBP/p300 for full activation, thus

they compete with each other for the rate-limiting availability of CBP/p300²²⁶. In addition, CREB induces transcription of the anti-inflammatory cytokine IL-10²²⁷ which is another mechanism by which CREB can exert anti-inflammatory activities.

In the context of IH, phosphorylated CREB (p-CREB) is increased in the CA1 region of the hippocampus following 14 and 30 days of IH²²⁸. This time point corresponds with a reduction in neuronal apoptosis. Decreased p-CREB is observed at 1, 3, and 7 days of IH, consistent with peak neuronal death and poor performance on the Morris-water maze task in the rodent model. Although p-CREB co-localized with neurons within the CA1 region, there were also non-neuronal cells expressing p-CREB, but they were not identified. The exact role of p-CREB during IH, and cell-specific regulation of immune responses and neuronal survival are yet unknown.

Secreted molecules produced by microglia

Microglia release extracellular signaling molecules that bind specific receptors on surrounding cells and induce a physiological change. The response is highly dependent on the particular signaling molecule and activating receptor, and this response can be cell-type specific. These signaling molecules are traditionally characterized as pro-inflammatory, anti-inflammatory, trophic, or chemotactic. However, these categories are not mutually exclusive, and a single molecule can fit into multiple categories. We will briefly discuss the main classes of extracellular signaling molecules produced by microglia and their possible role in IH-mediated neurotoxicity/protection.

Cytokines and Chemokines

Cytokines are small (~5-20kD), secreted signaling molecules that can act on surrounding cells in an autocrine or paracrine fashion. These molecules can exert pro-inflammatory, anti-

inflammatory, and/or trophic effects. There are many families of cytokines which include: interleukins (ILs), interferons (IFNs), tumor necrosis factors (TNFs), colony stimulating factors (CSFs), and transforming growth factors (TGFs). Cytokines are typically classified as either pro- or anti-inflammatory. As previously discussed, OSA increases the circulating levels of several inflammatory cytokines including TNF α , IL-1, IL-6, IL-8, and IL-18, whereas OSA decreases the expression of the anti-inflammatory cytokine IL-10^{13,69,229}. Interestingly, in the CNS, low levels of cytokines that are traditionally classified as “pro-inflammatory” such as TNF α , IL-1 β , IL-18, and IL-6, are important neuromodulators that promote neurogenesis and synaptic plasticity²³⁰. However, these molecules become neurotoxic at high concentrations and are commonly associated with neuropathologic events/diseases. HRO induces the production of pro-inflammatory cytokines IL-1 β , IL-18, IL-6, TNF α and the chemokine MIP-2 in cultured microglial cells^{116,118,120–123,175,213}. Inflammatory cytokine and chemokine production is associated with increased infarct size, peripheral immune cell infiltration, and neurotoxicity following ischemic injury²³¹. It is yet unknown if cytokines contribute to IH-mediated neurotoxicity.

Inflammatory Enzymes

In addition to increasing the production and release of pro-inflammatory cytokines and chemokines following an inflammatory stimuli, microglia upregulate enzymes such as iNOS and COX-2 which catalyze the production of nitric oxide (NO) and prostaglandins, respectively. iNOS and COX-2 are both implicated in IH-induced neuropathology in animal models^{16,231}.

There are 3 nitric oxide synthase enzymes that produce NO in the CNS, the constitutively active nitric oxide synthase enzymes eNOS (endothelial) and nNOS (neuronal), and the inducible isoform (iNOS). A large number of studies have demonstrated the important functional role of

NO in normal neuronal functioning. Indeed, NO production through nNOS is necessary for a form of spinal motor plasticity induced by a therapeutic form of IH²³². However, when NO is produced in large amounts, it can induce nitration of proteins and cause lipid peroxidation²³³. In addition, NO can induce excitotoxicity-mediated neuronal death through NMDA receptor activation¹⁰⁴. While all NOS isoforms can contribute to neuropathologies associated with ischemic and neurodegenerative injuries²³⁴, iNOS is the primary source for large quantities of NO production during injury²³⁴. iNOS is the primary isoform expressed in innate immune cells, and its levels are rapidly upregulated in microglia following inflammatory stimulation to promote NO production at concentrations known to be neurotoxic. HRO induces iNOS in cultured microglial cells in a p38-dependent manner²¹³. While a large body of research from animal models demonstrates that microglia are the primary source of iNOS and NO in the CNS in response to LPS stimulation, it is unclear whether this is true of human microglia, as several studies have found that human microglia do not induce NO production following activation with LPS.

COX-2 is an inducible cyclooxygenase enzyme that is rapidly upregulated in microglial cells following activation by an inflammatory stimulus. COX2 catalyzes the production of prostaglandins which, like NO, are neurotoxic at high concentrations and are associated with increased neuropathology following ischemic injury and in neurodegenerative diseases²³⁴.

MICROGLIAL RESPONSES TO IH: FRIEND OF FOE?

Thus far we have primarily focused on the potential deleterious activities of microglia in IH-induced neuropathology. While dysregulation of microglial inflammatory processes are implicated in virtually every neuropathology, microglia also have neuroprotective capabilities. Indeed, selective ablation of microglia in a rodent model of ischemia (MCAO) exacerbated

infarct size, thus suggesting microglia have a supportive role and protective capabilities²³⁵. In addition, microglial production of brain derived neurotrophic factor (BDNF) has recently been shown to be necessary for hippocampal long-term potentiation and synaptic remodeling^{236,237}, a form of synaptic plasticity that correlates with learning and memory. While OSA/IH can cause neuronal injury and cognitive deficits, the extent of pathology is relatively minor compared to those of other neurodegenerative and ischemic injury. In addition, in the rat IH model, neuronal apoptosis peaks after 3-7 days of IH exposure and ceases by 14 days²³⁸. Interestingly, following 14 days of IH there is evidence of neuro-regeneration in that there are increases in the number of neuronal precursor cells present in the hippocampus^{239,240}. Little is known about the mechanisms underlying this switch from IH-induced neuronal degeneration to regeneration, or whether microglia activities contribute to this transition.

Chronic exposure to IH may induce long-term adaptive changes in microglia to promote their neurotrophic phenotype to combat the repeated exposures to IH. Of particular interest is the potential for epigenetic modifications which may modify cellular responses to a given stimulus by changing DNA methylation states, remodeling the chromatin, or promoting gene silencing via miRNA production. Research into epigenetic regulation of microglia is still in its infancy. However, chromatin changes facilitated by the jmj-C domain containing histone demethylase, JMJD3, have recently been shown to mediate the transition between microglia inflammatory and anti-inflammatory phenotypes^{241,242}. Interestingly, JMJD3 is one of many jmj-C domain containing histone demethylases that are hypoxia-sensitive enzymes, and that are upregulated by hypoxia²⁴³. These enzymes are interesting in the context of IH because they require molecular oxygen for their catalytic activity, and their expression is also increased by hypoxia, making JMJD3 in particular, an intriguing target in the context of IH because both hypoxia and

molecular oxygen are intermittently abundant. In addition, several miRNAs are known to down regulate TLR4-induced inflammation by targeting key adaptor and signaling proteins in the signaling cascade. While this is an exciting avenue of research, more work needs to be done in order to understand how/if epigenetic mechanisms play a role in acute or adaptive microglial responses to chronic IH exposure.

CONCLUDING REMARKS

Overall health is significantly impacted by OSA and many of the deleterious cardiovascular and metabolic effects correlate with increased systemic inflammation. Here, we discuss existing evidence supporting the notion that inflammation also underlies OSA/IH-mediated neuronal injury and cognitive deficits. We speculate that microglia become reactive following exposure to IH contributing to neuroinflammation that underlies the associated neuronal injury and cognitive deficits. We have proposed a model (depicted in Fig. 1) whereby IH can induce microglial inflammation through systemic inflammation, activation by DAMPs, and/or direct IH-induced oxidative stress. However, more studies need to be performed to elucidate the role of microglia in IH induced neuropathology. In this thesis, we begin to address some of these gaps in knowledge by first investigating purinergic modulation of microglial inflammatory responses to HRO (Chapter 2). We then describe our newly developed flow cytometry method for analyzing multiple CNS cells simultaneously while retaining the ability to retrieve nucleic acids from the fixed samples (Chapter 3), and which will be utilized in chapters 5 and 6. Chapter 4 is the foundation for all subsequent chapters as it details for the first time, microglial responses to IH across CNS regions and at multiple time points. In chapters 5 and 6, we start to investigate the molecular mechanisms underlying microglial pro-inflammatory responses to IH with a focus on TLR4 (Chapter 5) and JMJD3 (Chapter 6).

FIGURE 1

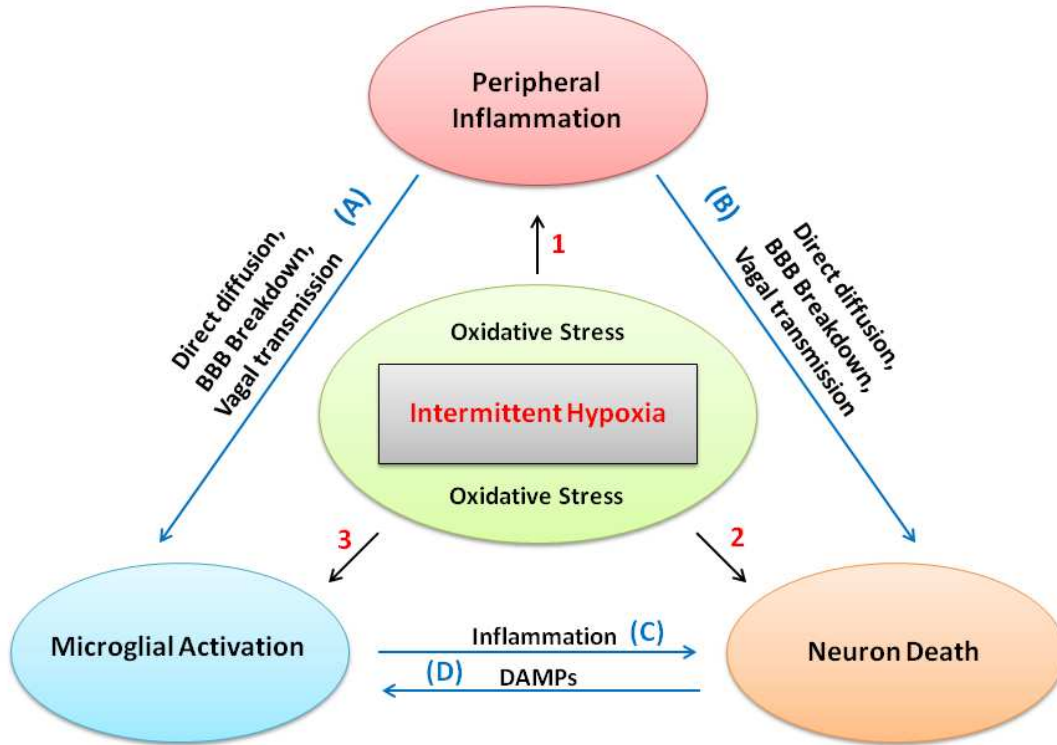


Figure 1 Legend***Schematic of potential inflammatory sources contributing to IH-associated neuropathology.***

Here we present a simplified schematic depicting the 3 central pathways that we hypothesize contribute to IH-induced inflammation and neuropathology (black arrows) and the potential cross-talk between these pathways (blue arrows). Through activation of oxidative stress pathways, IH induces 1) systemic inflammation, 2) neuronal injury, and 3) microglial inflammation. IH-induced peripheral inflammation promotes central inflammation through direct diffusion of inflammatory molecules across or breakdown of the blood brain barrier (BBB), and/or through activation of vagal neural afferents, all of which may promote microglial transition to a pro-inflammatory phenotype (A) and/or directly induce neuronal injury (B). Microglial production of pro-inflammatory/neurotoxic molecules induce neuronal injury/cell death (C). Damaged neurons release DAMPs into the extracellular space which can activate microglial inflammatory pathways through pattern recognition receptors (e.g. TLRs) or scavenger receptors (D).

FIGURE 2

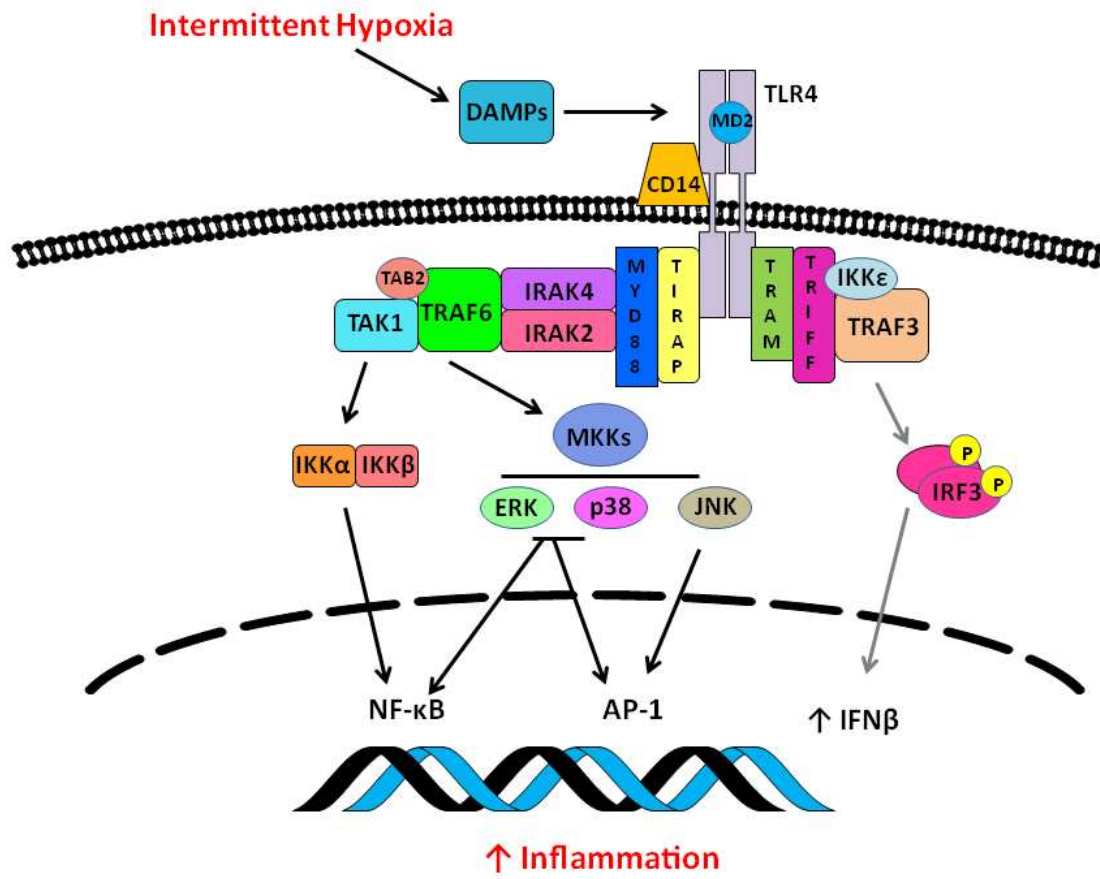


Figure 2 Legend***IH induced inflammation through TLR4 activation: model of TLR4 signaling cascade.***

Circulating endogenous TLR4 ligands are increased in the serum of patients with OSA and in the brain tissue of rodents exposed to IH (see main text reference information). Endogenous TLR4 ligands among the factors released from stressed/dying cells known as damage associated molecular patterns (DAMPs) that as ‘alarmins’ to alert surrounding immune cells of cellular damage. We hypothesize these DAMPs are released from peripheral and CNS cells in response to IH/OSA and induce inflammation through activation of TLR4. Here, we present a simplified diagram of the TLR4 signaling cascades. TLR4 signaling occurs through two different pathways: MYD88-dependent and TRIF-dependent. The MYD88-dependent pathway induces pro-inflammatory gene expression through activation of MAPKs and transcription factors such as NF- κ B and AP-1. The TRIF-dependent pathway induces phosphorylation of IRF3 which then translocates to the nucleus and induces expression of the neuroprotective cytokine, IFN β .

REFERENCES

1. Peppard, P. E., Young, T., Barnet, J. H., Palta, M., Hagen, E. W. & Hla, K. M. Increased prevalence of sleep-disordered breathing in adults. *American journal of epidemiology* **177**, 1006–1014 (2013).
2. Young, T., Palta, M., Dempsey, J., Skatrud, J., Weber, S. & Badr, S. The occurrence of sleep-disordered breathing among middle-aged adults. *New England Journal of Medicine* **328**, 1230–1235 (1993).
3. Kasai, T., Floras, J. S. & Bradley, T. D. Sleep Apnea and Cardiovascular Disease A Bidirectional Relationship. *Circulation* **126**, 1495–1510 (2012).
4. Redline, S. & Quan, S. F. Sleep Apnea: A Common Mechanism for the Deadly Triad—Cardiovascular Disease, Diabetes, and Cancer? *American journal of respiratory and critical care medicine* **186**, 123–124 (2012).
5. Pamidi, S., Aronsohn, R. S. & Tasali, E. Obstructive sleep apnea: role in the risk and severity of diabetes. *Best practice & research Clinical endocrinology & metabolism* **24**, 703–715 (2010).
6. Dempsey, J. A., Veasey, S. C., Morgan, B. J. & O'Donnell, C. P. Pathophysiology of sleep apnea. *Physiological reviews* **90**, 47–112 (2010).
7. Sawyer, A. M., Gooneratne, N. S., Marcus, C. L., Ofer, D., Richards, K. C. & Weaver, T. E. A systematic review of CPAP adherence across age groups: clinical and empiric insights for developing CPAP adherence interventions. *Sleep medicine reviews* **15**, 343–356 (2011).
8. Lumeng, C. N. & Saltiel, A. R. Inflammatory links between obesity and metabolic disease. *The Journal of clinical investigation* **121**, 2111 (2011).
9. Perry, V. H., Cunningham, C. & Holmes, C. Systemic infections and inflammation affect chronic neurodegeneration. *Nature Reviews Immunology* **7**, 161–167 (2007).
10. Epstein, F. H. & Ross, R. Atherosclerosis—an inflammatory disease. *New England journal of medicine* **340**, 115–126 (1999).
11. Selmi, C., Montano, N., Furlan, R., Keen, C. L. & Gershwin, M. E. Inflammation and oxidative stress in obstructive sleep apnea syndrome. *Experimental biology and medicine* **232**, 1409–1413 (2007).
12. Kasasbeh, E., Chi, D. S. & Krishnaswamy, G. Inflammatory aspects of sleep apnea and their cardiovascular consequences. *Southern medical journal* **99**, 58–67 (2006).

13. Lavie, L. & Polotsky, V. Cardiovascular aspects in obstructive sleep apnea syndrome-molecular issues, hypoxia and cytokine profiles. *Respiration* **78**, 361–370 (2009).
14. Amor, S., Puentes, F., Baker, D. & Van Der Valk, P. Inflammation in neurodegenerative diseases. *Immunology* **129**, 154–169 (2010).
15. Glass, C. K., Saijo, K., Winner, B., Marchetto, M. C. & Gage, F. H. Mechanisms underlying inflammation in neurodegeneration. *Cell* **140**, 918–934 (2010).
16. Li, R. C., Row, B. W., Gozal, E., Kheirandish, L., Fan, Q., Brittan, K. R., Guo, S. Z., Sachleben Jr, L. R. & Gozal, D. Cyclooxygenase 2 and intermittent hypoxia-induced spatial deficits in the rat. *American journal of respiratory and critical care medicine* **168**, 469 (2003).
17. Li, R. C., Row, B. W., Kheirandish, L., Brittan, K. R., Gozal, E., Guo, S. Z., Sachleben, L. R. & Gozal, D. Nitric oxide synthase and intermittent hypoxia-induced spatial learning deficits in the rat. *Neurobiol. Dis.* **17**, 44–53 (2004).
18. Patil, S. P., Schneider, H., Schwartz, A. R. & Smith, P. L. Adult obstructive sleep apneapathophysiology and diagnosis. *Chest Journal* **132**, 325–337 (2007).
19. Young, T., Peppard, P. E. & Gottlieb, D. J. Epidemiology of obstructive sleep apnea: a population health perspective. *American journal of respiratory and critical care medicine* **165**, 1217–1239 (2002).
20. Punjabi, N. M. in *Proceedings of the American Thoracic Society* **5**, 136 (2008).
21. Sforza, E. & Roche, F. Sleep apnea syndrome and cognition. *Frontiers in neurology* **3**, (2012).
22. Go, A. S., Mozaffarian, D., Roger, V. L., Benjamin, E. J., Berry, J. D., Blaha, M. J., Dai, S., Ford, E. S., Fox, C. S., Franco, S., Fullerton, H. J., Gillespie, C., Hailpern, S. M., Heit, J. A., Howard, V. J., Huffman, M. D., Judd, S. E., ... Turner, M. B. Heart disease and stroke statistics-2014 update: a report from the American Heart Association. *Circulation* **129**, e28–e292 (2014).
23. Malhotra, A. & White, D. P. Obstructive sleep apnoea. *The lancet* **360**, 237–245 (2002).
24. McArdle, N., Devereux, G., Heidarnejad, H., Engleman, H. M., Mackay, T. W. & Douglas, N. J. Long-term use of CPAP therapy for sleep apnea/hypopnea syndrome. *American Journal of Respiratory and Critical Care Medicine* **159**, 1108–1114 (1999).
25. Bhadriraju, S. & Collop, N. in *Essentials of Sleep Medicine* 143–153 (Springer, 2012).
26. Ferini-Strambi, L., Baietto, C., Di Gioia, M., Castaldi, P., Castronovo, C., Zucconi, M. & Cappa, S. Cognitive dysfunction in patients with obstructive sleep apnea (OSA): partial

- reversibility after continuous positive airway pressure (CPAP). *Brain research bulletin* **61**, 87–92 (2003).
27. Macey, P. M. Is brain injury in obstructive sleep apnea reversible. *Sleep* **35**, 9–10 (2012).
 28. Friedman, M., Wilson, M., Lin, H.-C. & Chang, H.-W. Updated systematic review of tonsillectomy and adenoidectomy for treatment of pediatric obstructive sleep apnea/hypopnea syndrome. *Otolaryngology-Head and Neck Surgery* **140**, 800–808 (2009).
 29. Brietzke, S. E. & Gallagher, D. The effectiveness of tonsillectomy and adenoidectomy in the treatment of pediatric obstructive sleep apnea/hypopnea syndrome: a meta-analysis. *Otolaryngology-Head and Neck Surgery* **134**, 979–984 (2006).
 30. Tauman, R., Gulliver, T. E., Krishna, J., Montgomery-Downs, H. E., O'Brien, L. M., Ivanenko, A. & Gozal, D. Persistence of obstructive sleep apnea syndrome in children after adenotonsillectomy. *The Journal of pediatrics* **149**, 803–808 (2006).
 31. Yang, I. V. Sleep, Immunology, and Epigenetics: Tip of an Iceberg. *American journal of respiratory and critical care medicine* **185**, 243–245 (2012).
 32. Cholidou, K. G., Kostakis, I. D., Manali, E. D., Perrea, D., Margeli, A., Vougas, K., Markozannes, E., Koulouris, N. & Alchanatis, M. Calprotectin: A protein related to cardiovascular risk in adult patients with obstructive sleep apnea. *Cytokine* **61**, 917–923 (2013).
 33. Marcus, C. L. Obstructive sleep apnea syndrome: differences between children and adults. *Sleep* **23**, S140 (2000).
 34. Capdevila, O. S., Kheirandish-Gozal, L., Dayyat, E. & Gozal, D. Pediatric obstructive sleep apnea: complications, management, and long-term outcomes. *Proceedings of the American Thoracic Society* **5**, 274 (2008).
 35. Beebe, W. Neurobehavioral morbidity associated with disordered breathing during sleep in children: a comprehensive review. *SLEEP-NEW YORK THEN WESTCHESTER*- **29**, 1115 (2006).
 36. Colt, H. G., Haas, H. & Rich, G. Hypoxemia vs sleep fragmentation as cause of excessive daytime sleepiness in obstructive sleep apnea. *CHEST Journal* **100**, 1542–1548 (1991).
 37. Barnes, M., McEvoy, R. D., Banks, S., Tarquinio, N., Murray, C. G., Vowles, N. & Pierce, R. J. Efficacy of positive airway pressure and oral appliance in mild to moderate obstructive sleep apnea. *American journal of respiratory and critical care medicine* **170**, 656–664 (2004).

38. Bucks, R. S., Olaithe, M. & Eastwood, P. Neurocognitive function in obstructive sleep apnoea: A meta-review. *Respirology* **18**, 61–70 (2013).
39. Beebe, D. W., Groesz, L., Wells, C., Nichols, A. & McGee, K. The neuropsychological effects of obstructive sleep apnea: a meta-analysis of norm-referenced and case-controlled data. *SLEEP-NEW YORK THEN WESTCHESTER* **26**, 298–307 (2003).
40. El-Ad, B. & Lavie, P. Effect of sleep apnea on cognition and mood. *International Review of Psychiatry* **17**, 277–282 (2005).
41. Alchanatis, M., Deligiorgis, N., Zias, N., Amfilochiou, A., Gotsis, E., Karakatsani, A. & Papadimitriou, A. Frontal brain lobe impairment in obstructive sleep apnoea: a proton MR spectroscopy study. *European Respiratory Journal* **24**, 980–986 (2004).
42. Joo, E. Y., Tae, W. S., Lee, M. J., Kang, J. W., Park, H. S., Lee, J. Y., Suh, M. & Hong, S. B. Reduced brain gray matter concentration in patients with obstructive sleep apnea syndrome. *Sleep* **33**, 235 (2010).
43. Zimmerman, M. E. & Aloia, M. S. A review of neuroimaging in obstructive sleep apnea. *J Clin Sleep Med* **2**, 461–471 (2006).
44. Macey, P. M., Henderson, L. A., Macey, K. E., Alger, J. R., Frysinger, R. C., Woo, M. A., Harper, R. K., Yan-Go, F. L. & Harper, R. M. Brain morphology associated with obstructive sleep apnea. *American journal of respiratory and critical care medicine* **166**, 1382–1387 (2002).
45. Sarchielli, P., Presciutti, O., Alberti, A., Tarducci, R., Gobbi, G., Galletti, F., Costa, C., Eusebi, P. & Calabresi, P. A 1H magnetic resonance spectroscopy study in patients with obstructive sleep apnea. *European Journal of Neurology* **15**, 1058–1064 (2008).
46. Yaouhi, K., Bertran, F., Clochon, P., Mézenge, F., Denise, P., Foret, J., Eustache, F. & Desgranges, B. A combined neuropsychological and brain imaging study of obstructive sleep apnea. *Journal of sleep research* **18**, 36–48 (2009).
47. Pae, E. K., Chien, P. & Harper, R. M. Intermittent hypoxia damages cerebellar cortex and deep nuclei. *Neuroscience letters* **375**, 123–128 (2005).
48. O'Donoghue, F. J., Wellard, R. M., Rochford, P. D., Dawson, A., Barnes, M., Ruehland, W. R., Jackson, M. L., Howard, M. E., Pierce, R. J. & Jackson, G. D. Magnetic resonance spectroscopy and neurocognitive dysfunction in obstructive sleep apnea before and after CPAP treatment. *Sleep* **35**, 41–48 (2012).
49. O'Donoghue, F. J., Briellmann, R. S., Rochford, P. D., Abbott, D. F., Pell, G. S., Chan, C. H. P., Tarquinio, N., Jackson, G. D. & Pierce, R. J. Cerebral structural changes in severe obstructive sleep apnea. *American journal of respiratory and critical care medicine* **171**,

- 1185–1190 (2005).
50. Torelli, F., Moscufo, N., Garreffa, G., Placidi, F., Romigi, A., Zannino, S., Bozzali, M., Fasano, F., Giulietti, G., Djonlagic, I., Malhotra, A., Marciani, M. G. & Guttmann, C. R. G. Cognitive profile and brain morphological changes in obstructive sleep apnea. *Neuroimage* **54**, 787–93 (2011).
 51. Row, B. W. in *Hypoxia and the Circulation* 51–67 (Springer, 2007).
 52. Squire, R. F., Noudoost, B., Schafer, R. J. & Moore, T. Prefrontal contributions to visual selective attention. *Annual review of neuroscience* **36**, 451–466 (2013).
 53. Jackson, M. L., Howard, M. E. & Barnes, M. Cognition and daytime functioning in sleep-related breathing disorders. *Progress in brain research* **190**, 53–68 (2011).
 54. Kim, H. C., Young, T., Matthews, C. G., Weber, S. M., Woodard, A. R. & Palta, M. Sleep-disordered breathing and neuropsychological deficits: a population-based study. *American journal of respiratory and critical care medicine* **156**, 1813–1819 (1997).
 55. Gosselin, N., Mathieu, A., Mazza, S., Décary, A., Malo, J. & Montplaisir, J. Deficits in involuntary attention switching in obstructive sleep apnea syndrome. *Neuroscience letters* **408**, 73–78 (2006).
 56. Twigg, G. L., Papaioannou, I., Jackson, M., Ghiassi, R., Shaikh, Z., Jaye, J., Graham, K. S., Simonds, A. K. & Morrell, M. J. Obstructive sleep apnea syndrome is associated with deficits in verbal but not visual memory. *American journal of respiratory and critical care medicine* **182**, 98 (2010).
 57. Naëgelé, B., Launois, S. H., Mazza, S., Feuerstein, C., Pépin, J.-L. & Lévy, P. Which memory processes are affected in patients with obstructive sleep apnea? An evaluation of 3 types of memory. *Sleep* **29**, 533–44 (2006).
 58. Saunamäki, T. & Jehkonen, M. A review of executive functions in obstructive sleep apnea syndrome. *Acta neurologica scandinavica* **115**, 1–11 (2007).
 59. Thomas, R. J., Rosen, B. R., Stern, C. E., Weiss, J. W. & Kwong, K. K. Functional imaging of working memory in obstructive sleep-disordered breathing. *Journal of Applied Physiology* **98**, 2226–2234 (2005).
 60. Findley, L., Unverzagt, M., Guchu, R., Fabrizio, M., Buckner, J. & Suratt, P. Vigilance and automobile accidents in patients with sleep apnea or narcolepsy. *CHEST Journal* **108**, 619–624 (1995).
 61. Bliwise, D. L. Sleep disorders in Alzheimer’s disease and other dementias. *Clinical Cornerstone* **6**, S16–S28 (2004).

62. Comella, C. L. Sleep disorders in Parkinson's disease: an overview. *Movement Disorders* **22**, S367–S373 (2007).
63. Zoccolella, S., Savarese, M., Lamberti, P., Manni, R., Pacchetti, C. & Logroscino, G. Sleep disorders and the natural history of Parkinson's disease: the contribution of epidemiological studies. *Sleep medicine reviews* **15**, 41–50 (2011).
64. Marcus, C. L., Keens, T. G., Bautista, D. B., von Pechmann, W. S. & Ward, S. L. D. Obstructive sleep apnea in children with Down syndrome. *Pediatrics* **88**, 132–139 (1991).
65. Morcos, Z. & Phadke, J. Re: Kaneko Y, Hajek VE, Zivanovic V et al. Relationship of sleep apnea to functional capacity and length of hospitalization following stroke. SLEEP 2003;26(3):293-7. *Sleep* **26**, 761; author reply 762 (2003).
66. Redline, S., Yenokyan, G., Gottlieb, D. J., Shahar, E., O'Connor, G. T., Resnick, H. E., Diener-West, M., Sanders, M. H., Wolf, P. A., Geraghty, E. M., Tauqeer, A., Lebowitz, M. & Punjabi, N. M. Obstructive sleep apnea-hypopnea and incident stroke: the sleep heart health study. *American journal of respiratory and critical care medicine* **182**, 269 (2010).
67. Ancoli-Israel, S., Palmer, B. W., Cooke, J. R., Corey-Bloom, J., Fiorentino, L., Natarajan, L., Liu, L., Ayalon, L., He, F. & Loreda, J. S. Cognitive effects of treating obstructive sleep apnea in Alzheimer's disease: a randomized controlled study. *Journal of the American Geriatrics Society* **56**, 2076–2081 (2008).
68. McNicholas, W. T. Obstructive sleep apnea and inflammation. *Progress in cardiovascular diseases* **51**, 392–399 (2009).
69. Ryan, S., Taylor, C. & McNicholas, W. Systemic inflammation: a key factor in the pathogenesis of cardiovascular complications in obstructive sleep apnoea syndrome? *Thorax* **64**, 631–636 (2009).
70. Goldbart, A. D. & Tal, A. Inflammation and Sleep Disordered Breathing in Children: A State-of-the-Art Review. *Pediatric pulmonology* **43**, 1151–1160 (2008).
71. Tasali, E. & Ip, M. S. Obstructive sleep apnea and metabolic syndrome: alterations in glucose metabolism and inflammation. *Proceedings of the American Thoracic Society* **5**, 207–217 (2008).
72. Haensel, A., Bardwell, W. A., Mills, P. J., Loreda, J. S., Ancoli-Israel, S., Morgan, E. E., Heaton, R. K. & Dimsdale, J. E. Relationship between inflammation and cognitive function in obstructive sleep apnea. *Sleep and Breathing* **13**, 35–41 (2009).
73. Reyad, E., Abdelaty, N. M., Prince, M. E., Farid, A. & El-Serougy, M. K. Plasma levels of TNF in obstructive sleep apnea syndrome (OSA) before and after surgical intervention. *Egyptian Journal of Chest Diseases and Tuberculosis* **61**, 179–185 (2012).

74. Ursava\cs, A., Karada\ug, M., Rodoplu, E., Y\ilmaztepe, A., Oral, H. B. & G□zü, R. O. Circulating ICAM-1 and VCAM-1 levels in patients with obstructive sleep apnea syndrome. *Respiration* **74**, 525–532 (2006).
75. Lindberg, E., Svensson, M., Venge, P. & Janson, C. Relationship Between Sleep-disordered Breathing And Markers Of Systemic Inflammation In Women From The General Population. *American Journal of Respiratory and Critical Care Medicine* **181**, A2476 (2010).
76. Dyugovskaya, L., Lavie, P. & Lavie, L. Phenotypic and functional characterization of blood $\gamma\delta$ T cells in sleep apnea. *American journal of respiratory and critical care medicine* **168**, 242–249 (2003).
77. Yaffe, K., Kanaya, A., Lindquist, K., Simonsick, E. M., Harris, T., Shorr, R. I., Tylavsky, F. A. & Newman, A. B. The metabolic syndrome, inflammation, and risk of cognitive decline. *Jama* **292**, 2237–2242 (2004).
78. Hotamisligil, G. S. Inflammation and metabolic disorders. *Nature* **444**, 860–867 (2006).
79. Yarchoan, M., Xie, S. X., Kling, M. A., Toledo, J. B., Wolk, D. A., Lee, E. B., Van Deerlin, V., Lee, V. M.-Y., Trojanowski, J. Q. & Arnold, S. E. Cerebrovascular atherosclerosis correlates with Alzheimer pathology in neurodegenerative dementias. *Brain* **135**, 3749–3756 (2012).
80. Kamba, M., Inoue, Y., Higami, S., Suto, Y., Ogawa, T. & Chen, W. Cerebral metabolic impairment in patients with obstructive sleep apnoea: an independent association of obstructive sleep apnoea with white matter change. *Journal of Neurology, Neurosurgery \& Psychiatry* **71**, 334–339 (2001).
81. Erecinska, M. & Silver, I. A. Tissue oxygen tension and brain sensitivity to hypoxia. *Respiration physiology* **128**, 263–276 (2001).
82. Peppard, P. E., Szklo-Coxe, M., Hla, K. M. & Young, T. Longitudinal association of sleep-related breathing disorder and depression. *Archives of internal medicine* **166**, 1709–1715 (2006).
83. Raison, C. L., Capuron, L. & Miller, A. H. Cytokines sing the blues: inflammation and the pathogenesis of depression. *Trends in immunology* **27**, 24–31 (2006).
84. Nácher, M., Farré, R., Montserrat, J. M., Torres, M., Navajas, D., Bulbena, O. & Serrano-Mollar, A. Biological consequences of oxygen desaturation and respiratory effort in an acute animal model of obstructive sleep apnea (OSA). *Sleep medicine* **10**, 892–897 (2009).
85. Drager, L. F., Jun, J. C. & Polotsky, V. Y. Metabolic consequences of intermittent hypoxia: relevance to obstructive sleep apnea. *Best Practice \& Research Clinical Endocrinology \&*

- Metabolism* **24**, 843–851 (2010).
86. Dematteis, M., Godin-Ribuot, D., Arnaud, C., Ribuot, C., Stanke-Labesque, F., Pépin, J.-L. & Lévy, P. Cardiovascular consequences of sleep-disordered breathing: contribution of animal models to understanding of the human disease. *ILAR journal* **50**, 262–281 (2009).
 87. Neubauer, J. A. Invited review: Physiological and pathophysiological responses to intermittent hypoxia. *Journal of applied physiology* **90**, 1593 (2001).
 88. Vinit, S., Lovett-Barr, M. R. & Mitchell, G. S. Intermittent hypoxia induces functional recovery following cervical spinal injury. *Respiratory physiology & neurobiology* **169**, 210–217 (2009).
 89. Dale-Nagle, E. A., Hoffman, M. S., MacFarlane, P. M., Satriotomo, I., Lovett-Barr, M. R., Vinit, S. & Mitchell, G. S. Spinal plasticity following intermittent hypoxia: implications for spinal injury. *Annals of the New York Academy of Sciences* **1198**, 252–259 (2010).
 90. Trumbower, R. D., Jayaraman, A., Mitchell, G. S. & Rymer, W. Z. Exposure to acute intermittent hypoxia augments somatic motor function in humans with incomplete spinal cord injury. *Neurorehabilitation and neural repair* **26**, 163–172 (2012).
 91. Gozal, D., Daniel, J. M. & Dohanich, G. P. Behavioral and anatomical correlates of chronic episodic hypoxia during sleep in the rat. *The Journal of Neuroscience* **21**, 2442 (2001).
 92. Xu, W., Chi, L., Row, B., Xu, R., Ke, Y., Xu, B., Luo, C., Kheirandish, L., Gozal, D. & Liu, R. Increased oxidative stress is associated with chronic intermittent hypoxia-mediated brain cortical neuronal cell apoptosis in a mouse model of sleep apnea. *Neuroscience* **126**, 313–323 (2004).
 93. Row, B. W., Liu, R., Xu, W., Kheirandish, L. & Gozal, D. Intermittent hypoxia is associated with oxidative stress and spatial learning deficits in the rat. *American journal of respiratory and critical care medicine* **167**, 1548–1553 (2003).
 94. Gozal, E., Gozal, D., Pierce, W. M., Thongboonkerd, V., Scherzer, J. A., R Sachleben Jr, L., Brittan, K. R., Guo, S. Z., Cai, J. & Klein, J. B. Proteomic analysis of CA1 and CA3 regions of rat hippocampus and differential susceptibility to intermittent hypoxia. *Journal of neurochemistry* **83**, 331–345 (2002).
 95. Burckhardt, I. C., Gozal, D., Dayyat, E., Cheng, Y., Li, R. C., Goldbart, A. D. & Row, B. W. Green tea catechin polyphenols attenuate behavioral and oxidative responses to intermittent hypoxia. *American journal of respiratory and critical care medicine* **177**, 1135 (2008).
 96. Hui-guo, L., Kui, L., Yan-ning, Z. & Yong-jian, X. Apocynin attenuate spatial learning deficits and oxidative responses to intermittent hypoxia. *Sleep medicine* **11**, 205–212

- (2010).
97. Nair, D., Dayyat, E. A., Zhang, S. X., Wang, Y. & Gozal, D. Intermittent hypoxia-induced cognitive deficits are mediated by NADPH oxidase activity in a murine model of sleep apnea. *PLoS One* **6**, e19847 (2011).
 98. Zhan, G., Fenik, P., Pratico, D. & Veasey, S. C. Inducible nitric oxide synthase in long-term intermittent hypoxia: hypersomnolence and brain injury. *American journal of respiratory and critical care medicine* **171**, 1414 (2005).
 99. Zhan, G., Serrano, F., Fenik, P., Hsu, R., Kong, L., Pratico, D., Klann, E. & Veasey, S. C. NADPH oxidase mediates hypersomnolence and brain oxidative injury in a murine model of sleep apnea. *American journal of respiratory and critical care medicine* **172**, 921–929 (2005).
 100. Li, C. & Jackson, R. M. Reactive species mechanisms of cellular hypoxia-reoxygenation injury. *American Journal of Physiology-Cell Physiology* **282**, C227–C241 (2002).
 101. Gao, H.-M., Zhou, H. & Hong, J.-S. NADPH oxidases: novel therapeutic targets for neurodegenerative diseases. *Trends in pharmacological sciences* **33**, 295–303 (2012).
 102. Block, M. L., Zecca, L. & Hong, J.-S. Microglia-mediated neurotoxicity: uncovering the molecular mechanisms. *Nature Reviews Neuroscience* **8**, 57–69 (2007).
 103. Luskin, M. B. Neuronal cell lineage in the vertebrate central nervous system. *The FASEB journal* **8**, 722 (1994).
 104. Cazevielle, C., Muller, A., Meynier, F. & Bonne, C. Superoxide and nitric oxide cooperation in hypoxia/reoxygenation-induced neuron injury. *Free Radical Biology and Medicine* **14**, 389–395 (1993).
 105. Frøyland, E., Skjæret, C., Wright, M. S., Dalen, M. L., Cvancarova, M., Kasi, C. & Rootwelt, T. Inflammatory receptors and pathways in human NT2-N neurons during hypoxia and reoxygenation. Impact of acidosis. *Brain research* **1217**, 37–49 (2008).
 106. Wang, D. D. & Bordey, A. The astrocyte odyssey. *Progress in neurobiology* **86**, 342–367 (2008).
 107. Aviles-Reyes, R. X., Angelo, M. F., Villarreal, A., Rios, H., Lazarowski, A. & Ramos, A. J. Intermittent hypoxia during sleep induces reactive gliosis and limited neuronal death in rats: implications for sleep apnea. *Journal of neurochemistry* **112**, 854–869 (2010).
 108. Maeda, Y., Matsumoto, M., Hori, O., Kuwabara, K., Ogawa, S., Yan, S. D., Ohtsuki, T., Kinoshita, T., Kamada, T. & Stern, D. M. Hypoxia/reoxygenation-mediated induction of astrocyte interleukin 6: a paracrine mechanism potentially enhancing neuron survival. *The*

- Journal of experimental medicine* **180**, 2297–2308 (1994).
109. Koehler, R. C., Roman, R. J. & Harder, D. R. Astrocytes and the regulation of cerebral blood flow. *Trends in neurosciences* **32**, 160–169 (2009).
 110. Kanaan, A., Farahani, R., Douglas, R. M., LaManna, J. C. & Haddad, G. G. Effect of chronic continuous or intermittent hypoxia and reoxygenation on cerebral capillary density and myelination. *American Journal of Physiology-Regulatory, Integrative and Comparative Physiology* **290**, R1105–R1114 (2006).
 111. Lim, D. C. & Pack, A. I. Obstructive sleep apnea and cognitive impairment: Addressing the blood-brain barrier. *Sleep medicine reviews* **18**, 35–48 (2014).
 112. Baumann, N. & Pham-Dinh, D. Biology of oligodendrocyte and myelin in the mammalian central nervous system. *Physiological reviews* **81**, 871–928 (2001).
 113. Macey, P. M., Kumar, R., Woo, M. A., Valladares, E. M., Yan-Go, F. L. & Harper, R. M. Brain structural changes in obstructive sleep apnea. *Sleep* **31**, 967 (2008).
 114. Cai, J., Tuong, C. M., Zhang, Y., Shields, C. B., Guo, G., Fu, H. & Gozal, D. Mouse intermittent hypoxia mimicking apnoea of prematurity: effects on myelinogenesis and axonal maturation. *The Journal of pathology* **226**, 495–508 (2012).
 115. Kettenmann, H., Hanisch, U.-K., Noda, M. & Verkhratsky, A. Physiology of microglia. *Physiological reviews* **91**, 461–553 (2011).
 116. Wang, J. & Wang, J. Hypoxia/Reoxygenation induces nitric oxide and TNF-alpha release from cultured microglia but not astrocytes of the rat. *Chinese Journal of Physiology* **50**, 127 (2007).
 117. Vogt, M., Bauer, M. K., Ferrari, D. & Schulze-Osthoff, K. Oxidative stress and hypoxia/reoxygenation trigger CD95 (APO-1/Fas) ligand expression in microglial cells. *FEBS letters* **429**, 67–72 (1998).
 118. Wang, J.-Y., Shum, A. Y., Chao, C. C., Kuo, J. S. & Wang, J.-Y. Production of macrophage inflammatory protein-2 following hypoxia/reoxygenation in glial cells. *Glia* **32**, 155–164 (2000).
 119. Spranger, M., Kiprianova, I., Krempien, S. & Schwab, S. Reoxygenation increases the release of reactive oxygen intermediates in murine microglia. *Journal of Cerebral Blood Flow & Metabolism* **18**, 670–674 (1998).
 120. Lai, A. Y. & Todd, K. G. Hypoxia-activated microglial mediators of neuronal survival are differentially regulated by tetracyclines. *Glia* **53**, 809–816 (2006).

121. Kim, N. G., Lee, H., Son, E., Kwon, O. Y., Park, J. Y., Park, J. H., Jae Cho, G., Sung Choi, W. & Suk, K. Hypoxic induction of caspase-11/caspase-1/interleukin-1 [beta] in brain microglia. *Molecular brain research* **114**, 107–114 (2003).
122. Lu, D.-Y., Liou, H.-C., Tang, C.-H. & Fu, W.-M. Hypoxia-induced iNOS expression in microglia is regulated by the PI3-kinase/Akt/mTOR signaling pathway and activation of hypoxia inducible factor-1 α . *Biochemical pharmacology* **72**, 992–1000 (2006).
123. Suk, K. Minocycline suppresses hypoxic activation of rodent microglia in culture. *Neuroscience letters* **366**, 167–171 (2004).
124. Pineau, I. & Lacroix, S. Endogenous signals initiating inflammation in the injured nervous system. *Glia* **57**, 351–361 (2009).
125. Ransohoff, R. M. & Perry, V. H. Microglial physiology: unique stimuli, specialized responses. *Annual review of immunology* **27**, 119–145 (2009).
126. Olah, M., Biber, K., Vinet, J. & WGM Boddeke, H. Microglia phenotype diversity. *Cns+ Neurological Disorders-Drug Targets* **10**, 108 (2011).
127. Crain, J. M., Nikodemova, M. & Watters, J. J. Microglia express distinct M1 and M2 phenotypic markers in the postnatal and adult central nervous system in male and female mice. *Journal of neuroscience research* **91**, 1143–1151 (2013).
128. Crain, J. M., Nikodemova, M. & Watters, J. J. Expression of P2 nucleotide receptors varies with age and sex in murine brain microglia. *J Neuroinflammation* **6**, 24 (2009).
129. Hanisch, U. K. & Kettenmann, H. Microglia: active sensor and versatile effector cells in the normal and pathologic brain. *Nature neuroscience* **10**, 1387–1394 (2007).
130. Pickering, M. & O'Connor, J. J. Pro-inflammatory cytokines and their effects in the dentate gyrus. *Progress in brain research* **163**, 339–354 (2007).
131. Schafers, M. & Sorkin, L. Effect of cytokines on neuronal excitability. *Neuroscience letters* **437**, 188–193 (2008).
132. Wilson, C. J., Finch, C. E. & Cohen, H. J. Cytokines and cognition—the case for a head-to-toe inflammatory paradigm. *Journal of the American Geriatrics Society* **50**, 2041–2056 (2002).
133. Konsman, J. P., Parnet, P. & Dantzer, R. Cytokine-induced sickness behaviour: mechanisms and implications. *Trends in neurosciences* **25**, 154–159 (2002).
134. Ek, M., Engblom, D., Saha, S., Blomqvist, A., Jakobsson, P.-J. & Ericsson-Dahlstrand, A. Inflammatory response: pathway across the blood-brain barrier. *Nature* **410**, 430–431

- (2001).
135. Bluthe, R.-M., Michaud, B., Kelley, K. W. & Dantzer, R. Vagotomy attenuates behavioural effects of interleukin-1 injected peripherally but not centrally. *Neuroreport* **7**, 1485–1488 (1996).
 136. Laye, S., Bluthe, R.-M., Kent, S., Combe, C., Medina, C., Parnet, P., Kelley, K. & Dantzer, R. Subdiaphragmatic vagotomy blocks induction of IL-1 beta mRNA in mice brain in response to peripheral LPS. *American Journal of Physiology-Regulatory, Integrative and Comparative Physiology* **268**, R1327–R1331 (1995).
 137. Kawai, T. & Akira, S. The roles of TLRs, RLRs and NLRs in pathogen recognition ARTICLE. *International immunology* **21**, 317–337 (2009).
 138. Carty, M. & Bowie, A. G. Evaluating the role of Toll-like receptors in diseases of the central nervous system. *Biochemical pharmacology* **81**, 825–837 (2011).
 139. Akira, S. & Takeda, K. Toll-like receptor signalling. *Nature Reviews Immunology* **4**, 499–511 (2004).
 140. O’Neill, L. A. J. The interleukin-1 receptor/Toll-like receptor superfamily: 10 years of progress. *Immunological reviews* **226**, 10–18 (2008).
 141. Kawai, T. & Akira, S. The role of pattern-recognition receptors in innate immunity: update on Toll-like receptors. *Nature immunology* **11**, 373–384 (2010).
 142. Hellwig-Bürgel, T., Stiehl, D. P., Wagner, A. E., Metzen, E. & Jelkmann, W. Review: hypoxia-inducible factor-1 (HIF-1): a novel transcription factor in immune reactions. *Journal of interferon & cytokine research* **25**, 297–310 (2005).
 143. Lu, Y. C., Yeh, W. C. & Ohashi, P. S. LPS/TLR4 signal transduction pathway. *Cytokine* **42**, 145–151 (2008).
 144. Doyle, S. L. & O’Neill, L. A. Toll-like receptors: from the discovery of NF κ B to new insights into transcriptional regulations in innate immunity. *Biochemical pharmacology* **72**, 1102–1113 (2006).
 145. Zughhaier, S. M., Zimmer, S. M., Datta, A., Carlson, R. W. & Stephens, D. S. Differential induction of the toll-like receptor 4-MyD88-dependent and-independent signaling pathways by endotoxins. *Infection and immunity* **73**, 2940–2950 (2005).
 146. Kagan, J. C., Su, T., Horng, T., Chow, A., Akira, S. & Medzhitov, R. TRAM couples endocytosis of Toll-like receptor 4 to the induction of interferon- β . *Nature immunology* **9**, 361–368 (2008).

147. Takeuchi, O. & Akira, S. Pattern recognition receptors and inflammation. *Cell* **140**, 805–820 (2010).
148. Olson, J. K. & Miller, S. D. Microglia initiate central nervous system innate and adaptive immune responses through multiple TLRs. *The Journal of Immunology* **173**, 3916–3924 (2004).
149. Okun, E., Griffioen, K. J. & Mattson, M. P. Toll-like receptor signaling in neural plasticity and disease. *Trends in neurosciences* (2011).
150. Akinnusi, M., Jaoude, P., Kufel, T. & El-Solh, A. A. Toll-like receptor activity in patients with obstructive sleep apnea. *Sleep and Breathing* **17**, 1009–1016 (2013).
151. Kim, S. Y., Choi, Y. J., Joung, S. M., Lee, B. H., Jung, Y. S. & Lee, J. Y. Hypoxic stress up-regulates the expression of Toll-like receptor 4 in macrophages via hypoxia-inducible factor. *Immunology* **129**, 516–524 (2010).
152. Kuhlicke, J., Frick, J. S., Morote-Garcia, J. C., Rosenberger, P. & Eltzschig, H. K. Hypoxia inducible factor (HIF)-1 coordinates induction of Toll-like receptors TLR2 and TLR6 during hypoxia. *PLoS One* **2**, e1364 (2007).
153. Kim, J., Bhattacharjee, R., Dayyat, E., Snow, A. B., Kheirandish-Gozal, L., Goldman, J. L., Li, R. C., Serpero, L. D., Clair, H. B. & Gozal, D. Increased cellular proliferation and inflammatory cytokines in tonsils derived from children with obstructive sleep apnea. *Pediatric research* **66**, 423–428 (2009).
154. Wu, K.-M., Lin, C.-C., Chiu, C.-H. & Liaw, S.-F. Effect of treatment by nasal continuous positive airway pressure on serum high mobility group box-1 protein in obstructive sleep apnea. *CHEST Journal* **137**, 303–309 (2010).
155. Kim, J., Bhattacharjee, R., Snow, A., Capdevila, O., Kheirandish-Gozal, L. & Gozal, D. Myeloid-related protein 8/14 levels in children with obstructive sleep apnoea. *European Respiratory Journal* **35**, 843–850 (2010).
156. Wessendorf, T. E., Thilman, A. F., Wang, Y.-M., Schreiber, A., Konietzko, N. & Teschler, H. Fibrinogen levels and obstructive sleep apnea in ischemic stroke. *American journal of respiratory and critical care medicine* **162**, 2039–2042 (2000).
157. Chin, K., Ohi, M., Kita, H., Noguchi, T., Otsuka, N., Tsuboi, T., Mishima, M. & Kuno, K. Effects of NCPAP therapy on fibrinogen levels in obstructive sleep apnea syndrome. *American journal of respiratory and critical care medicine* **153**, 1972–1976 (1996).
158. Saletu, M., Nosiska, D., Kapfhammer, G., Laluschek, W., Saletu, B., Benesch, T. & Zeitlhofer, J. Structural and serum surrogate markers of cerebrovascular disease in obstructive sleep apnea (OSA). *Journal of neurology* **253**, 746–752 (2006).

159. Bhattacharjee, R., Kheirandish-Gozal, L., Pillar, G. & Gozal, D. Cardiovascular complications of obstructive sleep apnea syndrome: evidence from children. *Progress in cardiovascular diseases* **51**, 416–433 (2009).
160. Kizawa, T., Nakamura, Y., Takahashi, S., Sakurai, S., Yamauchi, K. & Inoue, H. Pathogenic role of angiotensin II and oxidised LDL in obstructive sleep apnoea. *European Respiratory Journal* **34**, 1390–1398 (2009).
161. Lavie, L., Dyugovskaya, L., GOLAN-SHANY, O. & Lavie, P. Heat-shock protein 70: expression in monocytes of patients with sleep apnoea and association with oxidative stress and tumour necrosis factor- α . *Journal of sleep research* **19**, 139–147 (2010).
162. Stewart, C. R., Stuart, L. M., Wilkinson, K., van Gils, J. M., Deng, J., Halle, A., Rayner, K. J., Boyer, L., Zhong, R., Frazier, W. A., Lacy-Hulbert, A., El Khoury, J., Golenbock, D. T. & Moore, K. J. CD36 ligands promote sterile inflammation through assembly of a Toll-like receptor 4 and 6 heterodimer. *Nat. Immunol.* **11**, 155–61 (2010).
163. Hanamsagar, R., Hanke, M. L. & Kielian, T. Toll-like receptor (TLR) and inflammasome actions in the central nervous system. *Trends in immunology* **33**, 333–342 (2012).
164. Lehnardt, S. Innate immunity and neuroinflammation in the CNS: The role of microglia in Toll-like receptor-mediated neuronal injury. *Glia* **58**, 253–263 (2010).
165. Lehnardt, S., Massillon, L., Follett, P., Jensen, F. E., Ratan, R., Rosenberg, P. A., Volpe, J. J. & Vartanian, T. Activation of innate immunity in the CNS triggers neurodegeneration through a Toll-like receptor 4-dependent pathway. *Proceedings of the National Academy of Sciences* **100**, 8514–8519 (2003).
166. Lehnardt, S., Schott, E., Trimbuch, T., Laubisch, D., Krueger, C., Wulczyn, G., Nitsch, R. & Weber, J. R. A vicious cycle involving release of heat shock protein 60 from injured cells and activation of toll-like receptor 4 mediates neurodegeneration in the CNS. *The Journal of Neuroscience* **28**, 2320 (2008).
167. Ziegler, G., Prinz, V., Albrecht, M. W., Harhausen, D., Khojasteh, U., Nacken, W., Endres, M., Dirnagl, U., Nietfeld, W. & Trendelenburg, G. Mrp-8 and-14 mediate CNS injury in focal cerebral ischemia. *Biochimica et Biophysica Acta (BBA)-Molecular Basis of Disease* **1792**, 1198–1204 (2009).
168. Gao, H. M., Zhou, H., Zhang, F., Wilson, B. C., Kam, W. & Hong, J. S. HMGB1 acts on microglia Mac1 to mediate chronic neuroinflammation that drives progressive neurodegeneration. *The Journal of Neuroscience* **31**, 1081–1092 (2011).
169. Kim, J.-B., Choi, J. S., Yu, Y.-M., Nam, K., Piao, C.-S., Kim, S.-W., Lee, M.-H., Han, P.-L., Park, J. & Lee, J.-K. HMGB1, a novel cytokine-like mediator linking acute neuronal death and delayed neuroinflammation in the postischemic brain. *The Journal of*

- neuroscience* **26**, 6413–6421 (2006).
170. Faraco, G., Fossati, S., Bianchi, M., Patrone, M., Pedrazzi, M., Sparatore, B., Moroni, F. & Chiarugi, A. High mobility group box 1 protein is released by neural cells upon different stresses and worsens ischemic neurodegeneration in vitro and in vivo. *Journal of neurochemistry* **103**, 590–603 (2007).
 171. Yu, M., Wang, H., Ding, A., Golenbock, D. T., Latz, E., Czura, C. J., Fenton, M. J., Tracey, K. J. & Yang, H. HMGB1 signals through toll-like receptor (TLR) 4 and TLR2. *Shock* **26**, 174 (2006).
 172. Campana, L., Bosurgi, L. & Rovere-Querini, P. HMGB1: a two-headed signal regulating tumor progression and immunity. *Current opinion in immunology* **20**, 518–523 (2008).
 173. Vogl, T., Tenbrock, K., Ludwig, S., Leukert, N., Ehrhardt, C., van Zoelen, M. A. D., Nacken, W., Foell, D., van der Poll, T., Sorg, C. & Roth, J. Mrp8 and Mrp14 are endogenous activators of Toll-like receptor 4, promoting lethal, endotoxin-induced shock. *Nat. Med.* **13**, 1042–9 (2007).
 174. Lim, S. Y., Raftery, M. J., Goyette, J., Hsu, K. & Geczy, C. L. Oxidative modifications of S100 proteins: functional regulation by redox. *Journal of leukocyte biology* **86**, 577–587 (2009).
 175. Guo, G. & Bhat, N. R. Hypoxia/reoxygenation differentially modulates NF- κ B activation and iNOS expression in astrocytes and microglia. *Antioxidants & redox signaling* **8**, 911–918 (2006).
 176. Ock, J., Jeong, J., Choi, W. S., Lee, W. H., Kim, S. H., Kim, I. K. & Suk, K. Regulation of Toll-like receptor 4 expression and its signaling by hypoxia in cultured microglia. *Journal of neuroscience research* **85**, 1989–1995 (2007).
 177. Fields, R. D. & Stevens, B. ATP: an extracellular signaling molecule between neurons and glia. *Trends in neurosciences* **23**, 625–633 (2000).
 178. Sperlágh, B. & Illes, P. Purinergic modulation of microglial cell activation. *Purinergic signalling* **3**, 117–127 (2007).
 179. Smith, S. M., Mitchell, G. S., Friedle, S. A., Sibigtroth, C. M., Vinit, S. & Watters, J. J. Hypoxia attenuates purinergic P2X receptor-induced inflammatory gene expression in brainstem microglia. *Hypoxia* **2013**, (2013).
 180. Lai, A. Y. & Todd, K. G. Differential regulation of trophic and proinflammatory microglial effectors is dependent on severity of neuronal injury. *Glia* **56**, 259–270 (2007).

181. Färber, K. & Kettenmann, H. Purinergic signaling and microglia. *Pfluegers Archiv European Journal of Physiology* **452**, 615–621 (2006).
182. Inoue, K., Koizumi, S. & Tsuda, M. The role of nucleotides in the neuron-glia communication responsible for the brain functions. *Journal of neurochemistry* **102**, 1447–1458 (2007).
183. Haynes, S. E., Hollopeter, G., Yang, G., Kurpius, D., Dailey, M. E., Gan, W.-B. & Julius, D. The P2Y₁₂ receptor regulates microglial activation by extracellular nucleotides. *Nature neuroscience* **9**, 1512–1519 (2006).
184. Koizumi, S., Shigemoto-Mogami, Y., Nasu-Tada, K., Shinozaki, Y., Ohsawa, K., Tsuda, M., Joshi, B. V., Jacobson, K. A., Kohsaka, S. & Inoue, K. UDP acting at P2Y₆ receptors is a mediator of microglial phagocytosis. *Nature* **446**, 1091–1095 (2007).
185. Fields, R. D. & Burnstock, G. Purinergic signalling in neuron-glia interactions. *Nature Reviews Neuroscience* **7**, 423–436 (2006).
186. Brautigam, V. M., Frasier, C., Nikodemova, M. & Watters, J. J. Purinergic receptor modulation of BV-2 microglial cell activity: potential involvement of p38 MAP kinase and CREB. *Journal of neuroimmunology* **166**, 113–125 (2005).
187. Inoue, K. The function of microglia through purinergic receptors: neuropathic pain and cytokine release. *Pharmacology & therapeutics* **109**, 210–226 (2006).
188. Raouf, R., Chabot-Doré, A. J., Ase, A. R., Blais, D. & Séguéla, P. Differential regulation of microglial P2X₄ and P2X₇ ATP receptors following LPS-induced activation. *Neuropharmacology* **53**, 496–504 (2007).
189. Di Virgilio, F. Liaisons dangereuses: P2X₇ and the inflammasome. *Trends in pharmacological sciences* **28**, 465–472 (2007).
190. Watters, J. J., Sommer, J. A., Fisette, P. L., Pfeiffer, Z. A., Aga, M., Prabhu, U., Guerra, A. N., Denlinger, L. C. & Bertics, P. J. P2X₇ nucleotide receptor: Modulation of LPS-induced macrophage signaling and mediator production. *Drug development research* **53**, 91–104 (2001).
191. Sperlágh, B., Haskó, G., Németh, Z. & Vizi, E. S. ATP released by LPS increases nitric oxide production in raw 264.7 macrophage cell line via P2Z/P2X₇ receptors. *Neurochemistry international* **33**, 209–215 (1998).
192. Friedle, S., Brautigam, V., Nikodemova, M., Wright, M. & Watters, J. The P2X₇-Egr pathway regulates nucleotide-dependent inflammatory gene expression in microglia. *Glia* **59**, 1–13 (2011).

193. Boumechache, M., Masin, M., Edwardson, J. M., Górecki, D. C. & Murrell-Lagnado, R. Analysis of assembly and trafficking of native P2X4 and P2X7 receptor complexes in rodent immune cells. *Journal of Biological Chemistry* **284**, 13446 (2009).
194. Yamashita, T., Tsuda, M., Tozaki-Saitoh, H. & Inoue, K. in *JOURNAL OF PHARMACOLOGICAL SCIENCES* **118**, 101P–101P (2012).
195. Antonio, L., Stewart, A., Xu, X., Varanda, W., Murrell-Lagnado, R. & Edwardson, J. P2X4 receptors interact with both P2X2 and P2X7 receptors in the form of homotrimers. *British journal of pharmacology* **163**, 1069–1077 (2011).
196. Guo, C., Masin, M., Qureshi, O. S. & Murrell-Lagnado, R. D. Evidence for functional P2X4/P2X7 heteromeric receptors. *Molecular pharmacology* **72**, 1447–1456 (2007).
197. Bedard, K. & Krause, K.-H. The NOX family of ROS-generating NADPH oxidases: physiology and pathophysiology. *Physiological reviews* **87**, 245–313 (2007).
198. Hwang, K. Y., Oh, Y. T., Yoon, H., Lee, J., Kim, H., Choe, W. & Kang, I. Baicalein suppresses hypoxia-induced HIF-1 [alpha] protein accumulation and activation through inhibition of reactive oxygen species and PI 3-kinase/Akt pathway in BV2 murine microglial cells. *Neuroscience letters* **444**, 264–269 (2008).
199. Tschopp, J. & Schroder, K. NLRP3 inflammasome activation: The convergence of multiple signalling pathways on ROS production? *Nature Reviews Immunology* **10**, 210–215 (2010).
200. Yang, Q., Wang, Y., Feng, J., Cao, J. & Chen, B. Intermittent hypoxia from obstructive sleep apnea may cause neuronal impairment and dysfunction in central nervous system: the potential roles played by microglia. *Neuropsychiatric disease and treatment* **9**, 1077 (2013).
201. Schroder, K. & Tschopp, J. The inflammasomes. *Cell* **140**, 821–832 (2010).
202. Lamkanfi, M., Sarkar, A., Walle, L. V., Vitari, A. C., Amer, A. O., Wewers, M. D., Tracey, K. J., Kanneganti, T.-D. & Dixit, V. M. Inflammasome-dependent release of the alarmin HMGB1 in endotoxemia. *The Journal of Immunology* **185**, 4385–4392 (2010).
203. Kayagaki, N., Warming, S., Lamkanfi, M., Vande Walle, L., Louie, S., Dong, J., Newton, K., Qu, Y., Liu, J., Heldens, S., Zhang, J., Lee, W. P., Roose-Girma, M. & Dixit, V. M. Non-canonical inflammasome activation targets caspase-11. *Nature* **479**, 117–21 (2011).
204. Pétrilli, V., Dostert, C., Muruve, D. A. & Tschopp, J. The inflammasome: a danger sensing complex triggering innate immunity. *Current opinion in immunology* **19**, 615–622 (2007).
205. Chiu, G. S., Chatterjee, D., Darmody, P. T., Walsh, J. P., Meling, D. D., Johnson, R. W. & Freund, G. G. Hypoxia/reoxygenation impairs memory formation via adenosine-dependent activation of caspase 1. *The Journal of Neuroscience* **32**, 13945–13955 (2012).

206. Lavie, L. & Polotsky, V. Cardiovascular aspects in obstructive sleep apnea syndrome-molecular issues, hypoxia and cytokine profiles. *Respiration* **78**, 361–370 (2009).
207. Dyugovskaya, L., Lavie, P. & Lavie, L. Lymphocyte activation as a possible measure of atherosclerotic risk in patients with sleep apnea. *Annals of the New York Academy of Sciences* **1051**, 340–350 (2005).
208. Minoguchi, K., Yokoe, T., Tazaki, T., Minoguchi, H., Tanaka, A., Oda, N., Okada, S., Ohta, S., Naito, H. & Adachi, M. Increased carotid intima-media thickness and serum inflammatory markers in obstructive sleep apnea. *American journal of respiratory and critical care medicine* **172**, 625–630 (2005).
209. Koistinaho, M. & Koistinaho, J. Role of p38 and p44/42 mitogen-activated protein kinases in microglia. *Glia* **40**, 175–183 (2002).
210. Potucek, Y. D., Crain, J. M. & Watters, J. J. Purinergic receptors modulate MAP kinases and transcription factors that control microglial inflammatory gene expression. *Neurochemistry international* **49**, 204–214 (2006).
211. Nikodemova, M., Duncan, I. D. & Watters, J. J. Minocycline exerts inhibitory effects on multiple mitogen-activated protein kinases and κB degradation in a stimulus-specific manner in microglia. *Journal of neurochemistry* **96**, 314–323 (2005).
212. Oh, Y. T., Lee, J. Y., Lee, J., Kim, H., Yoon, K.-S., Choe, W. & Kang, I. Oleic acid reduces lipopolysaccharide-induced expression of iNOS and COX-2 in BV2 murine microglial cells: Possible involvement of reactive oxygen species, p38 MAPK, and IKK/NF- κB signaling pathways. *Neuroscience letters* **464**, 93–97 (2009).
213. Park, S. Y., Lee, H., Hur, J., Kim, S. Y., Kim, H., Park, J.-H., Cha, S., Kang, S. S., Cho, G. J., Choi, W. S. & Suk, K. Hypoxia induces nitric oxide production in mouse microglia via p38 mitogen-activated protein kinase pathway. *Brain Res. Mol. Brain Res.* **107**, 9–16 (2002).
214. Ryan, S., McNicholas, W. T. & Taylor, C. T. A critical role for p38 map kinase in NF- κB signaling during intermittent hypoxia/reoxygenation. *Biochemical and biophysical research communications* **355**, 728–733 (2007).
215. Sharp, F. R. & Bernaudin, M. HIF1 and oxygen sensing in the brain. *Nature Reviews Neuroscience* **5**, 437–448 (2004).
216. Yao, L., Kan, E. M., Lu, J., Hao, A., Dheen, S. T., Kaur, C. & Ling, E.-A. Toll-like receptor 4 mediates microglial activation and production of inflammatory mediators in neonatal rat brain following hypoxia: role of TLR4 in hypoxic microglia. *J Neuroinflammation* **10**, 23 (2013).

217. Nizet, V. & Johnson, R. S. Interdependence of hypoxic and innate immune responses. *Nature Reviews Immunology* **9**, 609–617 (2009).
218. Peyssonnaud, C., Cejudo-Martin, P., Doedens, A., Zinkernagel, A. S., Johnson, R. S. & Nizet, V. Cutting edge: essential role of hypoxia inducible factor-1 α in development of lipopolysaccharide-induced sepsis. *The Journal of Immunology* **178**, 7516–7519 (2007).
219. Blackwell, T. S. & Christman, J. W. The role of nuclear factor- κ B in cytokine gene regulation. *American journal of respiratory cell and molecular biology* **17**, 3–9 (1997).
220. Rius, J., Guma, M., Schachtrup, C., Akassoglou, K., Zinkernagel, A. S., Nizet, V., Johnson, R. S., Haddad, G. G. & Karin, M. NF- κ B links innate immunity to the hypoxic response through transcriptional regulation of HIF-1 α . *Nature* **453**, 807–811 (2008).
221. Greenberg, H., Ye, X., Wilson, D., Htoo, A. K., Hendersen, T. & Liu, S. F. Chronic intermittent hypoxia activates nuclear factor- κ B in cardiovascular tissues in vivo. *Biochemical and biophysical research communications* **343**, 591–596 (2006).
222. Ryan, S., Taylor, C. T. & McNicholas, W. T. Selective activation of inflammatory pathways by intermittent hypoxia in obstructive sleep apnea syndrome. *Circulation* **112**, 2660–2667 (2005).
223. Htoo, A. K., Greenberg, H., Tongia, S., Chen, G., Henderson, T., Wilson, D. & Liu, S. F. Activation of nuclear factor κ B in obstructive sleep apnea: a pathway leading to systemic inflammation. *Sleep and Breathing* **10**, 43–50 (2006).
224. Alberini, C. M. Transcription factors in long-term memory and synaptic plasticity. *Physiological reviews* **89**, 121–145 (2009).
225. Lendahl, U., Lee, K. L., Yang, H. & Poellinger, L. Generating specificity and diversity in the transcriptional response to hypoxia. *Nature Reviews Genetics* **10**, 821–832 (2009).
226. Parry, G. & Mackman, N. Role of cyclic AMP response element-binding protein in cyclic AMP inhibition of NF- κ B-mediated transcription. *The Journal of Immunology* **159**, 5450–5456 (1997).
227. Kreutzberg, G. W. Microglia: a sensor for pathological events in the CNS. *Trends in neurosciences* **19**, 312–318 (1996).
228. Goldbart, A., Row, B., Kheirandish-Gozal, L., Cheng, Y., Brittan, K. & Gozal, D. High fat/refined carbohydrate diet enhances the susceptibility to spatial learning deficits in rats exposed to intermittent hypoxia. *Brain research* **1090**, 190–196 (2006).
229. Ryan, S. & McNicholas, W. T. Intermittent hypoxia and activation of inflammatory molecular pathways in OSAS. *Archives of physiology and biochemistry* **114**, 261–266

- (2008).
230. Goshen, I. & Yirmiya, R. The role of pro-inflammatory cytokines in memory processes and neural plasticity. *Psychoneuroimmunology*. 4th ed: Elsevier (2007).
 231. Zoppo, G., Ginis, I., Hallenbeck, J. M., Iadecola, C., Wang, X. & Feuerstein, G. Z. Inflammation and stroke: putative role for cytokines, adhesion molecules and iNOS in brain response to ischemia. *Brain Pathology* **10**, 95–112 (2000).
 232. MacFarlane, P., Vinit, S. & Mitchell, G. Spinal nNOS regulates phrenic motor facilitation by a 5-HT_{2B} receptor-and NADPH oxidase-dependent mechanism. *Neuroscience* (2014).
 233. Li, J., Baud, O., Vartanian, T., Volpe, J. J. & Rosenberg, P. A. Peroxynitrite generated by inducible nitric oxide synthase and NADPH oxidase mediates microglial toxicity to oligodendrocytes. *Proceedings of the National Academy of Sciences of the United States of America* **102**, 9936–9941 (2005).
 234. Minghetti, L. & Levi, G. Microglia as effector cells in brain damage and repair: focus on prostanoids and nitric oxide. *Progress in neurobiology* **54**, 99–125 (1998).
 235. Lalancette-Hébert, M., Gowing, G., Simard, A., Weng, Y. C. & Kriz, J. Selective ablation of proliferating microglial cells exacerbates ischemic injury in the brain. *The Journal of neuroscience* **27**, 2596–2605 (2007).
 236. Lu, Y., Christian, K. & Lu, B. BDNF: a key regulator for protein synthesis-dependent LTP and long-term memory? *Neurobiology of learning and memory* **89**, 312–323 (2008).
 237. Blundon, J. A. & Zakharenko, S. S. Dissecting the components of long-term potentiation. *The Neuroscientist* **14**, 598–608 (2008).
 238. Gozal, E., Row, B. W., Schurr, A. & Gozal, D. Developmental differences in cortical and hippocampal vulnerability to intermittent hypoxia in the rat. *Neuroscience letters* **305**, 197–201 (2001).
 239. Zhu, L., Zhao, T., Li, H., Zhao, H., Wu, L., Ding, A., Fan, W. & Fan, M. Neurogenesis in the adult rat brain after intermittent hypoxia. *Brain research* **1055**, 1–6 (2005).
 240. Gozal, D., Row, B. W., Gozal, E., Kheirandish, L., Neville, J. J., Brittan, K. R., Sachleben, L. R. & Guo, S. Z. Temporal aspects of spatial task performance during intermittent hypoxia in the rat: evidence for neurogenesis. *European Journal of Neuroscience* **18**, 2335–2342 (2003).
 241. Tang, Y., Li, T., Li, J., Yang, J., Liu, H., Zhang, X. & Le, W. Jmjd3 is essential for the epigenetic modulation of microglia phenotypes in the immune pathogenesis of Parkinson's disease. *Cell Death & Differentiation* (2013).

242. Hanisch, U.-K. Linking STAT and TLR signaling in microglia: a new role for the histone demethylase Jmjd3. *Journal of Molecular Medicine* **92**, 197–200 (2014).
243. Kooistra, S. M. & Helin, K. Molecular mechanisms and potential functions of histone demethylases. *Nature reviews Molecular cell biology* **13**, 297–311 (2012).

CHAPTER 2

HYPOXIA ATTENUATES PURINERGIC P2X RECEPTOR-INDUCED INFLAMMATORY GENE EXPRESSION IN BRAINSTEM MICROGLIA

Stephanie M. C. Smith, Gordon S. Mitchell, Scott A. Friedle, Christine M. Sibigroth, Stéphane Vinit, and Jyoti J. Watters

The work from this chapter was published in *Hypoxia*, 2013 (1).

Hypoxia attenuates purinergic P2X receptor-induced inflammatory gene expression in brain stem microglia. Stephanie M. C. Smith, Gordon S. Mitchell, Scott A. Friedle, Christine M. Sibigroth, Stéphane Vinit, and Jyoti J. Watters.

ABSTRACT

Hypoxia and increased extracellular nucleotides are frequently coincident in the brainstem. Extracellular nucleotides are potent modulators of microglial inflammatory gene expression via P2X purinergic receptor activation. Although hypoxia is also known to modulate inflammatory gene expression, little is known about how hypoxia or P2X receptor activation alone affect inflammatory molecule production in brainstem microglia, nor how hypoxia and P2X receptor signaling interact when they occur together. In this study, we investigated the ability of a brief episode of hypoxia (2hrs) in the presence and absence of the non-selective P2X receptor agonist 2'(3')-O-(4-benzoylbenzoyl) adenosine-5'-triphosphate (BzATP) to promote inflammatory gene expression in brainstem microglia in adult rats. We evaluated inducible nitric oxide synthase (iNOS), tumor necrosis factor alpha (TNF α) and interleukin-6 (IL-6) mRNA levels in immunomagnetically-isolated brainstem microglia. Whereas iNOS and IL-6 gene expression increased with hypoxia and BzATP alone, TNF α expression was unaffected. Surprisingly, BzATP-induced inflammatory effects are lost after hypoxia, suggesting that hypoxia impairs pro-inflammatory P2X receptor signaling. We also evaluated the expression of key P2X receptors activated by BzATP, namely P2X1, P2X4 and P2X7 receptors. Whereas hypoxia did not alter their expression, BzATP upregulated P2X4 and P2X7 mRNAs; these effects were ablated in hypoxia. Although both P2X4 and P2X7 receptor expression correlated with increased microglial iNOS and IL-6 levels in microglia from normoxic rats, in hypoxia, P2X7 only correlated with IL-6, and P2X4 correlated only with iNOS. In addition, correlations between P2X7 and P2X4 were lost following hypoxia, suggesting that P2X4 and P2X7 receptor signaling differs in normoxia and hypoxia. Together, these data suggest that hypoxia suppresses P2X receptor-induced inflammatory gene expression, indicating a potentially

immunosuppressive role of extracellular nucleotides in brainstem microglia following exposure to hypoxia.

INTRODUCTION

Microglia are CNS resident immune cells that continuously survey their environment and respond to changes in cellular homeostasis resulting from infection, hypoxia, cell death and other stimuli to produce inflammatory molecules that are ultimately thought to be detrimental to neurons. Although mechanisms activating microglia are widely studied, little is known concerning the role of extracellular nucleotides, including ADP and ATP, in microglial activation and transcription of inflammatory genes *in vivo*. Extracellular nucleotides and their interactions with P2X and P2Y purinergic receptors are important signals permitting microglia to sense and respond to their local CNS environment^{1,2}. Nucleotides are co-packaged with neurotransmitters³ and released from astrocytes during calcium wave propagation,^{4,5} perhaps enabling microglia to sense synaptic health^{6,7}. Nucleotides also leak from damaged and/or dying cells,³ creating extracellular ATP concentrations sufficient to induce inflammatory activities via P2X7 receptor activation⁸.

Many disorders accompanied by microglial inflammation and high extracellular adenine nucleotide levels (i.e. cell death) are associated with hypoxia. For example, hypoxia is an element of ischemic injuries during stroke or myocardial infarction. Another example is the chronic intermittent hypoxia (repeated hypoxia/reoxygenation events) experienced during sleep disordered breathing, a frequent occurrence in many neurodegenerative, traumatic and genetic CNS disorders⁹⁻¹⁴. Although nucleotides and hypoxia each regulate microglial inflammatory activities (reviewed in^{15,16}), little is known concerning their interactions in regulating microglial activities when hypoxia and increased extracellular nucleotides occur together. These microglial stimuli are often coincident in pathology,¹⁷⁻²¹ and during normal CNS function in hypoxia-sensitive CNS regions, such as the brainstem where hypoxia-induced ATP release is important

for maintaining respiration²². Thus, we investigated the effects of a brief 2-hour period of hypoxia in the presence and absence of P2X receptor activation on microglial inflammatory gene expression *in vivo*. In specific, we tested the hypotheses that P2X receptor activation stimulates microglial inflammatory gene expression in normoxia, and that these effects would be potentiated in hypoxia.

In microglia, many immunomodulatory effects of ATP are mediated through the P2X receptor family member P2X7²³⁻²⁶. BzATP (3'-O-(4-benzoyl) benzoic ATP) is often regarded as a specific P2X7 receptor agonist, although it has at least some potency at all P2X receptor subtypes with the exception of P2X6²⁷. Here, we treated rats intracisternally with BzATP, and then exposed them to hypoxia or normoxia for 2 hours, followed by return to room air. We then evaluated the expression of several inflammatory genes including inducible nitric oxide synthase (iNOS), interleukin-6 (IL-6) and tumor necrosis factor alpha (TNF α) in freshly-isolated microglia. We chose iNOS as an endpoint because the inhibition or genetic deletion of this enzyme ameliorates brain damage in multiple ischemic, excitotoxic and hypoxic injury models²⁸⁻³². The pro-inflammatory cytokines TNF α and IL-6 were chosen because their upregulation is a hallmark of neuroinflammation, and they are often implicated in neuronal toxicity following many CNS insults, including hypoxia/ischemia, neurodegeneration and traumatic injury (reviewed in³³⁻³⁶).

MATERIALS AND METHODS

Materials:

3'-O-(4-benzoylbenzoyl)-adenosine 5'-triphosphate (BzATP) was purchased from Sigma Chemical Company (St. Louis, MO).

Animals:

Experiments were performed using 3- to 5-month-old adult male Sprague-Dawley rats (Harlan Laboratories, Madison, WI). Animals were maintained in an AAALAC-accredited animal facility according to protocols approved by the University of Wisconsin Institutional Animal Care and Use Committee. All animals were housed under standard conditions, with a 12 hour light/dark cycle and *ad libitum* food and water. All efforts were made to minimize animal distress and reduce the numbers used, while permitting the formation of statistically reliable conclusions.

Nucleotide (BzATP) treatment:

Rats were naïve (n=6) or treated intracisternally with vehicle (25 μ l of 250 mM Hepes) or BzATP (25 μ l of 0.3 μ M stock in 250 mM Hepes). Briefly, rats were presedated with dexmedetomidine (50-65 μ g/kg, s.c.), anesthetized with isoflurane (1.5%, 100% O₂ balanced), orotracheally intubated and ventilated (Harvard rodent ventilator). A tail vein catheter was placed in order to deliver fluids into the animal post-injection (Lactated Ringer, 2.5ml per hour, i.v.). After dorsal laminectomy at C2, the dura was cut to allow insertion of a silicone catheter into the cisterna magna (12 mm, inserted from the caudal end of the C1 vertebrae) through which vehicle or BzATP was delivered. The muscle and the skin were sutured closed, and atipamezole (500 μ g/kg, i.m.), buprenorphine (0.05 mg/kg, s.c.) and baytril (10 mg/kg, s.c.) were administered prior to termination of isoflurane anesthesia.

In vivo hypoxia exposures:

Exposures were performed by placing animals into individual chambers connected to a computer-driven controller that monitors O₂ and CO₂ within the exposure chamber and mixes O₂ and/or N₂ to achieve the desired inspired oxygen concentrations, with a CO₂ concentration <0.5%. Animals were exposed to either normoxia (vehicle, n=8; BzATP, n=8) or hypoxia (vehicle, n=7; BzATP, n=7) for 2 hours, with free access to food and fluids. This paradigm of hypoxia induces a rapid decrease in oxygen tension in the CNS³⁷, exerts measureable physiological changes in brainstem neuron excitability³⁸⁻⁴⁰ and promotes translocation to the nucleus of hypoxia inducible factor-1 α (HIF-1 α)⁴¹. In addition to vehicle-treated rats, naïve rats were also exposed to normoxia to control for non-specific, surgically-induced inflammation. At the end of the 2-hour exposure period, rats were removed from the chambers, the tail vein catheter was removed, and they were returned to their cages for 22 hours. At that time, the rats were euthanized, and brainstem microglia were immunomagnetically isolated for analysis of gene expression by qRT-PCR.

Immunomagnetic CD11b⁺ cell isolation:

CD11b⁺ cells were isolated from the brainstems of 6-13 individual animals/treatment group, as we have previously reported^{42,43}. The average purity of cells isolated from these animals that had the characteristics of microglia was >95% as determined by FSC/SSC scatter analysis and CD11b⁺/CD45^{low} staining^{42,43} (and data not shown), consistent with previous reports⁴⁴. These CD11b⁺ cells will subsequently be referred to as “microglia.”

RT-PCR:

Total RNA was isolated from freshly-isolated brain stem microglia (or whole brain as a positive control for primer set validation) using the TRI-reagent according to the manufacturer's

instructions. Purified RNA was then digested with DNase I (Invitrogen, Carlsbad, CA) according to the manufacturer's protocol. First-strand cDNA was synthesized from 1µg of total RNA using MMLV Reverse Transcriptase (Invitrogen) and an oligo(dT)/random hexamer cocktail (Promega). The cDNA was used for qPCR using Power SYBR (Applied Biosystems, Foster City, CA). Fluorescence was monitored in real-time using the TaqMan ABI 7300 Sequence Detection System (Applied Biosystems). The standard curve method⁴⁵ was used to determine the relative amounts of each gene between samples using the average of duplicate interpolated C_T values normalized to 18s rRNA. A 2-way ANOVA was used to determine whether treatment had any effect on the expression of 18s; we found no statistically significant differences in any treatment group (data not shown). The following primer sequences had efficiencies >97%, and were used for quantitative PCR; Genbank Accession numbers are provided in parentheses. iNOS (NM_012611.3) - 5' AGG GAG TGT TGT TCC AGG TG and 5' TCT GCA GGA TGT CTT GAA CG; IL-6 (NM_012589.2) - 5' GTG GCT AAG GAC CAA GAC CA and 5' GGT TTG CCG AGT AGA CCT CA; TNF-α (NM_012675.3) - 5' TCC ATG GCC CAG ACC CTC ACA C and 5' TCC GCT TGG TGG TTT GCT ACG; P2X1 (NM_001142367.1) - 5' AGC CCA AGG TAT TCG CAC AG and 5' TTC ACA GTG CCA TTG AAG GG; P2X2 (NM_053656.2) - 5' GTA GTC AGC ATC ATC ACC AGG and 5' TCA GAC AAG TCC AGG TCA CAG T; P2X3 (BC081783.1) - 5' TAC CAA GTC GGT GGT TGT GA and 5' CCA CCC CAC AAA GTA GGA GA; P2X4 (NM_031594.1) - 5' GTG GCG GAC TAT GTG ATT CC and 5' GGT GCT CTG TGT CTG GTT CA; P2X5 (NM_080780.2) - 5' TCT TGC ATC CAG TGA AGA CG and 5' AGT TCA GAG CTG TGG CCT GT; P2X6 (NM_012721.2) - 5' ACG TGT TCT TCC TGG TAA CCA ACT and 5' TGG ACA TCT GCC CTG GAC TT; P2X7 (NM_019256.1) - 5' GGC ACC ATC AAG TGG ATC TT and 5' CTT GTC GCT CAT CAA AGC AA; and 18s

(NR_046237.1) - 5' CGG GTG CTC TTA GCT GAG TGT CCC G and 3' CTC GGG CCT GCT TTG AAC AC. All primers were designed to span introns whenever possible, and primer efficiency was tested through the use of serial dilutions in standard curves. Primer specificity was assessed through NCBI BLAST analysis prior to use, and all dissociation curves had a single peak with an observed T_m consistent with the intended amplicon sequences. Samples with C_T values ≥ 34 cycles were considered undetectable, and were removed from statistical analyses.

Statistical analyses:

Statistical analyses were performed on the normalized, interpolated C_T values from the standard curves from each gene, as previously described⁴⁵. Outliers (identified using the Grubb's outlier test) were removed from the data set. When comparing two population means, statistical inferences were made using a Student's t-test. When comparing treatment and oxygen effects, comparisons were made using a two-way ANOVA (Sigma Stat version 11, Systat Software, San Jose, CA); Tukey *post hoc* tests were used to assess statistical significance in individual comparisons. Data sets that failed normality were logarithmically transformed prior to running the statistical analyses. Statistical significance was set at $p < 0.05$. There was no significant difference in gene expression between vehicle-treated and naïve normoxic animals for all genes studied, as determined by a Student's t-test (*data not shown*). Therefore, these groups were combined for subsequent statistical and graphical purposes. Mean data are expressed ± 1 SEM.

RESULTS

mRNA levels of pro-inflammatory genes are differentially increased by hypoxia in microglia

Hypoxia increased both iNOS and IL-6 mRNA levels (2.57 ± 0.63 fold, $p=0.02$ and 2.77 ± 0.56 fold, $p=0.04$ respectively) in freshly-isolated brainstem microglia (Fig. 1A, B). Interestingly, TNF α mRNA levels were not changed by hypoxia (0.89 ± 0.35 fold, $p>0.05$) (Fig. 1C), suggesting that the pro-inflammatory effects of hypoxia are gene-specific. Thus, hypoxia increases expression of some, but not all pro-inflammatory genes in brainstem microglia *in vivo*.

P2X receptor activation in normoxia upregulates inflammatory gene expression in brainstem microglia

To investigate the effects of P2X receptor activation on microglial inflammatory gene expression, rats were intracisternally injected with vehicle or BzATP, and exposed to normoxia or hypoxia. Similar to hypoxia alone, BzATP increased microglial iNOS (6.73 ± 2.17 fold, $p<0.001$) and IL-6 (2.32 ± 0.53 fold, $p=0.01$) mRNA levels, but not TNF α (1.47 ± 0.24 fold, $p>0.05$), demonstrating gene-specific regulation of pro-inflammatory molecules by P2X receptors (Fig. 1A, B, C). The stimulatory effects of BzATP on microglial IL-6 gene expression *in vivo* are consistent with our previous observations *in vitro*⁴⁶ where BzATP increased IL-6 mRNA levels.

BzATP-induced inflammation is prevented by exposure to hypoxia

Surprisingly, the effects of P2X receptor activation on microglial inflammatory gene expression in normoxia were lost in hypoxia. In hypoxia, BzATP failed to increase iNOS, IL-6 or TNF α mRNA levels compared to vehicle treatment (Fig. 1). The approximate seven-fold increase in iNOS expression stimulated by BzATP in normoxia was reduced by more than half

(2.37 ± 0.87 fold, $p=0.039$) in hypoxia, and was not different from the effects of hypoxia alone (2.57 ± 0.63 fold, $p=0.536$). Similarly, the ~ 2 -fold increase in IL-6 mRNA levels stimulated by BzATP in normoxia appeared to decrease (to 0.92 ± 0.25 fold), although these apparent changes were not significant with a 2-way ANOVA ($p=0.193$). However, there was a significant difference between BzATP effects in normoxia and hypoxia (Student's T-test; $p=0.045$). BzATP effects on IL-6 expression during hypoxia were not different from vehicle ($p=0.409$). Further, BzATP had no effect on TNF α mRNA expression ($p>0.05$) with hypoxia. Collectively, these data suggest that P2X receptor function differs in normoxia and hypoxia, and that the ability of P2X receptor signaling to induce inflammatory gene expression in microglia is ablated by hypoxia.

BzATP increases P2X4 and P2X7 mRNA levels

We evaluated the expression of all mammalian P2X receptors in brainstem microglia to narrow the potential list of P2X receptors that could be mediating the BzATP effects. The average C_T values for P2X receptors in brainstem microglia are as follows: P2X1- 29.89, P2X2- ND, P2X3- 30.34, P2X4- 28.14, P2X5- 30.48, P2X6- ND, P2X7- 28.15 and 18s rRNA- 14.41. Because P2X7, P2X4 and P2X1 receptors are the most highly expressed P2X receptors in brainstem microglia, and BzATP has the highest affinity for these same receptors²⁷, we evaluated BzATP effects on the expression of these receptors in normoxia versus hypoxia (Fig. 2). Hypoxia alone had no effect on P2X7 (1.51 ± 0.38 fold, $p=0.217$) (Fig. 2A), P2X4 (0.48 ± 0.13 fold, $p=0.565$) (Fig. 2B), or P2X1 (0.41 ± 0.18 fold, $p > 0.05$) (Fig. 2C) expression. In normoxia, BzATP increased expression of both P2X4 (4.12 ± 1.42 fold, $p=0.002$) and P2X7 (3.03 ± 0.70 fold, $p=0.002$) receptors, but not P2X1 receptors (0.78 ± 0.70 fold, $p>0.05$). As observed with the inflammatory genes, the effects of BzATP on P2X4 (1.05 ± 0.31 fold, $p<0.001$) and P2X7

(0.23 ± 0.07 fold, $p < 0.001$) mRNA levels were lost in hypoxia (Fig. 2A, B). Interestingly, while the effects of BzATP in hypoxia on P2X4 and P2X7 mRNA levels were not different from vehicle ($p = 0.227$ and $p = 0.509$, respectively), BzATP increased P2X1 mRNA levels ($p = 0.024$) in hypoxia (Fig. 2C).

P2X receptor expression correlates with inflammatory gene expression in brainstem microglia

Because of similarities between the regulation of inflammatory genes, P2X4 and P2X7 receptors in normoxia and hypoxia by BzATP, we sought to determine if correlations existed between these genes using regression analyses. We observed strong, positive correlations between both P2X7 and P2X4 receptors and iNOS (Figs. 3A and B) and IL-6 (Figs. 3C and D) expression, although some correlations differed in normoxia and hypoxia. In normoxia, iNOS mRNA correlated with both P2X7 (Fig. 3A) ($R^2 = 0.480$; $p = 0.003$) and P2X4 (Fig. 3B) mRNA levels ($R^2 = 0.644$; $p < 0.001$), although the correlation was stronger with P2X7 (correlation coefficient (r) = 0.936) than with P2X4 ($r = 0.771$). In contrast, the iNOS correlation with P2X7 mRNA was lost in hypoxia ($R^2 = 0.0689$; $p < 0.386$), whereas the correlation with P2X4 was increased ($R^2 = 0.936$; $r = 0.971$; $p < 0.001$).

Like iNOS, IL-6 positively correlated with both P2X7 (Fig. 3C) ($R^2 = 0.556$; $r = 0.936$; $p < 0.001$) and P2X4 expression (Fig. 3D) ($R^2 = 0.821$; $r = 1.02$; $p < 0.001$) in normoxia. However, the correlation with P2X4 was lost in hypoxia ($R^2 = 0.105$; $r = 0.359$; $p = 0.310$), whereas the correlation with P2X7 remained intact ($R^2 = 0.412$; $r = 0.314$; $p = 0.018$). IL-6 regulation by P2X7 *in vivo* is consistent with our previous *in vitro* observations using P2X7 RNAi⁴⁶ where we found that P2X7 receptor knockdown in N9 microglia ablated more than 90% of the BzATP-induced upregulation of IL-6. No correlation was observed between TNF α and either P2X4 or P2X7 (data

not shown), consistent with the lack of effect of BzATP on TNF α gene expression in any oxygen condition. In addition, P2X1 expression did not correlate with iNOS, TNF α , or IL-6 (data not shown). Interestingly, P2X4 and P2X7 receptor expression strongly correlated with each other in normoxia (Fig. 4A) ($R^2 = 0.815$; $r = 1.311$; $p < 0.001$), but not in hypoxia ($R^2 = 0.139$; $r = 0.412$; $p = 0.233$), suggesting an “uncoupling” of P2X4 and P2X7 regulation by hypoxia.

P2X1 mRNA did not correlate with P2X4 (Fig. 4B) ($R^2 = 0.0097$; $r = 0.119$; $p = 0.773$) or P2X7 (Fig. 4C) ($R^2 = 0.020$; $r = 0.17$; $p = 0.658$) in normoxia. In hypoxia, there was a marginal negative correlation between P2X1 and P2X4 expression ($R^2 = 0.346$; $r = -0.761$; $p = 0.073$, $n = 10$), and a significant correlation with P2X7 mRNA ($R^2 = 0.632$; $r = -1.283$; $p = 0.006$), suggesting that hypoxia may alter P2X receptor signaling by shifting the relative balance of P2X receptors.

DISCUSSION

This is the first report to describe the effects of P2X receptor activation and hypoxia on microglial inflammatory and P2X receptor gene expression *in vivo*. We found that exposure to hypoxia for only 2 hours is sufficient to induce microglial iNOS and IL-6 gene expression, detected the next day, although the effects of hypoxia are gene-specific since not all cytokines are similarly upregulated (i.e. TNF α). Because hypoxia and ATP release are often coincident, and P2X receptors are potent regulators of microglial activities, we also tested the impact of P2X receptor activation on iNOS, IL-6 and TNF α expression in hypoxia. We report here that, whereas P2X receptor activation in normoxia promotes iNOS and IL-6 gene expression (but not TNF α), these effects were nearly abolished by hypoxia. We also investigated if the apparent alteration in P2X receptor signaling by hypoxia was related to shifts in the balance of key microglial BzATP-responsive P2X receptors. Although hypoxia alone had no effect on P2X1, P2X4 or P2X7 receptor expression, BzATP-stimulated increases in P2X4 and P2X7 receptor expression in normoxia were prevented in hypoxia, similar to BzATP effects on iNOS and IL-6 gene expression. Because decreases in P2X receptor gene expression were not observed with hypoxia, P2X receptor signaling is likely altered by hypoxia via as yet, unknown mechanisms.

One possibility contributing to reduced P2X receptor signaling in hypoxia may be the altered composition of P2X receptor heterotrimers or altered interactions among homotrimers. These effects can conceivably occur relatively quickly (i.e. within the 2 hours of hypoxia exposure) due to rapid receptor subunit trafficking to the plasma membrane from intracellular pools. Intracellular pools of P2X4, P2X7 and P2X1 receptors have all been reported to influence ion channel function⁴⁷⁻⁵⁰. However, it should be noted that all gene expression analyses in our study were performed one day (22 hours) after the hypoxic exposure ended, so it is possible that

alterations in P2X receptor expression may also contribute to the modulation of inflammatory gene expression by BzATP reported here. In this study, we focused on the role of P2X1, P2X4 and P2X7 receptor regulation of microglial inflammatory activities for several reasons. 1) These receptors are among the most highly expressed in brainstem microglia (rank order abundance in freshly isolated adult brainstem microglia is: P2X4=P2X7 > P2X1 > P2X3=P2X5), and BzATP has the highest potency at P2X1 and P2X4 receptors²⁷. 2) BzATP has higher potency at P2X2, P2X5 and P2X7 receptors versus P2X3 receptors²⁷, P2X2 (and P2X6) mRNAs are undetectable in brainstem microglia, and P2X3 (and P2X5) are the least abundant of the P2X receptors in brainstem microglia. Thus, BzATP is most likely acting via P2X1, P2X4 and/or P2X7 receptors in brainstem microglia. 3) P2X4 and P2X7 receptors are the best characterized purinergic receptor subtypes in microglia^{51,52}. Little is known concerning P2X1 receptor function in adult microglia, although P2X1 receptors are present on microglia in the developing rat brain⁵³. P2X7 receptors mitigate microglial production of cytokines such as IL-1 β and IL-6^{46,54} as well as iNOS⁵⁵, whereas microglial P2X4 receptors contribute to neuropathic pain⁵⁶. Finally, 4) P2X receptors are homo- or hetero-trimeric proteins⁵⁷. P2X4 and P2X7 receptor subunits can form heterotrimers⁵⁸, although the preferred configuration in many tissues⁵⁹ and in cultured microglia appears to be homotrimers⁴⁸. Importantly, in cultured microglia there are also interactions between P2X4 and P2X7 homotrimers, suggesting cross-talk among these P2X receptors, even if they are not components of the same receptor trimer⁴⁸. Because P2X1 and P2X4 subunits can also trimerize⁶⁰, P2X4 subunits may be a common “partner” for P2X1 and P2X7 effects. In our studies, we found no effects of hypoxia or nucleotides on P2X1 receptor mRNA in normoxia; however, P2X1 receptor expression in hypoxia is negatively correlated with the P2X receptors. A negative association of P2X1 subunits may therefore reflect a complex shift in either the

composition of P2X4 and/or P2X7 trimers, and/or altered signaling interactions between these homomeric receptors. P2X receptor trimer composition, or between receptor interactions, have not been evaluated in hypoxia in any system. Thus, it is not yet known if alterations in these parameters contribute to the impaired ability of BzATP to signal to inflammatory genes during hypoxia.

To study the effects of exogenously administered nucleotides on microglial responses, we injected BzATP directly into the cisterna magna. Although the half-life of BzATP *in vivo* is unknown, this route of administration minimizes tissue trauma caused by direct injection into the brainstem parenchyma, while also maximizing exposure of brainstem cells to high nucleotide levels, the CNS region of interest in these studies. Interestingly, we found in pure microglial cultures *in vitro*, that between 1 and 8 hours of hypoxia ranging from 1-15%, followed by reoxygenation for 16-23 hours failed to induce any of the inflammatory genes assessed here (data not shown), suggesting that additional CNS cell types are likely necessary to recapitulate full microglial *in vivo* responses. This idea is consistent with the brainstem literature indicating an important role of astrocytes in sensing and responding to ATP during hypoxia^{61,62} to modulate respiratory rhythm generation and the hypoxic ventilatory response^{22,63-66}, key physiologic functions of the brainstem. It is also important to mention that we discuss the effects on microglial gene expression observed here as being the result of hypoxia. However, because we allowed the animals to control their own CO₂ during the hypoxic exposures, they also became hypocapnic. At this time, we cannot rule out the possibility that hypocapnia or a combination of both hypoxia and hypocapnia play a role in these observed effects.

Identifying individual contributions of P2X4 receptors to microglial activities in hypoxia *in vivo* is challenging because selective agonists or antagonists for P2X4 receptors are not

available. Most general P2 receptor antagonists have no affinity for P2X4. TNP-ATP has some ability to antagonize P2X4 receptors at high doses, but it has even higher potency at P2X7 receptors²⁷, making it difficult to pharmacologically distinguish P2X4 receptor-specific effects in cells such as microglia, where both receptor subtypes are highly expressed and likely play opposing roles. Moreover, antagonists such as iso-PPADS that lack the P2X7 receptor activities, have effects at P2X1 receptors which are also highly expressed in brainstem microglia and which we hypothesize play a role in responses to hypoxia. Due mostly to the lack of highly selective P2X receptor ligands, very little is known of P2X1 receptor activities in microglia in any situation, and little is known about P2X4 receptors in regulating microglial inflammatory gene expression *in vivo*. Indeed, the best studied role of P2X4 receptors is their function in tactile allodynia and neuropathic pain^{67,68}. Importantly, both P2X4 and P2X7 receptor protein levels are upregulated in microglia following ischemia⁶⁹⁻⁷¹, but no studies to our knowledge have evaluated P2X4 receptor levels in adult microglia after exposure to hypoxia alone⁷² or what the functional correlate is of P2X4 upregulation.

There are advantages and disadvantages to the immunomagnetic microglial isolation method used here. The major strength is that all experimental manipulations are performed *in vivo*, and microglia are rapidly isolated and analyzed. The ability to directly assess microglial gene expression in freshly-isolated cells is absolutely critical for making the most accurate conclusions about microglia. Typically, in the literature changes in microglial morphology are coupled with the presence of inflammatory mRNAs in whole tissue homogenates, the source of which is then ascribed to microglia. These conclusions may or may not be correct. However, the ability to perform these direct and microglia-specific analyses also comes at a cost. Microglia only comprise between 5 and 10% of all CNS cells, and unlike the cortex where 10% of the cells

are microglia in the rat, only about ~5% of brainstem cells are microglia (data not shown). Therefore, performing protein analyses by Western blots or ELISA assays are not feasible with such limited sample availability, and immunohistochemical (IHC) analyses are not appropriate for investigations of secreted molecules such as cytokines.

In this study, we were interested in identifying changes in mRNA levels for inflammatory genes induced by hypoxia and/or P2X receptor activation in microglia. In addition to the well-established roles of these inflammatory molecules in neurotoxicity as addressed above, we also chose to evaluate the expression of these particular genes because each one is inducible in microglia. They are regulated primarily at the level of transcription in response to common inflammatory stimuli such as LPS⁷³⁻⁷⁶. Thus, although concomitant increases in protein levels were not specifically investigated here, they are likely to occur. The transcriptional regulation of these genes is complex, and depending on the inflammatory stimulus used, may involve the transcriptional activities of several transcription factors including NF- κ B, AP-1, Egr factors and CREB^{46,77-79}. Important with regard to P2X receptor signaling in hypoxia is the fact that all of these transcription factors can be independently regulated by hypoxia⁸⁰⁻⁸² and P2X receptor activation^{46,83-85}. However, because both stimuli individually increase the activation of these transcription factors, we would predict that simultaneous activation of P2X receptors in hypoxia would result in augmented inflammatory gene expression if these transcription factors were involved, not the inhibition that we observed. Thus, it seems likely that the activation of a transcriptional repressor or the recruitment of a transcriptional co-repressor in the context of hypoxia may occur in response to P2X receptor activation. To our knowledge, no literature is available yet in support of or opposition to this hypothesis, and no information exists on specific activation or recruitment of transcriptional repressors or co-repressors by P2X receptors.

In summary, the present studies show that hypoxia prevents P2X receptor signaling to inflammatory gene expression in adult brainstem microglia *in vivo*. Detection of extracellular nucleotides by P2X receptors is likely one mechanism whereby microglia sense disturbances in cellular homeostasis in the CNS. That P2X receptor activation promotes inflammatory gene expression in microglia in normoxia suggests that, in pathologic situations when ATP is abundant, microglial inflammatory activities may contribute to neural injury. We suspect that downregulated P2X receptor signaling during hypoxia may be an adaptive measure used by microglia to prevent exaggerated inflammatory responses to the combined stimuli of increased extracellular nucleotides and hypoxia. This adaptation may represent a neuroprotective or anti-inflammatory function of microglia to mitigate hypoxic injury to neurons in this critical CNS region. These results indicate that microglia inherently adapt in hypoxia to mitigate their responsiveness to high concentrations of extracellular ATP when present. Indeed, if this is a generalized mechanism in microglial responses, this pathway could also be detrimental by inducing microglial quiescence during pathological periods of cellular dysregulation when microglial inflammatory activities would be beneficial. For example, the centers of growing tumors are hypoxic and contain high levels of extracellular ATP due to insufficient angiogenesis/vascularization⁸⁶ and cell death, respectively^{87,88}. The desired microglial response in this situation is an increased production of pro-inflammatory/anti-tumorigenic molecules. However, microglia located directly in the tumor microenvironment are generally immunologically suppressed (reviewed in⁸⁹), and underlying mechanisms of this may involve similar alterations in P2X receptor signaling in hypoxia. Thus, identifying mechanisms that regulate microglial responses to the combination of hypoxia and extracellular nucleotides will

provide new insights and understanding into microglial regulation and identify new therapeutic targets that can be used to manipulate microglial activities in various CNS pathologies.

ACKNOWLEDGEMENTS:

This work was supported by the NIH/NINDS R01NS049033 (JJW), the University of Wisconsin Alumni Research Foundation (JJW), the Respiratory Neurobiology Training Grant T32HL007654 (SMCS, SAF) and a Craig H. Neilsen Foundation Postdoctoral Fellowship (SV).

FIGURE 1

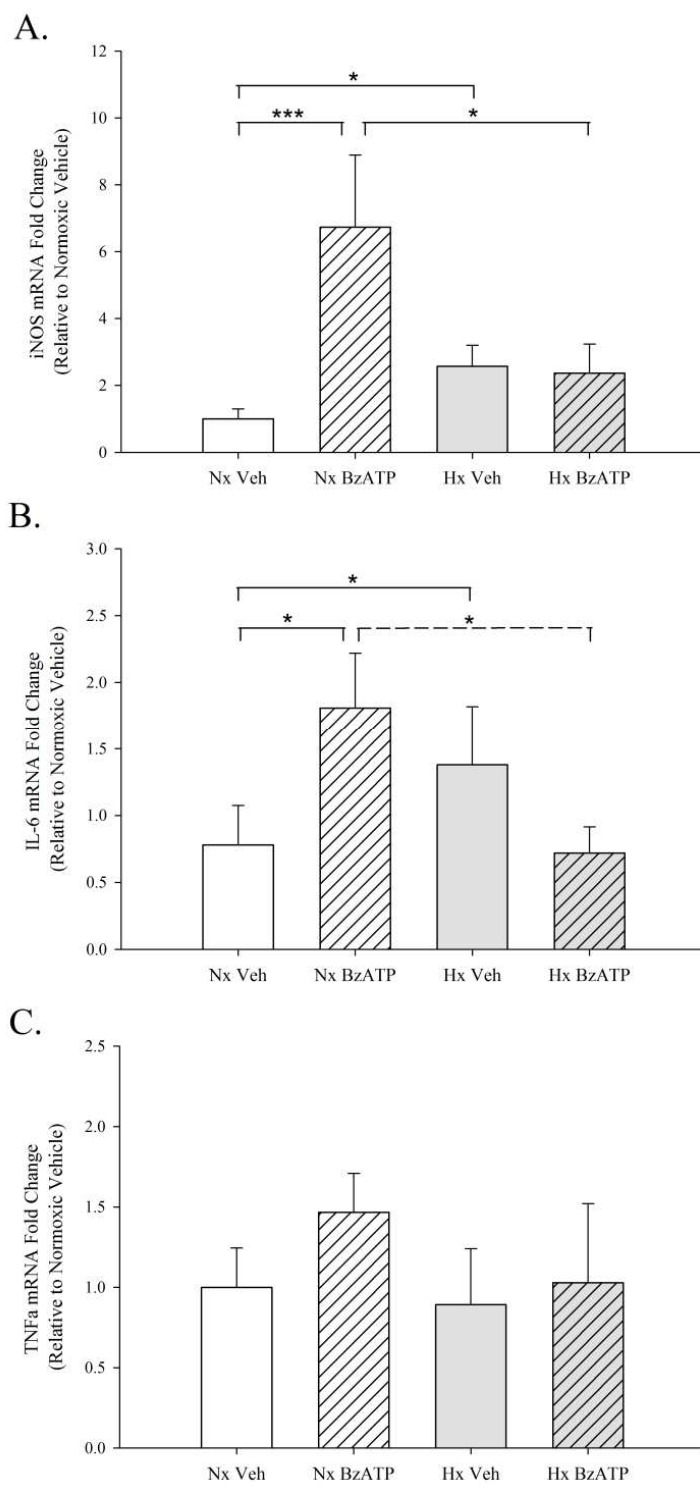


Figure Legend 1**Effects of BzATP treatment and hypoxia exposure on microglial inflammatory gene expression.**

Brainstem microglia were immunomagnetically isolated from animals treated with vehicle (Veh) or BzATP and exposed to normoxia (Nx) or hypoxia (Hx). Total RNA was isolated and subjected to qRT-PCR for analysis of: A) iNOS B) IL-6 and C) TNF α . Hypoxia for 2 hours increased the expression of iNOS and IL-6. BzATP treatment also increased iNOS and IL-6 expression in normoxia, but these effects were prevented in hypoxia. Neither treatment effected TNF α gene expression. Solid lines indicate statistically significant differences with a Two Way ANOVA and dashed lines with a t-test. *p<0.05; ***p<0.001. Data are graphed as fold change relative to vehicle treatment.

FIGURE 2

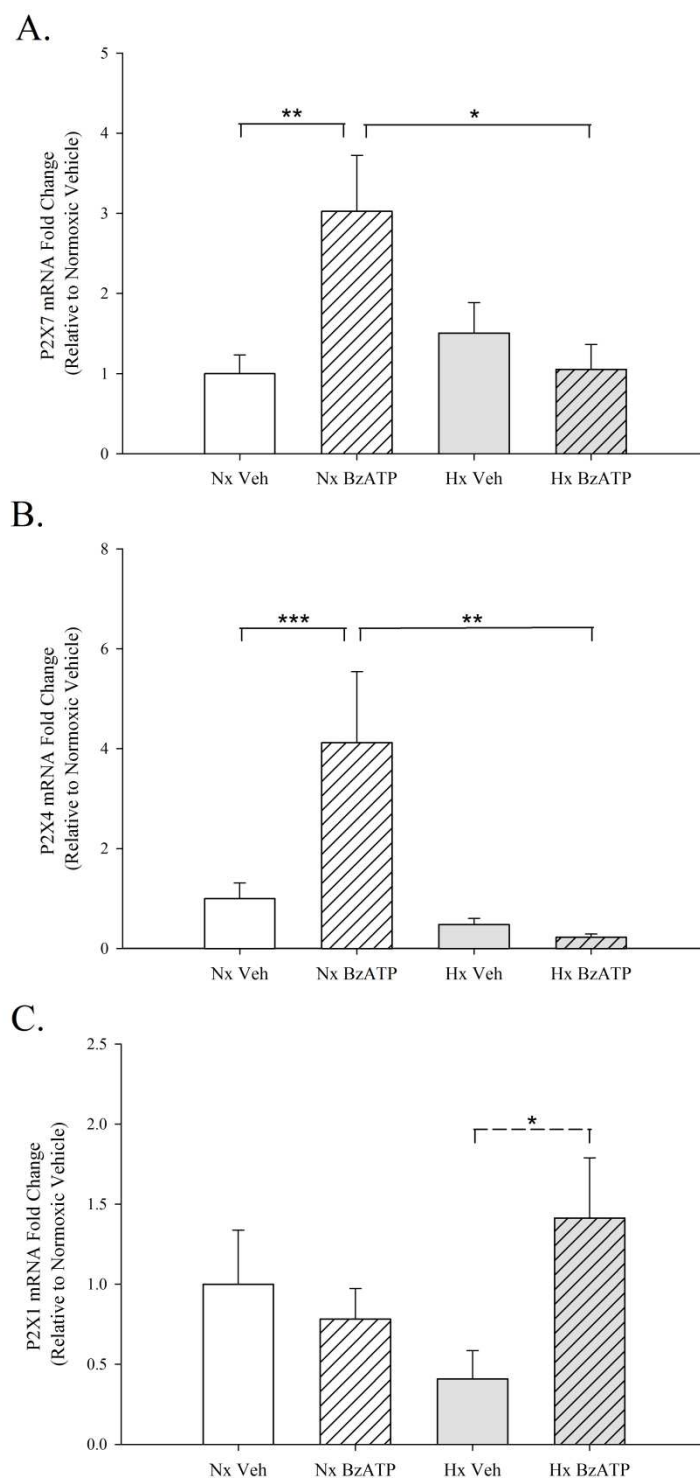


Figure Legend 2**Effects of BzATP treatment and hypoxia exposure on microglial P2X receptor gene expression.**

Brainstem microglia were immunomagnetically isolated from animals treated with vehicle (Veh) or BzATP and exposed to normoxia (Nx) or hypoxia (Hx). Total RNA was isolated and subjected to qRT-PCR for analysis of: A) P2X7 B) P2X4 and C) P2X1 receptors. Whereas hypoxia alone had no effect on P2X receptor expression, BzATP treatment increased P2X7 and P2X4 expression in normoxia, effects that were prevented in hypoxia. Neither BzATP treatment in normoxia, or hypoxia exposure affected P2X1 gene expression, but BzATP increased P2X1 mRNA levels in hypoxia. Solid lines indicate statistically significant differences determined by Two Way ANOVA and dashed lines by a t-test. * $p < 0.05$; ** $p < 0.01$; *** $p < 0.001$. Data are graphed as fold change relative to vehicle treatment.

FIGURE 3

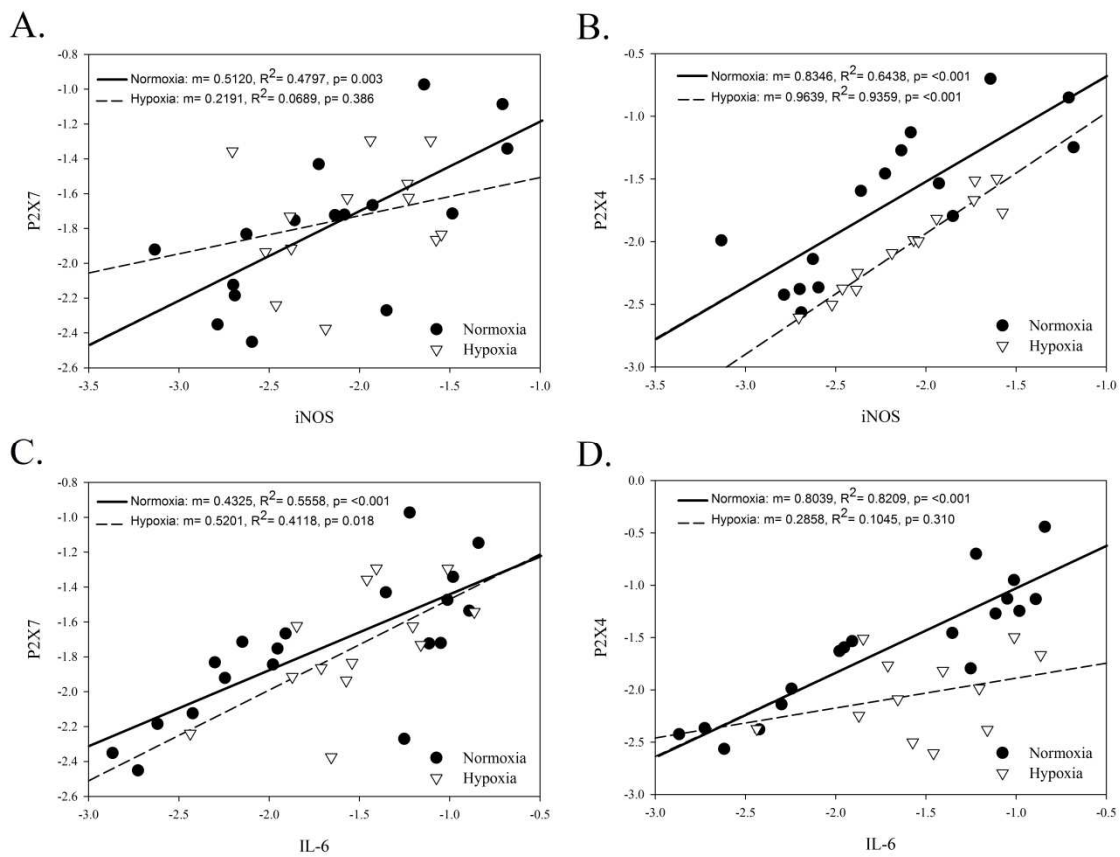


Figure Legend 3

Correlations between P2X4 and P2X7 receptor mRNAs and iNOS and IL-6 gene expression differ in normoxia and hypoxia. Multiple linear regression analyses were performed on inflammatory and P2X receptor gene expression data (logarithmically transformed interpolated C_T values) in normoxia and hypoxia. Correlations between A) iNOS and P2X7, B) iNOS and P2X4, C) IL-6 and P2X7 and D) IL-6 and P2X4 are shown. iNOS expression significantly correlated with both P2X7 and P2X4 receptors in normoxia whereas in hypoxia, correlation with P2X7 was lost. Likewise, IL-6 expression correlated with both P2X4 and P2X7 in normoxia, but correlation with P2X4 was lost in hypoxia.

FIGURE 4

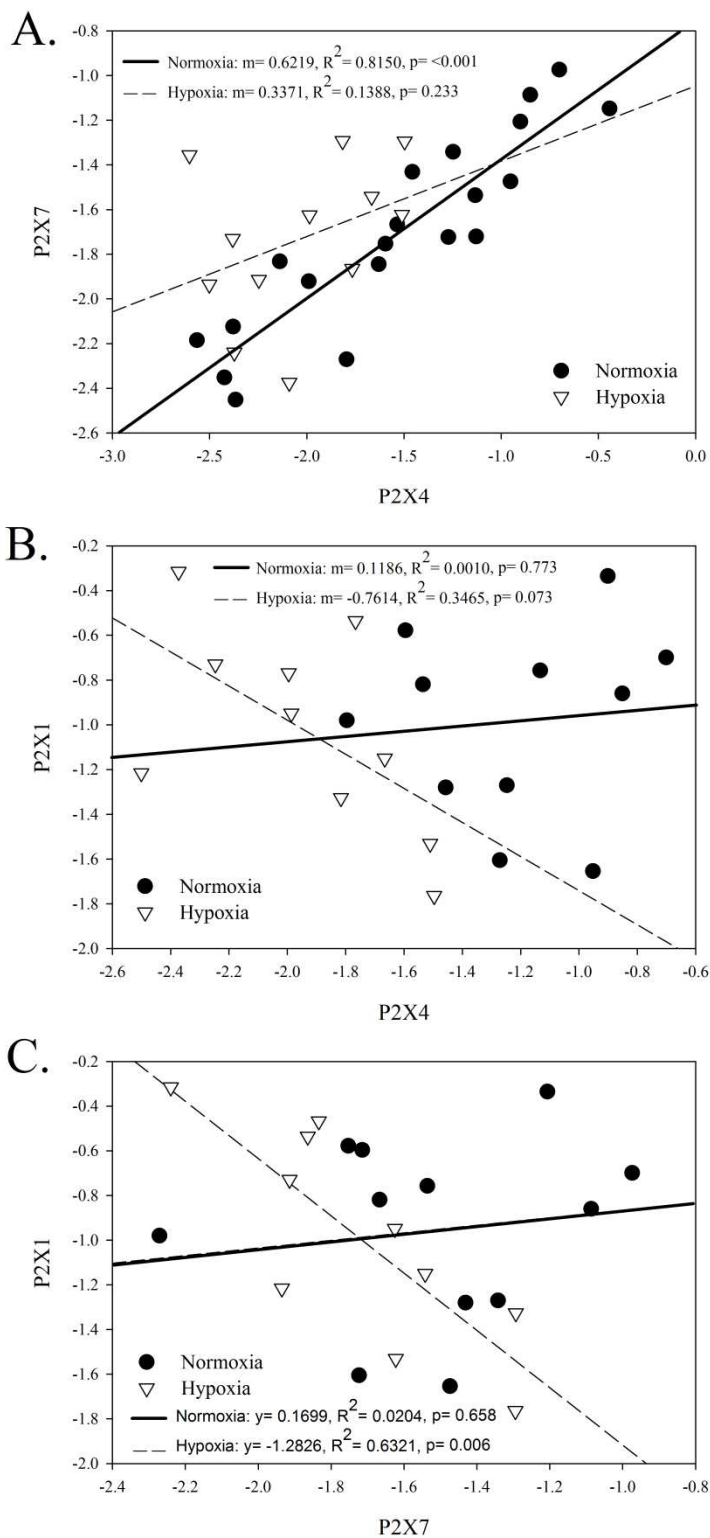


Figure Legend 4

The correlation between P2X4 and P2X7 receptor mRNAs in normoxia is lost in hypoxia when P2X1 receptor expression negatively correlates. Multiple linear regression analyses were performed between P2X receptor data (logarithmically transformed interpolated C_T values) in normoxia and hypoxia. Correlations between A) P2X4 and P2X7 B) P2X1 and P2X4, and C) P2X1 and P2X7 are shown. P2X4 expression significantly correlated with both P2X7 in normoxia, an effect that was lost hypoxia. In hypoxia, P2X1 negatively correlated with both P2X4 and P2X7.

REFERENCES

- 1 Corriden, R. & Insel, P. New insights regarding the regulation of chemotaxis by nucleotides, adenosine, and their receptors. *Purinergic Signalling* **8**, 587-598, doi:10.1007/s11302-012-9311-x (2012).
- 2 Koizumi, S., Ohsawa, K., Inoue, K. & Kohsaka, S. Purinergic receptors in microglia: Functional modal shifts of microglia mediated by P2 and P1 receptors. *Glia* **61**, 47-54, doi:10.1002/glia.22358 (2013).
- 3 Burnstock, G. Physiology and Pathophysiology of Purinergic Neurotransmission. *Physiol. Rev.* **87**, 659-797, doi:10.1152/physrev.00043.2006 (2007).
- 4 Guthrie, P. B. *et al.* ATP released from astrocytes mediates glial calcium waves. *Journal of Neuroscience*. **19**, 520-528 (1999).
- 5 Franke, H., Verkhratsky, A., Burnstock, G. & Illes, P. Pathophysiology of astroglial purinergic signalling. *Purinergic Signalling* **8**, 629-657, doi:10.1007/s11302-012-9300-0 (2012).
- 6 Wake, H., Moorhouse, A. J., Jinno, S., Kohsaka, S. & Nabekura, J. Resting Microglia Directly Monitor the Functional State of Synapses In Vivo and Determine the Fate of Ischemic Terminals. *J. Neurosci.* **29**, 3974-3980, doi:10.1523/jneurosci.4363-08.2009 (2009).
- 7 Davalos, D. *et al.* ATP mediates rapid microglial response to local brain injury in vivo. *Nat Neurosci* **8**, 752-758 (2005).
- 8 Bours, M. J., Dagnelie, P. C., Giuliani, A. L., Wesselius, A. & Di Virgilio, F. P2 receptors and extracellular ATP: a novel homeostatic pathway in inflammation. *Front Biosci (Schol Ed)* **3**, 1443-1456 (2011).
- 9 Hoch, C. C. *et al.* Sleep-disordered breathing in normal and pathologic aging. *J Clin Psychiatry* **47**, 499-503 (1986).
- 10 Atalaia, A., De Carvalho, M., Evangelista, T. & Pinto, A. Sleep characteristics of amyotrophic lateral sclerosis in patients with preserved diaphragmatic function. *Amyotroph Lateral Scler* **8**, 101-105, doi:777130549 [pii]10.1080/17482960601029883 [doi] (2007).
- 11 Manon-Espaillet, R., Gothe, B., Ruff, R. L. & Newman, C. Sleep Apnea in Multiple Sclerosis. *Neurorehabil Neural Repair* **3**, 133-136, doi:10.1177/136140968900300304 (1989).
- 12 Tran, K., Hukins, C., Geraghty, T., Eckert, B. & Fraser, L. Sleep-disordered breathing in spinal cord-injured patients: A short-term longitudinal study. *Respirology* **15**, 272-276, doi:10.1111/j.1440-1843.2009.01669.x (2010).
- 13 Bombois, S., Derambure, P., Pasquier, F. & Monaca, C. Sleep disorders in aging and dementia. *J Nutr Health Aging*. **14**, 212-217. (2010).

- 14 Marcus, C. L., Keens, T. G., Bautista, D. B., von Pechmann, W. S. & Ward, S. L. Obstructive sleep apnea in children with Down syndrome. *Pediatrics*. **88**, 132-139. (1991).
- 15 Di Virgilio, F., Ceruti, S., Bramanti, P. & Abbracchio, M. P. Purinergic signalling in inflammation of the central nervous system. *Trends in Neurosciences* **32**, 79-87, doi:10.1016/j.tins.2008.11.003 (2009).
- 16 Deng, Y. Y., Lu, J., Ling, E. A. & Kaur, C. Role of microglia in the process of inflammation in the hypoxic developing brain. *Front Biosci (Schol Ed)* **3**, 884-900 (2011).
- 17 Nau, R. & Bruck, W. Neuronal injury in bacterial meningitis: mechanisms and implications for therapy. *Trends Neurosci* **25**, 38-45 (2002).
- 18 Sawyer, R. G., Spengler, M. D., Adams, R. B. & Pruett, T. L. The peritoneal environment during infection. The effect of monomicrobial and polymicrobial bacteria on pO₂ and pH. *Ann Surg* **213**, 253-260 (1991).
- 19 Smith, A. L. Pathogenesis of Haemophilus influenzae meningitis. *Pediatr Infect Dis J* **6**, 783-786 (1987).
- 20 Ahlfors, C. E., Goetzman, B. W., Halsted, C. C., Sherman, M. P. & Wennberg, R. P. Neonatal listeriosis. *Am J Dis Child* **131**, 405-408 (1977).
- 21 Hantson, P. *et al.* Fatal Streptococcus suis meningitis in man. *Acta Neurol Belg* **91**, 165-168 (1991).
- 22 Gourine, A. V., Llaudet, E., Dale, N. & Spyer, K. M. Release of ATP in the Ventral Medulla during Hypoxia in Rats: Role in Hypoxic Ventilatory Response. *The Journal of Neuroscience* **25**, 1211-1218, doi:10.1523/jneurosci.3763-04.2005 (2005).
- 23 Di Virgilio, F., Sanz, J. M., Chiozzi, P. & Falzoni, S. The P2Z/P2X7 receptor of microglial cells: a novel immunomodulatory receptor. *Progress in Brain Research* **120**, 355-368 (1999).
- 24 Ferrari, D., Stroh, C. & Schulze-Osthoff, K. P2X7/P2Z purinoreceptor-mediated activation of transcription factor NFAT in microglial cells. *Journal of Biological Chemistry* **274**, 13205-13210 (1999).
- 25 Chessell, I. P., Michel, A. D. & Humphrey, P. P. Properties of the pore-forming P2X7 purinoceptor in mouse NTW8 microglial cells. *British Journal of Pharmacology* **121**, 1429-1437 (1997).
- 26 Ferrari, D., Chiozzi, P., Falzoni, S., Hanau, S. & Di Virgilio, F. Purinergic modulation of interleukin-1 beta release from microglial cells stimulated with bacterial endotoxin. *Journal of Experimental Medicine* **185**, 579-582 (1997).
- 27 Burnstock, G. & Knight, G. E. Cellular distribution and functions of P2 receptor subtypes in different systems. *Int Rev Cytol* **240**, 31-304 (2004).

- 28 Parmentier-Batteur, S. *et al.* Antisense oligodeoxynucleotide to inducible nitric oxide synthase protects against transient focal cerebral ischemia-induced brain injury. *Journal of Cerebral Blood Flow & Metabolism*. **21**, 15-21 (2001).
- 29 Acarin, L., Peluffo, H., Gonzalez, B. & Castellano, B. Expression of inducible nitric oxide synthase and cyclooxygenase-2 after excitotoxic damage to the immature rat brain. *Journal of Neuroscience Research*. **68**, 745-754 (2002).
- 30 Iadecola, C., Zhang, F., Casey, R., Nagayama, M. & Ross, M. E. Delayed reduction of ischemic brain injury and neurological deficits in mice lacking the inducible nitric oxide synthase gene. *Journal of Neuroscience*. **17**, 9157-9164 (1997).
- 31 Lecanu, L., Verrecchia, C., Margail, I., Boulu, R. G. & Plotkine, M. iNOS contribution to the NMDA-induced excitotoxic lesion in the rat striatum. *British Journal of Pharmacology*. **125**, 584-590 (1998).
- 32 Li, R. C. *et al.* Cyclooxygenase 2 and Intermittent Hypoxia-induced Spatial Deficits in the Rat. *Am. J. Respir. Crit. Care Med*. **168**, 469-475, doi:10.1164/rccm.200211-1264OC (2003).
- 33 Kraft, A. D., McPherson, C. A. & Harry, G. J. Heterogeneity of microglia and TNF signaling as determinants for neuronal death or survival. *Neurotoxicology* **30**, 785-793, doi:10.1016/j.neuro.2009.07.001 (2009).
- 34 Spooren, A. *et al.* Interleukin-6, a mental cytokine. *Brain Research Reviews* **67**, 157-183, doi:10.1016/j.brainresrev.2011.01.002 (2011).
- 35 Smith, J. A., Das, A., Ray, S. K. & Banik, N. L. Role of pro-inflammatory cytokines released from microglia in neurodegenerative diseases. *Brain Research Bulletin* **87**, 10-20, doi:http://dx.doi.org/10.1016/j.brainresbull.2011.10.004 (2012).
- 36 Lenzlinger, P., Morganti-Kossmann, M.-C., Laurer, H. & McIntosh, T. The duality of the inflammatory response to traumatic brain injury. *Molecular Neurobiology* **24**, 169-181, doi:10.1385/mn:24:1-3:169 (2001).
- 37 Fabian, R. H., Perez-Polo, J. R. & Kent, T. A. Extracellular superoxide concentration increases following cerebral hypoxia but does not affect cerebral blood flow. *International Journal of Developmental Neuroscience* **22**, 225-230, doi:http://dx.doi.org/10.1016/j.ijdevneu.2004.03.006 (2004).
- 38 Solomon, I. C., Edelman, N. H. & Neubauer, J. A. Pre-Bötzinger Complex Functions as a Central Hypoxia Chemosensor for Respiration In Vivo. *Journal of Neurophysiology* **83**, 2854-2868 (2000).
- 39 Sun, M. K. & Reis, D. J. Hypoxia selectively excites vasomotor neurons of rostral ventrolateral medulla in rats. *American Journal of Physiology - Regulatory, Integrative and Comparative Physiology* **266**, R245-R256 (1994).

- 40 Wasicko, M. J., Melton, J. E., Neubauer, J. A., Krawciw, N. & Edelman, N. H. Cervical sympathetic and phrenic nerve responses to progressive brain hypoxia. *Journal of Applied Physiology* **68**, 53-58 (1990).
- 41 Chávez, J. C., Agani, F., Pichiule, P. & LaManna, J. C. Expression of hypoxia-inducible factor-1 α in the brain of rats during chronic hypoxia. *Journal of Applied Physiology* **89**, 1937-1942 (2000).
- 42 Crain, J., Nikodemova, M. & Watters, J. Expression of P2 nucleotide receptors varies with age and sex in murine brain microglia. *Journal of Neuroinflammation* **6**, 24 (2009).
- 43 Nikodemova, M. & Watters, J. J. Efficient isolation of live microglia with preserved phenotypes from adult mouse brain. *J Neuroinflammation* **9**, 147, doi:10.1186/1742-2094-9-147 (2012).
- 44 Sedgwick, J. D. *et al.* Isolation and direct characterization of resident microglial cells from the normal and inflamed central nervous system. *Proceedings of the National Academy of Sciences of the United States of America* **88**, 7438-7442 (1991).
- 45 Rutledge, R. G. & Côté, C. Mathematics of quantitative kinetic PCR and the application of standard curves. *Nucleic Acids Research* **31**, e93, doi:10.1093/nar/gng093 (2003).
- 46 Friedle, S. A., Brautigam, V. M., Nikodemova, M., Wright, M. L. & Watters, J. J. The P2X7-Egr pathway regulates nucleotide-dependent inflammatory gene expression in microglia. *Glia*. **59**, 1-13. doi: 10.1002/glia.21071. Epub 22010 Sep 21027. (2011).
- 47 Qureshi, O. S., Paramasivam, A., Yu, J. C. H. & Murrell-Lagnado, R. D. Regulation of P2X4 receptors by lysosomal targeting, glycan protection and exocytosis. *Journal of Cell Science* **120**, 3838-3849, doi:10.1242/jcs.010348 (2007).
- 48 Boumechache, M., Masin, M., Edwardson, J. M., Gorecki, D. C. & Murrell-Lagnado, R. Analysis of Assembly and Trafficking of Native P2X4 and P2X7 Receptor Complexes in Rodent Immune Cells. *J. Biol. Chem.* **284**, 13446-13454, doi:10.1074/jbc.M901255200 (2009).
- 49 Gudipaty, L., Humphreys, B. D., Buell, G. & Dubyak, G. R. Regulation of P2X7 nucleotide receptor function in human monocytes by extracellular ions and receptor density. *Am J Physiol Cell Physiol* **280**, C943-953 (2001).
- 50 Lalo, U., Allsopp, R. C., Mahaut-Smith, M. P. & Evans, R. J. P2X1 receptor mobility and trafficking; regulation by receptor insertion and activation. *Journal of Neurochemistry* **113**, 1177-1187, doi:10.1111/j.1471-4159.2010.06730.x (2010).
- 51 Trang, T., Beggs, S. & Salter, M. W. ATP receptors gate microglia signaling in neuropathic pain. *Experimental Neurology* **234**, 354-361, doi:http://dx.doi.org/10.1016/j.expneurol.2011.11.012 (2012).
- 52 Skaper, S. D. Ion channels on microglia: therapeutic targets for neuroprotection. *CNS Neurol Disord Drug Targets* **10**, 44-56 (2011).

- 53 Xiang, Z. & Burnstock, G. Expression of P2X receptors on rat microglial cells during early development. *Glia* **52**, 119-126 (2005).
- 54 Ferrari, D. *et al.* The P2X7 Receptor: A Key Player in IL-1 Processing and Release. *J Immunol* **176**, 3877-3883 (2006).
- 55 Brautigam, V. M., Frasier, C., Nikodemova, M. & Watters, J. J. Purinergic receptor modulation of BV-2 microglial cell activity: Potential involvement of p38 MAP kinase and CREB. *Journal of Neuroimmunology* **166**, 113 (2005).
- 56 Trang, T. & Salter, M. P2X4 purinoceptor signaling in chronic pain. *Purinergic Signalling* **8**, 621-628, doi:10.1007/s11302-012-9306-7 (2012).
- 57 Murrell-Lagnado, R. D. & Qureshi, O. S. Assembly and trafficking of P2X purinergic receptors (Review). *Molecular Membrane Biology* **25**, 321-331, doi:doi:10.1080/09687680802050385 (2008).
- 58 Guo, C., Masin, M., Qureshi, O. S. & Murrell-Lagnado, R. D. Evidence for functional P2X4 / P2X7 heteromeric receptors. *Mol Pharmacol*, mol.107.035980, doi:10.1124/mol.107.035980 (2007).
- 59 Nicke, A. Homotrimeric complexes are the dominant assembly state of native P2X7 subunits. *Biochemical and Biophysical Research Communications* **377**, 803-808 (2008).
- 60 Nicke, A., Kerschensteiner, D. & Soto, F. Biochemical and functional evidence for heteromeric assembly of P2X1 and P2X4 subunits. *Journal of Neurochemistry* **92**, 925-933, doi:10.1111/j.1471-4159.2004.02939.x (2005).
- 61 Funk, G. D. The 'connexin' between astrocytes, ATP and central respiratory chemoreception. *J Physiol* **588**, 4335-4337, doi:10.1113/jphysiol.2010.200196 (2010).
- 62 Huxtable, A. G. *et al.* Glia contribute to the purinergic modulation of inspiratory rhythm-generating networks. *J Neurosci* **30**, 3947-3958, doi:10.1523/jneurosci.6027-09.2010 (2010).
- 63 Gourine, A. V. *et al.* Release of ATP and glutamate in the nucleus tractus solitarii mediate pulmonary stretch receptor (Breuer-Hering) reflex pathway. *J Physiol* **586**, 3963-3978, doi:10.1113/jphysiol.2008.154567 (2008).
- 64 Gourine, A. V., Llaudet, E., Dale, N. & Spyer, K. M. ATP is a mediator of chemosensory transduction in the central nervous system. *Nature* **436**, 108-111, doi:10.1038/nature03690 (2005).
- 65 Huckstepp, R. T. *et al.* Connexin hemichannel-mediated CO₂-dependent release of ATP in the medulla oblongata contributes to central respiratory chemosensitivity. *J Physiol* **588**, 3901-3920, doi:10.1113/jphysiol.2010.192088 (2010).
- 66 Spyer, K. M., Dale, N. & Gourine, A. V. ATP is a key mediator of central and peripheral chemosensory transduction. *Exp Physiol* **89**, 53-59 (2004).

- 67 Inoue, K., Koizumi, S. & Tsuda, M. The role of nucleotides in the neuron–glia communication responsible for the brain functions. *Journal of Neurochemistry* **102**, 1447-1458 (2007).
- 68 Tsuda, M. *et al.* P2X4 receptors induced in spinal microglia gate tactile allodynia after nerve injury. *Nature* **424**, 778-783 (2003).
- 69 Franke, H. *et al.* P2X7 receptor expression after ischemia in the cerebral cortex of rats. *J Neuropathol Exp Neurol* **63**, 686-699 (2004).
- 70 Le Feuvre, R. A., Brough, D., Touzani, O. & Rothwell, N. J. Role of P2X7 receptors in ischemic and excitotoxic brain injury in vivo. *Journal of Cerebral Blood Flow & Metabolism*. **23**, 381-384 (2003).
- 71 Wixey, J. A., Reinebrant, H. E., Carty, M. L. & Buller, K. M. Delayed P2X4R expression after hypoxia-ischemia is associated with microglia in the immature rat brain. *J Neuroimmunol* **212**, 35-43, doi:S0165-5728(09)00148-9 [pii]10.1016/j.jneuroim.2009.04.016 [doi] (2009).
- 72 Li, F. *et al.* Hypoxia induced amoeboid microglial cell activation in postnatal rat brain is mediated by ATP receptor P2X4. *BMC Neurosci* **12**, 111, doi:10.1186/1471-2202-12-111 (2011).
- 73 Kleinert, H., Schwarz, P. M. & Forstermann, U. Regulation of the expression of inducible nitric oxide synthase. *Biol Chem* **384**, 1343-1364, doi:10.1515/BC.2003.152 [doi] (2003).
- 74 Saha, R. N. & Pahan, K. Regulation of inducible nitric oxide synthase gene in glial cells. *Antioxid Redox Signal* **8**, 929-947 (2006).
- 75 Falvo, J. V., Tsytsykova, A. V. & Goldfeld, A. E. Transcriptional control of the TNF gene. *Curr Dir Autoimmun* **11**, 27-60, doi:10.1159/000289196 (2010).
- 76 Spooren, A. *et al.* Cooperation of NFκB and CREB to induce synergistic IL-6 expression in astrocytes. *Cellular Signalling* **22**, 871-881, doi:http://dx.doi.org/10.1016/j.cellsig.2010.01.018 (2010).
- 77 Potucek, Y. D., Crain, J. M. & Watters, J. J. Purinergic receptors modulate MAP kinases and transcription factors that control microglial inflammatory gene expression. *Neurochemistry International* **49**, 204-214 (2006).
- 78 Schonthaler, H. B., Guinea-Viniegra, J. & Wagner, E. F. Targeting inflammation by modulating the Jun/AP-1 pathway. *Annals of the Rheumatic Diseases* **70**, i109-i112, doi:10.1136/ard.2010.140533 (2011).
- 79 Hayden, M. S. & Ghosh, S. NF-κB, the first quarter-century: remarkable progress and outstanding questions. *Genes & Development* **26**, 203-234, doi:10.1101/gad.183434.111 (2012).

- 80 Taylor, C. T. & Cummins, E. P. The Role of NF- κ B in Hypoxia-Induced Gene Expression. *Annals of the New York Academy of Sciences* **1177**, 178-184, doi:10.1111/j.1749-6632.2009.05024.x (2009).
- 81 Nanduri, J., Yuan, G., Kumar, G. K., Semenza, G. L. & Prabhakar, N. R. Transcriptional responses to intermittent hypoxia. *Respiratory Physiology & Neurobiology* **164**, 277-281, doi:http://dx.doi.org/10.1016/j.resp.2008.07.006 (2008).
- 82 Herdegen, T. & Leah, J. D. Inducible and constitutive transcription factors in the mammalian nervous system: control of gene expression by Jun, Fos and Krox, and CREB/ATF proteins. *Brain Research Reviews* **28**, 370-490, doi:http://dx.doi.org/10.1016/S0165-0173(98)00018-6 (1998).
- 83 Ferrari, D., Wesselborg, S., Bauer, M. K. & Schulze-Osthoff, K. Extracellular ATP activates transcription factor NF-kappaB through the P2Z purinoreceptor by selectively targeting NF-kappaB p65. *Journal of Cell Biology* **139**, 1635-1643 (1997).
- 84 Budagian, V. *et al.* Signaling through P2X7 receptor in human T cells involves p56lck, MAP kinases, and transcription factors AP-1 and NF-kappa B. *J Biol Chem* **278**, 1549-1560 (2003).
- 85 Lenertz, L. Y. *et al.* Mutation of Putative N-Linked Glycosylation Sites on the Human Nucleotide Receptor P2X7 Reveals a Key Residue Important for Receptor Function. *Biochemistry* **49**, 4611-4619, doi:10.1021/bi902083n (2010).
- 86 Mongiardi, M. P. Angiogenesis and hypoxia in glioblastoma: a focus on cancer stem cells. *CNS Neurol Disord Drug Targets* **11**, 878-883 (2012).
- 87 Tamajusuku, A. S. K. *et al.* Characterization of ATP-induced cell death in the GL261 mouse glioma. *Journal of Cellular Biochemistry* **109**, 983-991, doi:10.1002/jcb.22478 (2010).
- 88 Martins, I. *et al.* Chemotherapy induces ATP release from tumor cells. *Cell Cycle* **8**, 3723-3728 (2009).
- 89 Watters, J. J., Schartner, J. M. & Badie, B. Microglia function in brain tumors. *Journal of Neuroscience Research* **81**, 447-455 (2005).

CHAPTER 3

**CELL-TYPE SPECIFIC JUMONJI HISTONE DEMETHYLASE GENE EXPRESSION
IN THE HEALTHY RAT CNS: DETECTION BY A NOVEL FLOW CYTOMETRY
METHOD**

Stephanie M.C. Smith, Rebecca S. Kimyon and Jyoti J. Watters

The work from this chapter was accepted for publication in *ASN Neuro* on April 14, 2014.

Published online ahead of print on April 15, 2014. Cell-Type Specific Jumonji Histone Demethylase Gene Expression in the Healthy Rat CNS: Detection by a Novel Flow Cytometry Method. Stephanie M.C. Smith, Rebecca S. Kimyon and Jyoti J. Watters

ABSTRACT

Our understanding of how histone demethylation contributes to the regulation of basal gene expression in the brain is largely unknown in any injury model, and especially in the healthy adult brain. Although Jumonji genes are often regulated transcriptionally, cell-specific gene expression of Jumonji histone demethylases in the brain remains poorly understood. Thus, in the present study we profiled the mRNA levels of 26 Jumonji genes in microglia (CD11b⁺), neurons (NeuN⁺) and astrocytes (GFAP⁺) from the healthy adult rat brain. We optimized a method combining a modified zinc-based fixative (mZBF) and flow cytometry (FCM) to simultaneously sort cells from non-transgenic animals. We evaluated cell-surface, intracellular and nuclear proteins, including histones, as well as messenger- and micro-RNAs in different cell types simultaneously from a single sorted sample. We found that 12 Jumonji genes were differentially expressed between adult microglia, neurons and astrocytes. While *JMJD2D* was neuron-restricted, *PHF8* and *JMJD1C* were expressed in all three cell types though expression was highest in neurons. *JMJD3* and *JMJD5* were expressed in all cell types, but were highly enriched in microglia; astrocytes had the lowest expression of *UTX* and *JHDM1D*. Levels of global H3K27 methylation varied among cell types and appeared to be lowest in microglia, indicating that differences in basal gene expression of specific Jumonji histone demethylases may contribute to cell-specific gene expression in the CNS. This multiparametric technique will be valuable for simultaneously assaying chromatin modifications and gene regulation in the adult CNS.

INTRODUCTION

The CNS is comprised of highly interconnected, yet functionally heterogeneous CNS cell populations. Understanding how these cells function both individually and within a network is crucial to unraveling their role in health and disease. Interpretation of many existing epigenetic and gene regulation studies in the adult CNS are complicated by the fact that they are typically performed on tissue homogenates, so effects within individual cell types cannot be distinguished. Another major technical hurdle in evaluating gene expression *in vivo* is the inability to efficiently isolate nucleic acids (RNA) from paraformaldehyde-fixed and sorted cells since major CNS cell types are best characterized by proteins expressed intracellularly. As a result, investigations of gene regulation in the brain often utilize cultured CNS cells that are usually derived from late embryonic or neonatal animals, confounding understanding of these processes in the adult. Laser capture microdissection^{1,2}, live cell sorting by flow cytometry from transgenic animals expressing fluorescent proteins driven by cell-type specific promoters³, ribosomal-tagging for mRNA isolation from transgenic animals⁴⁻⁶, and alcohol-based fixation to sort neurons for subsequent RNA analysis⁷ are commonly used methods permitting assessments of RNA in specific CNS cell populations, but each have their own drawbacks. Although each technique has enabled significant advances in neurobiology, their limitations include investigations of only a single cell type at a time, the need to use and maintain transgenic animals, and/or the inability to concurrently analyze nucleic acids and intracellular proteins in a single sample. Therefore, we endeavored to overcome these obstacles by optimizing a novel method using non-transgenic, adult rats where proteins and nucleic acids can be concurrently analyzed by flow cytometry (FCM) in multiple neurons and glial cell types simultaneously identified using a combination of intracellular and extracellular markers.

Although FCM is commonly used to analyze and sort pure cell populations, the ability to efficiently recover nucleic acids from formaldehyde-fixed cells is not ⁸. This limitation is particularly significant for neuroscience research because the best-characterized cell-type specific markers for neurons and astrocytes are intracellular, thus requiring fixation and permeabilization for immunostaining-based detection. Guez-Barber and colleagues ⁷ reported the use of an alcohol-based fixative to sort neurons from non-transgenic animals for subsequent RNA analysis, the utility of which for evaluating nucleic acids in sorted neurons has been demonstrated several times ⁹⁻¹¹. However, when endeavoring to isolate nucleic acids from identified and sorted neuron and glial cell populations simultaneously, based on a combination of intracellular and cell surface identification markers, alcohol fixation was ineffective in our studies. We thus turned to a zinc-based fixative (ZBF) which was previously shown to preserve cellular structure, proteins, and nucleic acids in histological and cellular studies ¹²⁻¹⁴. Because a modified ZBF (mZBF) was previously shown to preserve nucleic acids better than standard zinc fixation methods, we evaluated intracellular, extracellular and nuclear proteins, as well as post-translational modifications to histone tails with mZBF after a mechanical dissociation protocol. We found that all parameters were readily preserved. Fixed microglia, neurons and astrocytes were sorted based on cell surface (CD11b) and intracellular markers (NeuN and GFAP, respectively), and we obtained high quality messenger and small non-coding RNAs (miRNAs). We also observed differences in basal histone H3 lysine 27 (H3K27) methylation status among cell types, suggesting fundamental differences in chromatin structure between CNS cell types. The purity of sorted cell populations from the adult CNS was confirmed by evaluation of mRNA levels of cell-type specific genes in individual cell populations.

The importance of histone demethylation in the molecular regulation of CNS gene transcription is becoming increasingly appreciated. Our overall research goal is to understand the role of histone demethylation in regulating gene transcription in individual CNS cell types (microglia, neurons and astrocytes), since cell-specific gene regulation strongly contributes to cell-cell communication in CNS health and disease. Two families of histone demethylases have been identified: lysine specific demethylases (LSD) and Jumonji C (JmjC) domain family proteins¹⁵. Whereas the Jumonji demethylases comprise the largest gene family of histone demethylases, little is known about their expression or function in the adult CNS, in any cell type. To begin to understand how epigenetic regulation influences CNS cell function, and because so little is known about the expression of key Jumonji demethylases in any CNS cell type in the adult, we used the present method to independently profile the expression of the 26 best characterized Jumonji histone demethylase family members in microglia, neurons and astrocytes. We found that seven Jumonji genes had greater than a 3-fold change in mRNA expression levels between cell types. Of these, *PHF8*, *JMJD1C*, and *JMJD2D* had neuron-specific expression, whereas *JMJD3* and *JMJD5* were primarily expressed in microglia. *UTX* and *JHDM1D* had very low expression in astrocytes compared to neurons and microglia. Collectively, these data suggest that there is cell type-specific regulation of basal histone demethylase expression in the CNS. Moreover, because these enzymes have different histone targets and enzymatic specificities¹⁵, these results also suggest that histone demethylation likely plays different functional roles in the control of gene expression in neurons, astrocytes and microglia in the healthy brain. The present technique provides a simple experimental means with which to begin *in vivo* studies of cell-specific epigenetic gene regulation in multiple CNS cell types simultaneously.

MATERIALS AND METHODS

Animals

This study was carried out in strict accordance with the recommendations in the Guide for the Care and Use of Laboratory Animals of the National Institutes of Health. Experiments were performed on adult, male, Sprague-Dawley rats (Harlan, Indianapolis, IN) weighing 300 g \pm 50 g. Rats were housed and handled in accordance with the Guide for Care and Use of Laboratory Animals in an AAALAC-accredited facility. All surgical and experimental procedures were approved by the University of Wisconsin, Madison Institutional Animal Care and Use Committee. All efforts were made to minimize the number of animals used and their suffering.

Materials

Hank's Buffered Salt Solution (HBSS) was purchased from Cellgro (Herndon, VA). Calcium acetate, zinc chloride, zinc trifluoroacetate, glycerol, DEPC, EDTA, and TRI reagent were purchased from Sigma Aldrich (St. Louis, MO). Percoll was purchased from GE Healthcare (Waukesha, WI). DNase was purchased from Worthington Biochemicals (Lakewood, NJ). Lightning Link Antibody conjugation kit was purchased from Novus (Littleton, CO). Glycoblue reagent was purchased from Ambion (Austin, TX). NCode™ VILO™ miRNA cDNA Synthesis Kit, and RNase AWAY, and DAPI were purchased from Invitrogen (Carlsbad, CA). Primers were designed using Primer 3 software and were purchased from Integrated DNA Technologies (Coralville, IA). Power SYBR green was purchased from Applied Biosystems (Foster City, CA). CD11b and GFAP antibodies were purchased from BD Biosciences (San Jose, CA). NeuN, EAAT2 (GLT-1), H3K27me3, H3, and the rabbit IgG isotype control antibodies were purchased from Millipore (Billerica, MA). The H3K27me1 antibody was purchased from Epigentek

(Farmingdale, NY). The goat anti-rabbit PE-CY7 antibody, was purchased from Santa Cruz Biotechnology (Dallas, TX).

Control of RNase and DNase contamination

Special precautions were taken during sample collection and processing to preserve RNA integrity. Only certified nuclease-free plastic ware and/or glassware baked at 400°C for 4 hours were used. All surfaces and tools were treated with RNase AWAY (Invitrogen) to prevent RNase contamination. All solutions were prepared with DEPC-treated water.

Mechanical dissociation and fixation of neural tissue

Rats were euthanized with an overdose of isoflurane anesthetic, and perfused with cold 0.1M phosphate buffered saline (PBS). The brain, excluding olfactory bulbs, brainstem and cerebellum was dissected, and placed into cold HBSS on ice. Samples remained on ice for the duration of the procedure, and all centrifugation steps were performed at 4°C. We modified a mechanical dissociation protocol¹⁶ for creating single cell suspensions of CNS tissues by pushing the tissue through a pre-moistened 100µm filter with a syringe plunger and flushing the filter with ice-cold HBSS supplemented with 0.01mg/ml DNase and 0.1mM EDTA. Myelin was removed by high speed centrifugation at 850g for 15 minutes in a solution consisting of 26% Percoll in 0.1M PBS. Dissociated cells were washed in ice-cold HBSS and pelleted by centrifugation at 350g for 5 minutes. Cells were resuspended in a modified zinc-based fixative (mZBF) (0.5% zinc chloride, 0.5% zinc trifluoroacetate, 0.05% calcium acetate in 0.1M Tris-HCL, pH to 6.4-6.7) and glycerol (1:1), as previously described^{12,14}. Samples were stored at -20°C overnight or until ready to be used. Consistent with previous reports¹⁴, we have stored samples for several weeks with no detectable loss of cell integrity or immunostaining efficiency

(data not shown). To assess the effects of the fixation process on RNA quality, comparisons between fresh and fixed tissues, and fixed/sorted cells were performed.

Cell population analysis by flow cytometry

Fixed samples were washed 3X in ice-cold PBS and permeabilized on ice for 20 min in 1X PBS + 0.2% saponin + 0.1% BSA. All staining occurred on ice in the permeabilization buffer, protected from light. Cells were stained with anti-NeuN-Alexa 488 (1:200), anti-CD11b-PE-Cy7 or PE (1:200), and anti-GFAP- Alexa 647 (1:50) or anti-EAAT2 (GLT-1)-Alexa 647 (1:100) antibodies for 45 min on ice. Prior to staining, the EAAT2 (GLT-1) antibody was custom conjugated to Alexa 647 utilizing the Lightning-Link antibody conjugation kit, according to manufacturer's instructions. Samples were washed and resuspended for sorting in permeabilization buffer containing DAPI (1 µg/ml) to identify cells with intact nuclei. Flow cytometry analysis and cell sorting was performed using a FACSAria II equipped with 350-, 405-, 433-, 532-, and 633-nm lasers, a standard filter set, and FACSDiva software (BD Biosciences). All appropriate compensation and FMO controls were performed and utilized in the analysis. Intact cells were identified using forward and side-scatter parameters, singlet gates, and DAPI staining to identify cells in cell cycle at the time of fixation. Samples were first gated to exclude doublets and any events off scale with the following singlet gates: FSC-Width/SSC-Area, SSC-Width/FSC-Area. We then used a cell cycle gate to identify cells with intact nuclei based on DAPI-Width/DAPI-Area plotted on a linear scale. Cell populations were identified and gated using FMO controls. Cells were identified based on their fluorescence properties, and were sorted through a 120µM nozzle at 14 psi into 1.5 ml Ependorff tubes. Sorted cell populations were defined as the following: neurons (NeuN⁺/CD11b⁻/GFAP or GLT-1⁻), microglia (CD11b⁺/NeuN⁻/GFAP or GLT-1⁻), and astrocytes (GFAP or GLT-1⁺/CD11b⁻/NeuN⁻).

Immediately following the sort, the cells were pelleted and resuspended in Tri Reagent for RNA isolation. Following the sort, an aliquot of the remaining, unsorted, fixed and stained cells was taken for comparison to the unfixed and fixed/sorted cells. Post-sort population analyses and graphical representations were performed in FlowJo software v.10. (TreeStar Inc.). Data are representative of 3 separate experiments with 4 independent samples per experiment.

Cell-Type Identification on ImageStream

Cortical tissue was mechanically dissociated into a single cell suspension, fixed in mZBF, and stained with CD11b-PE, NeuN-Alexa488, GFAP- Alexa647, and DAPI as described above. Fluorescent images were visualized on the Amnis ImageStream. Cellular expression and distribution of these cell identifiers were analyzed in $\geq 20,000$ cells at 40X magnification, using IDEAS software (Amnis).

Detection of histone-tail post-translational modifications

To test whether the mZBF is compatible with detection of histone-tail post-translational modifications by flow cytometry, samples were prepared as described in the previous sections, with the following modifications. Cells were stained with anti-NeuN-Alexa 488 (1:200), anti-GFAP- Alexa 647 (1:50), anti-CD11b-PE (1:200), and rabbit-anti-H3K27me3 (1:100), rabbit-anti-H3K27me1 (1:100), or rabbit-anti-H3 (1:100) antibodies for 45 min on ice. Samples were washed, and stained on ice for 30 min with an anti-rabbit-PE-Cy7 (1:750) secondary antibody. Following incubation with the secondary antibody, the cells were washed and resuspended in permeabilization buffer containing DAPI (1 $\mu\text{g}/\text{ml}$). The cells were analyzed on a BD LSR II equipped with 350-, 405-, 433-, 561-, and 642-nm lasers, a standard filter set, and FACSDiva software (BD Biosciences). All single stain compensations and FMO controls were performed and utilized in the analysis. In single stains and FMO control samples, we included rabbit IgG

isotype control (1:100) for the histone antibodies plus secondary antibodies when appropriate, to control for nonspecific antibody binding. A total of 250,000 events were collected for each sample. Populations were identified and defined as previously described, and the median fluorescent intensity for H3, H3K27me3, and H3K27me1 were calculated for each cell population. All data analyses were performed using FlowJo software v. 10 (TreeStar Inc.). Data are representative of 4 independent rat brain samples.

DNA, mRNA & miRNA extraction/reverse transcription

Total RNA was extracted from fresh, fixed, and fixed/sorted cells according to the Tri Reagent protocol, with the addition of Glycoblue during the isopropanol incubation for RNA isolation. cDNA was synthesized from 0.25µg of total RNA using the NCode™ VILO™ miRNA cDNA Synthesis Kit according to manufacturer's protocol. This enables amplification of both mRNA and miRNAs by qPCR.

Custom Jumonji histone demethylase arrays

A custom Jumonji qRT-PCR array was performed in duplicate on pooled samples (n=4/pool) for the initial broad screen. mRNA expression levels of 26 characterized Jumonji genes were present on the array and results were normalized to the average C_T of the control genes 18s and β -tubulin, using the delta C_T method¹⁷. The expression of a given gene was averaged across all cell types, and expression within a given cell type was normalized to this average. The normalized values were subjected to a Log_2 transformation and were graphically displayed as a heat map created with TreeView software¹⁸. All genes whose expression differed among cell types by greater than 3-fold were independently confirmed by gene-specific qRT-PCR in each of 4 independent sorted samples, derived from 4 different animals.

Quantitative Real-Time PCR (qRT-PCR)

qRT-PCR was performed on cDNA using Power SYBR Green and quantified using an ABI 7500 Fast system. Primers were designed using Primer 3 software and specificity of target gene amplification was confirmed by NCBI BLAST searches and verification that the dissociation curves had a single peak with a T_m consistent with the expected amplicon. Primer efficiency was tested through the use of serial dilutions. Genes were considered non-detectable if the C_T value fell outside of the linear range of the given primer set serial dilution curve. Values from duplicate qPCR measurements were averaged, normalized to the average of two control genes (18s and β -tubulin, for mRNA analyses; and snoRNA135 and snoRNA234, for miRNA analyses), and relative expression was determined using the delta C_T method. Primer sequences are provided in Table 1.

Statistical analyses

Statistical analyses were performed on delta C_T values using Sigma Plot 11.0 software. A one-way ANOVA followed by the Tukey post hoc test was utilized when comparing multiple groups. The student t-test was utilized when comparing two groups. Statistical significance was set at the 95% confidence limit ($p < 0.05$). A single symbol above a bar represents $p < 0.05$; two symbols $p < 0.01$; and three symbols $p < 0.001$. Quantitative data are expressed as the mean \pm 1 SEM.

RESULTS

Mechanical dissociation and mZBF fixation is suitable for the processing of brain tissue for flow cytometry

Mechanically dissociated and fixed adult rat brain tissue samples were analyzed by flow cytometry. The gating strategy involved gating out doublets and off scale events based on the singlet gates obtained using FSC-width/SSC-area and SSC-width/FSC-area. The plots shown in Fig. 1 are from a single sample representative of four independent samples analyzed on the same day. Cells are readily distinguished from debris based on DAPI staining and forward-side scatter properties (Fig. 1A,B). There is a clear separation in the Forward-Side Scatter plot of mechanically dissociated brain tissue (Fig. 1A), representing a visible division between cells and debris. These results are consistent with a report performed on zinc-fixed epithelial cells, showing that ZBF preserves forward-side scatter properties¹⁴. We used DAPI to distinguish between debris and cells with intact nuclei/cells in the cell cycle at the time of fixation (Fig. 1B). DAPI fluorescence was plotted as DAPI-Area/DAPI-Width to both identify the DAPI⁺ cells while also serving as an additional singlet gate. The DAPI⁺ cell population accounts for $49.2 \pm 3.1\%$ (n=4) of the total number of events. The DAPI stain is essential, as it acts as an additional means to identify intact cells and to exclude debris from the sample (Fig. 1C). This reduces background autofluorescence and signal from non-specifically bound antibody.

Microglia, astrocytes, and neurons can be simultaneously identified in the non-transgenic, adult CNS

Dissociated and fixed samples were stained with antibodies to identify microglia (cell surface, anti-CD11b), astrocytes (intracellular, anti-GFAP or cell surface, anti-GLT-1), and neurons (intracellular, anti-NeuN). Distinct populations of DAPI⁺ microglia (Fig. 2A), neurons

(Fig. 2A,C), and astrocytes (Fig. 2B,C) were identified based on their immunofluorescent properties. There was clear separation between CD11b vs. NeuN (Fig. 2A) and CD11b vs. GFAP (Fig. 2B) immunostained cells. To determine if there was overlap between the NeuN and GFAP staining, we plotted NeuN vs. GFAP in the CD11b⁻ cell population (Fig. 2C). There were separate populations of cells that were single positive for NeuN (42.6% ± 2.29), GFAP (3.78% ± 0.28) and CD11b (11.3% ± 1.85) (n=4). However, there was also an unexpected population of cells that were double positive for NeuN and GFAP (0.94% ± 0.21, n=4). In addition, there was a population of DAPI⁺ cells that were triple negative for CD11b, NeuN, and GFAP (39.0 ± 1.3%, n=4). All CNS cells are not recognized by immunostaining with these three markers. On a per 100mg of tissue basis, Table 2 summarizes the cell population frequencies, as well as the average number of cells of each type obtained in 3 separate and independent sample sorts. A wide Forward Scatter (FSC)/Side Scatter (SSC) gate is necessary to encompass all neurons and astrocytes, and indicates that each cell type exhibits different but overlapping scatter properties (Fig. 2D). Single positive CD11b⁻, GFAP⁻, and NeuN-stained cells were visualized with an ImageStream analysis system where distribution and localization of immunostaining was evaluated in single cells (Fig. 2E). Data shown in Fig. 2A-D are from a single sample representative of four independent samples, analyzed on the same day.

mZBF permits retrieval of intact ribosomal-, messenger-, and micro- RNAs from sorted CNS cells

We next sought to determine if we could isolate RNA from the mZBF-fixed and sorted cells. Table 2 indicates the average RNA concentrations obtained from 50,000 cells, and the purity of RNA obtained from each cell population based on the 260/280 ratios. To assess whether RNAs isolated from mZBF-fixed and sorted CNS cells was of suitable quality for

downstream analyses, we utilized qRT-PCR to compare the levels of two commonly used “control genes”, the ribosomal RNA18s, and the messenger RNA, β -tubulin (n=8). We examined this in live cells (unfixed), and cells that were either fixed and unsorted, or fixed and sorted, to test the influence of both the fixation and sort processes. We found that the C_T values for both 18s and β -tubulin with zinc fixation were higher when compared to C_T values in live, unfixed cells (Fig. 3A), indicating that RNA quality is somewhat reduced by the fixation process, or that there are factor(s) acting as PCR inhibitors. Interestingly, 18s RNA appears to be more negatively affected by the fixation process than β -tubulin, suggesting a potential RNA size effect. When compared to live cells, the C_T values for 18s were increased by ~ 3 cycles in both the fixed/unsorted ($p < 0.001$) and fixed/sorted ($p < 0.001$) samples, whereas β -tubulin was increased by ~ 1 cycle in the fixed/unsorted samples ($p = 0.260$) and by 2 cycles in the fixed/sorted samples ($p = 0.024$). This suggests that larger RNAs may be more susceptible to degradation and/or that they are more difficult to isolate than smaller RNAs. Although there is indication that the fixation process causes some RNA degradation/PCR inhibition, mRNA levels are readily detectable, and the sorting process does not appear to further compromise downstream analyses. We next compared the levels of 18s and β -tubulin among microglia, astrocytes and neurons (Fig. 3B). We found that 18s levels were significantly lower in astrocytes (GFAP⁺) compared to levels in microglia (CD11b⁺; $p < 0.002$) and neurons (NeuN⁺; $p = 0.001$). In addition, the expression of β -tubulin was significantly higher in neurons compared to microglia ($p < 0.001$) and astrocytes ($p = 0.001$).

Since we were effective in retrieving both rRNA and mRNA from fixed/sorted cells, we next evaluated the compatibility of zinc fixation with the recovery of small RNAs in four independent samples derived from four separate animals. We screened two small noncoding

nuclear RNAs that are often used as loading controls for miRNA qRT-PCR studies, snoRNA135 and snoRNA234. We successfully detected both snoRNAs (Fig. 3C), and found no cell-type specific differences in the levels of either ($p=0.278$ and $p=0.463$, respectively). Finally, we screened two microRNAs (miRNAs): miR-26 highly expressed in the CNS¹⁹, and miR-146a, an important regulator of innate immune responses in microglia²⁰⁻²². Although they did not reach statistical significance, we found that compared to expression levels in microglia, miR-26 tended to be 2-3 fold more highly expressed in neurons ($p=0.051$) and astrocytes ($p=0.080$). miR-26 expression levels were comparable in astrocytes and neurons ($p=0.696$). miR-146a was highly expressed in microglia, but as expected, it was nearly undetectable in both astrocytes ($p=0.006$) and neurons ($p=0.001$).

It is unclear at this time if the differences in C_T values among cell types for 18s and β -tubulin are the result of cell type-specific differences in expression of these RNAs, or if there are inherent differences in the quality of RNA harvested from different cell populations. We suspect the latter because similar differences in expression patterns were observed with two other housekeeping RNAs (snoRNA135 and snoRNA234), although they were not statistically significant. snoRNA135 was similar in pattern to 18s whereas snoRNA234 was similar to β -tubulin. In addition, the quantity of RNA obtained from the same number of cells based on absorbance at 260nm appeared to be 3-4 times higher for astrocytes compared to neurons and microglia (Table 2). To account for these differences in subsequent gene expression analyses, we averaged the 18s and β -tubulin C_T values for ΔC_T calculations.

Cell-specific gene expression confirms purity of fixed, stained and sorted cells

Using qRT-PCR to analyze the expression of known cell-type specific genes, we assessed the purity of sorted neuron, microglia, and astrocyte cell populations from four independent cells

sorts. We found that the neuron specific genes NeuN, β -III tubulin, and neurofilament were highly expressed in NeuN⁺ cells, and that NeuN and β -III tubulin were lowly expressed or undetectable in microglia and astrocytes (Fig. 4A). Surprisingly, neurofilament was somewhat detectable in both microglia and astrocytes. The microglia-specific genes CD11b, Iba-1, and CD68 were highly expressed in microglial (CD11b⁺) cells, and lowly expressed or undetectable in astrocyte (GFAP⁺) and neuron (NeuN⁺) populations (Fig. 4B). Likewise, the astrocyte-specific genes GFAP, GLT-1, and ALDH1L1 were highly expressed in GFAP⁺ cells (Fig. 4C) and lowly expressed in microglia and neurons.

Cell-type specific expression of Jumonji histone demethylases

We used a custom qPCR array to analyze the expression of 26 JmjC-domain containing histone demethylases (Jumonji demethylases) in sorted microglia, neurons and astrocytes. For initial screening purposes, we pooled equal amounts of cDNA from 4 independent animal samples into a single sample (run in duplicate) to obtain the average expression of each Jumonji gene in all cell types. We found that 12 of the 26 Jumonji mRNAs were differentially expressed among cell types by at least 2-3 fold, and 7 had greater than a 3-fold change relative to the other cell types (Fig. 5A). We confirmed these results in samples from four independent cell sorts, obtained from four different animals, using qRT-PCR to profile the Jumonji mRNAs identified by the array as being the most differentially expressed in all three cell types: PHF8, JMJD2D, JMJD3, JMJD5, UTX, JHDM1D, and JMJD1C (Fig. 5B). We found the expression of PHF8, JMJD1C and JMJD2D to be highly specific to neurons. In addition, we found that JMJD3 and JMJD5 were primarily expressed in microglia (2.7 ± 0.60 and 2.2 ± 0.2 fold higher relative to neurons, respectively). Finally, UTX and JHDM1D mRNA levels were very low in astrocytes (0.17 ± 0.04 and 0.23 ± 0.04 fold relative to that in NeuN⁺ cells, respectively).

Identification of histone-tail post-translational modifications by flow cytometry

To determine if investigations of the functional role of Jumonji histone demethylases in sorted CNS cells could be performed using this method, we next assessed whether histone-tail post-translational modifications could be visualized by flow cytometry in mZBF-fixed microglia, neurons and astrocytes. We co-stained cells with antibodies against monomethylated lysine 27 on histone H3 (H3K27me1) (Fig. 6A,B) and trimethylated H3K27 (H3K27me3) (Fig. 6C,D), together with cell specific markers. As expected, we detected both H3K27me3 and H3K27me1 in all cell types. However, neurons and astrocytes appeared to have increased and more heterogeneous expression of mono- and tri-methylated H3K27 than microglia as evidenced by broader peaks on the histogram. We also used an antibody against the H3 histone protein that recognizes an epitope on the carboxy terminus of the core histone not readily accessible in its native conformation. With this antibody, we observed only a slight shift in the mean fluorescent intensity (Fig 6E,F) although pan H3 immunostaining in microglia, in contrast to the methylated immunostaining at H3K27, appeared to be greater than in neurons and astrocytes. These results indicate that native histone structure is maintained in the mZBF-fixed cells, that histone tail post-translational modifications can be visualized by flow cytometry in this fixative, and that levels of methylated histones differ among CNS cell types.

DISCUSSION

To our knowledge, this is the first study to successfully identify and isolate distinct CNS neuron and glial cell populations simultaneously from the adult, non-transgenic, rodent brain based on a combination of intra- and extra-cellular markers by flow cytometry. The modified zinc-based fixative used here preserves cell surface, intracellular, and nuclear protein structure, and we have used it to perform analyses of cell cycle, histone tail modifications, and other proteins prior to cell sorting, maximizing the information obtainable from a single CNS tissue sample. We show that the quality of ribosomal, messenger, and micro RNAs retrieved from the sorted cells is adequate for subsequent downstream qRT-PCR analyses, providing a means to study epigenetic regulation of gene expression in specific CNS populations from the same sample. This important technical advance represents a particularly significant step forward for gene expression studies in non-neuronal cell types for which intracellular epitopes are the best characterized, and/or for which antibodies against extracellular epitopes of cell type-specific surface markers are not widely available. An additional benefit of this method is the ability to store samples for many weeks for later analyses.

Cellular fixation and permeabilization are necessary for antibody-mediated detection of intracellular antigens by FCM. Recovery of RNAs from standard formaldehyde- or paraformaldehyde-fixed cells is poor^{8,23} especially when cell numbers are limiting, and alcohol fixation is not ideal for extracellular marker-based cell identification (data not shown, and^{24,25}). Several recent studies have successfully used an alcohol-based fixation method for recovery of RNA from intracellularly-identified neuron populations^{9,11,26}. However, because we wished to use a combination of intracellular and cell surface markers for cell identification, we applied the modified zinc-based fixation method to isolate RNAs from fixed and sorted neurons and glia.

Consistent with previous reports¹²⁻¹⁴, DNA could also be successfully isolated from zinc-fixed cells (data not shown), increasing the utility of this technique for the study of epigenetic DNA modifications. Many fields are plagued by the need/desire to fix samples prior to flow cytometric analysis and/or cell sorting, and more information can be obtained from fixed cells (because intracellular proteins can be quantified). Fixation often adds a level of safety for more biohazardous samples since significant biosafety concerns are present when working with human, pathogen-infected or virally-transduced cells, particularly in flow cytometry facilities where the potential for aerosolization is high²⁷. Although not tested here, this fixation method may also be a useful alternative to live sorting when nucleic acid recovery is desired from biohazardous samples.

We undertook the present study to begin to investigate the epigenetic control of gene expression in microglia and neurons as it relates to cell-cell communication in pathology. Although live microglia can easily be identified and sorted based on cell surface marker identification (e.g. CD11b)²⁸, the same cannot be done with live neurons, as the best-characterized markers are intracellular. Adult astrocyte identification also suffers from the same issues as neurons with regard to intracellular markers and/or antibodies only being available towards intracellular epitopes of cell surface markers (e.g. GLT-1). Indeed, the dissociation procedure reported here is not optimized for astrocytes as the mechanical disruption decreases astrocyte viability, reducing their recovery. However, the mechanical method was optimal for the retrieval of neurons and microglia, which are the major cell types of interest to us. In the course of optimizing this technique for our purposes, we found that enzymatic dissociation with papain²⁸ permitted much better astrocyte recovery, although it greatly decreased neuron retrieval (data not shown). Efficiency of microglial recovery with both methods was not different. The overlap

observed between the GFAP⁺ and NeuN⁺ cells (<1%; Fig. 2C) is likely a product of the mechanical dissociation process. For example, incomplete dissociation may result in astrocyte debris sticking to neuronal cells. Alternatively, GFAP/NeuN double positive cells could represent a population of neural progenitor cells expressing both NeuN and GFAP markers²⁹. Results from the ImageStream analyses supported both notions: whereas there were true NeuN⁺/GFAP⁺ double positive cells (likely precursor cells), most were double positive because of cell debris stuck to an intact cell (data not shown). In addition, there was a large proportion of cells (~39%) that were triple negative for the three cell identification markers used here. Although additional studies are needed to specifically identify the members of this cell population, we speculate that these are likely to be astrocyte/glia cells and endothelial cells that were not identified by the primary markers used here. For example, whereas GFAP is the most commonly used marker for astrocytes, it is only expressed by a fraction of astrocytes, the intensity and percentage of which varies throughout the brain³⁰. Thus, while the present dissociation method is not ideal for GFAP⁺ astrocyte recovery, more efficient and universal astrocyte identification may require simultaneous staining with multiple astrocyte markers (e.g. GFAP, GLT-1, ALDH1L1), regardless of dissociation method.

Because histone demethylation is commonly associated with the activation/repression of gene transcription^{15,31}, and many microglial inflammatory activities require new gene transcription of cytokines and other mediators of inflammation^{32,33}, we were particularly interested in which histone demethylase enzymes were expressed in microglia and neurons. In this study, we focused on the Jumonji histone demethylase gene family that contains 30 members based on sequence homology¹⁵. The Jumonji demethylases catalyze a dioxygenase reaction to remove mono-, di- and tri-methyl groups from lysine and arginine residues, primarily on histone

H3, H4 and H1 substrates. This reaction is dependent on Fe (II) and α -ketoglutarate¹⁵. There is very little known about the role of Jumonji histone demethylases in the regulation of CNS function in general, and nothing is known about their cell-specific expression in the adult CNS. Given the significant differences in gene expression profiles in microglia, neurons and astrocytes, we hypothesized that there would be cell type-specific differences in the basal expression of the Jumonji demethylase genes.

We found that seven Jumonji family genes were most differentially expressed between neurons, microglia and astrocytes. PHF8, JMJD1C, and JMJD2D were highly neuron-specific as they were undetectable or very lowly expressed in microglia and astrocytes. Neuronal expression of PHF8 and JMJD1C is consistent with previous reports^{34,35}. PHF8 is important for proper neural development³⁴, and its mutation is associated with Fragile X syndrome, believed in part to be responsible for the associated cognitive deficits^{36,37}. JMJD1C protein levels are high in androgen-responsive neurons where it is proposed to be involved in the co-activation of the androgen receptor³⁵. Although mutations in the JMJD1C gene are linked to the development of autism^{38,39}, this relationship is not fully understood as the histone substrate for this enzyme has not yet been identified¹⁵. Very little is known about the role of JMJD2D in the CNS. However, similar to JMJD1C, JMJD2D acts as an androgen receptor co-activator in the prostate⁴⁰. Perhaps in the CNS, JMJD2D plays a similar role to JMJD1C. We found that JMJD3 and JMJD5 were more highly expressed in microglia than in astrocytes or neurons. JMJD3 is an important regulator of both inflammatory⁴¹⁻⁴³ and anti-inflammatory activities in macrophages⁴⁴, and JMJD5 expression in osteoclasts is an important regulator of osteoclastogenesis⁴⁵. There is now one report of a Jumonji gene family member (JMJD3) in microglia⁴⁶. JMJD3 was shown to be critical for switching between inflammatory and anti-inflammatory/reparative phenotypes in

immortalized microglia, consistent with reported effects in macrophages. Finally, we found UTX and JHDM1D to be more lowly expressed in astrocytes, compared to neurons and microglia. UTX is an X-chromosome-linked gene and is more highly expressed in the female brain ⁴⁷, but nothing is known about its expression in astrocytes. Only male rats were included in our study; thus, it is possible that UTX levels may be higher in astrocytes isolated from female rats. Interestingly, a point mutation in the UTX gene results in Kabuki syndrome ^{48,49} characterized by developmental delay, cognitive disabilities, and craniofacial abnormalities. Because these morbidities are also associated with aberrant astrocyte activity (e.g. Alexander disease, Fragile X disease) ⁵⁰, impaired or overactive UTX activity in astrocytes specifically, may play an important physiological role in neuropsychiatric disease. Lastly, little information is available on the role of JHDM1D in the brain. It is known to regulate neural differentiation ⁵¹ and neural fate specification ⁵² during embryogenesis. We find its expression in the adult CNS to be lowest in astrocytes and highest in neurons, consistent with the idea that the JHDM1D gene may be down-regulated in astrocytes after progenitors have committed to the glial phenotype. Whether differences in basal Jumonji demethylase gene expression contribute to cell type-specific regulation of gene expression in the adult CNS is not yet known, but the present data are consistent with this possibility.

There are apparent differences in the magnitude of mono and tri-methylated H3K27 among CNS cell types, with neurons having the highest expression of both marks. While the significance of this is not yet clear, differences in H3K27 methylation at specific gene promoters may contribute to fundamental, cell-specific differences in gene expression profiles among these cell types. Additional studies involving chromatin immunoprecipitations are necessary to test this hypothesis further. In addition to histone modifications, miRNAs are another important aspect of

epigenetic gene regulation. In this study, we evaluated levels of miR-146a and miR-26 in sorted microglia, astrocytes, and neurons to determine if the quality of recovered miRNAs from cells processed in this way was adequate for subsequent investigation. While we could easily amplify miRNAs, we found cell type specificity of the 2 miRNAs we evaluated. We found that miR-146a was highly expressed in microglia (but was very low in neurons and astrocytes), consistent with its expression primarily in myeloid lineage cells^{20,53}. Because miR-26 is reported to be preferentially expressed in astrocytes¹⁹, we were surprised to find it equally detectable in astrocytes and neurons. However, the astrocyte-specific expression of miR-26 was determined in differentiated murine stem cells *in vitro*¹⁹. Our samples are rat, and there are significant species differences in miRNAs. Alternatively, differences may be related to cell age. Our studies were performed on adult cells isolated from the whole brain; stem cells differentiated *in vitro* may not accurately reflect identical gene expression levels and patterns of 3 month-old adult cells *in vivo*. Further, gene expression in neurons and astrocytes *in vivo* are highly influenced by the CNS microenvironment and cannot be identically recapitulated *in vitro* during stem cell differentiation. Together, these results reinforce the need to study miRNAs in specific cell types *in vivo*.

In conclusion, this technique adapts known flow cytometry and cell fixation methods to the field of neuroscience, advancing our ability to study epigenetics and gene regulation simultaneously in glia and neurons. To lay the foundation for future studies of histone demethylation-regulated gene expression, we utilized this procedure to investigate the profile of Jumonji gene family histone demethylase expression in neurons, microglia and astrocytes from the healthy CNS. Our findings are consistent with the limited available literature. More importantly, the results provide new information about cell-specific Jumonji gene expression in

the adult CNS, underscoring the importance of understanding cell-specific regulation of epigenetic modifiers in the adult, non-transgenic brain.

ACKNOWLEDGEMENTS

We would like to thank Drs. Tracy Baker-Herman and Gordon Mitchell for helpful discussions and their continued support of this project, and Dagna Sheerar and Jamie Boyd from the UW-Madison flow core facility for their assistance with the flow cytometry aspects of this study. We also wish to specially acknowledge Dr. Robert Thacker from Amnis for his assistance with the ImageStream data acquisition and analyses. Supported by the National Institutes of Health [NS049033, HL111598 and T32HL007654] and the BD Biosciences Research Innovation Award in Immunology.

FIGURE 1

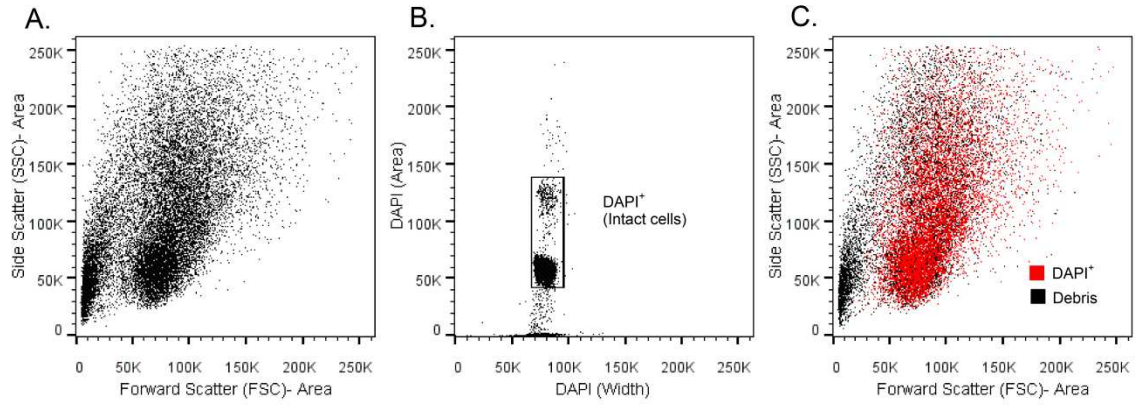


Figure Legend 1

FSC/SSC and DAPI staining identifies intact CNS cells. Rat brain tissue was mechanically dissociated into a single cell suspension, fixed in mZBF, and processed for flow cytometry, as described in the Methods. Doublets and off scale events were gated out based on FSC-Area/SSC-Width and SSC-Area/FSC-Width. All plots started with the same singlet gate. (A) Typical Forward/Side Scatter plot for rat brain cells. (B) To remove dead cells and debris from the analysis, we used DAPI staining to gate on cells that were in the cell cycle at time of fixation. (C) Backgating on DAPI⁺ cells identified where debris and intact cells appeared on the Forward/Side Scatter plot. Data shown are representative of 4 independent experiments.

FIGURE 2

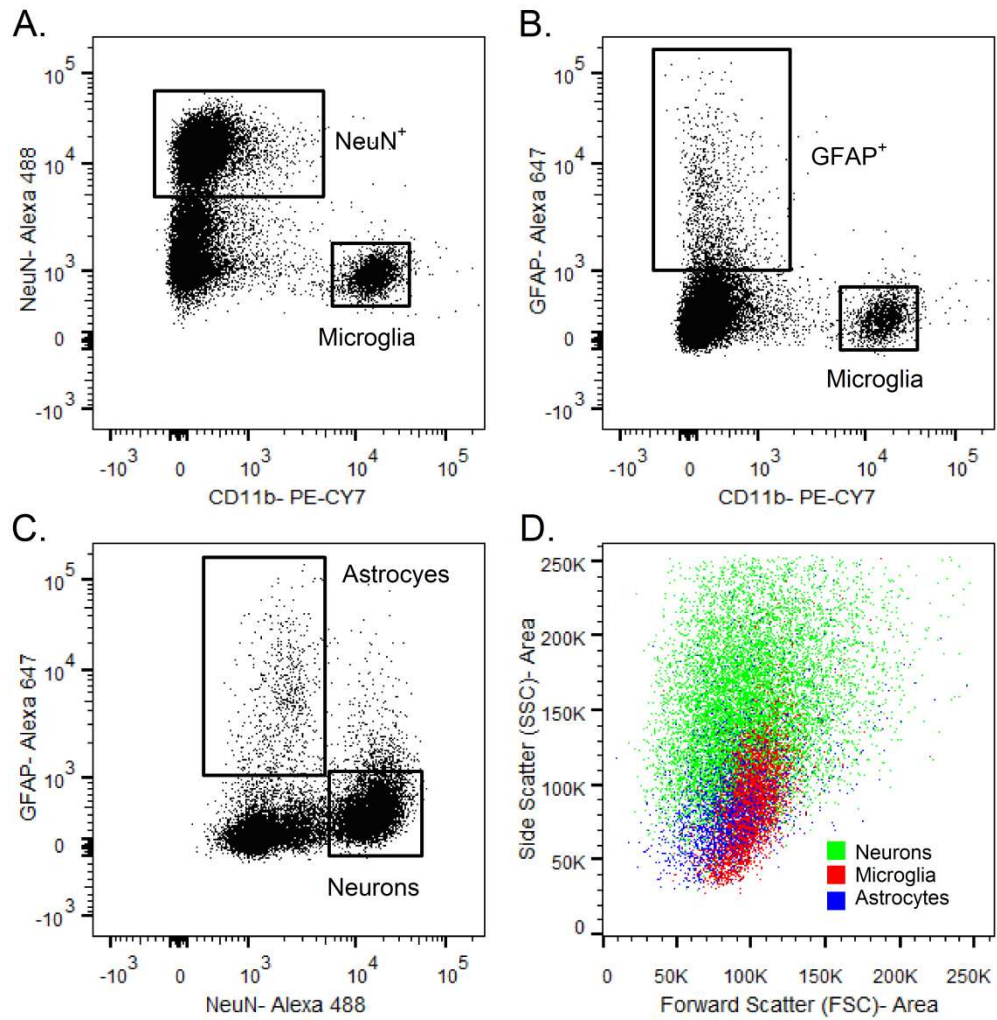


Figure Legend 2

Neurons, microglia, and astrocytes are simultaneously identified by FCM. Single cell mZBF-fixed suspensions were processed for flow cytometry. Singlet cells were gated as described above, and then gated on DAPI as in Fig. 1B. DAPI⁺ neurons, microglia, and astrocytes were identified using antibodies against the cell-specific markers NeuN (neurons; A,C), CD11b (microglia; A,B), and GFAP (astrocytes; B,C). (C) CD11b⁻ cells were plotted against GFAP and NeuN, revealing single positive GFAP and NeuN populations as well as a small GFAP and NeuN double positive population. (D) An overlay of the single positive CD11b, NeuN, and GFAP populations reveals that they have overlapping and variable Forward/Side Scatter properties indicating that these parameters alone are not useful on their own for cell-type identification in the CNS. The data shown are from a single sample that is representative of 4 independent experiments. (E) Representative images of DAPI⁺ cells staining single positive for CD11b, GFAP or NeuN from a single experiment of $\geq 20,000$ cells, at 40X magnification obtained using ImageStream analysis.

FIGURE 3

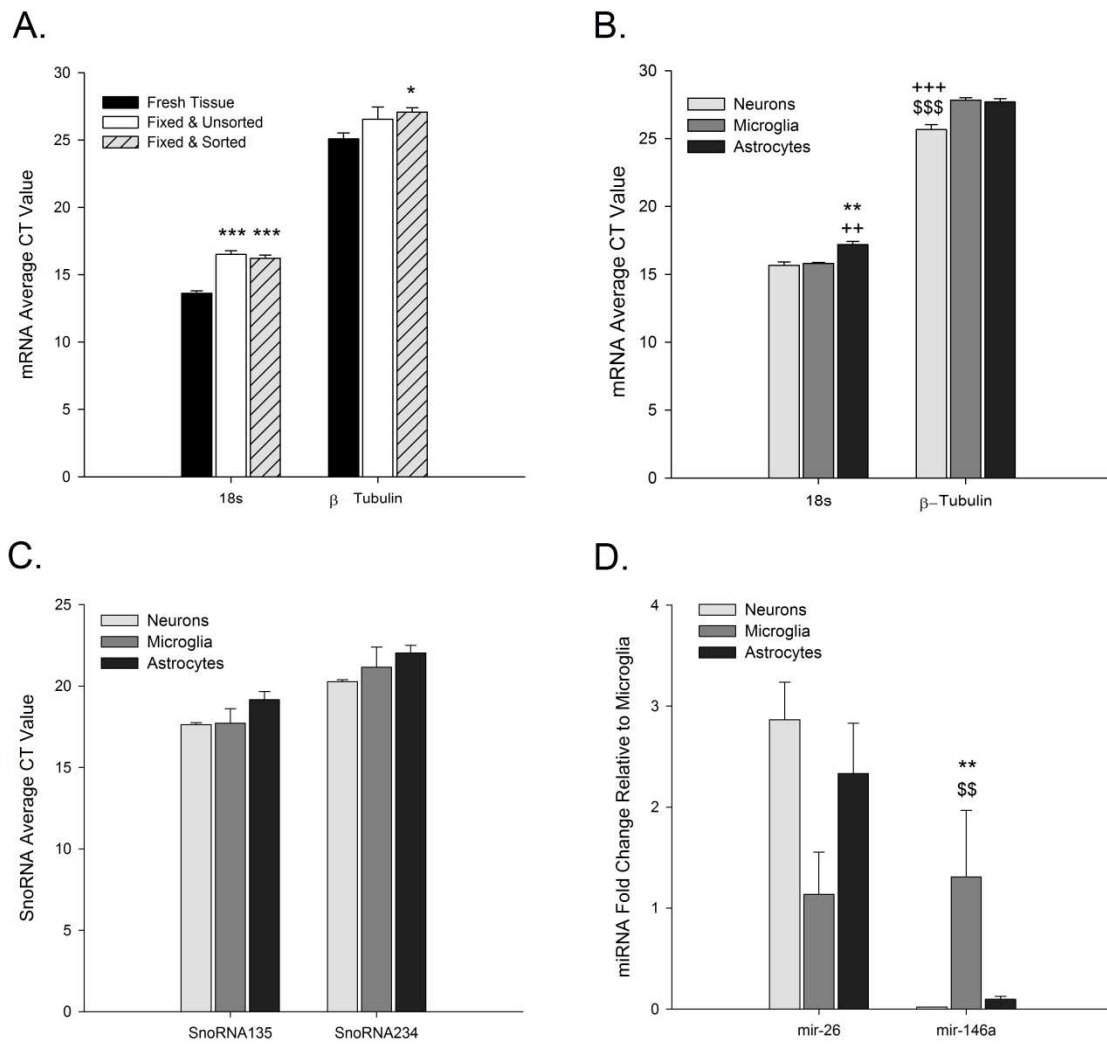


Figure Legend 3

Retrieved RNAs from sorted cells are suitable for analysis by qRT-PCR. RNA was harvested and qRT-PCR was used to analyze the levels of two commonly used housekeeping genes: 18s rRNA and β -tubulin mRNA. Comparisons were made between (A) fresh tissue, fixed/unsorted cells, and fixed/sorted cells (n=4-8), or (B) sorted neurons (NeuN⁺), microglia (CD11b⁺), and astrocytes (GFAP⁺) (n=8). (C) The expression of two commonly used housekeeping small non-coding RNAs (SnoRNA-135 and -234) and (D) two microRNAs miR-26 and miR-146a in neurons (NeuN⁺), microglia (CD11b⁺), and astrocytes (GLT1⁺) were also evaluated (n=4). Symbols indicate significant differences between samples as assessed by a One-Way ANOVA. * vs. fresh tissue (A) or neurons (B-D); + vs. microglia; and \$ vs. astrocytes. 1 symbol p<0.05; 2 symbols p<0.01; 3 symbols p<0.001.

FIGURE 4

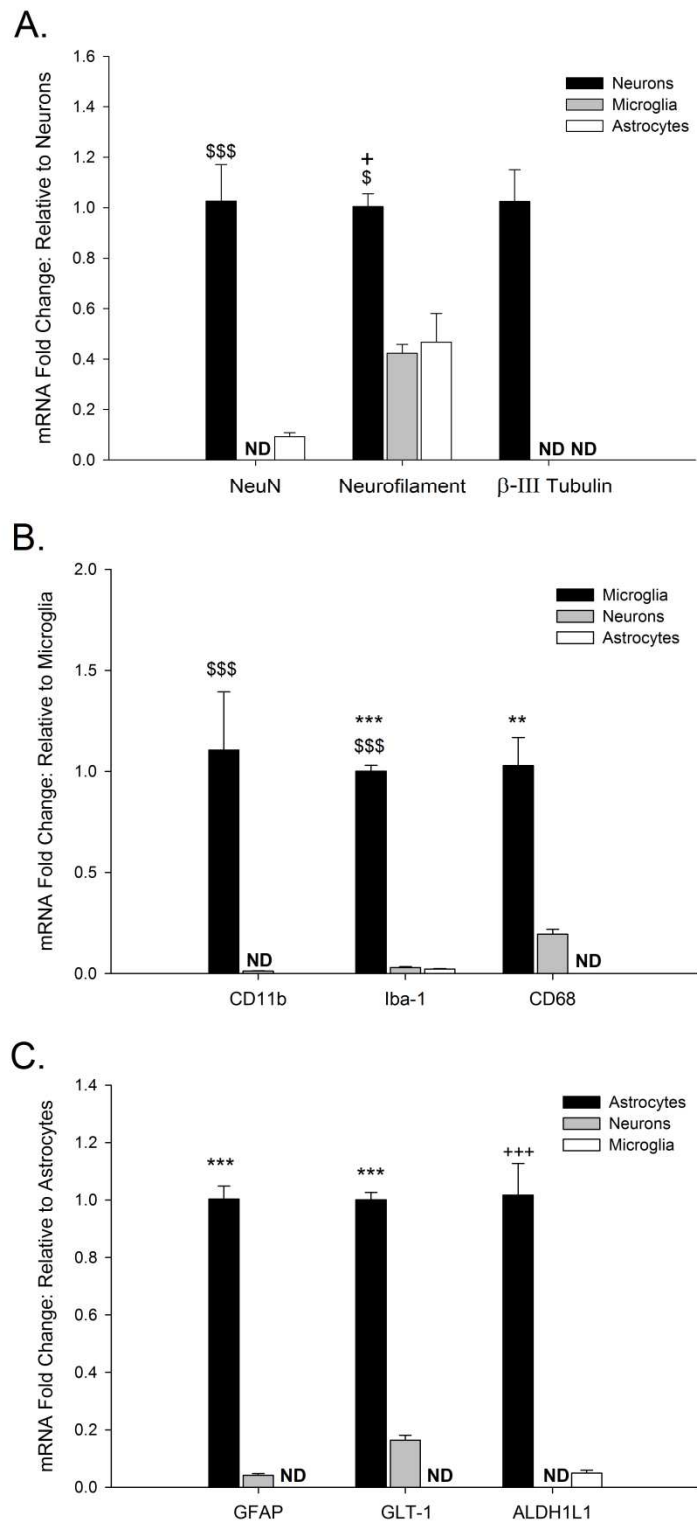


Figure Legend 4

qRT-PCR of cell-specific genes confirms sorted CNS cell purity. Total RNA harvested from fixed/sorted cells was utilized for qRT-PCR of cell-type specific genes to confirm the purity of the sort. (A) The neuron-specific genes NeuN, neurofilament, and β (III)- tubulin), (B) the microglia-specific genes CD11b, Iba-1, and CD68, and (C) the astrocyte-specific genes GFAP, GLT-1, and ALDH1L1 were evaluated in all three cell populations (n=4-8). Symbols indicate significant differences between samples as assessed by a One-Way ANOVA. * vs. neurons; + vs. microglia; and \$ vs. astrocytes. 1 symbol $p < 0.05$; 2 symbols $p < 0.01$; 3 symbols $p < 0.001$.

FIGURE 5

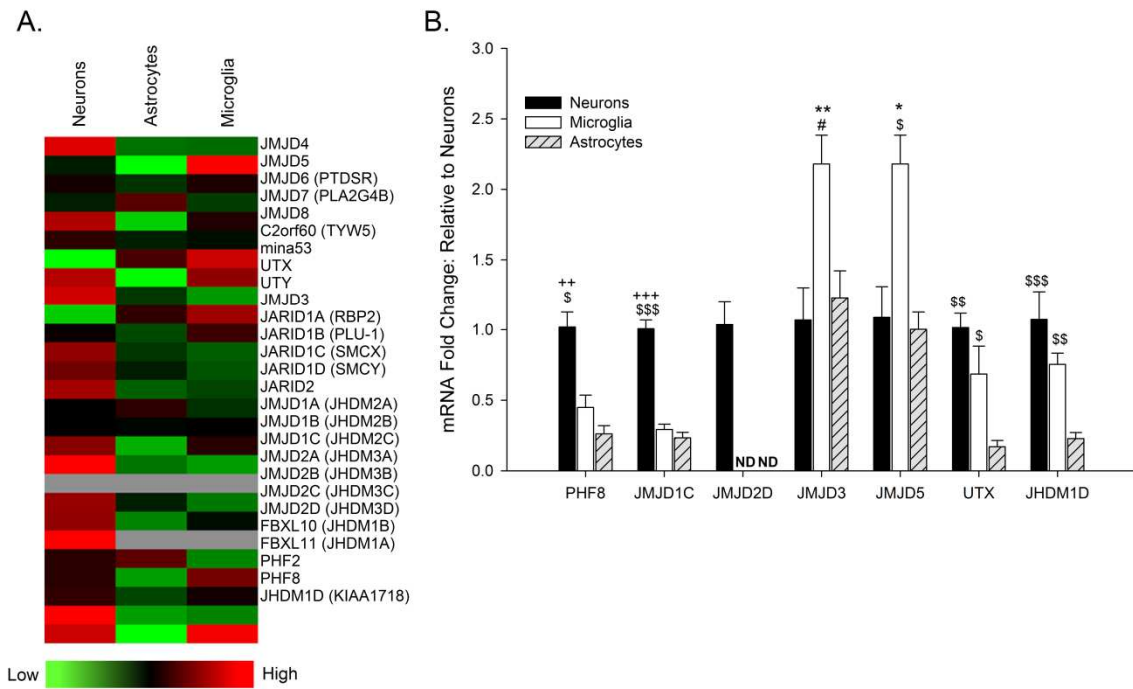


Figure Legend 5

Jumonji histone demethylase gene expression is cell-type specific in the CNS. (A) Total RNA was harvested from sorted cell populations, a portion of the cDNA was pooled, and screened in a custom-made qRT-PCR array consisting of 26 Jumonji histone demethylases. (B) Genes with a greater than 3-fold difference between cell types were confirmed by qRT-PCR in 4 independent samples. Symbols indicate significant differences between samples as assessed by a One-Way ANOVA. * vs. neurons; + vs. microglia; \$ vs. astrocytes; and # $p=0.060$ vs. astrocytes. 1 symbol $p<0.05$; 2 symbols $p<0.01$; 3 symbols $p<0.001$.

FIGURE 6

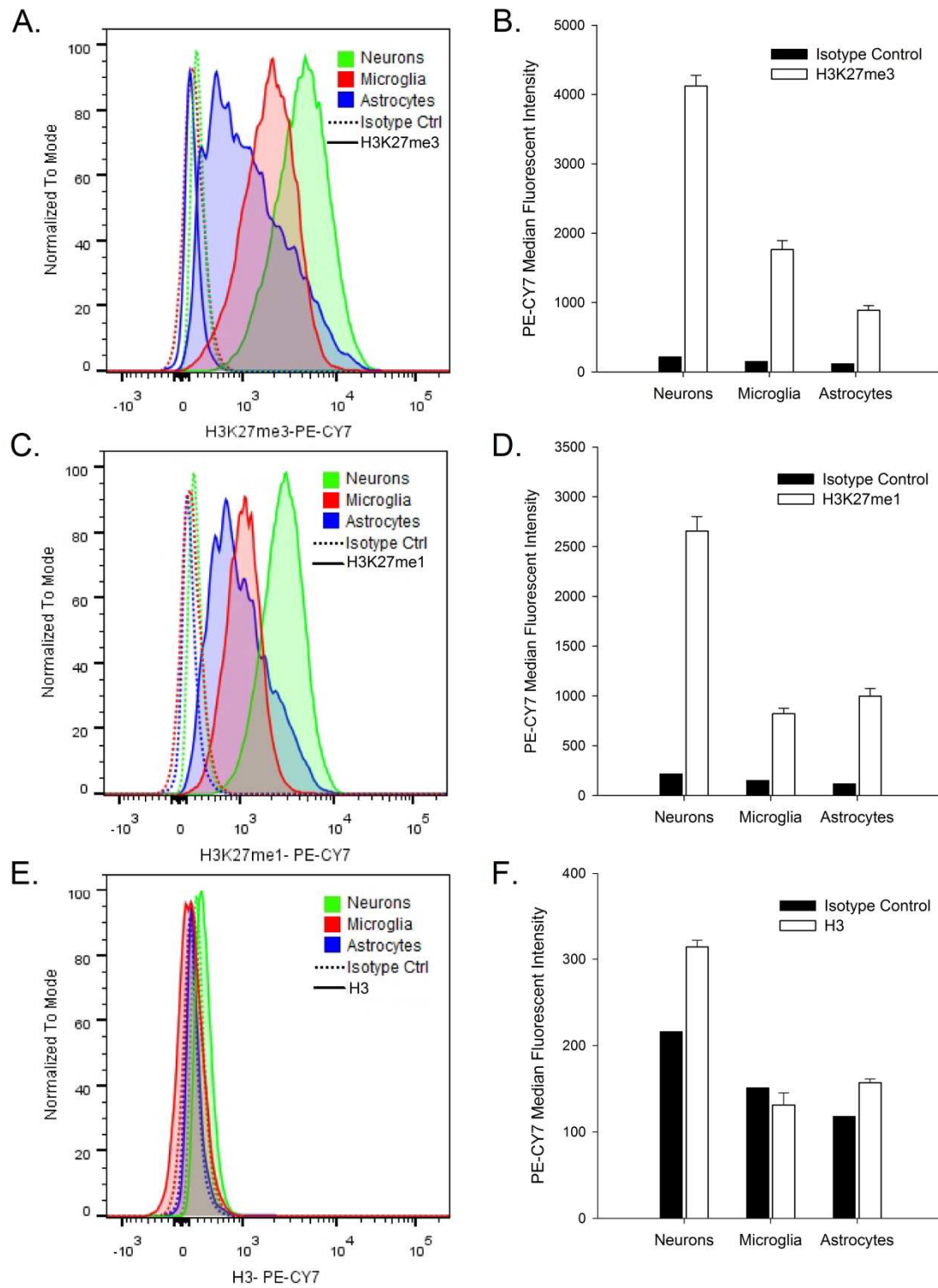


Figure Legend 6

Post-translational histone modifications can be analyzed by FCM in zinc-fixed cells. mZBF-fixed cell suspensions were stained with antibodies against NeuN, CD11b, and GFAP to identify neurons, microglia and astrocytes respectively, in the presence of antibodies against the histone mark (A,B) H3K27me1, (C,D) H3K27me3, or (E,F) pan-H3. Singlet and DAPI⁺ gated populations were subsequently gated by cell-type, and changes in the median fluorescent intensity (MFI) of the respective histone marks were assessed. Shifts in the MFI with primary antibody relative to signal with IgG isotype control antibody are shown in the histograms, and averaged data (n=4 independent samples) are shown in the bar graphs.

TABLE 1

<u>Protein Name</u>	<u>Gene Name</u>	<u>NCBI Reference Sequence</u>	<u>Forward Primer (5')</u>	<u>Reverse Primer (5')</u>
	18s	M11188.1	CGG GTG CTC TTA GCT GAG TGT CCC G	CTC GGG CCT GCT TTG AAC AC
β -Tubulin	Tubb2a	NM_001109 119.1	AGA CCA TGC TGG AGG ACA ACA	AGG ATG CCA CGG CTG ATG
NeuN	Rbfox3	NM_001134 498.2	TGC CAA TGG CTG GAA GCT AA	TAG GGG AAA CTG GTC ACT GC
Neurofilament - heavy chain	Nefh	NM_012607. 2	GGC CTC CTA CCA GGA TGC AAT TCA G	TGC GCG GCC ATC TCC CAT TT
β -III Tubulin	Tubb3	NM_139254. 2	TAG CCG AGT GAA GTC AGC ATG AGG G	ACC TCC CAG AAC TTG GCC CCT ATC
cd11b	Itgam	NM_012711. 1	GGG CAG GAG ACG TTT GTG AA	TGC CCA CAA TGA GTG GTA CAG
Iba-1	Aif1	NM_017196. 3	TCA TCG TCA TCT CCC CAC CT	GCT TTT CCT CCC TGC AAA TCC
CD68	CD68	NM_001031 638.1	GGA CTA ATG GTT CCC AGC CA	TGG GTC AGG TAC AAG ATG CG
GFAP	GFAP	NM_017009. 2	GGG CGA AGA AAA CCG CAT CAC CA	ATG ACC TCG CCA TCC CGC ATC
ALDH1L1	Aldh1l1	NM_022547. 1	CCT GGA CAC TGG TGA CCT TC	ACG ATT GTA CAG CGT GCT CA
GLT-1	Slc1a2	NM_017215. 2	GCA TCA ACC GAG GGT GCC AAC AA	CCC AGG TTT CGG TGC TTT GGC T
C2orf60	Tyw5	NM_001170 473.1	TTA CCC GCA GAG AAA GCC TC	ACT GCA GCG ACG TGA ATC TT
Jarid1A	Kdm5a	NM_001277 177.1	TGA ACT GTC TTC TGC CCT GG	AGT GTC CCT GTA AGT CTG GAT TG
Jarid1B	Kdm5b	NM_001107 177.1	GCC ACC ATT CGC TTG TGA TG	TTA CAC GTG TTT GGG CCT CC
Jarid1C	Kdm5c	XM_241817. 7	GGT TCC TTG CTA CGC TCT CA	TAC ACT GCA CAA GGT TGG CT
Jarid1D	Kdm5d	FJ775729.1	ATG CCT CTG CAA CCT CCA TC	AGA TCA CAC CGC AGA GCT TC
Jarid2	Jarid2	XM_003752 957.1	GCA GGC GAA TCT GGT TTT GG	GCT GAT TGC AAA AGG GGA CA
JHDM1A	Kdm2a	NM_001108 515.1	GCA TCC CTG GAG TGG TTT CT	TAC CAC GCA ATC TCT GGC TG
JHDM1B	Kdm2b	NM_001100 679.1	CTT TCC CCC TCC GCC AAA AT	GTC GTA TCT CTG GCG GTC AAT
JHDM1D	Jhdm1d	XM_003749 720.1	TGA TGG CTC CAA ACC TGT TCA	TTC ATC GGC ACT TGG GAA GAC
JMJD1A	Kdm3a	NM_175764 .2	TTG CTC TGA GGT CTC TCC CA	GCA GTA CAG CCA AGC AGG AT
JMJD1B	Kdm3b	XM_001061	GGA CCT AGC GAT	AGC GTG AAC CTT

		636.2	CTT TGT GGA	AAC CCA GG
JMJD1C	Jmjd1c	NM_001191 719.1	TGC GCT GAC CTT CAA ACC AT	GTT CGG GCT TTA GGC TGT CT
JMJD2A	Kdm4a	NM_001107 966.1	AAA GAC AGT GGG ATC GGC G	ACC TGG AGC CTA AAG CCC TA
JMJD2B	Kdm4b	NM_001044 236.2	ACT GCG CTG GAT CGA CTA TG	GCT GCA GGA TGC GTA CAA AC
JMJD2C	Kdm4c	NM_001106 663.2	TGG AGA GTC CCC TAA ATC CCA	TTG GCA AGA CCT GCT CGA TG
JMJD2D	Kdm4d	NM_001079 712.1	AGG CGC AAA TAA GTA CGG GG	GGG GTG CAG CAG ATT CTC TT
JMJD3	Kdm6B	NM_001108 829.1	CAA ACC CCC GCT TTT CTG TG'	ATT TGG GTG GCA GGA GGA GG
JMJD4	Jmjd4	NM_001105 784.1	AGG GAG GCT ACT CCT CTC CAA	ATC CAC CAA GGA GTC TCT GC
JMJD5	Kdm8	NM_001037 196.1	CCG TGG AAG TGG GTT CAA GA	CAT CCT TTG CCT CGC TCA GA
JMJD6	Jmjd6	NM_001012 143.2	TAG CAG CTA TGG CGA ACA CC	CCC CAT CAC AAA CCA CCT GTA
JMJD7	Jmjd7	NM_001114 656.1	TGC TCG CGA CCT CAA TGT A	GGT AGA AGC AGA GCG GAC TT
JMJD8	Jmjd8	NM_001014 116.1	TGG ACG ATT CGG TCT GCT TT	ACT CTG TTT CCA TCC CCC TTC
Mina53	Mina53	NM_153309 .2	ATG CCA AAG AAA GTG AAG CCC	GTA GCT CCT CTT TCA CCT GCT
PHF2	Phf2	NM_001107 342.1	TCA GAC ACC AGA ATG TCC AGC	TCG GGC CAG TAG TTT TCC AC
PHF8	Phf8	NM_001108 253.1	TTT GGG ACC GTG GAC GTT T	GTC AGA AAG GCA GCA ACA AGC
UTX	Kdm6a	NM_009483 .1	CCA CCC TGC CTA GCA ATT CA	CCA CCT GAG GTA GCA GTG TG
UTX	Uty	NM_009484	ATT ATC TCT CAC TAC TGC TGC CC	CGA AGA AGC TGC TGT CTA ATC CAC
	snoRNA135 / Snord65	NR_028541. 1	AGT ACT TTT TGA ACC CTT TTC CA	
	snoRNA234 /Snord70	NR_028554. 1	TTA ACA AAA ATT CGT CAC TAC CA	
	mir-26	NR_029742. 1	GGT TCA AGT AAT CCA GGA TAG GCT	
	mir-146a	NR_031892. 1	TGA GAA CTG AAT TCC ATG GGT T	

Table Legend 1

Primer Table. The table includes the primer sequences used to assess gene expression by qPCR, the associated protein name, gene name, and the NCBI accession number for the gene on which the primer sequences are based.

TABLE 2

	% of DAPI⁺ Cells	# of cells/100mg tissue	RNA (ng)/50,000 cells	RNA 260/280
NeuN⁺	42.7 ± 1.14	275,972 ± 16,950	24.57 ± 5.04	1.93 ± 0.05
CD11b⁺	11.3 ± 0.92	44,526 ± 3,877	33.64 ± 5.15	1.85 ± 0.09
GFAP⁺	3.8 ± 0.14	12,325 ± 1,243	111.05 ± 11.29	1.86 ± 0.06

Table Legend 2

Expected cell numbers and cell-specific RNA quantification and purity from mZBF-fixed and sorted rat brain cells. Half of a rat brain was weighed (~650mg), mechanically dissociated, and processed for flow cytometry as described in the Methods. Doublets and off scale events were gated out based on FSC-Area/SSC-Width and SSC-Area/FSC-Width, and intact cells were gated based on DAPI positivity (Fig. 1B). Single positive CD11b, NeuN, and GFAP cells were sorted from the entire tissue sample. The total number of neurons (NeuN⁺), microglia (CD11b⁺), and astrocytes (GFAP⁺) obtained from the sort were normalized to tissue weight, and total RNA isolated from the sorted cells was normalized to the number of cells sorted. The % of DAPI⁺ cells, the number of cells obtained per 100mg of tissue, the total RNA per 50,000 cells, and the average RNA 260/280 ratios are presented in the table for each of the three cell populations (average ± the SEM, from n=4 independent samples).

REFERENCES

- 1 Luo, C. X. *et al.* Reduced neuronal nitric oxide synthase is involved in ischemia-induced hippocampal neurogenesis by up-regulating inducible nitric oxide synthase expression. *Journal of neurochemistry* **103**, 1872-1882 (2007).
- 2 Vincent, V. A., DeVoss, J. J., Ryan, H. S. & Murphy, G. M. Analysis of neuronal gene expression with laser capture microdissection. *Journal of neuroscience research* **69**, 578-586 (2002).
- 3 Lobo, M. K., Karsten, S. L., Gray, M., Geschwind, D. H. & Yang, X. W. FACS-array profiling of striatal projection neuron subtypes in juvenile and adult mouse brains. *Nature neuroscience* **9**, 443-452 (2006).
- 4 Doyle, J. P. *et al.* Application of a translational profiling approach for the comparative analysis of CNS cell types. *Cell* **135**, 749-762 (2008).
- 5 Heiman, M. *et al.* A translational profiling approach for the molecular characterization of CNS cell types. *Cell* **135**, 738-748 (2008).
- 6 Sanz, E. *et al.* Cell-type-specific isolation of ribosome-associated mRNA from complex tissues. *Proceedings of the National Academy of Sciences* **106**, 13939-13944, doi:10.1073/pnas.0907143106 (2009).
- 7 Guez-Barber, D. *et al.* FACS identifies unique cocaine-induced gene regulation in selectively activated adult striatal neurons. *J Neurosci* **31**, 4251-4259, doi:10.1523/jneurosci.6195-10.2011 (2011).
- 8 Diez, C., Bertsch, G. & Simm, A. Isolation of full-size mRNA from cells sorted by flow cytometry. *Journal of Biochemical and Biophysical Methods* **40**, 69-80, doi:http://dx.doi.org/10.1016/S0165-022X(99)00020-2 (1999).
- 9 Fanous, S. *et al.* Unique gene alterations are induced in FACS-purified Fos-positive neurons activated during cue-induced relapse to heroin seeking. *Journal of Neurochemistry* **124**, 100-108, doi:10.1111/jnc.12074 (2013).
- 10 Guez-Barber, D. *et al.* FACS purification of immunolabeled cell types from adult rat brain. *Journal of neuroscience methods* **203**, 10-18 (2012).
- 11 Liu, Q.-R. *et al.* Detection of molecular alterations in methamphetamine-activated Fos-expressing neurons from a single rat dorsal striatum using fluorescence-activated cell sorting (FACS). *Journal of Neurochemistry* **128**, 173-185, doi:10.1111/jnc.12381 (2014).
- 12 Lykidis, D. *et al.* Novel zinc-based fixative for high quality DNA, RNA and protein analysis. *Nucleic Acids Research* **35**, e85, doi:10.1093/nar/gkm433 (2007).

- 13 Wester, K. *et al.* Zinc-based fixative improves preservation of genomic DNA and proteins in histoprocessing of human tissues. *Laboratory investigation* **83**, 889-899 (2003).
- 14 Jensen, U. B., Owens, D. M., Pedersen, S. & Christensen, R. Zinc fixation preserves flow cytometry scatter and fluorescence parameters and allows simultaneous analysis of DNA content and synthesis, and intracellular and surface epitopes. *Cytometry Part A* **77A**, 798-804, doi:10.1002/cyto.a.20914 (2010).
- 15 Kooistra, S. M. & Helin, K. Molecular mechanisms and potential functions of histone demethylases. *Nature reviews Molecular cell biology* **13**, 297-311 (2012).
- 16 Chassevent, A. *et al.* Comparative flow DNA analysis of different cell suspensions in breast carcinoma. *Cytometry*. **5**, 263-267. (1984).
- 17 Livak, K. J. & Schmittgen, T. D. Analysis of Relative Gene Expression Data Using Real-Time Quantitative PCR and the $2^{-\Delta\Delta CT}$ Method. *Methods* **25**, 402-408, doi:http://dx.doi.org/10.1006/meth.2001.1262 (2001).
- 18 Saldanha, A. J. Java Treeview—extensible visualization of microarray data. *Bioinformatics* **20**, 3246-3248, doi:10.1093/bioinformatics/bth349 (2004).
- 19 Smirnova, L. *et al.* Regulation of miRNA expression during neural cell specification. *European Journal of Neuroscience* **21**, 1469-1477 (2005).
- 20 Ponomarev, E. D., Veremeyko, T. & Weiner, H. L. MicroRNAs are universal regulators of differentiation, activation, and polarization of microglia and macrophages in normal and diseased CNS. *Glia* **61**, 91-103 (2013).
- 21 Rom, S. *et al.* CCL8/MCP-2 is a target for mir-146a in HIV-1-infected human microglial cells. *The FASEB Journal* **24**, 2292-2300 (2010).
- 22 Saba, R. *et al.* MicroRNA 146a (miR-146a) is over-expressed during prion disease and modulates the innate immune response and the microglial activation state. *PLoS One* **7**, e30832 (2012).
- 23 Esser, C., Gottlinger, C., Kremer, J., Hundeiker, C. & Radbruch, A. Isolation of full-size mRNA from ethanol-fixed cells after cellular immunofluorescence staining and fluorescence-activated cell sorting (FACS). *Cytometry*. **21**, 382-386. (1995).
- 24 Perez, O. D. *et al.* in *Current Protocols in Cytometry* (John Wiley & Sons, Inc., 2001).
- 25 Shapiro, H. *Parameters and Probes. In: Practical Flow Cytometry*, . 2 edn, pp 168–170. (Alan R. Liss 1988).

- 26 Guez-Barber, D. *et al.* FACS Identifies Unique Cocaine-Induced Gene Regulation in Selectively Activated Adult Striatal Neurons. *The Journal of Neuroscience* **31**, 4251-4259, doi:10.1523/jneurosci.6195-10.2011 (2011).
- 27 Schmid, I., Merlin, S. & Perfetto, S. P. Biosafety concerns for shared flow cytometry core facilities. *Cytometry Part A* **56A**, 113-119, doi:10.1002/cyto.a.10085 (2003).
- 28 Nikodemova, M. & Watters, J. J. Efficient isolation of live microglia with preserved phenotypes from adult mouse brain. *Journal of Neuroinflammation* **9**, 147 (2012).
- 29 Sanchez-Ramos, J. *et al.* Adult Bone Marrow Stromal Cells Differentiate into Neural Cells *in Vitro*. *Experimental neurology* **164**, 247-256 (2000).
- 30 Kimelberg, H. K. The problem of astrocyte identity. *Neurochemistry International* **45**, 191-202 (2004).
- 31 Takeuchi, T., Watanabe, Y., Takano-Shimizu, T. & Kondo, S. Roles of jumonji and jumonji family genes in chromatin regulation and development. *Developmental dynamics* **235**, 2449-2459 (2006).
- 32 Doyle, S. L. & O'Neill, L. A. Toll-like receptors: from the discovery of NF κ B to new insights into transcriptional regulations in innate immunity. *Biochemical pharmacology* **72**, 1102-1113 (2006).
- 33 Blackwell, T. S. & Christman, J. W. The Role of Nuclear Factor- κ B in Cytokine Gene Regulation. *American Journal of Respiratory Cell and Molecular Biology* **17**, 3-9, doi:10.1165/ajrcmb.17.1.f132 (1997).
- 34 Qiu, J. *et al.* The X-linked mental retardation gene PHF8 is a histone demethylase involved in neuronal differentiation. *Cell research* **20**, 908-918 (2010).
- 35 Wolf, S. S., Patchev, V. K. & Obendorf, M. A novel variant of the putative demethylase gene, s-JMJD1C, is a coactivator of the AR. *Archives of biochemistry and biophysics* **460**, 56-66 (2007).
- 36 Kleine-Kohlbrecher, D. *et al.* A functional link between the histone demethylase PHF8 and the transcription factor ZNF711 in X-linked mental retardation. *Molecular cell* **38**, 165-178 (2010).
- 37 Laumonier, F. *et al.* Mutations in PHF8 are associated with X linked mental retardation and cleft lip/cleft palate. *Journal of Medical Genetics* **42**, 780-786, doi:10.1136/jmg.2004.029439 (2005).
- 38 Castermans, D. *et al.* Identification and characterization of the TRIP8 and REEP3 genes on chromosome 10q21.3 as novel candidate genes for autism. *European Journal of Human Genetics* **15**, 422-431 (2007).

- 39 Shulha, H. P. *et al.* Epigenetic signatures of autism: trimethylated H3K4 landscapes in prefrontal neurons. *Archives of general psychiatry* **69**, 314 (2012).
- 40 Shin, S. & Janknecht, R. Activation of androgen receptor by histone demethylases JMJD2A and JMJD2D. *Biochemical and Biophysical Research Communications* **359**, 742-746, doi:http://dx.doi.org/10.1016/j.bbrc.2007.05.179 (2007).
- 41 De Santa, F. *et al.* Jmjd3 contributes to the control of gene expression in LPS-activated macrophages. *The EMBO journal* **28**, 3341-3352 (2009).
- 42 Das, N. D., Jung, K. H. & Chai, Y. G. The role of NF-kappaB and H3K27me3 demethylase, Jmjd3, on the anthrax lethal toxin tolerance of RAW 264.7 cells. *PLoS One* **5**, e9913, doi:10.1371/journal.pone.0009913 (2010).
- 43 Luo, X. *et al.* A Selective Inhibitor and Probe of the Cellular Functions of Jumonji C Domain-Containing Histone Demethylases. *Journal of the American Chemical Society* **133**, 9451-9456, doi:10.1021/ja201597b (2011).
- 44 Satoh, T. *et al.* The Jmjd3-Irf4 axis regulates M2 macrophage polarization and host responses against helminth infection. *Nature immunology* **11**, 936-944 (2010).
- 45 Youn, M.-Y. *et al.* JMJD5, a Jumonji C (JmjC) domain-containing protein, negatively regulates osteoclastogenesis by facilitating NFATc1 protein degradation. *Journal of Biological Chemistry* **287**, 12994-13004 (2012).
- 46 Tang, Y. *et al.* Jmjd3 is essential for the epigenetic modulation of microglia phenotypes in the immune pathogenesis of Parkinson's disease. *Cell Death Differ* **21**, 369-380, doi:10.1038/cdd.2013.159 (2014).
- 47 Xu, J., Deng, X., Watkins, R. & Disteché, C. M. Sex-specific differences in expression of histone demethylases Utx and Uty in mouse brain and neurons. *J Neurosci* **28**, 4521-4527, doi:10.1523/jneurosci.5382-07.2008 (2008).
- 48 Lederer, D. *et al.* Deletion of KDM6A, a Histone Demethylase Interacting with MLL2, in Three Patients with Kabuki Syndrome. *American journal of human genetics* **90**, 119-124 (2012).
- 49 Miyake, N. *et al.* MLL2 and KDM6A mutations in patients with Kabuki syndrome. *American Journal of Medical Genetics Part A* (2013).
- 50 Molofsky, A. V. *et al.* Astrocytes and disease: a neurodevelopmental perspective. *Genes & development* **26**, 891-907 (2012).
- 51 Huang, C. *et al.* Dual-specificity histone demethylase KIAA1718 (KDM7A) regulates neural differentiation through FGF4. *Cell research* **20**, 154-165 (2010).

- 52 Huang, C. *et al.* The dual histone demethylase KDM7A promotes neural induction in early chick embryos. *Developmental Dynamics* **239**, 3350-3357, doi:10.1002/dvdy.22465 (2010).
- 53 O'Connell, R. M., Zhao, J. L. & Rao, D. S. MicroRNA function in myeloid biology. *Blood* **118**, 2960-2969 (2011).

CHAPTER 4

CHRONIC INTERMITTENT HYPOXIA EXERTS CNS REGION-SPECIFIC EFFECTS ON RAT MICROGLIAL INFLAMMATORY AND TLR4 GENE EXPRESSION

Stephanie M.C. Smith, Scott A. Friedle and Jyoti J. Watters

The work from this chapter was published in: *PloS One*, 2013. 8. e81584.

Chronic Intermittent Hypoxia Exerts CNS Region-Specific Effects on Rat Microglial
Inflammatory and TLR4 Gene Expression. Stephanie M.C. Smith, Scott A. Friedle and Jyoti J.
Watters.

ABSTRACT

Intermittent hypoxia (IH) during sleep is a hallmark of sleep apnea, causing significant neuronal apoptosis, and cognitive and behavioral deficits in CNS regions underlying memory processing and executive functions. IH-induced neuroinflammation is thought to contribute to cognitive deficits after IH. In the present studies, we tested the hypothesis that IH would differentially induce inflammatory factor gene expression in microglia in a CNS region-dependent manner, and that the effects of IH would differ temporally. To test this hypothesis, adult rats were exposed to a paradigm of intermittent hypoxia (2 min intervals of 10.5% O₂) for 8 hours/day during their respective sleep cycles for 1, 3 or 14 days. Cortex, medulla and spinal cord tissues were dissected, microglia were immunomagnetically isolated and mRNA levels of the inflammatory genes iNOS, COX-2, TNF α , IL-1 β and IL-6 and the innate immune receptor TLR4 were compared to levels in normoxia. Inflammatory gene expression was also assessed in tissue homogenates (containing all CNS cells). We found that microglia from different CNS regions responded to IH differently. Cortical microglia had longer lasting inflammatory gene expression whereas spinal microglial gene expression was rapid and transient. We also observed that inflammatory gene expression in microglia frequently differed from that in tissue homogenates from the same region, indicating that cells other than microglia also contribute to IH-induced neuroinflammation. Lastly, microglial TLR4 mRNA levels were strongly upregulated by IH in a region- and time-dependent manner, and the increase in TLR4 expression appeared to coincide with timing of peak inflammatory gene expression, suggesting that TLR4 may play a role in IH-induced neuroinflammation. Together, these data indicate that microglial-specific neuroinflammation may play distinct roles in the effects of intermittent hypoxia in different CNS regions.

INTRODUCTION

Intermittent hypoxia (IH) during sleep is a hallmark feature of sleep apnea. IH induces significant cognitive and behavioral deficits that involve disruptions of connections among CNS regions underlying memory processing and executive function. For example, IH promotes apoptosis of hippocampal CA1 and frontal cortical neurons^{1,2} as well as cerebellar Purkinje and fastigial neurons³ in rodents. Similar gray matter losses have also been observed in hippocampal and para-hippocampal brain regions^{4,5}, and the temporal gyrus and cerebellum⁶ in humans with sleep apnea. Interestingly, there also appears to be CNS region-specific neuronal vulnerability to IH. Neurons in the hippocampal CA3 region do not undergo apoptosis as a result of IH, whereas CA1 neurons are highly sensitive^{1,2}. To the best of our knowledge, there are no reports of neuronal loss occurring in the brainstem or spinal cord of adult animals exposed to IH protocols. Indeed, the dorsocaudal brainstem and the CA3 regions are considered to be protected from IH-induced neuronal apoptosis⁷.

Many mechanisms are thought to contribute to neuronal death following chronic exposure to IH including oxidative stress^{8,9} and inflammation^{10,11}. In particular, enzymatic inhibition and/or genetic deletion of NADPH oxidase^{9,12-14}, cyclooxygenase-2¹⁰, and inducible nitric oxide synthase¹¹ protect against IH-induced neuronal apoptosis and cognitive impairment, suggesting that inflammatory processes play an important role in IH-induced neuropathology. Neuronal apoptosis in the CA1 region and cortex (as assessed by single stranded DNA immunostaining) indicates that apoptosis peaks between 1 and 2 days of IH, is significantly decreased by 7 days, and has returned to baseline levels by 14 days¹. This neuronal apoptosis profile coincides with iNOS and COX-2 gene expression in cortical homogenates where mRNA and protein levels peak at 1 day of IH and then decline thereafter^{10,11}. Although COX-2 levels

remain elevated above baseline at 14 days of IH¹⁰, iNOS levels remain elevated above basal only for 3 to 7 days¹¹, suggesting differential gene regulation of these inflammatory molecules in cortical homogenates.

Whether inflammatory molecules besides iNOS and COX-2 are produced in the CNS during IH is not known, nor is the cellular source of these molecules, although iNOS has been attributed to neurons¹¹. Microglia, CNS resident immune cells are considered to be contributors to IH-induced neuroinflammation⁷, but their activities have never directly been tested in this model of IH^{15,16}. Thus, a major goal of the present studies was to determine the contributions of microglia to IH-induced neuroinflammation over time, and to elucidate the expression profile of inflammatory factor genes. Microglia can be major sources of inducible nitric oxide synthase (iNOS) and cyclooxygenase-2 (COX-2) in the CNS in other models of CNS neuroinflammation¹⁷⁻¹⁹, and Toll-like receptor 4 (TLR4) activation is involved in microglial inflammatory responses to many insults²⁰⁻²³. TLR4 is a key pattern recognition receptor whose prototypical ligand is gram-negative lipopolysaccharide (LPS). In addition to iNOS and COX-2, TLR4 activation also leads to the production and release of cytokines including interleukin (IL)-1 β , IL-6 and tumor necrosis factor (TNF) α ^{20,21,24}. All of these molecules have been implicated in neuronal injury, death and/or functional impairments in the CNS^{10,25-32}.

Importantly, it is now well established that TLR4 also mediates “sterile inflammation” in the CNS, primarily by responding to a host of endogenous ligands including, proteins associated with cell damage (e.g. heat shock proteins 60 and 70), extracellular matrix turnover, and oxidatively modified lipids³³. A proteomic study comparing the profile of IH-induced proteins in sensitive (CA1) and resistant (CA3) hippocampal regions showed that several heat shock proteins were upregulated by IH, and some differentially in CA1 versus CA3³⁴, suggesting that

IH may region-specifically increase endogenous ligands for TLR4 that could contribute to microglial activation and IH-induced neuroinflammation in this region. Interestingly, serum levels of the TLR4 ligands myeloid related proteins (MRP) 8 and 14³⁵ correlate with severity of disease in children with OSA³⁶, suggesting a relationship between IH-induced inflammation and TLR4 activity. No studies to our knowledge have evaluated the levels of TLR4 in the CNS, although recently, upregulated TLR4 levels have been reported on circulating monocytes in adults with obstructive sleep apnea³⁷.

Because there is CNS regional susceptibility to neuronal damage during chronic IH, in the present studies, we tested the hypothesis that microglia differentially induce inflammatory factor gene expression in response to IH, and that the expression profiles of these genes would differ over time in IH-sensitive and -resistant CNS regions. Adult rats were exposed to a paradigm of intermittent hypoxia (2 min intervals of 10.5% O₂) for 8 hours/day during their respective sleep cycles for 1, 3 or 14 days. Cortex, medulla and spinal cord tissues were dissected, microglia were immunomagnetically isolated and mRNA levels of inflammatory genes were compared to those in tissue homogenates containing all CNS cells. We found that the inflammatory genes induced by IH differed in microglia from different CNS regions, and that the general temporal profiles of inflammatory gene expression differed in IH-sensitive and -resistant CNS regions. Further, we observed that the expression of inflammatory genes in microglia compared to that in regional tissue homogenates frequently differed, especially at the 14 day timepoint, indicating that cells other than microglia also produce inflammatory factors in response to chronic IH exposure. Lastly, microglial TLR4 mRNA levels were strongly upregulated in a region- and time-dependent manner, and that its expression frequently coincided

with increased inflammatory gene expression, suggesting that TLR4 may play a role in IH-induced neuroinflammation.

MATERIALS AND METHODS

Animals

Ethics Statement: This study was carried out in strict accordance with the recommendations in the Guide for the Care and Use of Laboratory Animals of the National Institutes of Health. All surgical and experimental procedures were approved by the University of Wisconsin Madison Institutional Animal Care and Use Committee. All efforts were made to minimize the number of animals used and their suffering. Experiments were performed on Sprague-Dawley rats weighing $150 \text{ g} \pm 20 \text{ g}$ (Harlan, Indianapolis, IN). All animals were maintained in an AAALAC-accredited animal facility and housed under standard conditions, with a 12 hour light/dark cycle with food and water available *ad libitum*.

Reagents

Neural Tissue Dissociation Kit, anti-PE magnetic beads, and MS columns were purchased from Miltenyi Biotech (Germany). PE-Mouse anti-rat CD11b was purchased from BD Biosciences (San Jose, CA). Hank's Buffered Salt Solution (HBSS) was purchased from Cellgro (Herndon, VA). TRI reagent was purchased from Sigma Aldrich (St. Louis, MO). Glycoblue reagent was purchased from Ambion (Austin, TX). MMLV Reverse transcriptase was purchased from Invitrogen (Carlsbad, CA). Oligo dT, Random Primers, and RNase inhibitor were purchased from Promega (Madison, WI). Primers were designed using Primer 3 software and were purchased from Integrated DNA Technologies (Coralville, IA). Power SYBR green was purchased from Applied Biosystems (Foster City, CA).

Intermittent Hypoxia (IH) Exposures

Animals were placed in computer controlled, custom-manufactured chambers that mix O₂, N₂, and CO₂ to the desired concentration with a flow rate of 4 L/min to enable rapid dynamics and minimal CO₂ accumulation. The treatment groups were exposed to alternating 2 minute episodes of hypoxia (10.5% inspired O₂) and normoxia (21% inspired O₂) for 8 h/day during their respective night cycle for 1, 3, or 14 days. The control group underwent identical handling, but their chambers were continually flushed with room air (21% inspired O₂). Following exposure, rats were returned to their cages.

CD11b⁺ Cell Isolation

Rats were harvested 16 hours after their last hypoxic exposure, and CD11b⁺ cells were isolated using previously described methods^{38,39}. Briefly, rats were euthanized and perfused with cold phosphate buffered saline (PBS). The cortex, medulla (pontomedullary junction to obex) and spinal cord (C1-L6) were removed, and dissociated into a single cell suspension using the neural tissue dissociation kit (Miltenyi) according to the manufacturer's protocol. Myelin was removed by high speed centrifugation at 850g in a 0.9 M solution of sucrose in HBSS. CD11b⁺ cells were tagged with a PE-conjugated anti-CD11b⁺ antibody followed by an anti-PE antibody conjugated to a magnetic bead. Magnetically-tagged CD11b⁺ cells were isolated using MS columns according to the Miltenyi MACS protocol. Prior to CD11b⁺ cell isolation an aliquot of tissue cell suspension was taken for CNS homogenate tissue analysis. Reagents were kept chilled at 4°C and cells were kept on ice whenever possible. As we have previously shown, this method results in >97% pure population of CD11b⁺/CD45^{low} cells^{38,39}. Isolated CD11b⁺ cells will subsequently be referred to as "microglia."

RNA extraction/ reverse transcription

RNA was extracted from tissue homogenates and freshly-isolated microglia according to the TriReagent protocol, with the addition of Glycoblue during the isopropanol incubation. cDNA was synthesized from 1 μ g of total RNA using MMLV Reverse Transcriptase as previously described ³⁸.

Quantitative PCR

cDNA was used in real-time quantitative PCR with Power SYBR Green using either the ABI StepOne or ABI 7500 Fast system. Primers (Table 1) were designed using Primer 3 software and the specificity was assessed through NCBI BLAST. Primer efficiency was tested through the use of serial dilutions. Verification that the dissociation curve had a single peak with an observed T_m consistent with the amplicon length was performed for every PCR reaction. C_T values from duplicate measurements were averaged and normalized to levels of the ribosomal RNA, 18s. Relative gene expression was determined using the relative standard curve method as previously described ³⁸.

Statistical analysis

Statistical analyses were performed on the normalized, interpolated C_T values from the standard curves for each gene, as previously described ⁴⁰, using a one-way ANOVA followed by the Holm-Sidak multiple comparisons post hoc test using Sigma Plot 11.0 software (San Jose, CA). Data sets that failed normality were logarithmically transformed prior to statistical analyses. Statistical significance was set at the 95% confidence limit ($p < 0.05$). A single symbol above a bar represents $p < 0.05$; two symbols $p < 0.01$; and three symbols $p < 0.001$. Quantitative data are expressed as the mean \pm SEM of up to 3 independent experiments containing $n=4-6$ animals/group for normoxia and IH treatments.

RESULTS

IH time-dependently increases the expression of inflammatory genes (but not TNF α) in cortical microglia.

IH treatment increased cortical microglial inflammatory gene expression (compared to normoxic controls) over the course of the 14 day IH exposure. There was a statistically significant 4-fold increase in COX-2 ($p=0.002$) and 6-fold increase in IL-1 β ($p<0.001$) mRNA levels after 14 days of IH. Although there was an apparent 5-fold increase in the expression of IL-6 after 14 days ($p=0.09$) and a 4-fold increase in iNOS expression at 3 days ($p=0.074$), these genes did not reach statistical significance by ANOVA. Interestingly, relative to expression in normoxia, TNF α mRNA levels significantly decreased at 1 day ($p=0.024$) but had returned to baseline levels by 3 days. In contrast, in cortical tissue homogenates, although the mRNA levels of all genes showed an increase of approximately 2- fold after 3 days of IH and this increase is maintained after 14 days, these increases did not reach statistical significance as determined by ANOVA although TNF α came close ($p=0.055$; iNOS $p=0.09$; COX-2 $p=0.299$; IL-1 β $p=0.25$; IL-6 $p=0.11$).

IH promotes early and long-lasting increases in IL-1 β and IL-6 gene expression in medullary microglia, but multiple inflammatory genes are upregulated by IH in homogenates.

Medullary microglia appeared to have a more rapid inflammatory response to IH relative to cortical microglia. Whereas in cortical microglia IL-1 β and IL-6 mRNA levels did not appear to peak until 14 days of IH, in the medulla, microglia, IL-1 β and IL-6 mRNA levels were increased at 1 day of IH and remained elevated at 14 days. Interestingly, microglial IL-1 β and IL-6 expression profiles paralleled each other in both the medulla and cortex. In addition, while

cortical microglial COX-2 mRNA levels were highest at 14 days, in the medulla, microglial COX-2 was elevated at 3 days of IH and seemed to be returning to baseline levels by 14 days. IH exposure did not change iNOS ($p=0.56$) or TNF α ($p=0.71$) mRNA levels at any timepoint tested here. Unlike microglia, medullary homogenates behaved similarly to cortical homogenates. COX-2, TNF α , IL-1 β and IL-6 mRNA levels were significantly increased (~2-3 fold) at 3 days of IH, and with the exception of TNF α , the expression of these genes remained elevated at 14 days. iNOS levels in medullary homogenates remained unchanged over the course of IH treatment ($p=0.479$).

IH promotes transient inflammatory gene expression in spinal microglia but longer lasting effects in homogenates

IL-1 β expression was the only inflammatory gene to exhibit a strong upregulation after 1 day of IH in spinal microglia ($p<0.001$). However, by 3 days of IH, iNOS, COX-2, IL-1 β and IL-6 mRNA levels were increased by 3-5 fold, but only COX-2 ($p=0.007$) and IL-1 β ($p<0.001$) levels attained statistical significance (iNOS $p=0.12$; TNF α $p=0.28$; IL-6 $p=0.099$). COX-2 and IL-1 β expression returned to basal levels by 14 days of IH. IH did not appear to increase microglial IL-6 mRNA levels until 14 days although this 3-fold change was not statistically significant ($p=0.099$). Spinal homogenates behaved very similarly to brainstem homogenates where the expression of all inflammatory genes examined was increased between 3 and 8-fold at 3 days of IH. COX-2 and IL-1 β expression remained elevated at 14 days of IH ($p=0.003$ and $p=0.033$ respectively), but iNOS mRNA levels were returning to baseline despite remaining significantly elevated above basal levels in normoxia ($p=0.044$). Also, as in medullary homogenates, spinal homogenate IL-6 mRNA levels were highest at 14 days of IH ($p<0.001$) while TNF α levels peaked at 3 days (though not statistically significantly; $p=0.074$).

IH differentially increases microglial TLR4 expression in cortex, medulla and spinal cord

Because TLR4 plays an important role in mediating inflammatory gene induction in microglia, and endogenous TLR4 ligands are increased in IH-susceptible CNS regions, we evaluated the expression of TLR4 over time following IH exposure. Very interestingly, the largest increase in TLR4 mRNA levels occurred in microglia from the cortex where expression was increased by approximately 12-fold at 14 days of IH ($p=0.001$). The apparent 2-fold increase at 1 day of IH was not significant ($p=0.398$ by ANOVA). TLR4 expression in microglia from the medulla was increased by 7-fold at 3 days of IH ($p<0.001$), and remained elevated (by 4-fold at 14 days ($p=0.001$)). In spinal microglia, TLR4 expression was not significantly increased at any time point tested, although an approximate 3-fold increase at 3 days of IH was observed ($p=0.085$ by ANOVA).

DISCUSSION

In this study we were interested in understanding whether microglial inflammatory gene expression was altered by IH, whether those responses differed based on CNS region from which the microglia were derived, if there was temporal regulation of IH-induced inflammatory gene expression, and whether assessments of neuroinflammation in tissue homogenates were accurately reflective of microglial activities in specific. We show here that IH induces differential inflammatory gene profiles in microglia from different CNS regions, and that patterns of IH-induced inflammatory gene expression differ in tissue homogenates (in which all cell types are present) versus isolated microglia from the same region. Lastly, we find that the expression of the pattern recognition receptor TLR4 is time- and CNS region-dependently upregulated by IH in microglia in a manner that coincides with microglial inflammatory gene expression. This report is the first to directly evaluate microglial phenotype following intermittent hypoxia exposure, and to reveal differences in microglial responses based on CNS region and time of exposure. Our data also indicate that microglia are likely not the only CNS cell type contributing to neuroinflammation following chronic exposure to IH.

Microglia make up approximately 5-10% of all CNS cells, with the cortex having more microglia than caudal CNS regions such as the brainstem and spinal cord⁴¹. Because microglia comprise such a small percentage of total CNS cells, changes in microglial gene expression may not necessarily be evident in tissue homogenates unless the changes are very strong. For example, the approximately 50% reduction in TNF α or the 4-fold increase in COX-2 mRNA levels in cortical microglia are not apparent in cortical homogenates. Our data also indicate that cell types other than microglia can and do synthesize inflammatory molecules in response to IH exposure. For example, in spinal tissue homogenates, the mRNA levels of iNOS, COX-2 and IL-

6 are significantly elevated above normoxic levels at 14 days of IH when expression of these genes in microglia are not different from controls. The identity of the cells contributing to the expression of these neuroinflammatory mediators is not yet known, but such results suggest that conclusions made about microglial activities based on the expression/presence of inflammatory molecules in tissue homogenates may not always be accurate.

The observation that microglia respond to the same IH stimulus differently in different parts of the CNS may be related to differences in the local CNS environment as well as potential fundamental differences in the microglia themselves. In the cortex, microglial inflammatory gene expression (COX-2, IL-1 β , and IL-6) appears to increase over time after IH. However, these effects are gene-specific because iNOS expression had returned to baseline by 14 days and TNF α expression was not increased at any time point evaluated. Indeed, TNF α expression was significantly decreased in cortical microglia at 1 day of IH. This was the only CNS region in which we observed a decrease in the expression of any inflammatory gene. We do not yet know the significance of this rapid and acute TNF α downregulation as the biological functions of microglial produced TNF α versus TNF α produced by other cell types have not been distinguished. Additional studies are necessary to delineate mechanisms underlying this microglial-specific inhibition of TNF α in the cortex.

When comparing the cortex where IH-induced neuronal apoptosis occurs^{1,34}, to the spinal cord where there are no reports of IH-induced neuronal loss, we find that microglia from these two CNS regions behave very differently from each other. In cortical microglia, we observe a general pattern of time-dependent increases in inflammatory gene expression that appear to be peaking at 14 days of IH. Spinal microglia on the other hand, respond acutely and transiently to the IH stimulus such that the expression of inflammatory genes had returned to

basal levels by 14 days. Although we do not yet know the reasons underlying these regional differences, we hypothesize that the availability of endogenous TLR4 ligands may play a role, at least in part. Endogenous TLR4 ligands are increased in the IH-susceptible CA1 hippocampal region, but not in the CA3 region where the neurons appear to resistant to apoptotic effects of IH^{34,42}. Whereas similar proteomic studies have not been performed in the cortex, because there is significant IH-induced cortical neuron loss, we suspect that cortical results would be similar to those in the CA1 region. Why certain CNS regions appear to be susceptible to or protected from IH-induced neuronal loss is not yet clear, but differential induction of IH-regulated proteins⁴² and changes in basal metabolism in different regions³⁴ have been suggested. Regardless, we hypothesize that these differences contribute to region-specific alterations in microglial inflammatory gene expression profiles and temporal dynamics.

To the best of our knowledge, there are no reports of neuronal loss occurring in the dorsocaudal brainstem of adult animals exposed to IH protocols^{7,43}, although some brainstem regions including the nucleus tractus solitarius (nTS) and the nucleus ambiguus in the ventrolateral medulla are susceptible in the developing CNS⁴⁴. However, in the dorsocaudal brainstem, IH increases NMDA receptor subunit expression⁴⁵ and alters antioxidant responses in pontine neurons⁴⁶. Thus, although the dorsocaudal brainstem is protected from IH-induced neuronal apoptosis, neuronal function in several brainstem nuclei are altered by IH. Our observations that inflammatory gene expression in isolated microglia and homogenates from the medulla had some similarities to both the cortex and spinal cord are consistent with the varied activities of IH in different brainstem nuclei. The changes in microglial inflammatory and TLR4 gene expression in our medullary samples may therefore reflect responses of heterogeneous

microglial populations that cannot be distinguished using the present immunomagnetic isolation methodology.

TLR4 expression and activity is increased on monocytes from patients with sleep apnea³⁷, and ligands for TLR4 are increased in the serum of children with sleep apnea³⁶. TLR4 is also upregulated in the CNS in many injuries and neurodegenerative disease processes^{24,47-50}. Although TLR4 mRNA and protein levels are increased by chronic sustained hypoxia in microglia *in vitro*⁵¹, whether this also occurs following exposure to intermittent patterns of hypoxia, *in vivo*, was not known prior to this study. We found that TLR4 was very strongly upregulated in cortical microglia after 14 days of IH, and in medullary microglia at 3 and 14 days, consistent with the timing of peak inflammatory gene expression in the respective CNS regions. Since the function of upregulated TLR4 in CNS disease is thought to promote and/or maintain neuroinflammation, chronically upregulated microglial TLR4 in the cortex may contribute to IH-induced neuroinflammation and neuronal loss. *In vitro*, sustained hypoxia transcriptionally upregulates TLR4 expression via transactivation of the TLR4 promoter by hypoxia inducible factor (HIF)1 α in macrophages⁵². Interestingly, we also observe a strong increase in HIF-1 α mRNA at 14 days of IH in microglia (data not shown), supporting the idea that IH may contribute to chronically elevated microglial TLR4 levels via similar HIF-1-dependent transcriptional mechanisms.

The biological significance of microglia-mediated neuroinflammation in response to IH may be different in different CNS regions, especially given the differences in time domains. For example, in the cortex, microglial inflammatory gene expression appears to be maximal at 14 days (the longest time point measured here), suggesting that microglia may contribute to neuroinflammation and neuronal loss/damage in the chronic state. In contrast, spinal microglia

also respond to IH by increasing inflammatory gene expression, but these effects appear to be rapid and acute as inflammatory mRNA levels had returned to baseline by 14 days. Although the function of transient microglial inflammation in the spinal cord is not yet known, our recent studies have suggested that acute spinal inflammation, contributed to in part by microglia, can abrogate phrenic nerve long-term facilitation (pLTF), a form of spinal motor neuron plasticity⁵³. Interestingly, in rats exposed to IH for 7 days, pLTF is greatly enhanced compared to normoxia-exposed rats⁵⁴, suggesting that this form of motor neuron plasticity may return when IH-induced microglial inflammation subsides.

The IH model used here simulates a hallmark feature of sleep apnea. Recent estimates indicate that up to 34% of men and 13% of women between 30 and 70 yrs of age are affected by obstructive sleep apnea⁵⁵ which causes serious neural morbidities including neuroinflammation, neuronal death and cognitive impairment^{7,56}. However, equally as important, sleep disordered breathing and associated IH is also severe in >50% of patients with other major health problems including ischemic (e.g. stroke), traumatic (e.g. spinal injury), neurodegenerative (e.g. Alzheimer's, Parkinson's, ALS, MS) and genetic neural disorders (e.g. Down's syndrome, Fragile X)⁵⁷⁻⁶³. IH triggers the upregulation of endogenous TLR4 ligands in the CNS³⁴, and we find that TLR4 expression is upregulated in microglia by IH. Because TLR4 activation causes neurodegeneration⁴⁷, and several neurodegenerative diseases (e.g. AD, ALS and MS) are associated with abnormal TLR4 function^{24,48-50}, collectively, our data suggest that IH-induced TLR4 upregulation may play a previously unrecognized role in many CNS disorders. Thus, IH-induced neuroinflammation and neuronal death may accelerate or exacerbate ongoing pathology associated with other primary disorders. We suggest that IH-induced microglial activation may

therefore be a critical, underappreciated contributor to many seemingly unrelated neural disorders.

ACKNOWLEDGEMENTS

We wish to thank Mr. Bradley Wathan, Mr. Alex Wessel, Ms. Alissa Small and Ms. Rebecca Kimyon for excellent technical assistance. We are also grateful to Drs. Gordon Mitchell and Barbara Morgan for allowing us to use their hypoxia exposure chambers. We also wish to thank Dr. Mitchell for helpful collaborative and scientific discussions. This work was supported by NIH NS049033 and HL111598, and the University of Wisconsin Graduate School.

FIGURE 1

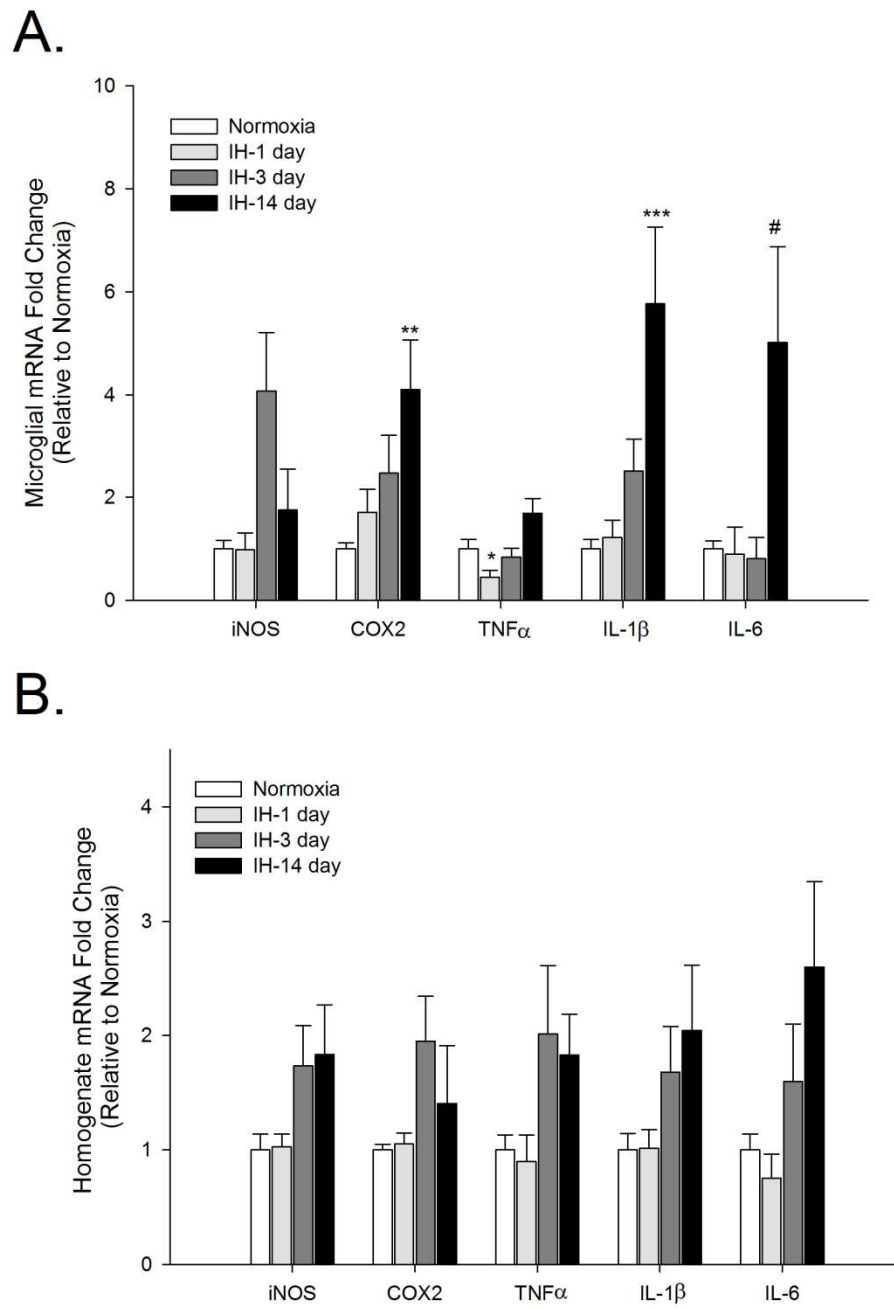


Figure Legend 1**Intermittent hypoxia-induced inflammatory gene expression peaks in cortical microglia at**

14 days of exposure. iNOS, COX-2, TNF α , IL-1 α and IL-6 gene expression was analyzed by qRT-PCR in immunomagnetically-separated microglia (A) or tissue homogenates (B) from the

cortex of healthy male rats exposed either to normoxia or IH for 1, 3 or 14 days. Means \pm 1

SEM are presented relative to expression in normoxic controls. * p <0.05; ** p <0.01; *** p <0.001;

p =0.09.

FIGURE 2

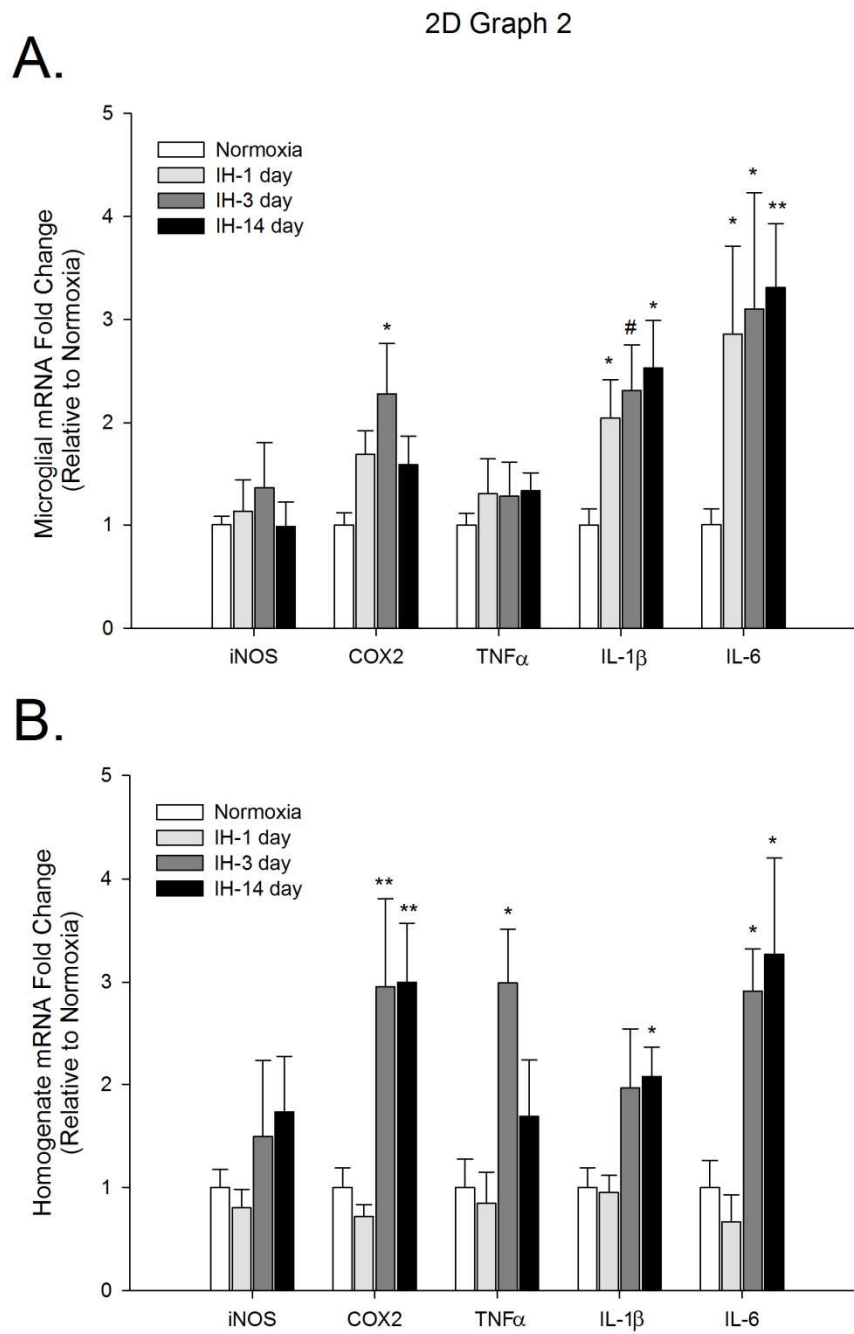


Figure Legend 2**Intermittent hypoxia-induced inflammatory gene expression differs temporally in**

brainstem microglia and brainstem tissue homogenates. iNOS, COX-2, TNF α , IL-1 β and IL-6 gene expression was analyzed by qRT-PCR in immunomagnetically-separated microglia (A) or tissue homogenates (B) from the brainstem of healthy male rats exposed either to normoxia or IH for 1, 3 or 14 days. Means \pm 1 SEM are presented relative to expression in normoxic controls.

*p<0.05; **p<0.01; #p=0.06.

FIGURE 3

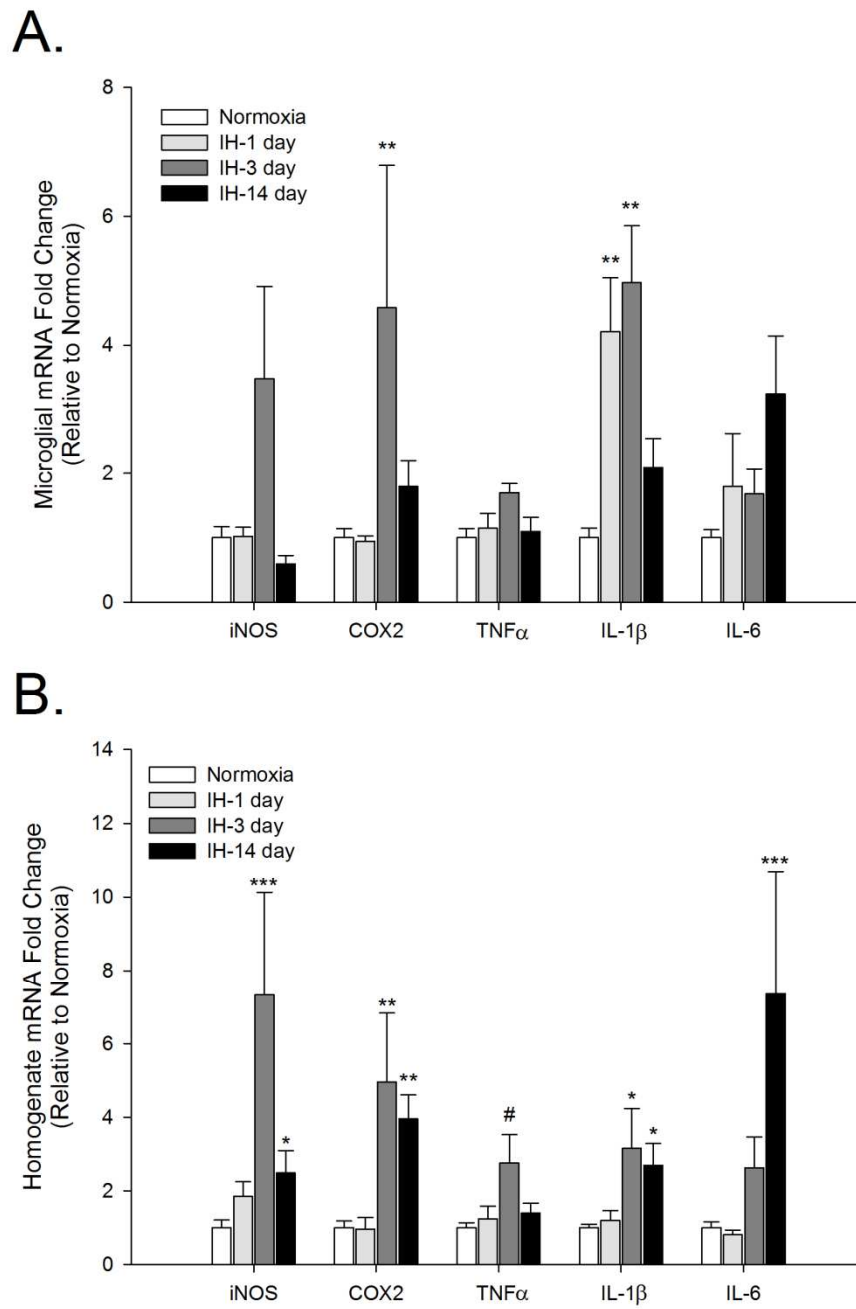


Figure Legend 3:

Intermittent hypoxia-induced inflammatory gene expression is rapid and transient in spinal microglia but sustained in spinal tissue homogenates. iNOS, COX-2, TNF α , IL-1 β and IL-6 gene expression was analyzed by qRT-PCR in immunomagnetically-separated microglia (A) or tissue homogenates (B) from the spinal cord of healthy male rats exposed either to normoxia or IH for 1, 3 or 14 days. Means \pm 1 SEM are presented relative to expression in normoxic controls. * p <0.05; ** p <0.01; *** p <0.001; # p =0.074.

FIGURE 4

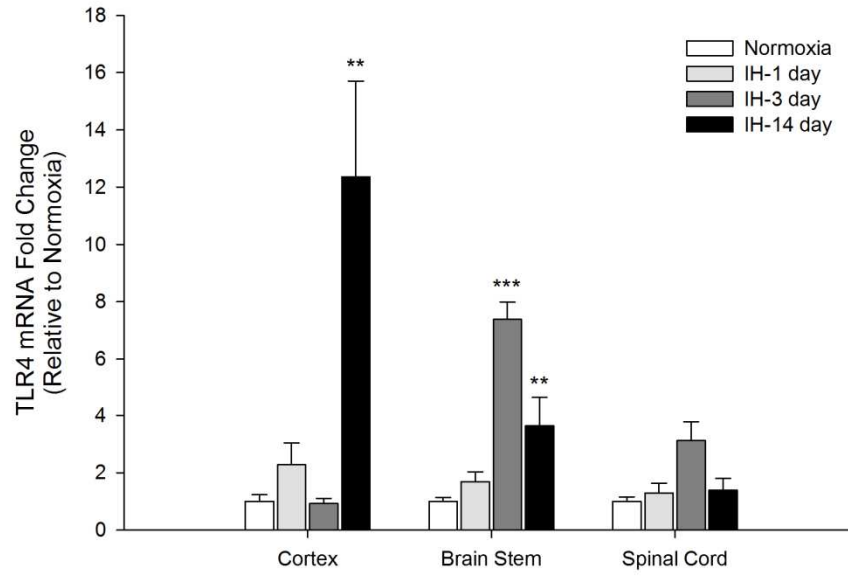


Figure Legend 4**Intermittent hypoxia-induced TLR4 gene expression in microglia differs by time and CNS**

region. TLR4 gene expression was analyzed by qRT-PCR in immunomagnetically-separated microglia from the cortex, brainstem and spinal cord of healthy male rats exposed either to normoxia or IH for 1, 3 or 14 days. Means \pm 1 SEM are presented relative to expression in normoxic controls. ** $p < 0.01$; *** $p < 0.001$; # $p = 0.085$.

TABLE 1

Gene	Forward Primer (5')	Reverse Primer (5')
18s	AACGAGACTCTCGG ATGCTAA	CCGGACATCTAAGGGCATCA
Cyclooxygenase 2 (COX-2)	TGTTCCAACCCATGTCAAAA	CGTAGAATCCAGTCCGGGTA
Inducible nitric oxide synthetase (iNOS)	AGGGAGTGTTGTTCCAGGTG	TCTGCAGGATGTCTTGAACG
Tumor necrosis factor- α (TNF- α)	TCCATGGCCCAGACCCTCACAC	TCCGCTTGGTTTGCTACG
Interleukin-1 β (IL-1 β)	CTGCAGATGCAATGGAAAGA	TTGCTTCCAAGGCAGACTTT
Interleukin-6 (IL-6)	GTGGCTAAGGACCAAGACCA	GGTTTGCCGAGTAGACCTCA
TLR4	AGGCAGCAGGTGGAATTGTATC	TCGAGGCTTTTCCATCCAATAG

REFERENCES

- 1 Gozal, D., Daniel, J. M. & Dohanich, G. P. Behavioral and Anatomical Correlates of Chronic Episodic Hypoxia during Sleep in the Rat. *The Journal of Neuroscience* **21**, 2442-2450 (2001).
- 2 Aviles-Reyes, R. X. *et al.* Intermittent hypoxia during sleep induces reactive gliosis and limited neuronal death in rats: implications for sleep apnea. *Journal of Neurochemistry* **112**, 854-869, doi:10.1111/j.1471-4159.2009.06535.x (2010).
- 3 Pae, E.-K., Chien, P. & Harper, R. M. Intermittent hypoxia damages cerebellar cortex and deep nuclei. *Neuroscience Letters* **375**, 123-128, doi:http://dx.doi.org/10.1016/j.neulet.2004.10.091 (2005).
- 4 Morrell, M. J. & Twigg, G. Neural consequences of sleep disordered breathing: the role of intermittent hypoxia. *Adv Exp Med Biol* **588**, 75-88 (2006).
- 5 Morrell, M. J. *et al.* Changes in brain morphology associated with obstructive sleep apnea. *Sleep Medicine* **4**, 451-454, doi:http://dx.doi.org/10.1016/S1389-9457(03)00159-X (2003).
- 6 Morrell, M. J. *et al.* Changes in brain morphology in patients with obstructive sleep apnoea. *Thorax* **65**, 908-914, doi:10.1136/thx.2009.126730 (2010).
- 7 Zhang, S. X., Wang, Y. & Gozal, D. Pathological consequences of intermittent hypoxia in the central nervous system. *Compr Physiol* **2**, 1767-1777, doi:10.1002/cphy.c100060 (2012).
- 8 Row, B. W., Liu, R., Xu, W., Kheirandish, L. & Gozal, D. Intermittent Hypoxia Is Associated with Oxidative Stress and Spatial Learning Deficits in the Rat. *Am. J. Respir. Crit. Care Med.* **167**, 1548-1553, doi:10.1164/rccm.200209-1050OC (2003).
- 9 Xu, W. *et al.* Increased oxidative stress is associated with chronic intermittent hypoxia-mediated brain cortical neuronal cell apoptosis in a mouse model of sleep apnea. *Neuroscience* **126**, 313-323, doi:10.1016/j.neuroscience.2004.03.055 [doi]S0306452204002477 [pii] (2004).
- 10 Li, R. C. *et al.* Cyclooxygenase 2 and Intermittent Hypoxia-induced Spatial Deficits in the Rat. *Am. J. Respir. Crit. Care Med.* **168**, 469-475, doi:10.1164/rccm.200211-1264OC (2003).
- 11 Li, R. C. *et al.* Nitric oxide synthase and intermittent hypoxia-induced spatial learning deficits in the rat. *Neurobiology of Disease* **17**, 44-53 (2004).
- 12 Nair, D., Dayyat, E. A., Zhang, S. X., Wang, Y. & Gozal, D. Intermittent hypoxia-induced cognitive deficits are mediated by NADPH oxidase activity in a murine model of sleep apnea. *PLoS One.* **6**, e19847. Epub 12011 May 19823. (2011).

- 13 Nair, D. *et al.* Sleep Fragmentation Induces Cognitive Deficits Via Nicotinamide Adenine Dinucleotide Phosphate Oxidase–dependent Pathways in Mouse. *American Journal of Respiratory and Critical Care Medicine* **184**, 1305-1312, doi:10.1164/rccm.201107-1173OC (2011).
- 14 Shan, X. *et al.* Manganese superoxide dismutase protects mouse cortical neurons from chronic intermittent hypoxia-mediated oxidative damage. *Neurobiology of Disease* **28**, 206-215, doi:10.1016/j.nbd.2007.07.013 (2007).
- 15 Nagata, N. *et al.* Repetitive intermittent hypoxia-ischemia and brain damage in neonatal rats.[comment]. *Brain & Development*. **22**, 315-320 (2000).
- 16 Prout, A. P. *et al.* Systemic and cerebral inflammatory response to umbilical cord occlusions with worsening acidosis in the ovine fetus. *American Journal of Obstetrics and Gynecology* **202**, 82.e81-82.e89, doi:http://dx.doi.org/10.1016/j.ajog.2009.08.020 (2010).
- 17 Lee, H.-K. *et al.* Anti-inflammatory effects of OBA-09, a salicylic acid/pyruvate ester, in the postischemic brain. *Brain Research*, doi:http://dx.doi.org/10.1016/j.brainres.2013.06.026.
- 18 Nikodemova, M. & Watters, J. J. Outbred ICR/CD1 mice display more severe neuroinflammation mediated by microglial TLR4/CD14 activation than inbred C57Bl/6 mice. *Neuroscience* **190**, 67-74, doi:10.1016/j.neuroscience.2011.06.006 (2011).
- 19 Ghoshal, A. *et al.* Proinflammatory mediators released by activated microglia induces neuronal death in Japanese encephalitis. *Glia* **55**, 483-496, doi:10.1002/glia.20474 (2007).
- 20 Yao, L. *et al.* Toll-like receptor 4 mediates microglial activation and production of inflammatory mediators in neonatal rat brain following hypoxia: role of TLR4 in hypoxic microglia. *Journal of Neuroinflammation* **10**, 23 (2013).
- 21 Fellner, L. *et al.* Toll-like receptor 4 is required for α -synuclein dependent activation of microglia and astroglia. *Glia* **61**, 349-360, doi:10.1002/glia.22437 (2013).
- 22 Sansing, L. H. *et al.* Toll-like receptor 4 contributes to poor outcome after intracerebral hemorrhage. *Annals of Neurology* **70**, 646-656, doi:10.1002/ana.22528 (2011).
- 23 Hines, D. J., Choi, H. B., Hines, R. M., Phillips, A. G. & MacVicar, B. A. Prevention of LPS-induced microglia activation, cytokine production and sickness behavior with TLR4 receptor interfering peptides. *PLoS One* **8**, e60388, doi:10.1371/journal.pone.0060388 (2013).
- 24 Jin, J. J., Kim, H. D., Maxwell, J. A., Li, L. & Fukuchi, K. Toll-like receptor 4-dependent upregulation of cytokines in a transgenic mouse model of Alzheimer's disease. *J Neuroinflammation*. **5**, 23. (2008).

- 25 Parmentier-Batteur, S. *et al.* Antisense oligodeoxynucleotide to inducible nitric oxide synthase protects against transient focal cerebral ischemia-induced brain injury. *Journal of Cerebral Blood Flow & Metabolism*. **21**, 15-21 (2001).
- 26 Acarin, L., Peluffo, H., Gonzalez, B. & Castellano, B. Expression of inducible nitric oxide synthase and cyclooxygenase-2 after excitotoxic damage to the immature rat brain. *Journal of Neuroscience Research*. **68**, 745-754 (2002).
- 27 Iadecola, C., Zhang, F., Casey, R., Nagayama, M. & Ross, M. E. Delayed reduction of ischemic brain injury and neurological deficits in mice lacking the inducible nitric oxide synthase gene. *Journal of Neuroscience*. **17**, 9157-9164 (1997).
- 28 Lecanu, L., Verrecchia, C., Margaille, I., Boulu, R. G. & Plotkine, M. iNOS contribution to the NMDA-induced excitotoxic lesion in the rat striatum. *British Journal of Pharmacology*. **125**, 584-590 (1998).
- 29 Kraft, A. D., McPherson, C. A. & Harry, G. J. Heterogeneity of microglia and TNF signaling as determinants for neuronal death or survival. *Neurotoxicology* **30**, 785-793, doi:10.1016/j.neuro.2009.07.001 (2009).
- 30 Spooren, A. *et al.* Interleukin-6, a mental cytokine. *Brain Research Reviews* **67**, 157-183, doi:10.1016/j.brainresrev.2011.01.002 (2011).
- 31 Smith, J. A., Das, A., Ray, S. K. & Banik, N. L. Role of pro-inflammatory cytokines released from microglia in neurodegenerative diseases. *Brain Research Bulletin* **87**, 10-20, doi:http://dx.doi.org/10.1016/j.brainresbull.2011.10.004 (2012).
- 32 Lenzlinger, P., Morganti-Kossmann, M.-C., Laurer, H. & McIntosh, T. The duality of the inflammatory response to traumatic brain injury. *Molecular Neurobiology* **24**, 169-181, doi:10.1385/mn:24:1-3:169 (2001).
- 33 Erridge, C. Endogenous ligands of TLR2 and TLR4: agonists or assistants? *J Leukoc Biol* **87**, 989-999, doi:jlb.1209775 [pii]10.1189/jlb.1209775 [doi] (2010).
- 34 Gozal, E. *et al.* Proteomic analysis of CA1 and CA3 regions of rat hippocampus and differential susceptibility to intermittent hypoxia. *Journal of Neurochemistry* **83**, 331-345, doi:10.1046/j.1471-4159.2002.01134.x (2002).
- 35 Vogl, T. *et al.* Mrp8 and Mrp14 are endogenous activators of Toll-like receptor 4, promoting lethal, endotoxin-induced shock. *Nat Med* **13**, 1042-1049, doi:http://www.nature.com/nm/journal/v13/n9/suppinfo/nm1638_S1.html (2007).
- 36 Kim, J. *et al.* Myeloid-related protein 8/14 levels in children with obstructive sleep apnoea. *European Respiratory Journal* **35**, 843-850, doi:10.1183/09031936.00075409 (2010).

- 37 Akinnusi, M., Jaoude, P., Kufel, T. & El-Solh, A. Toll-like receptor activity in patients with obstructive sleep apnea. *Sleep Breath*, 1-8, doi:10.1007/s11325-012-0791-2 (2012).
- 38 Crain, J., Nikodemova, M. & Watters, J. Expression of P2 nucleotide receptors varies with age and sex in murine brain microglia. *Journal of Neuroinflammation* **6**, 24 (2009).
- 39 Nikodemova, M. & Watters, J. J. Efficient isolation of live microglia with preserved phenotypes from adult mouse brain. *J Neuroinflammation* **9**, 147, doi:10.1186/1742-2094-9-147 (2012).
- 40 Rutledge, R. G. & Côté, C. Mathematics of quantitative kinetic PCR and the application of standard curves. *Nucleic Acids Research* **31**, e93, doi:10.1093/nar/gng093 (2003).
- 41 Nikodemova, M., Small, A. L., Smith, S. M. C., Mitchell, G. S. & Watters, J. J. Spinal but not cortical microglia acquire an atypical phenotype with high VEGF, galectin-3 and osteopontin, and blunted inflammatory responses in ALS rats. *Submitted* (2013).
- 42 Klein, J. B. *et al.* Proteomic identification of a novel protein regulated in CA1 and CA3 hippocampal regions during intermittent hypoxia. *Respiratory Physiology & Neurobiology* **136**, 91-103, doi:http://dx.doi.org/10.1016/S1569-9048(03)00074-0 (2003).
- 43 Simakajornboon, N., Szerlip, N. J., Gozal, E., Anonetapipat, J. W. & Gozal, D. In vivo PDGF β receptor activation in the dorsocaudal brainstem of the rat prevents hypoxia-induced apoptosis via activation of Akt and BAD. *Brain Research* **895**, 111-118, doi:http://dx.doi.org/10.1016/S0006-8993(01)02054-6 (2001).
- 44 Reeves, S. R., Guo, S. Z., Brittan, K. R., Row, B. W. & Gozal, D. Anatomical changes in selected cardio-respiratory brainstem nuclei following early post-natal chronic intermittent hypoxia. *Neurosci Lett* **402**, 233-237, doi:S0304-3940(06)00381-8 [pii]10.1016/j.neulet.2006.04.013 [doi] (2006).
- 45 Reeves, S. R. *et al.* Effect of long-term intermittent and sustained hypoxia on hypoxic ventilatory and metabolic responses in the adult rat. *Journal of Applied Physiology* **95**, 1767-1774, doi:10.1152/jappphysiol.00759.2002 (2003).
- 46 Ramanathan, L., Gozal, D. & Siegel, J. M. Antioxidant responses to chronic hypoxia in the rat cerebellum and pons. *J Neurochem* **93**, 47-52, doi:JNC2988 [pii]10.1111/j.1471-4159.2004.02988.x [doi] (2005).
- 47 Lehnardt, S. *et al.* Activation of innate immunity in the CNS triggers neurodegeneration through a Toll-like receptor 4-dependent pathway. *PNAS* **100**, 8514-8519 (2003).
- 48 Balistreri, C. R. *et al.* Association between the polymorphisms of TLR4 and CD14 genes and Alzheimer's disease. *Curr Pharm Des.* **14**, 2672-2677. (2008).

- 49 Zhao, W. *et al.* Extracellular mutant SOD1 induces microglial-mediated motoneuron injury. *Glia* **58**, 231-243, doi:10.1002/glia.20919 (2010).
- 50 Marta, M. Toll-like receptors in multiple sclerosis mouse experimental models. *Ann N Y Acad Sci.* **1173**, 458-462. (2009).
- 51 Ock, J. *et al.* Regulation of Toll-like receptor 4 expression and its signaling by hypoxia in cultured microglia. *J Neurosci Res* **85**, 1989-1995, doi:10.1002/jnr.21322 [doi] (2007).
- 52 Kim, S. Y. *et al.* Hypoxic stress up-regulates the expression of Toll-like receptor 4 in macrophages via hypoxia-inducible factor. *Immunology* **129**, 516-524, doi:10.1111/j.1365-2567.2009.03203.x (2010).
- 53 Huxtable, A. G., Smith, S. M. C., Vinit, S., Watters, J. J. & Mitchell, G. S. Systemic LPS induces spinal inflammatory gene expression and impairs phrenic long-term facilitation following acute intermittent hypoxia. *Journal of Applied Physiology* **114**, 879-887, doi:10.1152/jappphysiol.01347.2012 (2013).
- 54 Ling, L. *et al.* Chronic Intermittent Hypoxia Elicits Serotonin-Dependent Plasticity in the Central Neural Control of Breathing. *The Journal of Neuroscience* **21**, 5381-5388 (2001).
- 55 Peppard, P. E. *et al.* Increased prevalence of sleep-disordered breathing in adults. *American Journal of Epidemiology* **in press** (2013).
- 56 Wang, Y., Zhang, S. X. L. & Gozal, D. Reactive oxygen species and the brain in sleep apnea. *Respiratory Physiology & Neurobiology* **174**, 307-316, doi:http://dx.doi.org/10.1016/j.resp.2010.09.001 (2010).
- 57 Hoch, C. C. *et al.* Sleep-disordered breathing in normal and pathologic aging. *J Clin Psychiatry* **47**, 499-503 (1986).
- 58 Atalaia, A., De Carvalho, M., Evangelista, T. & Pinto, A. Sleep characteristics of amyotrophic lateral sclerosis in patients with preserved diaphragmatic function. *Amyotroph Lateral Scler* **8**, 101-105, doi:777130549 [pii] 10.1080/17482960601029883 [doi] (2007).
- 59 Manon-Espaillet, R., Gothe, B., Ruff, R. L. & Newman, C. Sleep Apnea in Multiple Sclerosis. *Neurorehabil Neural Repair* **3**, 133-136, doi:10.1177/136140968900300304 (1989).
- 60 Tran, K., Hukins, C., Geraghty, T., Eckert, B. & Fraser, L. Sleep-disordered breathing in spinal cord-injured patients: A short-term longitudinal study. *Respirology* **15**, 272-276, doi:10.1111/j.1440-1843.2009.01669.x (2010).

- 61 Bombois, S., Derambure, P., Pasquier, F. & Monaca, C. Sleep disorders in aging and dementia. *J Nutr Health Aging*. **14**, 212-217. (2010).
- 62 Marcus, C. L., Keens, T. G., Bautista, D. B., von Pechmann, W. S. & Ward, S. L. Obstructive sleep apnea in children with Down syndrome. *Pediatrics*. **88**, 132-139. (1991).
- 63 Ali, L. K. & Avidan, A. Y. Sleep-disordered breathing and stroke. *Rev Neurol Dis* **5**, 191-198 (2008).

CHAPTER 5

**MICROGLIAL INFLAMMATORY RESPONSES TO CHRONIC INTERMITTENT
HYPOXIA ARE MEDIATED IN PART THROUGH TLR4 ACTIVATION**

Stephanie M.C. Smith, Alex W. Wessell, and Jyoti J. Watters

In preparation for publication

ABSTRACT

Intermittent Hypoxia (IH), a hallmark of sleep apnea, causes severe neurologic deficits. Inflammation underlies much IH-induced neuropathology, including cortical/hippocampal neuronal apoptosis and cognitive deficits. In the rat model, we recently demonstrated that IH-induced microglial pro-inflammatory gene expression. Additionally, microglial TLR4 mRNA was significantly up-regulated by IH. In these studies, we test whether TLR4 regulates microglial inflammation following IH. Rodents were exposed to alternating intervals of hypoxia and normoxia during their respective night cycles for 1, 4, 7, 14, and 28 days. We utilized multi-color flow cytometry to analyze the protein levels of pro-inflammatory molecules expressed by microglia following IH exposure. We found that IH differentially increases microglial expression of CD11b, CD45, IL-1 β , and TLR4 over the course of IH exposure. To investigate the mechanism whereby IH activates microglia, we treated microglial cultures with CNS supernatants. The soluble factors from IH-treated animals induced activation of cultured microglia, pro-inflammatory effects that were absent in microglia with nonfunctional TLR4. These data suggest that endogenous molecule(s) released during IH may signal through TLR4 to promote microglial activation and neuroinflammation *in vivo*. Additionally, microglia exposed to IH *in vitro* increase pro-inflammatory gene expression, and this IH-induced inflammatory gene expression is mediated, at least in part through TLR4-mediated signaling. Finally, we tested if microglial TLR4 up-regulation *in vivo* primes microglia to become more pro-inflammatory to a secondary inflammatory exposure. Surprisingly, microglial inflammatory responses to a systemic administration of LPS were attenuated in microglia exposed to 14 days of IH, suggesting that microglia may undergo a phenotypic transition during chronic exposure to

IH that attenuates inflammatory processes. This is the first study to investigate the role of TLR4 in IH-induced microglial gene expression.

INTRODUCTION

Intermittent hypoxia (IH) is a hallmark feature of sleep disordered breathing and is most commonly experienced in the form of obstructive sleep apnea (OSA). By recent estimates, 13% of men and 6% of women between the ages of 30-70 experience moderate-severe sleep disordered breathing¹, a condition that if left untreated, can have significant deleterious effects on mood², behavior³⁻⁵, and cognitive processing^{6,7} in addition to increasing risk for developing cardiovascular^{8,9} and metabolic disorders⁹. In rodent models, IH protocols designed to simulate moderate-severe sleep apnea cause significant cognitive deficits that are attributed to increases in neuron death in hippocampal and frontal cortical regions¹⁰⁻¹². Much of this IH-induced neuropathology is thought to be a result of increased oxidative stress and inflammation^{13,14} as pharmacologic inhibition and/or genetic deletion of NADPH oxidase^{10,15-17}, cyclooxygenase-2 (COX-2)¹³, and inducible nitric oxide synthase (iNOS)¹⁴ significantly protect against IH-induced cognitive impairments and neuronal death.

Recent work from our laboratory demonstrated that cortical, spinal, and medullary microglia, resident CNS immune cells, increase pro-inflammatory gene expression in response to IH in the rat, and the inflammatory profile differs regionally and temporally following chronic IH exposure¹⁸. In addition to increased production of COX-2 and iNOS, we found significant increases in the expression of the pro-inflammatory cytokines interleukin (IL)- 1 β and -6 in microglia from all regions studied (although regional expression varied temporally), while tumor necrosis factor-alpha (TNF α) levels decreased or remained largely unchanged. Interestingly, microglial expression of IL-1 β increased acutely after just 1 day of IH and returned to control levels by 14 days in the medulla and spinal cord, whereas IL-1 β expression did not increase in cortical microglia until 14 days of IH exposure, suggesting significant regional differences in

microglial responses to IH¹⁸. However, the functional importance of and the mechanisms underlying the regional heterogeneity of microglial inflammatory responses to IH are yet unknown.

Despite comprising only 5-10% of the total CNS cell population, microglia play essential roles in the maintenance of healthy brain functioning^{19,20} and they provide the first line of defense against invading pathogens and tissue damage^{21,22}. When disturbances in cellular homeostasis are detected, microglia rapidly transition to an 'active' phenotype marked by morphologic changes, increased pro- or anti- inflammatory molecule production, proliferation, migration, and/or phagocytosis^{23,24}. Acute inflammation following insult is necessary and beneficial in the CNS as it eliminates pathogens, removes cellular debris, and promotes tissue repair²⁵. However, chronic/prolonged inflammation is neurotoxic and is believed to be a common factor contributing to all neuronal disorders²⁶. Additionally, many cytokines traditionally characterized as pro-inflammatory have concentration-dependent effects in the CNS where low levels promote neurogenesis and synaptic plasticity, but high levels contribute to neurotoxicity^{25,27,28}. Among the cytokines found to have dual, concentration-dependent functions within the CNS are IL-1 β ^{29,30}, IL-6^{31,32}, and TNF α ^{33,34}, the expression of all of which we found to be altered in some capacity by IH in microglial cells¹⁸.

Toll-like receptors (TLRs), a family of pattern recognition receptors (PRRs) highly expressed by microglial cells^{35,36}, are becoming increasingly appreciated for mediating sterile inflammation in the CNS^{37,38}, as is experienced during IH and OSA. They are best known for their ability to recognize highly conserved motifs expressed by microbial cells, known as pathogen-associated molecular patterns (PAMPs)³⁹. However, dozens of endogenously produced proteins, known collectively as damage associated molecular patterns (DAMPs) have

been identified as putative TLR ligands^{40,41}. The majority of these endogenous TLR ligands are intracellular proteins that under normal conditions are not freely available to interact with TLR receptors. Consequently, when they are released into the extracellular space by stressed, damaged, and/or dying cells, they act as danger signals or ‘alarmins’ that initiate microglial inflammatory pathways via TLR activation.

We previously reported that microglial TLR4 gene was upregulated in rats exposed to IH, in a time course that largely corresponded with induction of pro-inflammatory gene expression¹⁸. Consistent with these findings, a recent study showed that monocytes isolated from patients with OSA have increased expression of TLR4 and TLR2, as well as pro-inflammatory cytokines, when compared to matched control (non-OSA) subjects, effects which were reduced following 8 weeks of continuous positive airway pressure (CPAP)⁴². Additionally, TLR4 expression is increased in microglia by sustained hypoxia *in vitro*^{43,44} and mediates microglial inflammation in neonatal rats exposed to sustained hypoxia for 2 hours⁴³. Several known endogenous TLR4 ligands (DAMPs)⁴⁵ are increased in the serum of patients with OSA including: ligand monocyte responsive protein (MRP)-8/14 (S100A8/S100A9, or calprotectin)^{46,47}, high mobility group box-1(HMGB1)⁴⁸, heat shock protein (HSP)-70⁴⁹, fibrinogen⁵⁰⁻⁵², and oxidized LDL^{53,54}. However their cellular source(s), and whether they are also released into the extracellular space in the CNS are currently unknown. In addition to these circulating DAMPs that are increased in OSA patients, HMGB1 and HSP60^{55,56} are also released from stressed/dying CNS cells, and they act on microglia to promote their inflammatory activities- via TLR4 activation?. HSP60 is also acutely and selectively increased in the CA1, but not CA3 region of the hippocampus (within 6 hours), a major site of IH-induced neuron death following IH exposure⁵⁷. However, it is

unknown if this protein is increased intracellularly, and/or if it is released into the extracellular space to act as a DAMP.

In the present studies, we tested the hypothesis that TLR4 plays a role in controlling IH-induced microglial inflammatory responses in the frontal cortex and hippocampus, the most susceptible CNS regions to IH-induced neuron death. We used flow cytometry to assess microglial production of inflammatory proteins and TLR4 expression in mice exposed to IH (90 sec intervals of 6% and 21% O₂) for 12 hours/day during their respective night cycles for 1, 4, 7, 14, and 28 days. We found pro-inflammatory proteins and TLR4 to be upregulated in a time- and gene-specific manner. Since we hypothesized that endogenous TLR4 ligands were increased in the brains of IH-exposed animals, we treated microglial cultures with soluble proteins isolated from frontal cortical and hippocampal tissue of mice exposed to IH, and found that pro-inflammatory gene expression was increased in a manner that required TLR4. Direct exposure of microglial cultures to IH also promoted pro-inflammatory gene expression, but the induction of only certain genes appeared to require TLR4 activity, at least in part. Lastly, because we hypothesized that increased TLR4 levels on the microglial surface would “prime” them to be more pro-inflammatory to a subsequent inflammatory stimulus, we exposed mice to IH for 14 days after which time systemic inflammation was induced by LPS treatment. Surprisingly, we found that not only was LPS-induced pro-inflammatory gene expression in microglia reduced compared to normoxia treated controls, but anti-inflammatory gene expression was potentiated in the IH animals, suggesting that the early pro-inflammatory activities of TLR4 may be somehow altered by chronic IH exposure. Altered TLR4 signaling in microglia may enable their adaptation to a more anti-inflammatory/neuroprotective phenotype to minimize the neuroinflammatory effects of chronic IH.

METHODS

Materials

LPS (E.coli 0111:B4) Sigma Chemical Company (St. Louis, MO). Hank's Buffered Salt Solution (HBSS) was purchased from Cellgro (Herndon, VA). Glycoblue reagent was purchased from Ambion (Austin, TX). Oligo dT, Random Primers, and RNase inhibitor were purchased from Promega (Madison, WI). Power SYBR green was purchased from Applied Biosystems (Foster City, CA). Calcium acetate, zinc chloride, zinc trifluoroacetate, glycerol, DEPC, EDTA, and TRI reagent were purchased from Sigma Aldrich (St. Louis, MO). Percoll was purchased from GE Healthcare (Waukesha, WI). DNase was purchased from Worthington Biochemicals (Lakewood, NJ). Gas permeable 24-well tissue culture plates were purchased from Coy Laboratories (Great Lake, Michigan). TAK-242 was purchased from Invivogen (San Diego, CA). SB202190 and U0126 were purchased from Calbiochem (Billerica, MA). MMLV reverse transcriptase, RNase AWAY, and DAPI were purchased from Invitrogen (Carlsbad, CA). IL-6, TNF α , and caspase-3 antibodies were purchased from BD Biosciences (San Jose, CA). CD11b antibody was purchased from eBioscience (San Diego, CA). NeuN antibody was purchased from Millipore (Billerica, MA). TLR4 antibody was purchased from Biolegend (San Diego, CA). pro-IL-1 β antibody was purchased from R&D Systems (Minneapolis, MN).

Animals

Experiments were performed on adult, male, C57/BL6 (Harlan Laboratories, Madison, WI) or B6.B10ScN-Tlr4^{lps-del/JthJ} (Jackson Laboratory, Bar Harbor, ME) mice, weighing 25-28g. Mice were randomly assigned to intermittent hypoxia or room air groups. Mice were housed in clear polycarbonate cages under standard conditions conditions, with a 12 hour light/dark cycle (6:00am-6:00pm) and *ad libitum* food and water. All protocols were approved by

the University of Wisconsin Institutional Animal Care and Use Committee All efforts were made to minimize animal distress and reduce the numbers used, while permitting the formation of statistically reliable conclusions.

Intermittent Hypoxia (IH) Exposure

All animal exposures were performed using a commercially-designed system (BioSpherix, Redfield, NY). Animals were housed in standard polycarbonate cages with access to food at water *ad libitum* and maintained in a specialized chamber (12x20x30). Oxygen and carbon dioxide concentrations were continuously measured by an O₂ and CO₂ analyzer and were changed by a computerized system controlling gas outlets (Oxycycler model G2 and Watview software). During the sleep cycle (light-on hours), oxygen concentrations were modified to generate a cyclical pattern of either 6% or 21% oxygen every 90 seconds (intermittent hypoxia)^{58,59}. During their awake period (lights-off), O₂ concentration was maintained at a steady 21%. During the IH exposure, the rapid airflow was sufficient to prevent CO₂ accumulation, and during the normoxia period, room air was periodically flushed through the system maintain a CO₂ concentration below 0.3%. Normoxic control animals were either housed outside of the hypoxia chamber in room air or maintained inside the chamber with circulating room air to mimic the IH exposure.

Mechanical dissociation and fixation of neural tissue for flow cytometry

CNS tissues were dissociated as previously described⁶⁰ (Chapter 3). Briefly, mice euthanized with an overdose of isoflurane and perfused intra-aortically with cold 0.1M phosphate buffered saline (PBS). The frontal cortex and hippocampus were dissected out, placed into cold HBSS on ice, and mechanically dissociated by pushing tissue through a pre-moistened 100 μ M cell strainer with a syringe plunger and washed with cold HBSS supplemented with

0.01mg/ml DNase. Dissociated tissues were resuspended in 26% Percoll in 0.1M PBS and centrifuged at 850g for 15 minutes to remove myelin. Samples were divided, where half was taken for analysis of non-secreted proteins and was immediately fixed in a modified zinc-based fixative (mZBF) (0.5% zinc chloride, 0.5% zinc trifluoroacetate, 0.05% calcium acetate in 0.1M Tris-HCL, pH to 6.4-6.7)⁶¹ and glycerol (1:1), and stored at -20°C overnight or until ready to be stained for flow cytometry^{61,62}. The other half was taken for intracellular cytokine staining and incubated at 37°C for 4 hours in 1 ml of DMEM supplemented with 10% FBS, 100 U mL⁻¹ penicillin/streptomycin, and 3µl of GolgiPlug, a Brefeldin-A – containing compound that blocks the canonical secretory pathways through interactions with golgi apparatus⁶³ prior to mZBF fixation.

Staining for Flow Cytometry

Fixed samples were washed 3X in ice-cold PBS. Cell surface protein stains CD11b-APC-Cy7 (1:150), CD45-APC (1:100), and/or TLR4-PE-CY7 (1:25) were performed on ice in 50µl of 1X PBS supplemented with 0.1% BSA for 25 minutes. Cells were washed 3X and re-suspended in permeabilization buffer (1X PBS + 0.2% saponin + 0.1% BSA). Intracellular staining was performed in 50µl permeabilization buffer on ice for 45 minutes. The cytokine panel consisted of: IL-6- PE (1:100), TNFα- PE-CY7 (1:100), and pro-IL-1β- FITC, and the non-cytokine panels was stained with NeuN-Alexa 488 (1:500), and caspase-3- PE (1:20). Samples were washed and resuspended for in permeabilization buffer containing DAPI (1 µg/ml) to identify cells with intact nuclei. Cells were analyzed on a BD LSR II equipped with 350-, 405-, 433-, 561-, and 642-nm lasers, a standard filter set, and FACSDiva software (BD Biosciences). All appropriate compensation and FMO controls were performed and utilized in the analysis. Intact cells were identified using forward and side-scatter parameters, singlet gates, and DAPI

staining to identify cells in cell cycle at the time of fixation. Samples were first gated to exclude doublets and any events off scale with the following singlet gates: FSC-Width/SSC-Area, SSC-Width/FSC-Area. We then used a cell cycle gate to identify cells with an intact nuclei based on DAPI-Width/DAPI-Area plotted on a linear scale. Cell populations were identified and gated using the FMO controls. Microglia were identified based on CD11b and CD45 surface markers. See supplementary figure 1 for a representative example of the gating strategy utilized in these studies. Analysis of flow cytometry data was performed in FlowJo software v.10. (TreeStar Inc.). Regions from 2 animals were pooled to create a single individual sample. Data are representative of 4 individuals.

Cell Culture

Murine BV2 microglial cells⁶⁴ were routinely cultured in Dulbecco's modified Eagle's medium (DMEM; Cellgro, Herndon, VA) supplemented with 10% fetal bovine growth serum (FBS, Hyclone, Logan, UT) in 100 mm BD Falcon plates. Cells were grown to ~90% confluency and passaged every 1-3 days. For IH supernatant experiments, cells were seeded at a density of 2.5×10^4 per well and the following day were treated with tissue supernatants. For IH experiments, cells were grown on a gas-permeable membrane in a specialized 24-well plate to facilitate rapid gas exchange at the cellular level. For overnight IH experiments, cells were seeded at a density of 3.5×10^4 per well in a 24 well plate and 6 hours later were treated and exposed to IH.

Primary microglial cultures were prepared as previously described⁶⁵. Briefly, mixed glial cultures were prepared from C57/BL6 or B6.B10ScN-Tlr4lps-del/JthJ mice (postnatal days 3-7) and cultured in DMEM supplemented with 10% fetal bovine serum and 100 U mL^{-1} penicillin/streptomycin. Primary microglia were shaken from the mixed glial cultures and were

seeded at a density of 150,000 cells/well in a 24-well gas permeable tissue culture plates, and IH exposures started the following day.

***In Vitro* IH Supernatant Treatments**

CNS tissues were mechanically dissociated to single-cell suspensions as described above. Cells were pelleted and supernatants were saved for treatment of microglial cells *in vitro*. Protein concentrations in the supernatants collected from the *in vivo* IH studies above were determined by BCA assay. BV2 microglia were treated *in vitro* with 20 μ g of cellular supernatants \pm a TLR4 inhibitor (TAK-242, 1 μ M, 1hr pre-treatment) for 18hrs. mRNA was collected for qRT-PCR analyses of pro-inflammatory cytokines.

***In vitro* intermittent hypoxia exposure:**

Intermittent hypoxia exposures were performed using a commercially-designed cell culture system (BioSpherix, Redfield, NY). Cells were maintained in a specialized incubator chamber at 37°C. O₂ and CO₂ concentrations were continuously measured with O₂ and CO₂ analyzers, and were changed with a computerized system controlling gas outlets (Oxycycler model C42, Biospherix, Redfield, NY). Cells were exposed to normoxia (Nx; 21% O₂, 5% CO₂, balance N₂), or intermittent hypoxia (IH; 10min cycles of 1% and 21% O₂ held at a constant 5% CO₂, balance N₂).

Immunomagnetic Microglia (CD11b+) Cell Isolation from IH Treated Mice \pm LPS

Mice were exposed to 14 days of IH. Immediately following the last hypoxic exposure, mice were injected intraperitoneally with 1mg/kg LPS in sterile HBSS or sterile HBSS vehicle control, and were harvested 13 \pm 1.5 hours after LPS or vehicle administration. CD11b+ cells were isolated using previously described methods^{66,67}. Briefly, mice were euthanized with an overdose of isoflurane and perfused with cold 0.1M PBS. The whole brain minus (the

cerebellum, medulla, and olfactory bulbs) was dissected out and dissociated into a single cell suspension using 0.7mg/ml Papain and 50 μ g/ml DNase in HBSS. Myelin was removed by high speed centrifugation at 850g in a 26% solution of Percoll in 1X PBS. CD11b⁺ cells were tagged with an anti-CD11b antibody conjugated to a magnetic bead. Magnetically-tagged CD11b⁺ cells were isolated using MS columns according to the Miltenyi MACS protocol. Reagents were kept chilled at 4°C and cells were kept on ice whenever possible to preserve microglial phenotypes. We have previously shown, this method results in a >97% pure CD11b⁺/CD45^{low} cell population^{66,67}, and thus, this population will subsequently be referred to as “microglia.”

RNA extraction/ reverse transcription

RNA was extracted from BV2 and, primary, and immunomagnetically isolated microglia according to the TriReagent protocol, with the addition of Glycoblue during the isopropanol incubation. First-strand cDNA was synthesized from total RNA using MMLV Reverse Transcriptase, and an oligo(dT)/random hexamer cocktail. cDNA was used for qRT-PCR analysis.

Quantitative-Real Time PCR:

cDNA was used in real-time quantitative PCR with Power SYBR Green using either the ABI StepOne or ABI 7500 Fast system (Applied Biosystems/Life Technologies). Primers (Table 1) were designed using Primer 3 software and the specificity was assessed through NCBI BLAST. Primer efficiency was tested through the use of serial dilutions. Verification that the dissociation curve had a single peak with an observed T_m consistent with the amplicon length was performed for every PCR reaction. CT values from duplicate measurements were averaged and normalized to levels of the ribosomal RNA, 18s. Relative gene expression was determined using the $\Delta\Delta$ CT method⁶⁸.

Statistical analyses:

When comparing two population means, statistical inferences were made using a Student's t-test or a paired Student's t-test, where applicable. When three or more groups were compared across 2 parameters, comparisons were made using a two-way ANOVA or two-way RM ANOVA, where applicable. Holm-Sidak post hoc tests were used to assess statistical significance in individual comparisons. All statistical analyses were performed in SigmaPlot (Sigma Stat version 11(Systat Software, San Jose, CA). Statistical significance was set at $p < 0.05$. Mean data are expressed ± 1 SEM.

RESULTS:**IH bi-phasically increases the percentage of IL-1 β + and reduces the frequency of IL-6+ microglia in the frontal cortex and hippocampus**

IH induced a bi-phasic increase in the percentage of microglia (CD11b+ cells) expressing pro-IL-1 β in the frontal cortex and hippocampus, peaking at 1 and 7 days of IH (Fig. 1, Supp. Fig. 2). The proportion of IL-1 β + cells following 1 day of IH was increased in the frontal cortex ($41.40\% \pm 7.22$, $p < 0.001$) and hippocampus ($36.08\% \pm 7.01$, $p < 0.001$) compared to normoxia ($1.51\% \pm 0.38$ and $1.08\% \pm 0.29$, respectively). This population decreased to $7.63\% \pm 3.40$ in the frontal cortex and $9.67\% \pm 3.76$ in the hippocampus after 4 days of IH, though it remained significantly elevated over levels in normoxia ($p = 0.002$ and $p = 0.005$, respectively). After 7 days of IH, the percentage of IL-1 β + microglia again increased to $42.90\% \pm 2.72$ ($p < 0.001$) and 24.28 ± 3.2 ($p < 0.001$) respectively in the frontal cortex and hippocampus, and then declined to $21.95\% \pm 1.64$ and $12.54\% \pm 4.16$ at 14 days of IH, though again, remaining significantly elevated over control levels in normoxia ($p < 0.001$ for both). However, by 28 days of IH the percentage of IL-1 β + microglia returned to normoxic levels in both the frontal cortex and hippocampus ($2.15\% \pm 0.36$, $p = 0.618$ and $0.83\% \pm 0.27$, $p = 0.437$).

Whereas the frequency of microglia expressing IL-1 β was low in control animals, more microglia in the frontal cortex and hippocampus express detectable levels of IL-6 ($9.99\% \pm 1.14$ and $9.39\% \pm 1.94$, respectively) (Fig. 2, Supp. Fig. 3). Interestingly, IH decreased this population by ~70% at the 4 and 14 day time points ($p = 0.005$ and 0.008) in the frontal cortex. Similar trends were observed in the hippocampus where IH reduced the percentage of IL-6+ microglia by ~40%, although this did not reach statistical significance by an ANOVA ($p = 0.066$). Similarly, a large percentage of microglia expressed TNF α ($22.22\% \pm 3.71$ and $20.40\% \pm 2.93$)

in the frontal cortex and hippocampus (Fig. 3, Supp. Fig. 4). IH had no significant effect on the frequency of TNF α + microglia at any time point tested in either the frontal cortex ($p=0.068$) or hippocampus ($p=0.215$), although there appeared to be a trend towards reduced levels at 4 and 7 days in the hippocampus.

IH induces early and persistent increases in microglial CD45 and CD11b expression.

Since CD11b and CD45 marker upregulation are often used as indicators of pro-inflammatory activity of macrophages and microglia, we evaluated their expression following IH. We found that IH induced a significant increase in microglial expression of both CD11b and CD45 in frontal cortical and hippocampal microglia, as reflected by an increase in their respective median fluorescent intensities (MFI) (Fig. 4, Supp. Fig. 5). In the frontal cortex, the CD11b levels were significantly increased by ~36% ($p=0.001$), ~29% ($p=0.013$), and ~44% ($p<0.001$) following 1, 7, and 14 days of IH, respectively, but not at 4 or 28 days ($p=0.147$ and $p=0.502$) (Fig. 4B). CD45 levels followed a similar trend in the frontal cortex with significant increases in after 1 (~36%, $p<0.001$), 7 (~25%, $p<0.001$), 14 (~40%, $p<0.001$), and 28 days of IH (~16%, 0.010) relative to normoxic controls, although these increases were not observed at 4-days of IH ($p=0.336$) (Fig. 4C). In the hippocampus, CD11b levels were increased by ~37% ($p<0.001$), ~30% (0.001), ~31% (0.003), and ~33% (0.004) at 1, 4, 7, and 14 days of IH, respectively, and had returned to normoxic levels by 28 days ($p=0.515$) (Fig. 4D, Supp. Fig. 5) as in the cortex. CD45 levels were significantly increased over normoxic levels at all IH time points examined by ~35% ($p<0.001$), ~17% ($p=0.017$), ~32% ($p<0.001$), ~39% ($p<0.001$), and ~20% ($p=0.004$) following 1, 4, 7, 14, and 28 days, respectively.

IH long-lasting increases the percentage of microglia expressing complexed TLR4/MD2

We had previously observed that microglial TLR4 gene expression was increased by IH in a time course that corresponded with pro-inflammatory gene expression in the rat⁷. However, it was unknown whether this increase in gene expression translated into increased functional TLR4 protein *in vivo*. Since TLR4 requires the adaptor protein MD2 for functional activity, we used an antibody that recognizes the TLR4/MD2 complex to determine if IH increases cell surface expression of functional TLR4 protein. The frequency of TLR4/MD2+ microglia in the frontal cortex and hippocampus was almost doubled at 14 and 28 days of IH, although changes were not evident at earlier time points (Fig. 5, Supp. Fig. 6). In the frontal cortex, the percentage of TLR4/MD2+ microglia increased from 7.10% \pm 0.62 in normoxia to 13.60% \pm 2.24 (p=0.001) at 14 days and to 10.99 \pm 0.53 (p=0.016) at 28 days of IH (Fig. 5A,B). Similarly, the proportion of hippocampal microglia expressing TLR4/MD2 increased from 5.45% \pm 0.38 in normoxia to 10.06% \pm 1.62 (p=0.002) and 10.65% \pm 0.80 (p=<0.001) after 14 and 28 days of IH, respectively. Interestingly, the increased frequency of TLR4/MD2+ microglia remained observable at 28 days of IH when other markers of microglial activation including IL-1 β (Fig. 1) and CD11b (Fig. 4) had returned to normoxic levels.

Supernatants from frontal cortex and hippocampus of IH-treated animals induce pro-inflammatory gene expression in cultured BV2 microglia via a TLR4-dependent mechanism

Since TLR4 is up-regulated during IH and endogenous TLR4 ligands (DAMPs) may be released by stressed and/or dying cells in response to IH, we hypothesized that IH would increase DAMPs that would signal through TLR4 to induce microglial inflammation. Thus, we treated BV2 microglial cultures with supernatants collected following mechanical dissociation from the frontal cortex and hippocampus of mice exposed to normoxia (Nx), 1, 3, 7, 14, and 28 days of

IH. We found that frontal cortex (Fig. 6) and hippocampus (Fig. 7) supernatants from mice exposed to IH induced cyclooxygenase-2 (COX-2) and IL-6, but not IL-1 β or TNF α mRNAs in BV2 microglia when compared to supernatants from animals treated with Nx, and that these increases were prevented in the presence of the TLR4 inhibitor, TAK-242.

COX-2 mRNA levels were significantly increased by frontal cortex supernatants from mice exposed to 4, 14, and 28 days of IH by 2.17 ± 0.15 ($p=0.039$), 6.13 ± 2.15 ($p=0.002$), and 3.80 ± 0.91 ($p=0.010$) fold respectively (Fig. 6A). Although supernatants from 1 and 7 day IH animals also increased COX-2 mRNA levels by 2.48 ± 0.40 and 2.96 ± 0.93 fold, these did not quite reach statistical significance ($p=0.05$ and 0.083 , respectively). In the presence of the TLR4 inhibitor, TAK-242, the induction of COX-2 gene expression by these supernatants was abolished, with statistically significant decreases observed in COX-2 expression induced by supernatants from animals exposed to IH-1 ($p=0.025$), IH-4 ($p=0.009$), IH-7 ($p=0.008$), IH-14 ($p=0.004$), and IH-28 (0.002). IL-6 gene expression was likewise increased in BV2 microglia treated with supernatants from mice exposed to IH for 14 (7.45 ± 2.24 fold; $p=0.018$) and 28 days (6.12 ± 1.41 fold; $p=0.019$), and this induction was blocked by the TLR4 inhibitor ($p<0.001$ at both time points) (Fig. 6B). Additionally, TAK-242 significantly decreased the IL-6 expression in microglia treated with 4 ($p<0.001$) and 7 day ($p=0.008$) supernatants, despite the lack of significant IL-6 gene induction by supernatants at these time points ($p=0.667$ and 0.224 , respectively). While there were modest increases in IL-1 β (Fig. 6C) and TNF α (Fig. 6D) gene expression in these samples, they did not reach statistical significance at any time point. However, interestingly, there were significant reductions in the expression of both genes in the presence of TAK-242.

Findings from hippocampal supernatants were similar to those from the frontal cortex. COX-2 gene expression was increased in BV2 microglia treated with hippocampal supernatants from animals exposed to IH for 4, 7, 14, and 28 days by 3.66 ± 0.59 ($p=0.003$), 2.65 ± 0.44 ($p=0.035$), 3.58 ± 0.59 ($p=0.003$), and 3.08 ± 0.45 ($p=0.021$) fold, when compared to normoxic controls (Fig. 7A). In contrast to the complete abolition by TAK-242 of COX-2 gene expression induced by frontal cortex supernatants, TAK-242 significantly reduced COX-2 gene expression in microglia treated with hippocampal supernatants from 4 ($p=0.022$) and 14 day ($p=0.002$) IH exposed animals, but levels were not decreased to control levels. They tended to remain approximately 1.6- 2.5 fold higher than control levels although p-values were not significant (ranged from $p=0.187$ to 0.339). IL-6 gene expression was significantly increased by hippocampal supernatants from 1, 4, 7, and 28 day supernatants by 8.33 ± 3.73 ($p=0.009$), 9.64 ± 4.26 ($p=0.007$), 10.57 ± 4.58 ($p=0.003$), and 10.27 ± 3.28 ($p=0.002$) fold, respectively and by 3.01 ± 0.66 fold in 14 day samples, though it did not reach statistical significance ($p=0.062$). TAK-242 completely abolished IL-6 gene induction by hippocampal supernatants at all IH time points ($p<0.001$ for IH-1, IH-4, IH-7, and IH-14 and a $p=0.001$ for IH-28) (Fig. 7B). In addition, there was no statistically significant difference among supernatants in TAK-242 treated cells (p values ranged from 0.325 to 0.685). Similar to results from the frontal cortex, hippocampal supernatants from IH-treated animals induced modest increases in IL-1 β gene expression with fold changes ranging from 1.9-2.7 when compared to normoxic controls, although they did not reach statistical significance (2-way ANOVA p values ranged from 0.077 to 0.296) (Fig. 7C). However, there were significant reductions in IL-1 β gene expression with TAK-242 treatment at all IH time points (IH-1 $p=0.010$; IH-4, $p=0.003$; IH-7, $p=0.007$; IH-14, $p=0.020$) except for IH-28 ($p=0.267$). There was no observable induction of TNF α gene expression at any time point by

hippocampal supernatants ($p=0.273-0.917$). Surprisingly, TAK-242 induced TNF α gene expression in cells treated with supernatants from 28 day IH-exposed animals ($p=0.032$) (Fig. 7D).

Microglia exposed to IH *in vitro* increase pro-inflammatory gene expression through TLR4-dependent and independent mechanisms.

To study the direct effects of IH on microglia specifically, we exposed primary microglia to IH *in vitro*. IH increased pro-inflammatory gene expression relative to cells exposed to room air (normoxia). COX-2 mRNA levels were increased by 13.31 ± 4.99 fold ($p=0.003$), IL-6 by 5.01 ± 1.48 fold ($p=0.003$), and TNF α by 3.69 ± 0.24 fold ($p<0.001$) (Fig. 8A). IL-1 β appeared to be mildly increased with a 2.12 ± 0.39 fold increase over normoxia, although it did not reach statistical significance ($p=0.077$). Additionally, we examined the expression of the inflammatory/chemoattractant cytokines, macrophage inflammatory protein (MIP)-1 α (or CCL3) and MIP-1 β (or CCL4) to determine if IH altered their expression. Interestingly, IH significantly increased the expression of both molecules by 3.69 ± 0.24 ($p<0.001$) and 3.53 ± 0.47 ($p=0.003$) fold, respectively (Fig. 8C). Since TLR4 gene¹⁸ and protein expression (Fig. 5) were up-regulated in microglia by exposure to IH *in vivo*, we examined whether microglia exposed to IH *in vitro* had a similar response. We did not observe an IH-induced increase in TLR4 mRNA in primary microglial cultures (Fig. 8E). However, CD14, a scavenger receptor that complexes with TLR4 to confer responsiveness to LPS, was up-regulated by IH (2.42 ± 0.46 fold, $p=0.023$), as was TLR2 (1.54 ± 0.14 fold, $p=0.045$), a TLR that shares many functional similarities to TLR4 and can also be activated by DAMPs.

To test whether TLR4 was involved in IH-induced inflammation, we compared responsiveness to IH in primary microglia derived from wild-type (WT) and B6.B10ScN-

Tlr4^{lps-del/JthJ} (TLR4^{del}) mice. These mice harbor a naturally occurring deletion of the TLR4 gene locus⁶⁹. There were no significant differences in basal gene expression levels between WT and TLR4^{del} microglia for all genes studied, as determined by a student's t-test on the Δ CT-values, with the exception of IL-1 β , where the WT Δ CT values were \sim 2 cycles lower (i.e. higher basal expression) compared to the TLR4^{del} microglia (p=0.003). Data are graphed relative to their respective normoxic controls.

The IH-induced expression of COX-2 (p=0.049) and IL-1 β (p=0.003) was attenuated in TLR4^{del} microglia (Fig. 8B), and IL-6 mRNA levels trended towards a decrease, but they did not attain statistical significance (p=0.075). Interestingly, IH-induced expression of TNF α , MIP-1 α , and MIP-1 β were not affected in the TLR4^{del} microglia (p=0.736, 0.736, and 0.908 respectively) (Fig. 8D). Similarly, IH-induced expression of CD14 and TLR2 were not changed in microglia without TLR4 (p=0.637 for both) (Fig. 8E) suggesting that IH is sufficient to induce pro-inflammatory gene expression in microglial cultures, but TLR4 only plays gene-specific roles.

Microglia exposed to IH *in vitro* have heightened inflammatory responses to TLR4 ligands

We next wanted to test the hypothesis that IH exposed microglia would have exacerbated pro-inflammatory responses to subsequent inflammatory stimuli, perhaps as a result of increased TLR4 activity. However, primary microglia did not recapitulate the increase in TLR4 levels observed following IH exposure *in vivo*, so we turned to BV2 microglia to evaluate the effects of IH on TLR4 and TLR2 levels. We found that IH upregulated TLR4 mRNA by 1.79 ± 0.18 fold (p=0.012) and TLR2 by 1.72 ± 0.22 fold, although TLR2 did not reach statistical significance (p=0.061) (Fig. 9C A). We also assessed their ability to respond to IH with an increase in pro-inflammatory gene expression (Fig. 9A, B, C). Whereas IH also increased the expression of

inflammatory genes in BV2 cells, their gene expression profiles differed somewhat in their magnitudes compared to primary microglia (Fig. 8, Fig. 9D). IH-induced the expression of TNF α (1.92 ± 0.24 fold, $p=0.038$), MIP-1 α (2.71 ± 0.50 fold, $p=0.028$), MIP-1 β (2.14 ± 0.24 , $p=0.023$), IL-1 β (8.17 ± 1.77 - fold, $p=0.006$) and COX-2 (1.57 ± 0.34 - fold, $p=0.200$) in BV2 microglia. Having identified similarities between IH responses in BV2 microglia and microglia *in vivo*, we then exposed them to either IH or Nx for 16hrs, and then stimulated them with LPS or vehicle control for 6 hours (Fig. 9D). We found that LPS-induced IL-6 ($p=0.006$), COX-2 ($p=0.029$), and MIP-1 α ($p=0.005$) gene expression was potentiated in cells pre-treated with IH.

Chronic IH exposure *in vivo* attenuates microglial inflammatory responses in response to systemic inflammation

To test if exposure to IH *in vivo* would also “prime” microglia to become more pro-inflammatory to a subsequent inflammatory stimulus, we exposed mice to 14 days of IH followed immediately by an intraperitoneal injection of LPS or vehicle control. Microglia were isolated from the whole brain approximately 14 hours later, and inflammatory gene expression was evaluated. To our surprise, we found that the ability of LPS to induce microglial pro-inflammatory gene expression was attenuated in mice exposed to 14 days of IH (Fig.10). LPS significantly increased pro-inflammatory gene expression of: COX-2 (6.65 ± 1.87 -fold), IL-1 β (8.47 ± 1.53 -fold), TNF α (17.05 ± 4.89 -fold), MIP-1 α (5.42 ± 0.84 - fold), MIP-1 β (2.78 ± 0.46 -fold) as well as the anti-inflammatory cytokine IL-10 (4.23 ± 0.63 -fold) ($p < 0.001$ for all molecules). However, the expression of IL-1 β , TNF α , and MIP-1 α were significantly decreased by ~50% in IH-exposed mice ($p = 0.044$, 0.008 , and 0.042 , respectively), although LPS-induced COX-2 expression was not significantly reduced, although it appeared to trend lower ($p=0.118$). Likewise, IH had no effect on the LPS-induced expression of IL-10 ($p=0.228$) or MIP-1 β

($p=0.914$). But interestingly, IH alone significantly increased the expression of IFN β and BDNF by 5.32 ± 0.90 ($p=0.007$) and 5.40 ± 1.19 ($p=0.038$) fold, respectively, and LPS treatment did not alter this.

DISCUSSION:

Previously, we showed that IH-induced microglial pro-inflammatory gene expression varied regionally and temporally in a rat model of IH, and that observed increases in inflammatory gene expression correlated with upregulated TLR4 mRNA levels¹⁸. In order to better understand the role of microglia in the pathophysiology of IH-induced neural injury, we studied microglial gene expression in the CNS regions most susceptible to IH-induced neuronal death, the frontal cortex and hippocampus^{12,17,70}. Additionally, we sought to expand our previous observations implicating TLR4 as a potential mediator of IH-induced microglial activation, and to further explore its potential role in microglial responses to IH.

Here, we show that microglial activation by IH in the mouse is bi-phasic with an acute/early phase followed by a slower and more long-lasting chronic activation state that subsides by 28 days of IH. We found that the percentage of microglia expressing detectable levels of the functional TLR4/MD2 complex on their cell surface increased at later IH time points and remained elevated when other indicators of pro-inflammatory activation were decreasing or had already returned baseline levels. Additionally, we identified that microglial inflammatory responses to IH are mediated through TLR4-dependent and independent mechanisms. This report is the first to directly evaluate the functional significance of TLR4 in IH-induced microglial activation and indicate a mechanism for microglial adaptation to the chronic neuroinflammatory IH stimulus, making them less reactive and more anti-inflammatory/neurotrophic.

We used flow cytometry to quantify the effects of IH on microglial protein levels over a time course spanning 1 to 28 days. Flow cytometry poses unique advantages over other protein analysis methods including immunohistochemical and immunoblot assays, as flow cytometry

enables sensitive, multi-parametric analysis of proteins in specific cell populations, while also distinguishing between cell surface and intracellular protein expression. This is essential as the microglial inflammatory response often includes increased production and subsequent release of small (~5-20kD), secreted cytokines and chemokines that are difficult, if not impossible to detect by other methods. Additionally, we previously showed that IH increased the expression of pro-inflammatory genes in both microglia and non-microglial CNS cells¹⁸, so analyzing protein expression in microglia specifically is an advantage. The optimized tissue processing and fixation methods used here to study CNS cells by flow cytometry were recently developed in our laboratory⁶⁰ (Chapter 3).

IH-induced microglial production of IL- β in microglia is bi-modal, where the proportion of microglia expressing detectable levels of pro-IL-1 β was transiently increased at 1 day, and then again increased at 7 and 14 days, before returning to normoxic levels at 28 days of IH exposure. Similarly, the expression of the CD11b and CD45 scavenger receptors on the microglial cell surface increased similarly to IL-1 β . Increased CD11b and CD45 expression is common in the activated or pro-inflammatory state⁷¹, consistent with the notion that microglia become activated by IH. The biphasic changes in the expression of these activation markers suggest that microglial activities during chronic IH exposure change with time. We also observed changes in the cell cycle of microglia following IH exposure, where we observed more microglial cells in the S- and G2- phases, as assessed by DAPI staining, following 1, 4, and 28 days of IH in the frontal cortex, and 4 and 28 days in the hippocampus (Supp. Figs. 7 and 8). These results suggest that IH may promote microglial proliferation in these regions. Interestingly, this response was also bi-phasic, but peak frequency of microglia in S/G2- phases was highest when microglial activation markers were low. While there was essentially no

detectable microglial expression of IL-1 β in normoxia, we did observe that ~10% and ~20% of microglia from the healthy CNS contain IL-6 and TNF α proteins, respectively. While IL-6 and TNF α are traditionally regarded as pro-inflammatory molecules, they can be neuroprotective at low concentrations, and they are necessary for some forms of neuroplasticity^{27,28,31,33,34}.

Consistent with our previous findings in the rat model, we did not observe increases in TNF α mRNA levels; if anything, basal levels of TNF α decreased with IH. Similarly, we found that the frequency of IL-6+ microglia decreased at 4 and 14 days of IH in the hippocampus. While the significance of decreasing basal TNF α and IL-6 are unknown, if basal expression of these molecules is indeed neuroprotective and required for neuronal plasticity, then IH-induced decreases may contribute to IH-induced injury.

Surface TLR4 protein expression was increased on microglia following 14 and 28 days of IH exposure. Several endogenous TLR4 ligands, including HSP60 and HMGB1, are released from damaged/dying neurons which can in turn, induce microglial-mediated inflammation through TLR4 activation^{55,56,72,73}. We observed increased expression of the pro-apoptotic marker caspase-3 in frontal cortical and hippocampal neurons as early as 4 days following IH (Supp. Figs. 9 and 10), supporting our hypothesis that IH is inducing neuronal death/stress which may contribute to increased microglial activation. Additionally, HSP60 is selectively increased in the IH-sensitive CA1 region of the hippocampus compared to the resistant CA3 region⁵⁷. We hypothesized that TLR4 played a crucial role in the initiation of IH-induced inflammation, via TLR4-mediated activation by DAMPs. To test this, we treated BV2 microglia with tissue supernatants collected from the frontal cortex and hippocampus of mice exposed to IH. These supernatants significantly increased COX-2 and IL-6 expression relative to supernatants from normoxic controls, and these increases were blocked in the presence of the selective TLR4

inhibitor, TAK-242^{74,75}. These data suggest that IH may increase levels of yet unidentified endogenous TLR4 ligands in the hippocampus and frontal cortex, and that they may facilitate IH-induced inflammation via microglial TLR4 activation. Preliminary *in vitro* studies currently underway support this hypothesis, where microglia treated with conditioned medium from IH-treated neuronal cultures increase microglial inflammation and this is partially blocked in the presence of a TLR4 inhibitor (Supp. Fig. 12). However, larger N are needed to confirm the validity of these results.

Exposure of primary and BV2 microglia to IH *in vitro* increased the expression of pro-inflammatory molecules. IH induced increases in COX-2, IL-1 β , and IL-6 expression were abolished in TLR4 deficient microglia, whereas IH-induced TNF α , MIP-1 α , and MIP-1 β mRNA levels were unaffected. Thus, IH appears to induce inflammatory gene expression through both TLR4-dependent and -independent mechanisms *in vitro*, potentially through the activation of mitogen activated protein kinase (MAPK) pathways (Supp. Fig. 11). The observation that IH could activate microglia via a TLR4-dependent mechanism, in the absence of known TLR4 ligand, was unexpected. We hypothesize that IH may induce the autocrine/paracrine release of a TLR4 ligand that acts to activate microglia via a TLR4-dependent mechanism. MRP8/14 and HMGB1 are putative TLR4 ligands that could be regulated in this manner^{76,77}. For example, MRP8/14 is highly expressed in the cytosol of monocytes, and it was recently shown to be released from monocytes following LPS activation to enhance LPS-induced inflammation⁷⁷, and during ischemic injury to induce TLR4-mediated inflammation⁷⁸. However, it is unknown if MRP8/14 is released from microglia in response to IH. HMGB1 is a nuclear protein that is rapidly trafficked to the cytosol following cellular stress, and it can be released through a NLRP3 inflammasome-mediated, non-canonical secretory pathway, similar to that of IL-1 β and IL-

18^{72,79}. In addition to activating TLR4, HMGB1 can also signal through TLR2⁷⁶ and CD11b⁵⁵ to induce inflammation, both of which we found to be increased by IH.

Based on tissue culture studies where we found that LPS-induced microglial pro-inflammatory gene expression was exacerbated in cells that had been previously exposed to IH, we hypothesized that IH would also prime microglia to be more pro-inflammatory to a subsequent inflammatory stimulus *in vivo*. Microglia from mice exposed to 14 days of IH followed by an acute peripheral injection of LPS, showed attenuation in pro-inflammatory gene expression such that LPS was less efficacious at inducing inflammation in the microglia from IH mice even though TLR4/MD2 levels were elevated. Also interesting is the gene-specific effects of LPS since the ability of LPS to alter anti-inflammatory/neurotrophic factor gene expression IL-10 and BDNF were not changed by IH, whereas IFN β was further upregulated. These data suggest that the chronic up-regulation of TLR4 during IH correlates with reduced microglial inflammatory activities and increased neurotrophic factor production, suggesting the potential for a neuroprotective role of TLR4 and microglia. The data also indicate that microglia adapt to the chronic IH exposure, and that they change their responses over time.

Together, the results presented here implicate an important role for TLR4 in mediating at least some aspects of IH-induced neuroinflammatory gene expression, suggesting the potential for TLR4 inhibitors to be beneficial for reducing neuroinflammation and its CNS morbidities in disorders characterized by chronic IH. Further, IH may be a useful model for promoting both inflammatory and neurotrophic activities of microglia, as it creates a situation in which natural microglial adaptation to the chronic inflammatory IH stimulus can be studied. This has application and significance to many neurodegenerative/inflammatory disorders.

ACKNOWLEDGEMENTS

We would like to thank Rebecca Kimyon, Thomas Dietz, and Scott Ray for their technical support on this project. We would also like to thank Bradley Wathen for his continued support and assistance with the intermittent hypoxia exposures, and Dagna Sheerar from the UW-Madison flow core facility for their assistance with the flow cytometry aspects of this study. We would also like to thank Drs. Tracy Baker-Herman and Gordon Mitchell for helpful discussions and their continued support of this project, and Supported by the National Institutes of Health [NS049033, HL111598 and T32HL007654] and the BD Biosciences Research Innovation Award in Immunology.

FIGURE 1

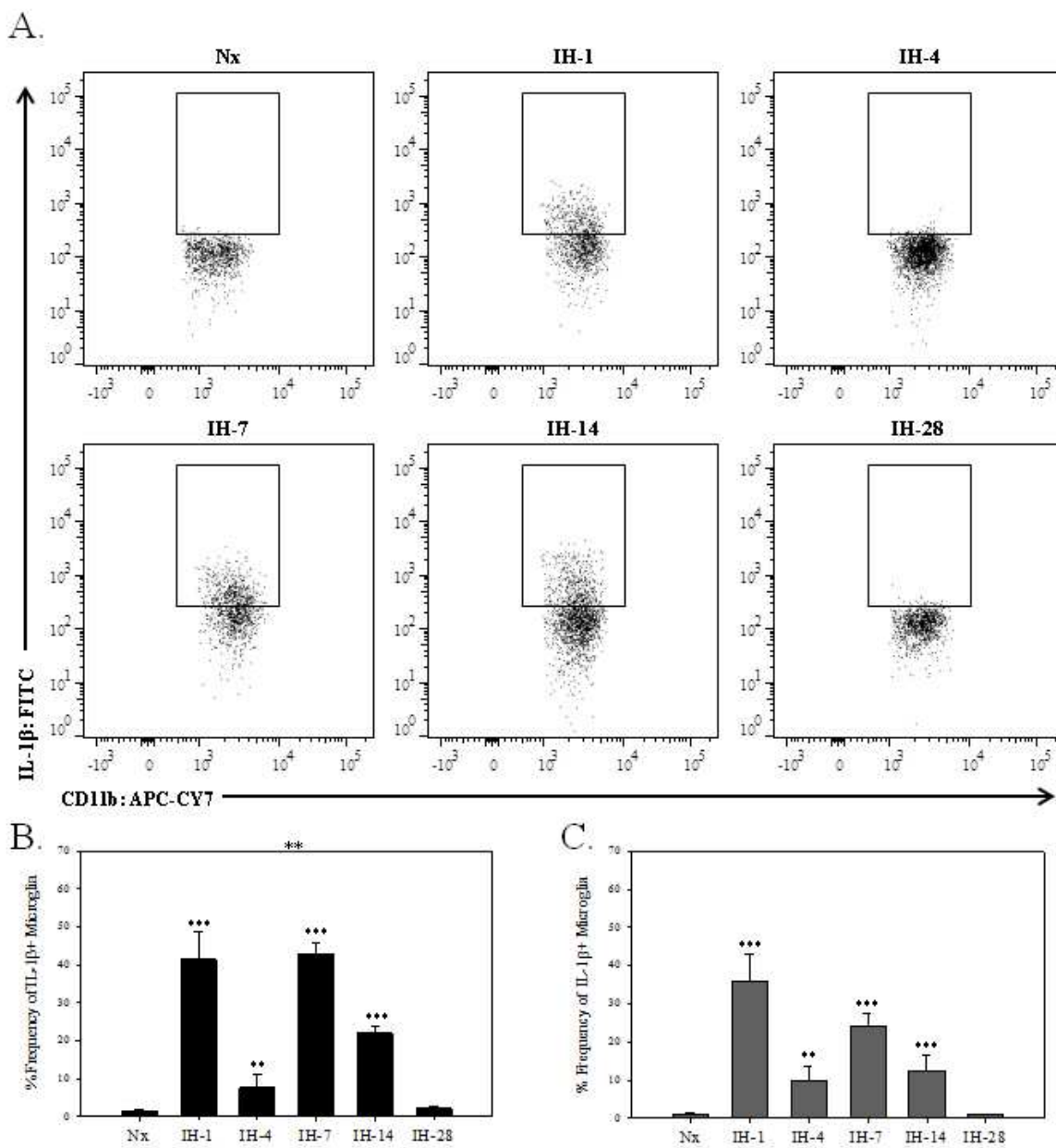


Figure Legend 1**Microglia exhibit a bi-phasic induction of pro-IL-1 β over the IH time course**

Mice were exposed to Nx, 1, 4, 7, 14, or 28 days of IH. 14 hours following the last hypoxic exposure, microglia were harvested for analysis by flow cytometry. Single cell mZBF-fixed suspensions were processed for flow cytometry. Singlet cells were gated based on FSC-H/SSC-A, and SSC-H/FSC-A, and then gated on DAPI to identify cells with an intact nucleus at time of fixation. We then plotted SSC-W vs. CD11b, and the cells that were CD11b⁺ per the FMO controls were gated on for subsequent analysis and will hereby be referred to as microglia. (A) Representative dot plots of IL-1 β vs. CD11b from frontal cortical tissue for all IH-timepoints (B) Frontal cortex, graphed average data of the percentage of microglia expressing IL-1 β . (C) Hippocampus, graphed average data of the percentage of microglia expressing IL-1 β . Respective tissues from 2 animals were pooled to create 1 sample. Data are representative of at least 4 individual samples. Mean % Frequency + 1 SEM are presented relative to expression in normoxic controls. Statistical significance was determined by a One-Way ANOVA, and a Holm-Sidak post-hoc test. * symbol represents statistical significant differences from normoxic control. *p<0.05; **p<0.01; ***p<0.001

FIGURE 2

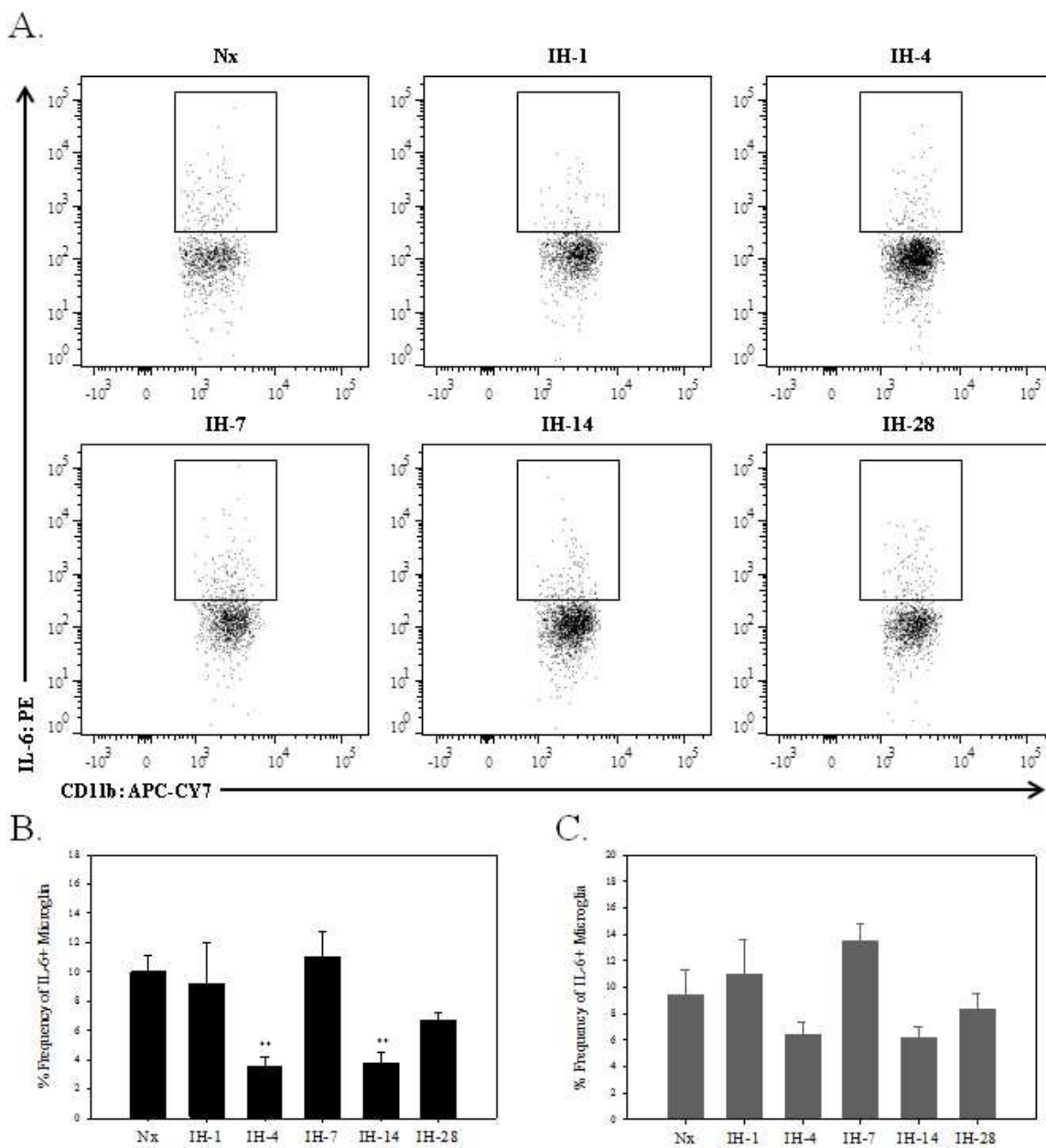


Figure legend 2**Microglia decrease IL-6 expression following 4 and 14 days of IH**

Mice were exposed to Nx, 1, 4, 7, 14, or 28 days of IH. 14 hours following the last hypoxic exposure, microglia were harvested for analysis by flow cytometry. Single cell mZBF-fixed suspensions were processed for flow cytometry. Singlet cells were gated based on FSC-H/SSC-A, and SSC-H/FSC-A, and then gated on DAPI to identify cells with an intact nucleus at time of fixation. We then plotted SSC-W vs. CD11b, and the cells that were CD11b⁺ per the FMO controls were gated on for subsequent analysis and will hereby be referred to as microglia. (A) Representative dot plots of IL-6 vs. CD11b from frontal cortical tissue for all IH-timepoints (B) Frontal cortex, graphed average data of the percentage of microglia expressing IL-6. (C) Hippocampus, graphed average data of the percentage of microglia expressing IL-6. Respective tissues from 2 animals were pooled to create 1 sample. Data are representative of at least 4 individual samples. Mean % Frequency + 1 SEM are presented relative to expression in normoxic controls. Statistical significance was determined by a One-Way ANOVA, and a Holm-Sidak post-hoc test. * symbol represents statistical significant differences from normoxic control. *p<0.05; **p<0.01; ***p<0.001

FIGURE 3

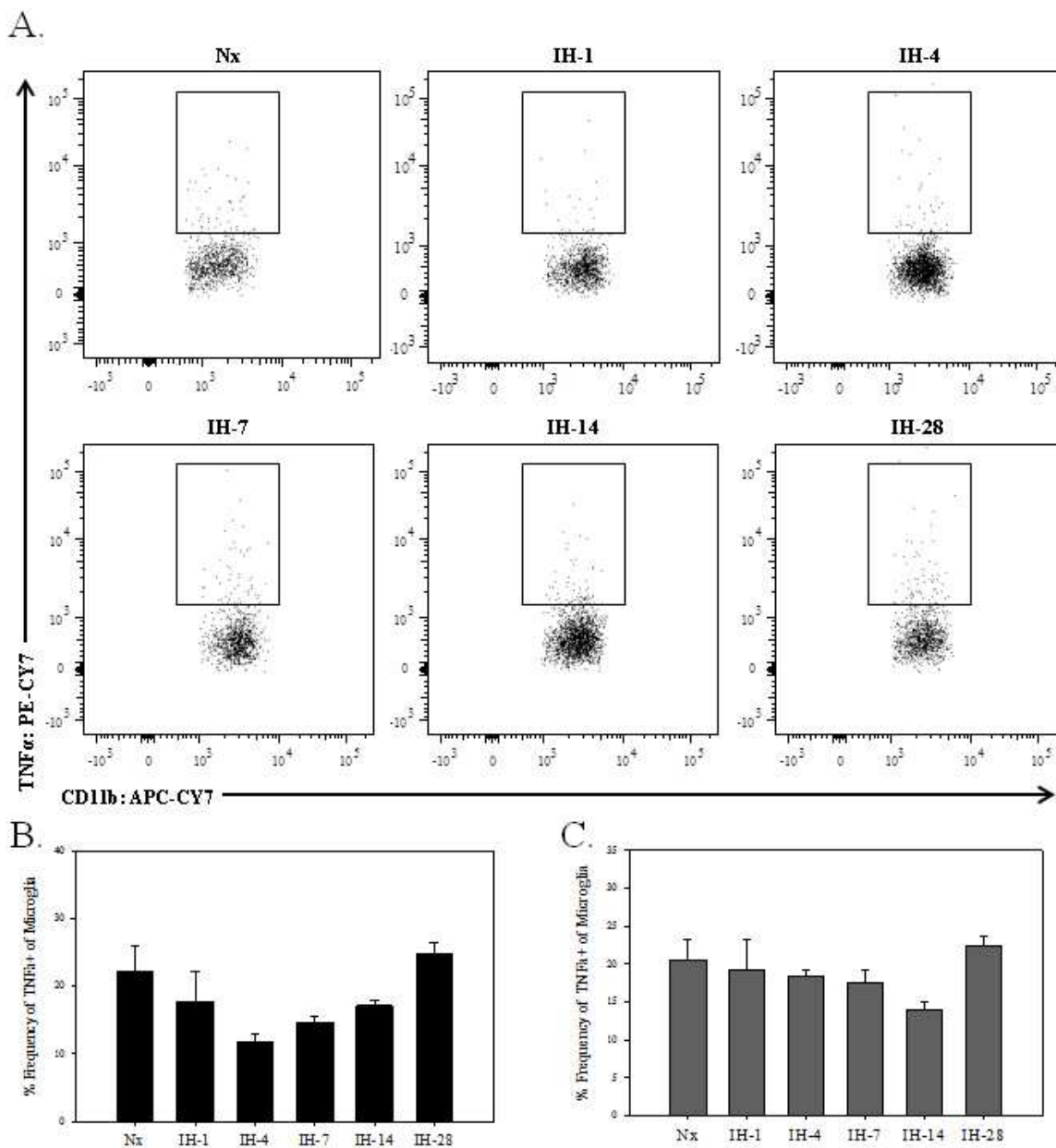


Figure Legend 3

Microglial expression of TNF α does not change with *in vivo* IH treatment

Mice were exposed to Nx, 1, 4, 7, 14, or 28 days of IH. 14 hours following the last hypoxic exposure, microglia were harvested for analysis by flow cytometry. Single cell mZBF-fixed suspensions were processed for flow cytometry. Singlet cells were gated based on FSC-H/SSC-A, and SSC-H/FSC-A, and then gated on DAPI to identify cells with an intact nucleus at time of fixation. We then plotted SSC-W vs. CD11b, and the cells that were CD11b⁺ per the FMO controls were gated on for subsequent analysis and will hereby be referred to as microglia. (A) Representative dot plots of TNF α vs. CD11b from frontal cortical tissue for all IH-timepoints (B) Frontal cortex, graphed average data of the percentage of microglia expressing TNF α . (C) Hippocampus, graphed average data of the percentage of microglia expressing TNF α . Respective tissues from 2 animals were pooled to create 1 sample. Data are representative of at least 4 individual samples. Mean % Frequency + 1 SEM are presented relative to expression in normoxic controls. Statistical significance was determined by a One-Way ANOVA, and a Holm-Sidak post-hoc test. * symbol represents statistical significant differences from normoxic control. *p<0.05; **p<0.01; ***p<0.001

FIGURE 4

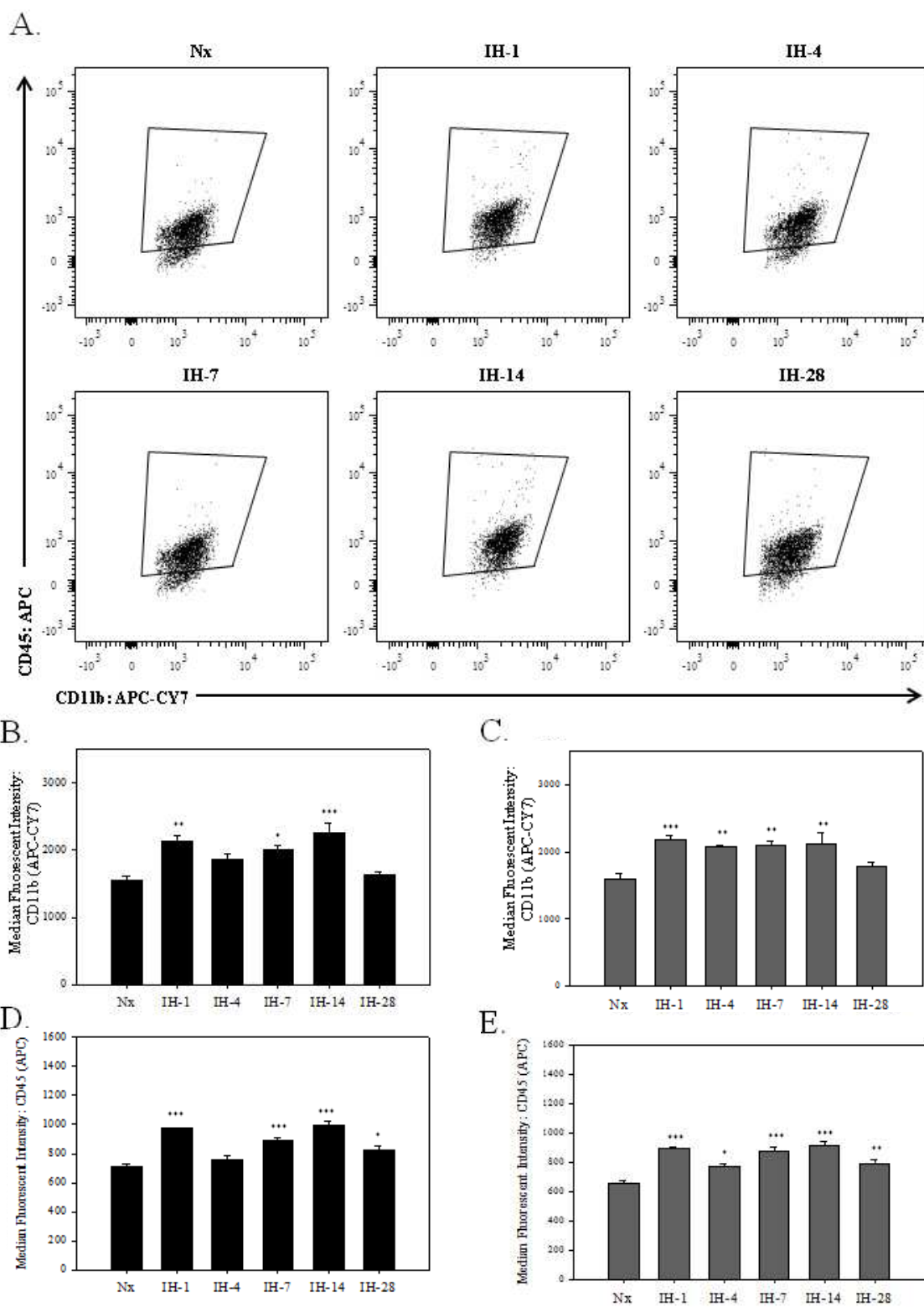


Figure Legend 4**Microglial expression of CD11b and CD45 increase following IH treatment.**

Mice were exposed to Nx, 1, 4, 7, 14, or 28 days of IH. 14 hours following the last hypoxic exposure, microglia were harvested for analysis by flow cytometry. Single cell mZBF-fixed suspensions were processed for flow cytometry. Singlet/DAPI+/NeuN-/ CD11b+ cells were identified based on FSC/SSC and staining properties and will hereby be referred to as microglia. See Supp. Fig. 1 for the detailed gating strategy. (A) Representative dot plots of CD45 vs. CD11b from frontal cortical tissue for all IH-timepoints (B) Frontal cortex, graphed average data of the mean fluorescent intensity of CD11b (C) Hippocampus, graphed average data of the mean fluorescent intensity of CD11b. (D) Frontal cortex, graphed average data of the mean fluorescent intensity of CD45 (E) Hippocampus, graphed average data of the mean fluorescent intensity of CD45. Respective tissues from 2 animals were pooled to create 1 sample. Data are representative of at least 4 individual samples. Mean MFI + 1 SEM are presented relative to expression in normoxic controls. Statistical significance was determined by a One-Way ANOVA, and a Holm-Sidak post-hoc test. * symbol represents statistical significant differences from normoxic control. * $p < 0.05$; ** $p < 0.01$; *** $p < 0.001$

FIGURE 5

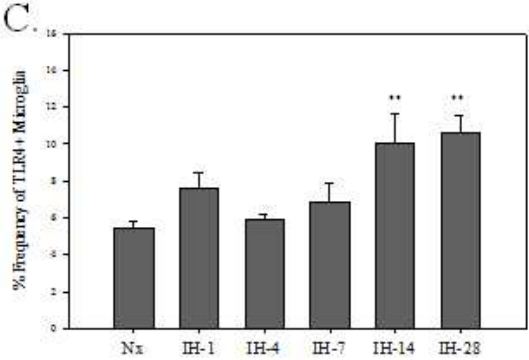
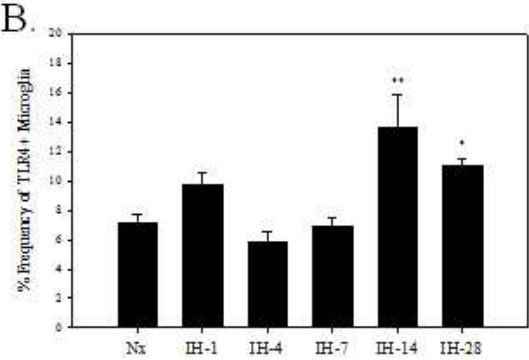
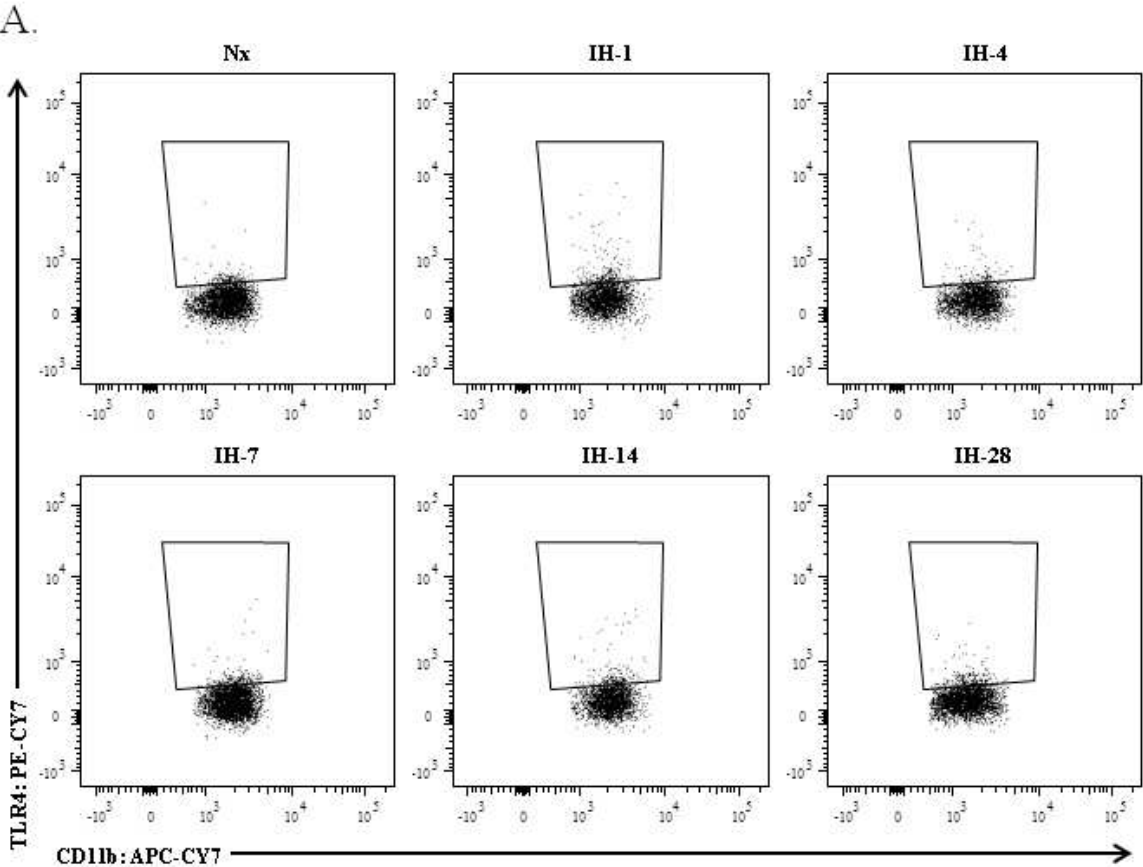


Figure Legend 5**Microglial surface expression of TLR4/MD2 increase following 14 and 28 day of IH**

Mice were exposed to Nx, 1, 4, 7, 14, or 28 days of IH. 14 hours following the last hypoxic exposure, microglia were harvested for analysis by flow cytometry. Single cell mZBF-fixed suspensions were processed for flow cytometry. Singlet/DAPI+/NeuN-/ CD11b+ cells were identified based on FSC/SSC and staining properties and will hereby be referred to as microglia. See Supp. Fig. 1 for the detailed gating strategy. (A) Representative dot plots of TLR4/MD2 vs. CD11b from frontal cortical tissue for all IH-timepoints (B) Frontal cortex, graphed average data of the percentage of microglia expressing TLR4/MD2. (C) Hippocampus, graphed average data of the percentage of microglia expressing TLR4/MD2. Respective tissues from 2 animals were pooled to create 1 sample. Data are representative of at least 4 individual samples. Mean % Frequency + 1 SEM are presented relative to expression in normoxic controls. Statistical significance was determined by a One-Way ANOVA, and a Holm-Sidak post-hoc test. * symbol represents statistical significant differences from normoxic control. + symbol represents statistical significant differences from veh control. * $p < 0.05$; ** $p < 0.01$; *** $p < 0.001$, + symbol

FIGURE 6

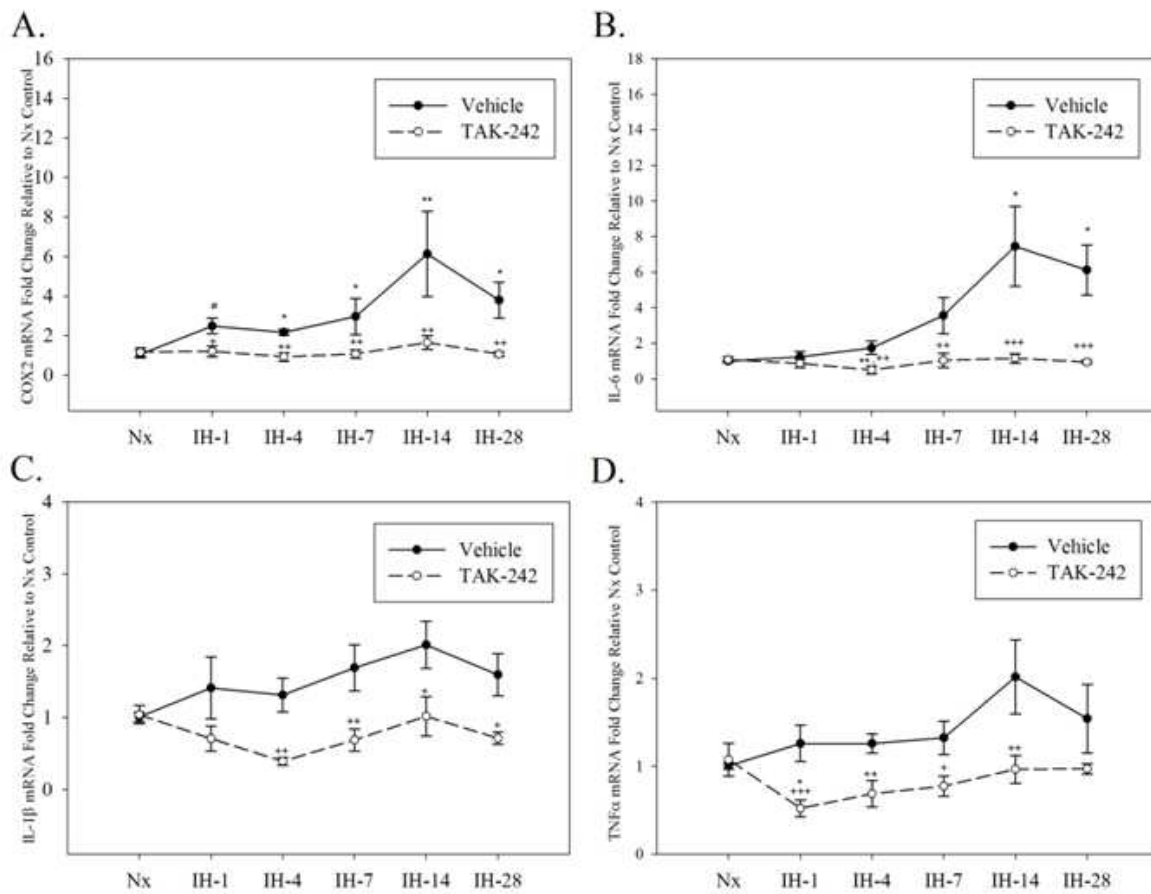


Figure Legend 6**Frontal cortical supernatants from IH treated animals increase expression of proinflammatory genes through a TLR4 dependent mechanism**

Frontal cortical tissues were isolated from mice exposed to Nx, 1, 4, 7, 14, or 28 days of IH.

Tissues were mechanically dissociated, the cellular fraction was removed through centrifugation, and the supernatants were collected. BV2 microglia in culture were treated with the isolated supernatant (20 μ g) in the presence/absence of the TLR4 inhibitor TAK-242 (1 μ M), and were harvested for gene expression analysis 18 hours post-treatment. (A) COX-2 expression (B) IL-6 expression, (C) IL-1 β , and (D) TNF α . Data are representative of at two independent experiments each with an n= 2-4, total n=6-8. Mean fold changes + 1 SEM are presented relative to respective normoxic controls. Statistical significance was determined by a two-way RM ANOVA on Δ CT values, and a Holm-Sidak post hoc. * symbol represents statistical significant differences from normoxic control. + symbol represents statistical significant differences from veh control.

*p<0.05; **p<0.01; ***p<0.001

FIGURE 7

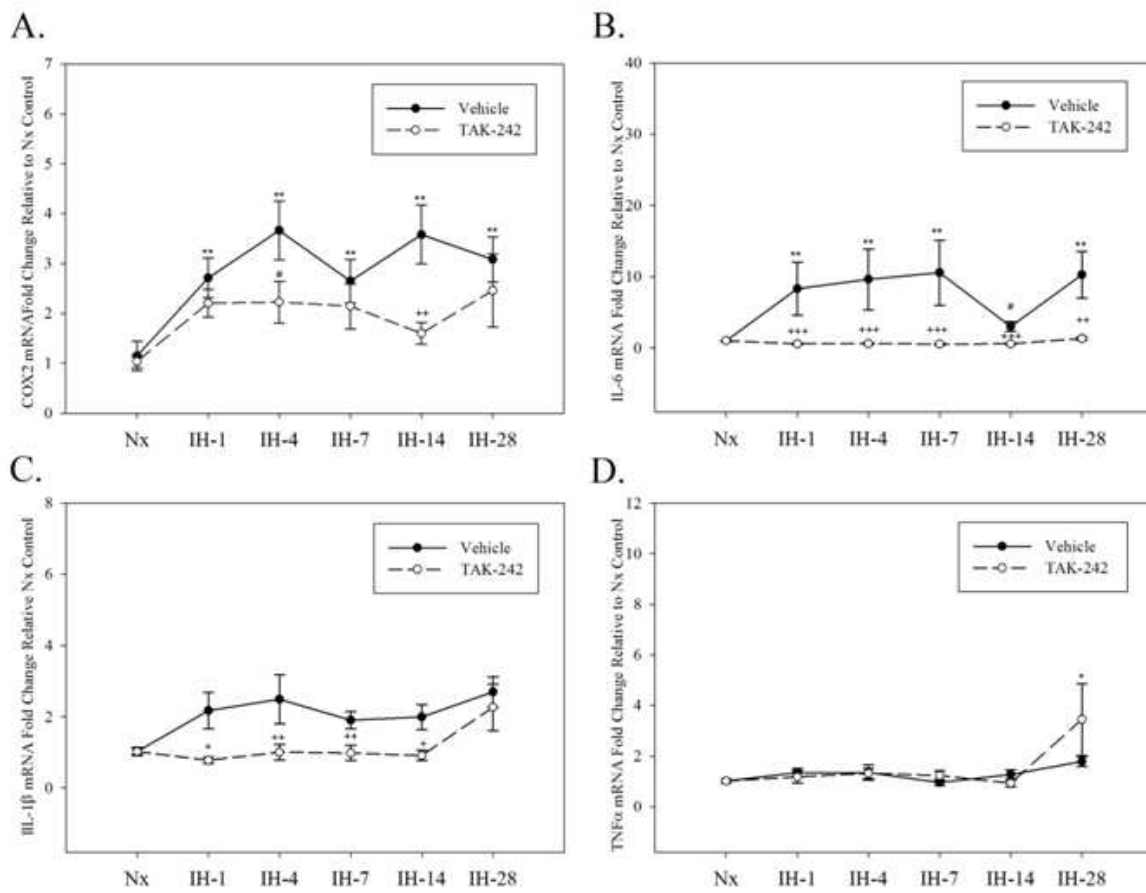


Figure Legend 7**Hippocampal supernatants from IH treated animals increase expression of proinflammatory genes through a TLR4 dependent mechanism**

Hippocampal tissues were isolated from mice exposed to Nx, 1, 4, 7, 14, or 28 days of IH.

Tissues were mechanically dissociated, the cellular fraction was removed through centrifugation, and the supernatants were collected. BV2 microglia in culture were treated with the isolated supernatant (20 μ g) in the presence/absence of the TLR4 inhibitor TAK-242 (1 μ M), and were harvested for gene expression analysis 18 hours post-treatment. (A) COX-2 expression (B) IL-6 expression, (C) IL-1 β , and (D) TNF α . Data are representative of at two independent experiments each with an n= 2-4, total n=6-8. Mean fold changes + 1 SEM are presented relative to respective normoxic controls. Statistical significance was determined by a two-way RM ANOVA on Δ CT values, and a Holm-Sidak post hoc. *p<0.05; **p<0.01; ***p<0.001

FIGURE 8

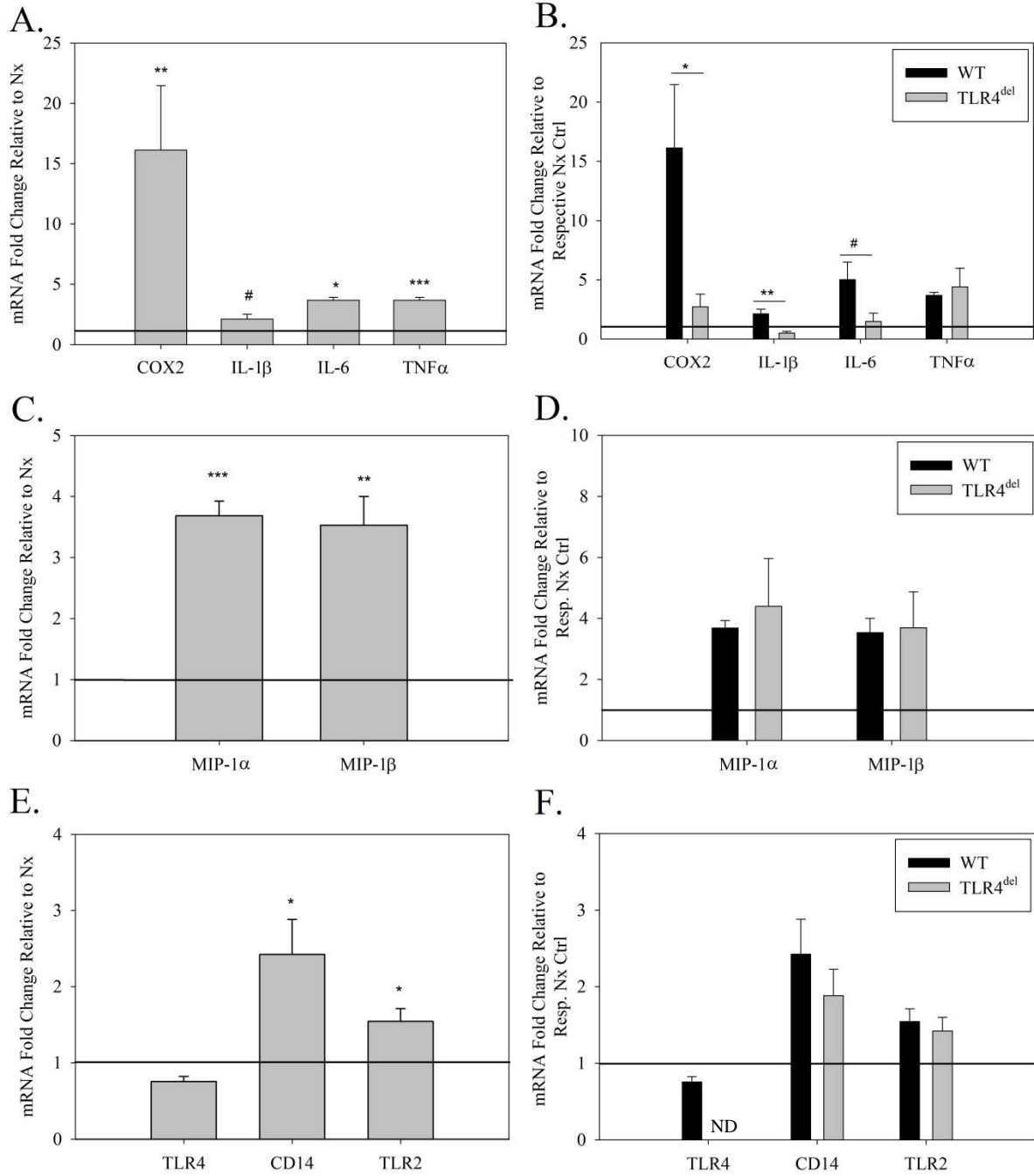


Figure Legend 8***In vitro* IH-treatment increases microglial pro-inflammatory gene expression which is mediated in part through TLR4**

WT or TLR4^{del} primary microglia were exposed to IH *in vitro* for 18 hour and were then harvested for mRNA gene expression analysis. (A) IH-treated WT microglia with COX2, IL-1 β , IL-6, and TNF α . (B) IH-treated WT and TLR4^{del} microglia with COX2, IL-1 β , IL-6. (C) IH-treated WT microglia with MIP-1 α and MIP-1 β . (D) IH-treated WT and TLR4^{del} microglia with with MIP-1 α and MIP-1 β . (E) IH-treated WT microglia with TLR4, CD14, and TLR2. (D) IH-treated WT and TLR4^{del} microglia with with TLR4, CD14, and TLR2. N=4-6. Means fold changes + 1 SEM are presented relative to respective normoxic controls. Statistical significance was determined by a paired T-test on Δ CT values for graphs (A, C, and E). Students T-test was performed on IH fold changes normalized to respective normoxic control for graphs (B, D, and F). * symbol respresents statistical significance from Nx (A, C, and E) or WT IH (B, D, and F). *p<0.05; **p<0.01; ***p<0.001

FIGURE 9

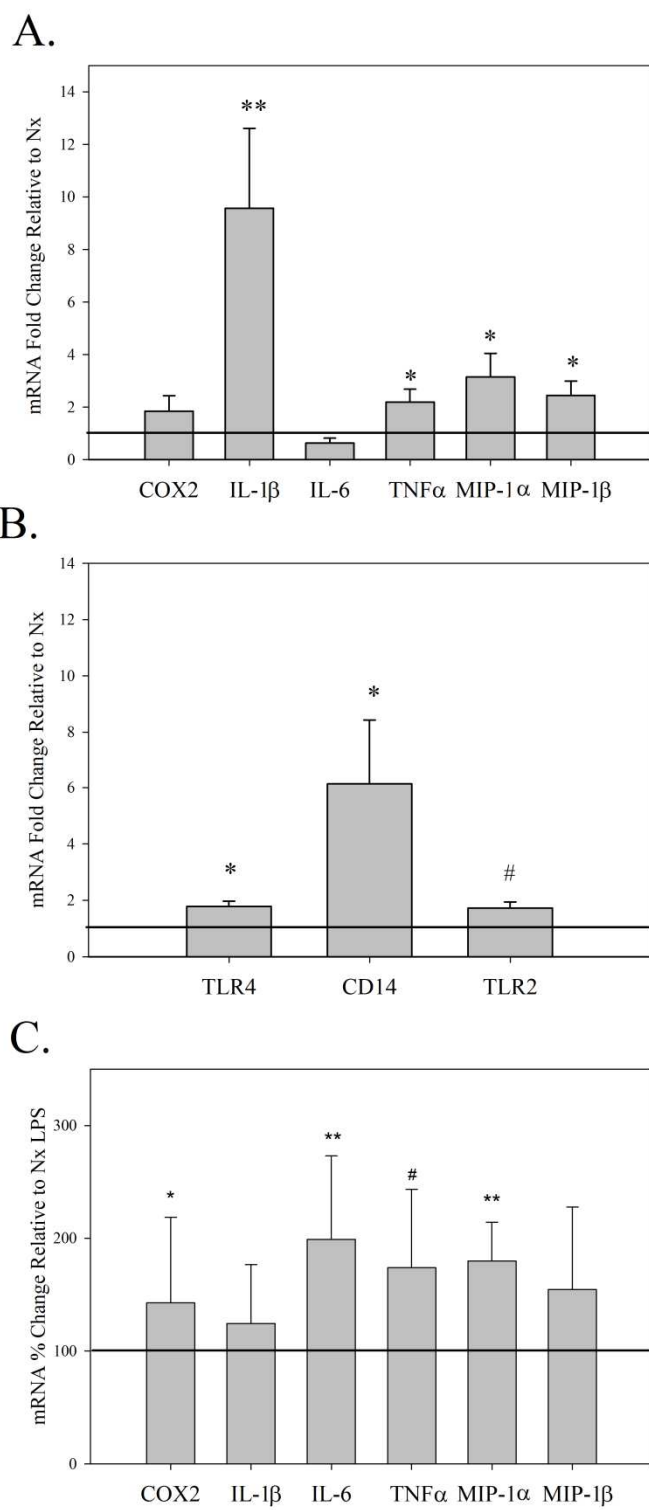


Figure Legend 9

BV2 microglial cells exhibit similar responses to IH. LPS mediated signaling is potentiated in IH-treated microglia.

BV2 microglia were exposed to IH *in vitro* for 18 hour and were then harvested for mRNA gene expression analysis or exposed to 6 hours of LPS (500ng/ml) or a vehicle control. (A) IH-treated BV2 microglia with COX2, IL-1 β , IL-6, TNF α , MIP-1 α and MIP-1 β . (B) IH-treated BV2 microglia with TLR4, CD14 and TLR2. (C) IH-treated BV2 microglia exposed to LPS with COX2, IL-1 β , IL-6, MIP-1 α and MIP-1 β . N=4. Mean fold changes + 1 SEM are presented relative to respective normoxic controls. Statistical significance was determined by a paired T-test on Nx and IH veh Δ CT values for graphs (A and B) and Nx and IH LPS Δ CT values for graph (C). * symbol represents statistical significance from Nx (A and B) or LPS treatment in Nx (C). *p<0.05; **p<0.01; ***p<0.001

FIGURE 10

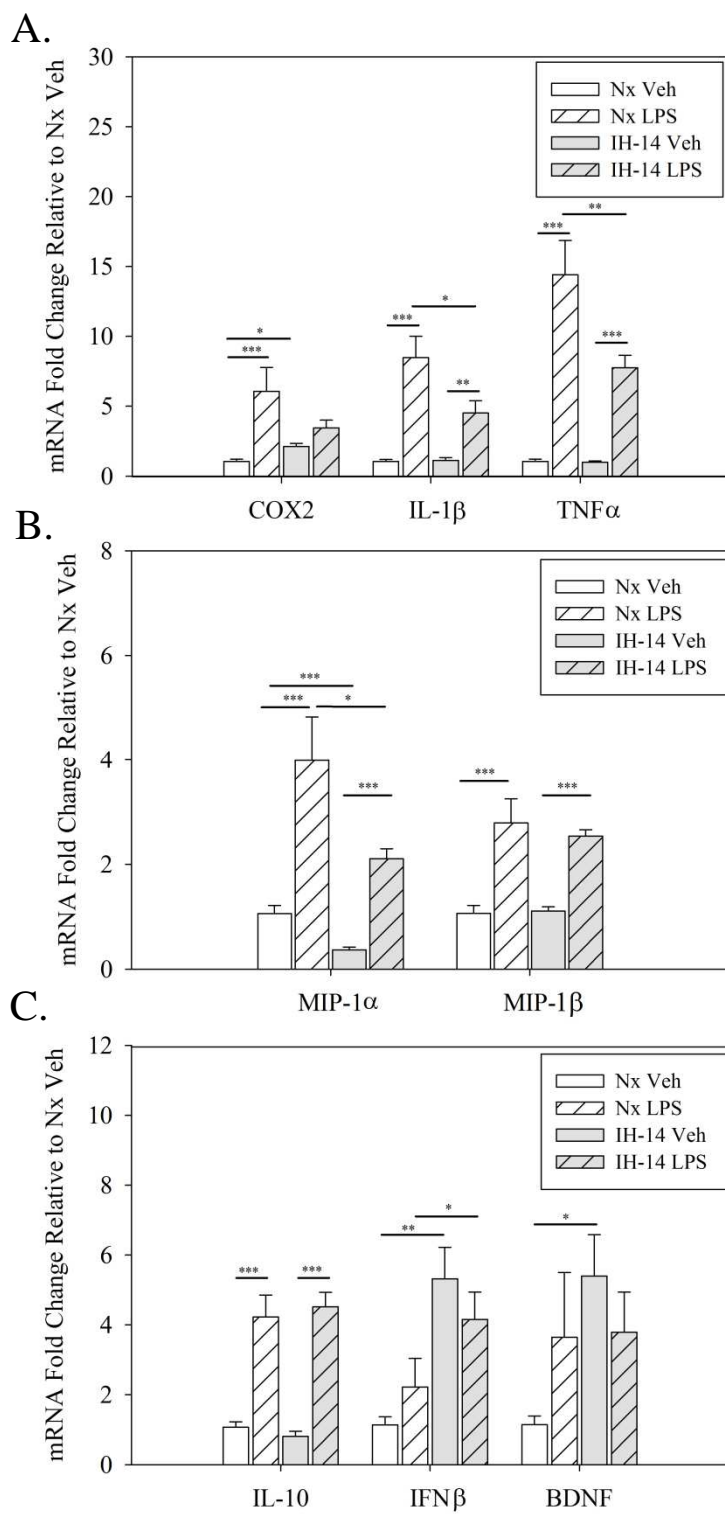


Figure Legend 10

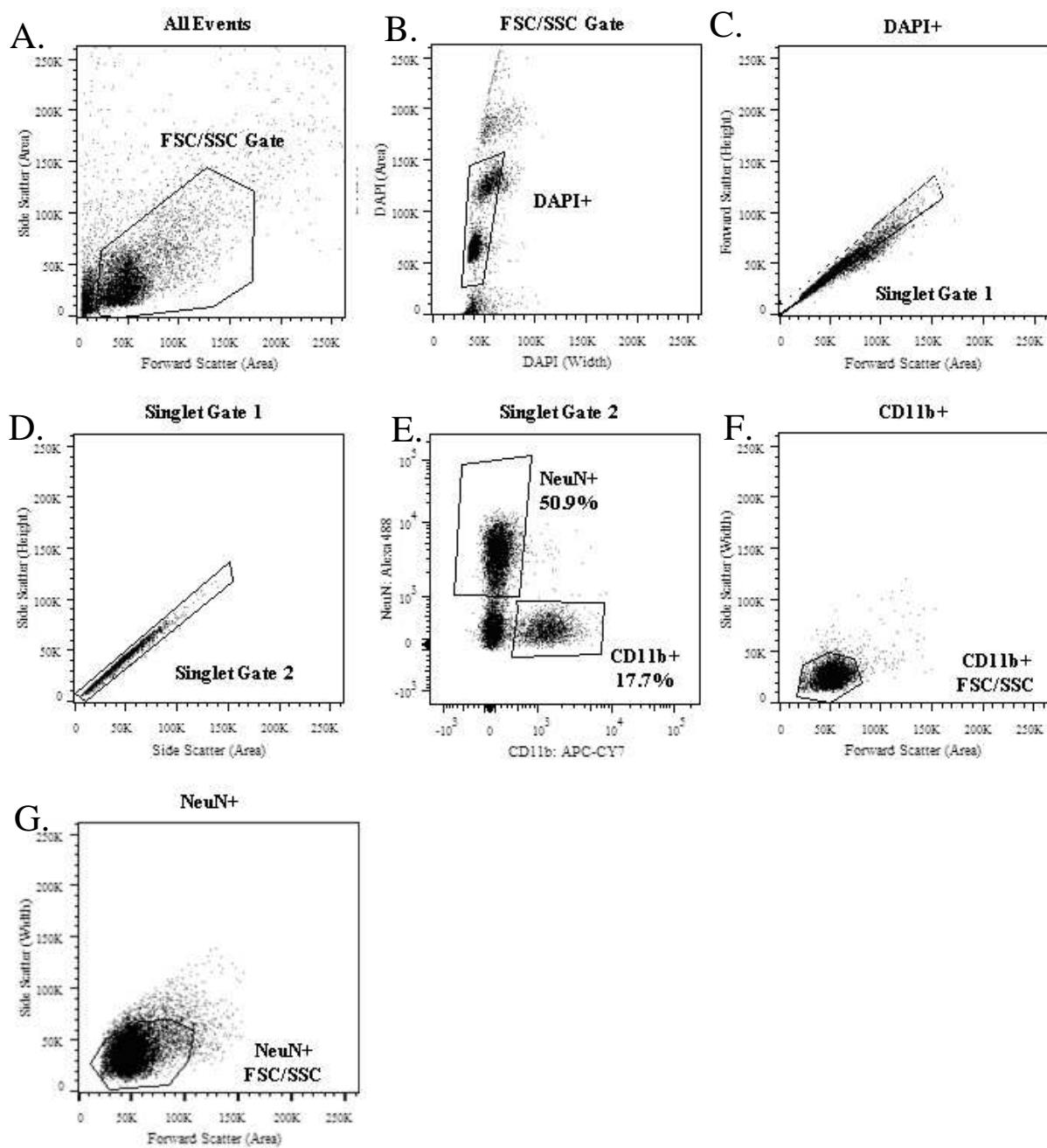
Microglia isolated from mice exposed to IH-14 exhibit a decreased inflammatory response to systemic LPS.

Mice were exposed to Nx or 14 days of IH. Immediately following the last hypoxic exposure mice were either treated with Veh or LPS (IP, 1mg/kg). Microglia were immunomagnetically isolated from the whole brain for qRT-PCR analysis. (A) Fold changes in COX2, IL-1 β , IL-6, and TNF α . (B) Fold changes in MIP-1 α and MIP-1 β . (C) Fold Changes in IL-10, IFN β , and BDNF N=4. Mean fold changes + 1 SEM are presented relative to the veh normoxic control. Statistical significance was determined by a 2-Way ANOVA with the Holm-Sidak post-hoc test. N=6-7 for each group. *p<0.05; **p<0.01; ***p<0.001

TABLE 1

Gene	Forward Primer (5'→3')	Reverse Primer (5'→3')
18S	CGGGTGCTCTTAGCTGAGTGTC	CTCGGGCCTGCTTTGAACAC
COX2	TGTTCCAACCCATGTCAAAA	CGTAGAATCCAGTCCGGGTA
IL-6	ACTTCCATCCAGTTGCCTTC	GTCTCCTCTCCGGACTTGTG
IL-1 β	TCAAAGTGCCAGTGAACCCC	GGTCACAGCCAGTCCTCTTAC
TNF α	TGTAGCCCACGTCGTAGCAA	AGGTACAACCCATCGGCTGG
MIP-1 α (CCL3)	TACAGCCGGAAGATTCCACG	TCAGGAAAATGACACCTGGCT
MIP-1 β (CCL4)	TGTGATGGATTACTATGAGACCAGC	GCCTCTTTTGGTCAGGAATACCA
TLR4	GAGGCAGCAGGTGGAATTGTAT	TTCGAGGCTTTTCCATCCAA
CD14	GCCAAATTGGTCGAACAAGC	CCATGGTCGGTAGATTCTGAAAGT
TLR2	CGAGTGGTGCAAGTACGAACTG	TGGTGTTCATTATCTTGCGCAG
IL-10	GCCTTATCGGAAATGATCCA	TCTCACCCAGGGAATTCAAA
IFN β	TCTCCATCGACTACAAGCAG	GTCTCATTCCACCCAGTGCT
BDNF	TGCTTTACTGGCGTAAGGGAC	TCCATCCCTACTCCGGGTG

SUPPLEMENTARY FIGURE 1

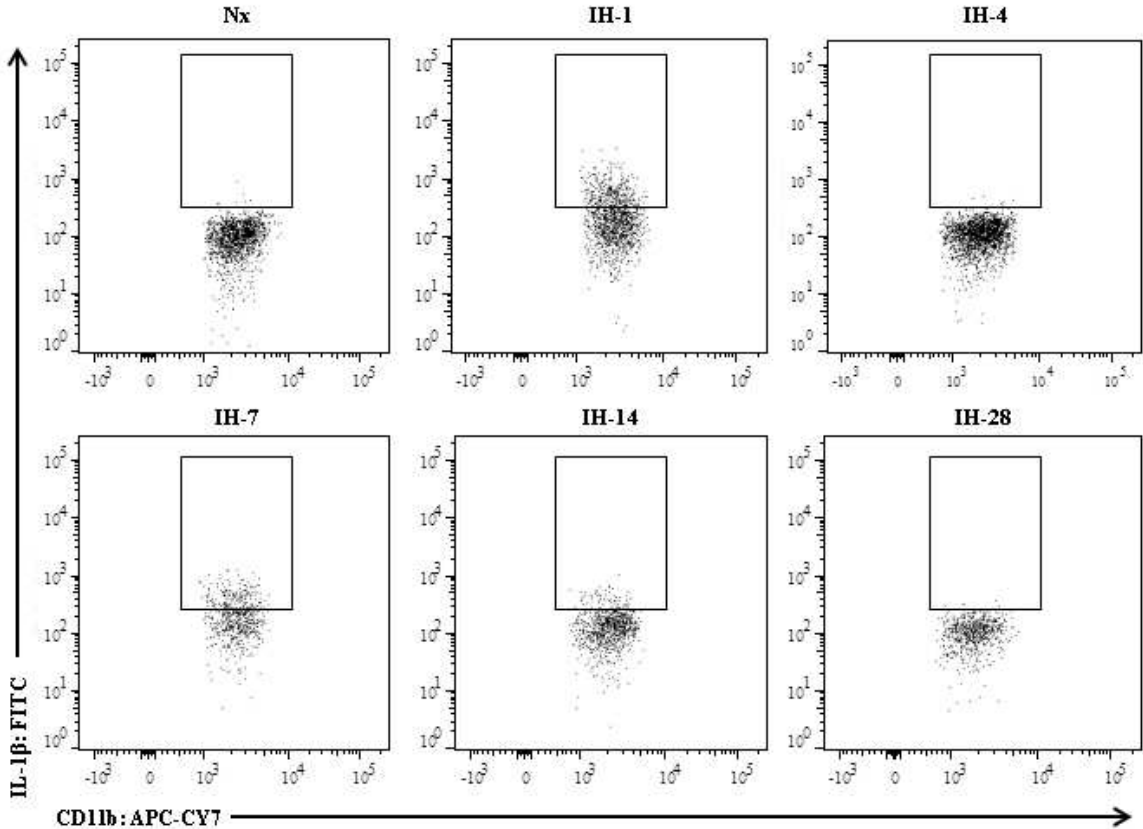


Supplementary Figure Legend 1

Representative gating strategy for identification of CD11b+ (microglia) and NeuN+ (neurons) cells.

Frontal cortical tissue was mechanically dissociated into a single cell suspension, fixed with mZBF, and stained for flow cytometric analysis as described in the methods section. A) 1st gate: FSC/SSC parameters, cells with low or high FSC/SSC properties were excluded from analysis. B) 2nd gate: events falling within gate 1 were plotted DAPI (width) vs. DAPI (area). DAPI+ events were gated on and represent cells with an intact nuclei at the time of fixation. C) 3rd gate: singlet gate on DAPI+ cells based on FSC parameters. D) 4th gate: second singlet gate on DAPI+ cells based on SSC parameters. E) 5th gate: singlet DAPI+ cells were plotted CD11b vs. NeuN. Single positive CD11b+ (microglia) and NeuN+ (neurons) gates were drawn based on FMO controls. F) CD11b+ cells with high FSC/SSC parameters were excluded from analysis. This population of CD11b+ cells were used for subsequent analyses, and are referred to as microglia. G) NeuN+ cells with high FSC/SSC parameters were excluded from analysis. This population of NeuN+ cells were used for subsequent analyses, and are referred to as neurons.

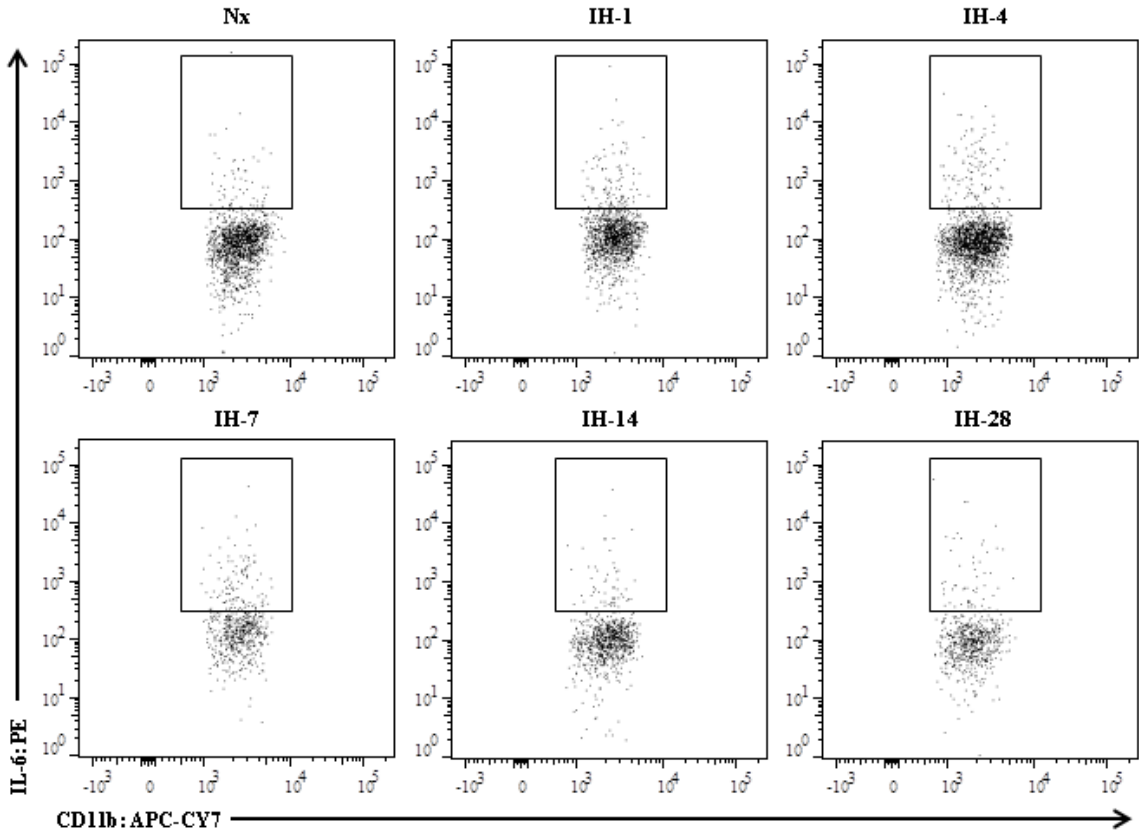
SUPPLEMENTARY FIGURE 2



Supplementary Figure Legend 2**Representative IL-1 β flow cytometry data from hippocampal microglia**

Mice were exposed to Nx, 1, 4, 7, 14, or 28 days of IH. 14 hours following the last hypoxic exposure, microglia were harvested for analysis by flow cytometry. Single cell mZBF-fixed suspensions were processed for flow cytometry. Singlet cells were gated based on FSC-H/SSC-A, and SSC-H/FSC-A, and then gated on DAPI to identify cells with an intact nucleus at time of fixation. We then plotted SSC-W vs. CD11b, and the cells that were CD11b⁺ per the FMO controls were gated on for subsequent analysis and will hereby be referred to as microglia. Data are representative dot plots of IL-1 β vs. CD11b from hippocampal tissue for all IH-timepoints.

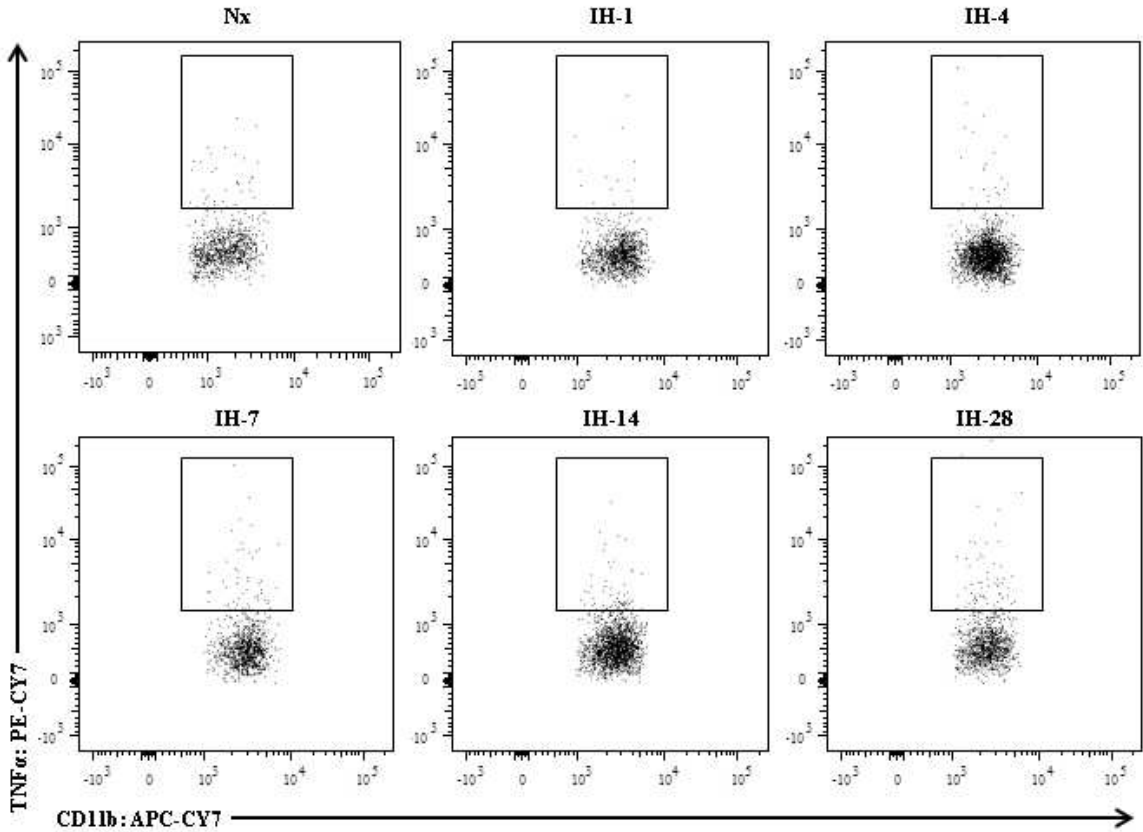
SUPPLEMENTARY FIGURE 3



Supplementary Figure Legend 3**Representative IL-6 flow cytometry data from hippocampal microglia**

Mice were exposed to Nx, 1, 4, 7, 14, or 28 days of IH. 14 hours following the last hypoxic exposure, microglia were harvested for analysis by flow cytometry. Single cell mZBF-fixed suspensions were processed for flow cytometry. Singlet cells were gated based on FSC-H/SSC-A, and SSC-H/FSC-A, and then gated on DAPI to identify cells with an intact nucleus at time of fixation. We then plotted SSC-W vs. CD11b, and the cells that were CD11b⁺ per the FMO controls were gated on for subsequent analysis and will hereby be referred to as microglia. Data are representative dot plots of IL-6 vs. CD11b from hippocampal tissue for all IH-timepoints.

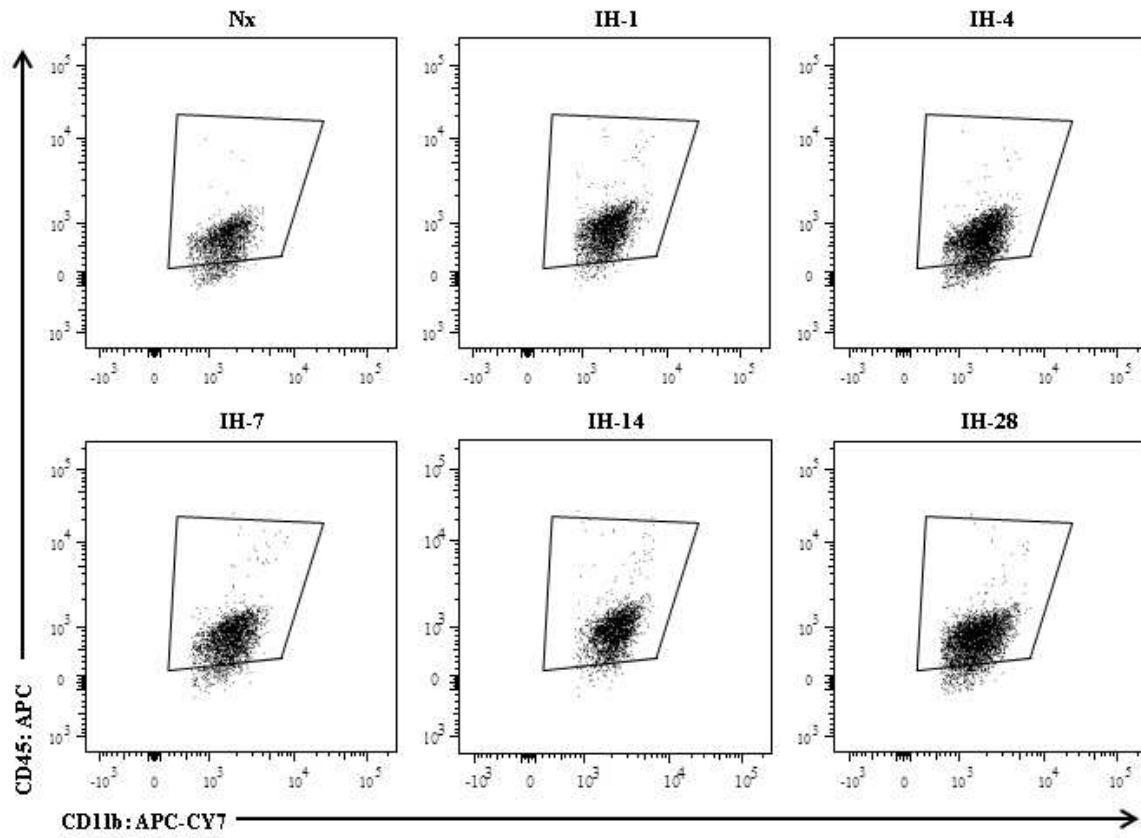
SUPPLEMENTARY FIGURE 4



Supplementary Figure Legend 4**Representative TNF α flow cytometry data from hippocampal microglia**

Mice were exposed to Nx, 1, 4, 7, 14, or 28 days of IH. 14 hours following the last hypoxic exposure, microglia were harvested for analysis by flow cytometry. Single cell mZBF-fixed suspensions were processed for flow cytometry. Singlet cells were gated based on FSC-H/SSC-A, and SSC-H/FSC-A, and then gated on DAPI to identify cells with an intact nucleus at time of fixation. We then plotted SSC-W vs. CD11b, and the cells that were CD11b⁺ per the FMO controls were gated on for subsequent analysis and will hereby be referred to as microglia. Data are representative dot plots of TNF α vs. CD11b from hippocampal tissue for all IH-timepoints.

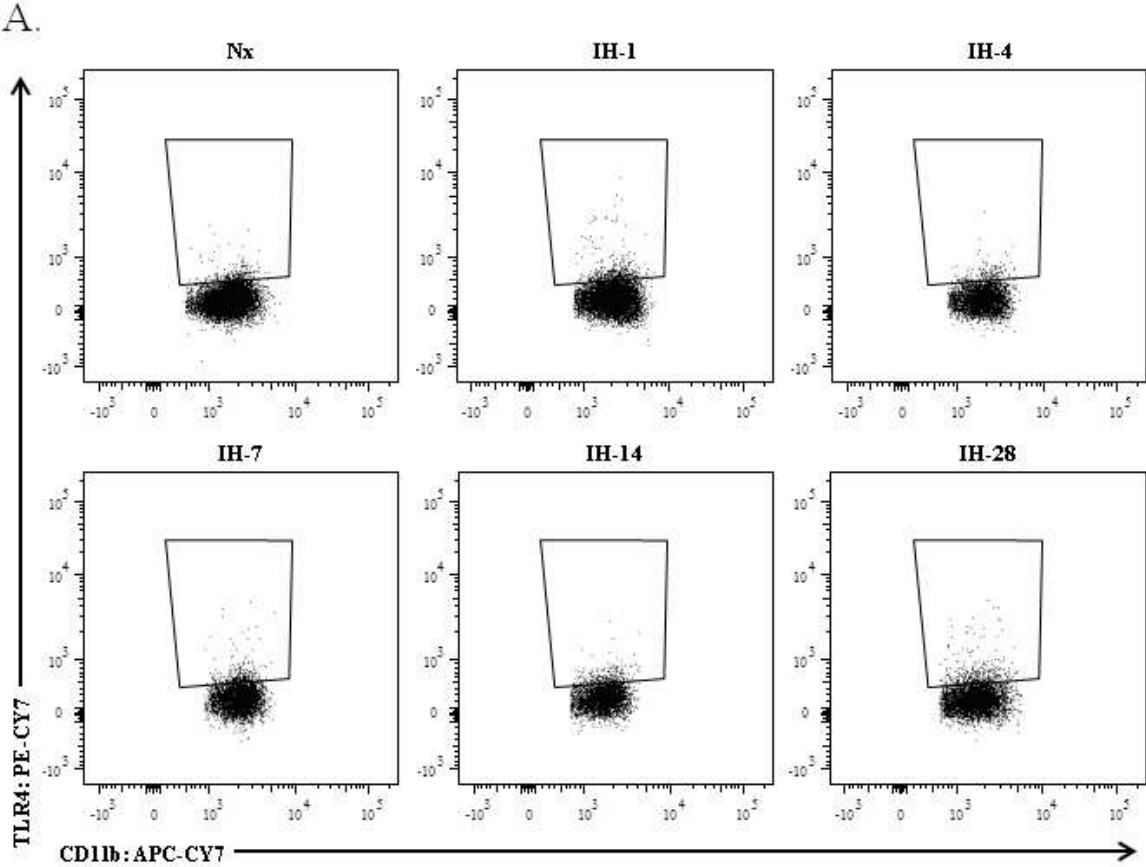
SUPPLEMENTARY FIGURE 5



Supplementary Figure Legend 5**Representative CD11b and CD45 flow cytometry data from hippocampal microglia**

Mice were exposed to Nx, 1, 4, 7, 14, or 28 days of IH. 14 hours following the last hypoxic exposure, microglia were harvested for analysis by flow cytometry. Single cell mZBF-fixed suspensions were processed for flow cytometry. Singlet/DAPI+/NeuN-/ CD11b+ cells were identified based on FSC/SSC and staining properties and will hereby be referred to as microglia. See Supp. Fig. 1 for the detailed gating strategy. Data are representative dot plots of CD45 vs. CD11b from hippocampal tissue for all IH-timepoints.

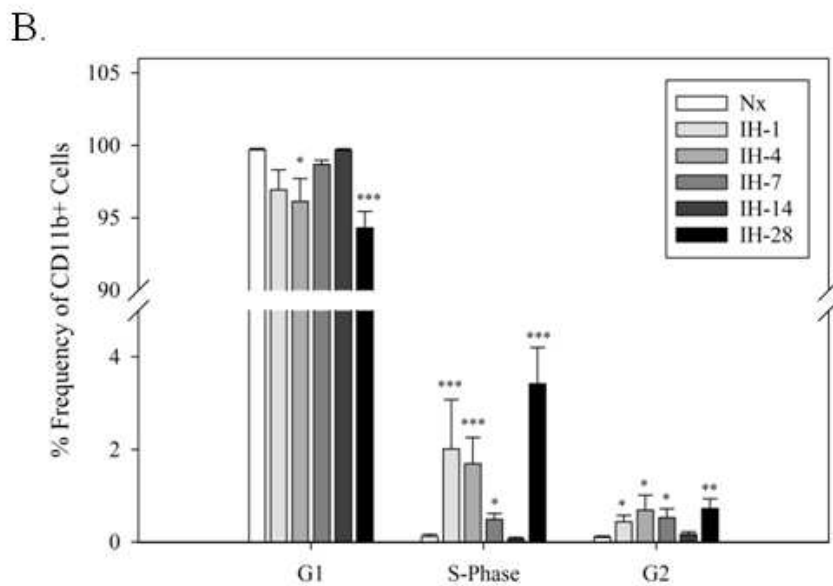
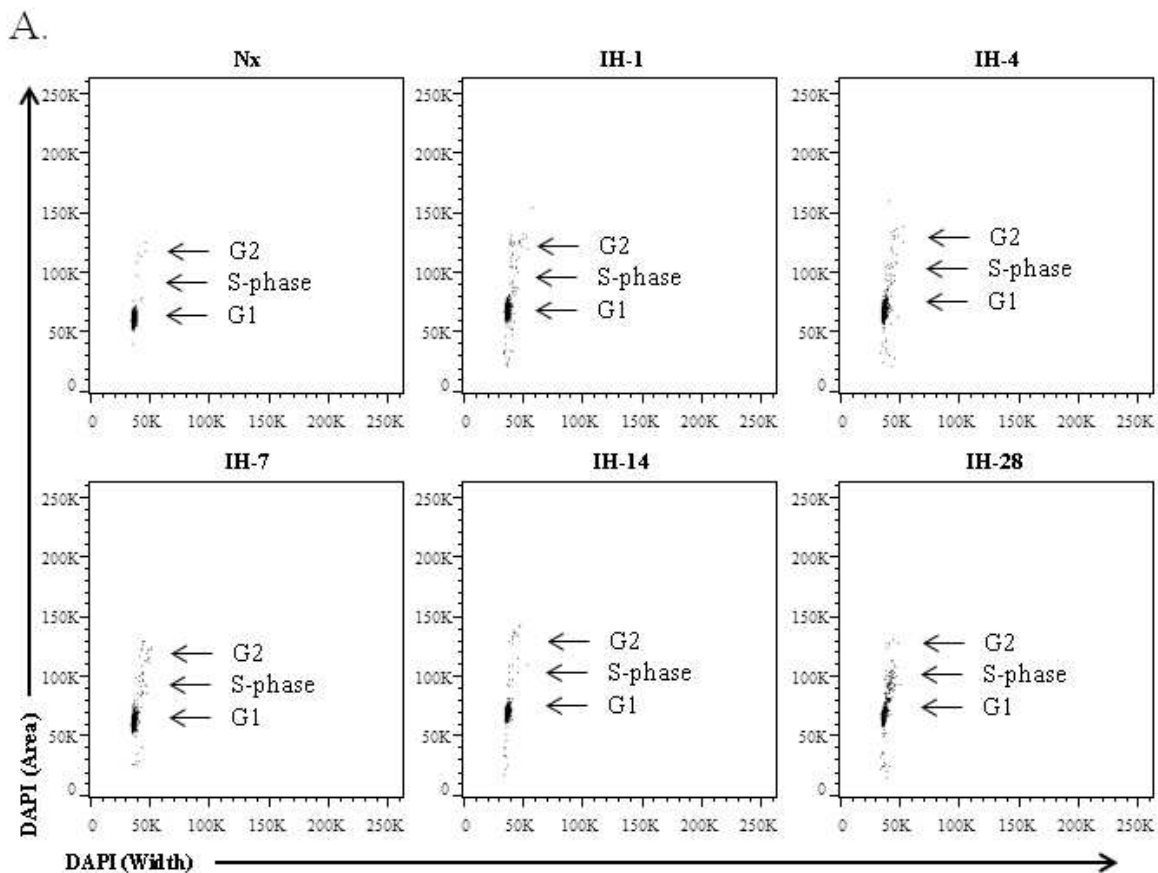
SUPPLEMENTARY FIGURE 6



Supplementary Figure Legend 6**Representative TLR4 flow cytometry data from hippocampal microglia**

Mice were exposed to Nx, 1, 4, 7, 14, or 28 days of IH. 14 hours following the last hypoxic exposure, microglia were harvested for analysis by flow cytometry. Single cell mZBF-fixed suspensions were processed for flow cytometry. Singlet/DAPI+/NeuN-/ CD11b+ cells were identified based on FSC/SSC and staining properties and will hereby be referred to as microglia. See Supp. Fig. 1 for the detailed gating strategy. Data are representative dot plots of TLR4 vs. CD11b from hippocampal tissue for all IH-timepoints.

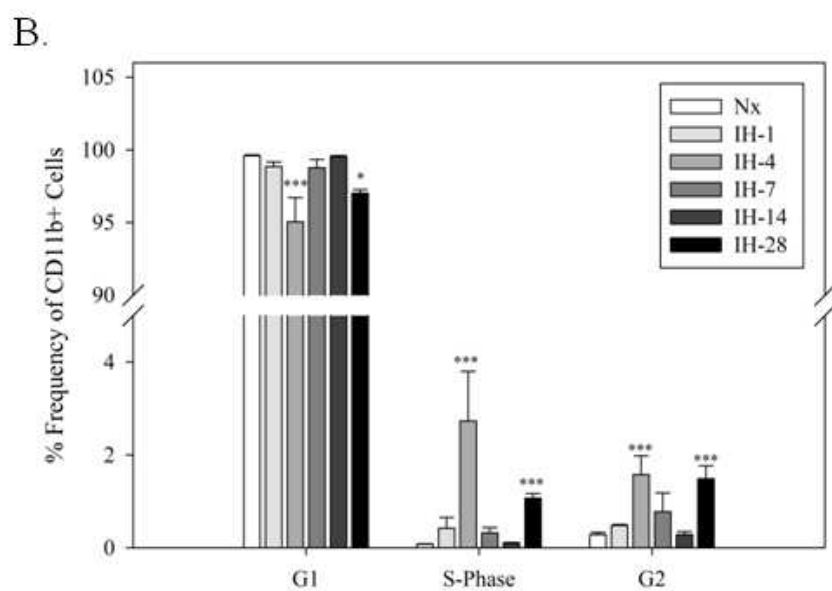
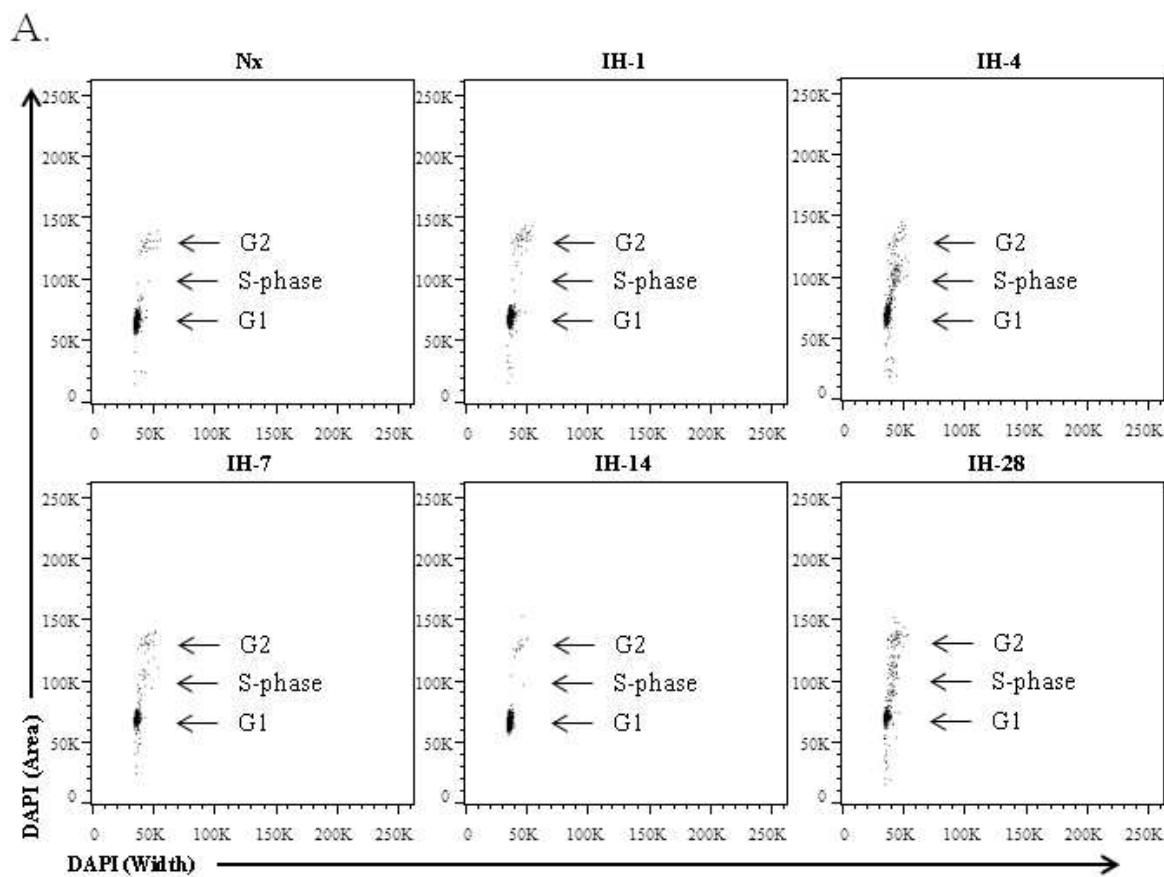
SUPPLEMENTARY FIGURE 7



Supplementary Figure Legend 7**IH increases the percentage of frontal cortical microglia in G2 and S-phase.**

Mice were exposed to Nx, 1, 4, 7, 14, or 28 days of IH. 14 hours following the last hypoxic exposure, microglia were harvested for analysis by flow cytometry. Singlet/DAPI+/NeuN-/CD11b+ cells were identified based on FSC/SSC and staining properties and will hereby be referred to as microglia. See Supp. Fig. 1 for the detailed gating strategy. (A) Representative dot plots of microglia plotted DAPI (width) vs. DAPI (area) from frontal cortical tissue for all IH-timepoints. Extent of DAPI staining in microglial cells represent different cell cycle stages, where DAPI staining is lowest in G1, doubled in G2, and between G1 and G2 during S-phase. (B) Frontal cortex, graphed average data of the percentage of microglia in G1, G2, or S-phase at each IH time point analyzed. Respective tissues from 2 animals were pooled to create 1 sample. Data are representative of the means +/- 1 SEM of at least 4 individual samples. Statistical significance was determined by a One-Way ANOVA, and a Holm-Sidak post hoc test on the. * symbol represents statistically significant differences from normoxia. * $p < 0.05$; ** $p < 0.01$; *** $p < 0.001$

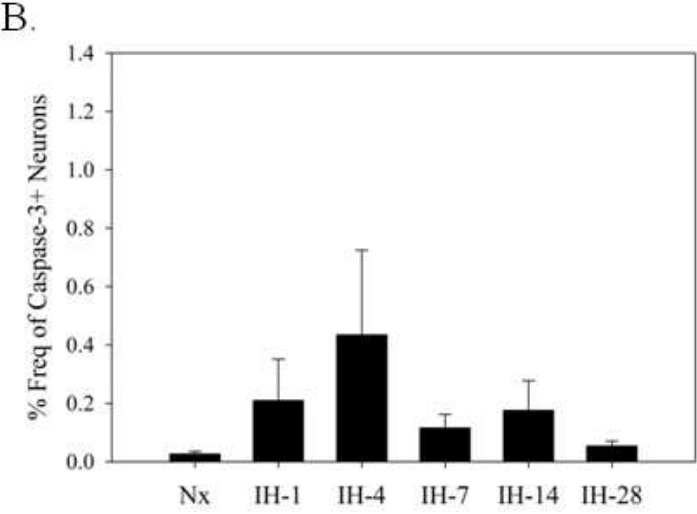
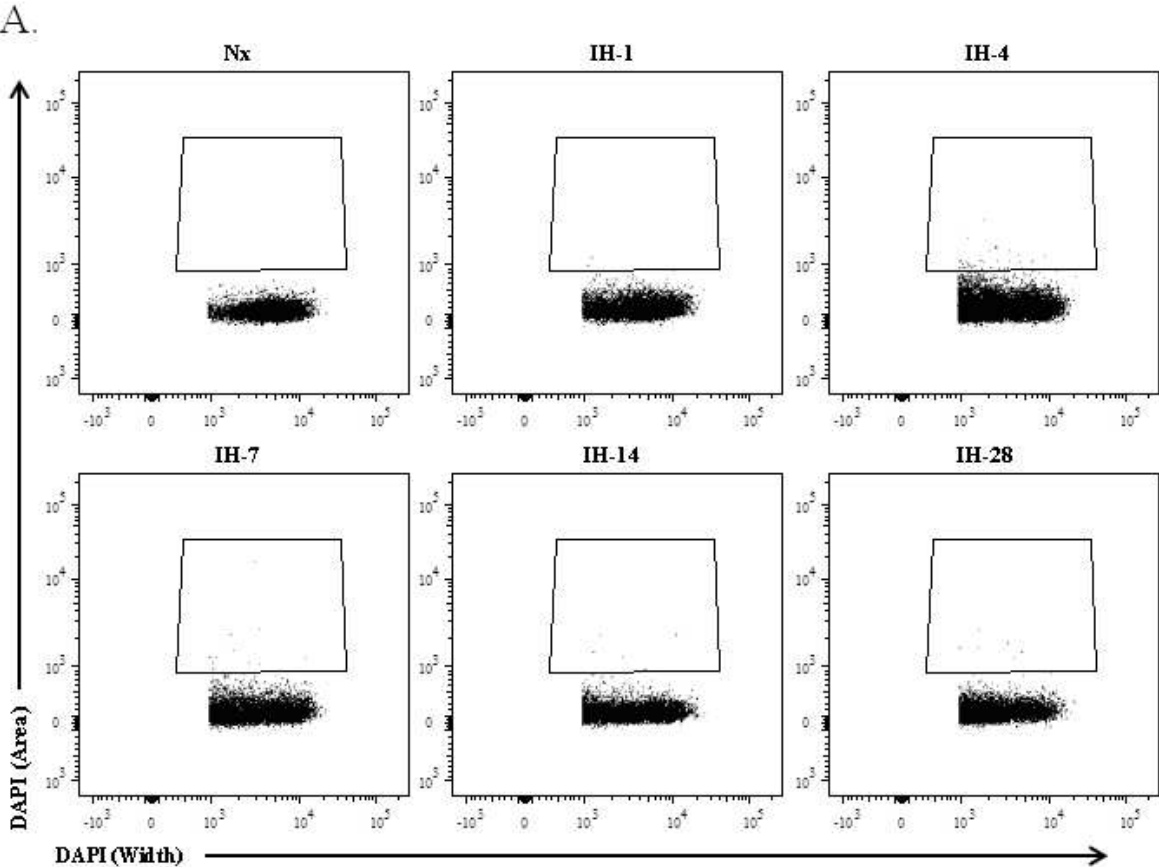
SUPPLEMENTARY FIGURE 8



Supplementary Figure Legend 8**IH increases the percentage of hippocampal microglia in G2 and S-phase.**

Mice were exposed to Nx, 1, 4, 7, 14, or 28 days of IH. 14 hours following the last hypoxic exposure, microglia were harvested for analysis by flow cytometry. Singlet/DAPI+/NeuN-/CD11b+ cells were identified based on FSC/SSC and staining properties and will hereby be referred to as microglia. See Supp. Fig. 1 for the detailed gating strategy. (A) Representative dot plots of microglia plotted DAPI (width) vs. DAPI (area) from hippocampal tissue for all IH-timepoints. Extent of DAPI staining in microglial cells represent different cell cycle stages, where DAPI staining is lowest in G1, doubled in G2, and between G1 and G2 during S-phase. (B) Hippocampal, graphed average data of the percentage of microglia in G1, G2, or S-phase at each IH time point analyzed. Respective tissues from 2 animals were pooled to create 1 sample. Data are representative of the means +/- 1 SEM of at least 4 individual samples. Statistical significance was determined by a One-Way ANOVA, and a Holm-Sidak post hoc test on the. * symbol represents statistically significant differences from normoxia. * $p < 0.05$; ** $p < 0.01$; *** $p < 0.001$

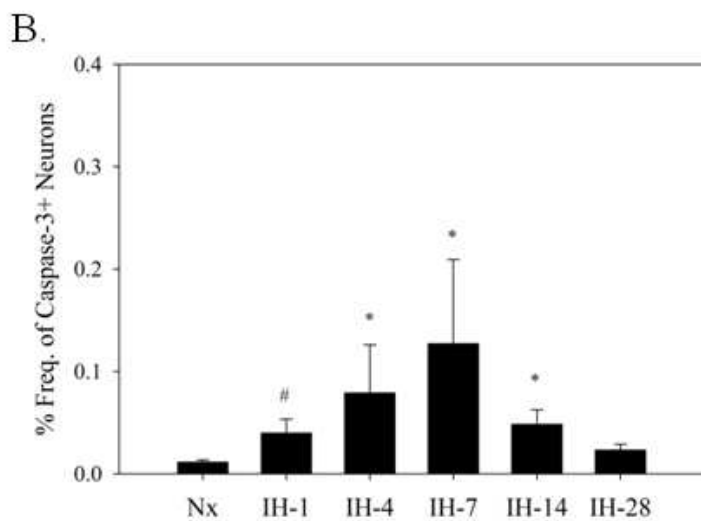
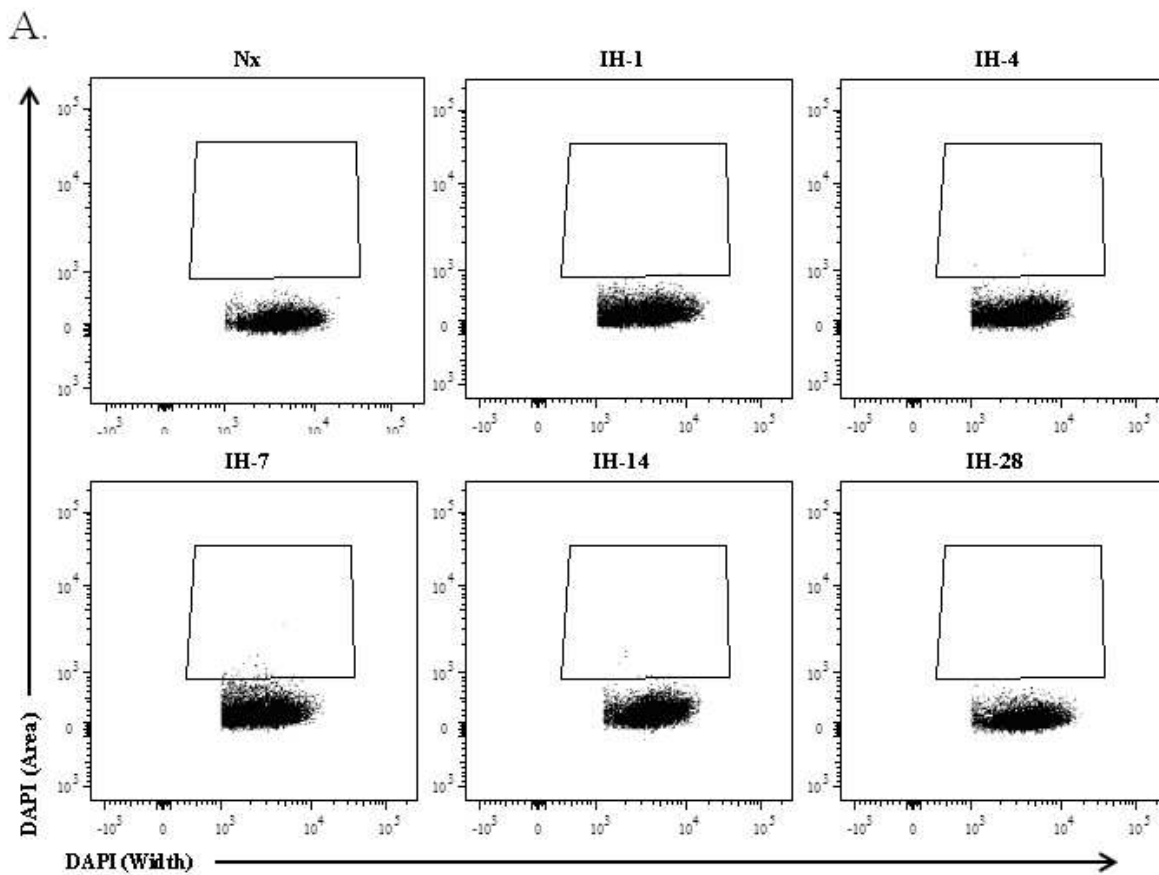
SUPPLEMENTARY FIGURE 9



Supplementary Figure Legend 9**IH-induced increases the percentage of frontal cortical neurons expressing caspase-3.**

Mice were exposed to Nx, 1, 4, 7, 14, or 28 days of IH. 14 hours following the last hypoxic exposure, microglia were harvested for analysis by flow cytometry. Singlet/DAPI+/CD11b-/NeuN+ cells were identified based on FSC/SSC and staining properties and will hereby be referred to as neurons. See Supp. Fig. 1 for the detailed gating strategy. (A) Representative dot plots of NeuN vs. caspase-3 from frontal cortical tissue for all IH-timepoints. (B) Frontal cortex, graphed average data of the percentage of neurons expressing caspase-3 at each IH time point analyzed. Respective tissues from 2 animals were pooled to create 1 sample. Data are representative of the means \pm 1 SEM of at least 4 individual samples. Data did not reach statistical significance was determined by a One-Way ANOVA, and a Holm-Sidak post hoc test, p -value = 0.084.

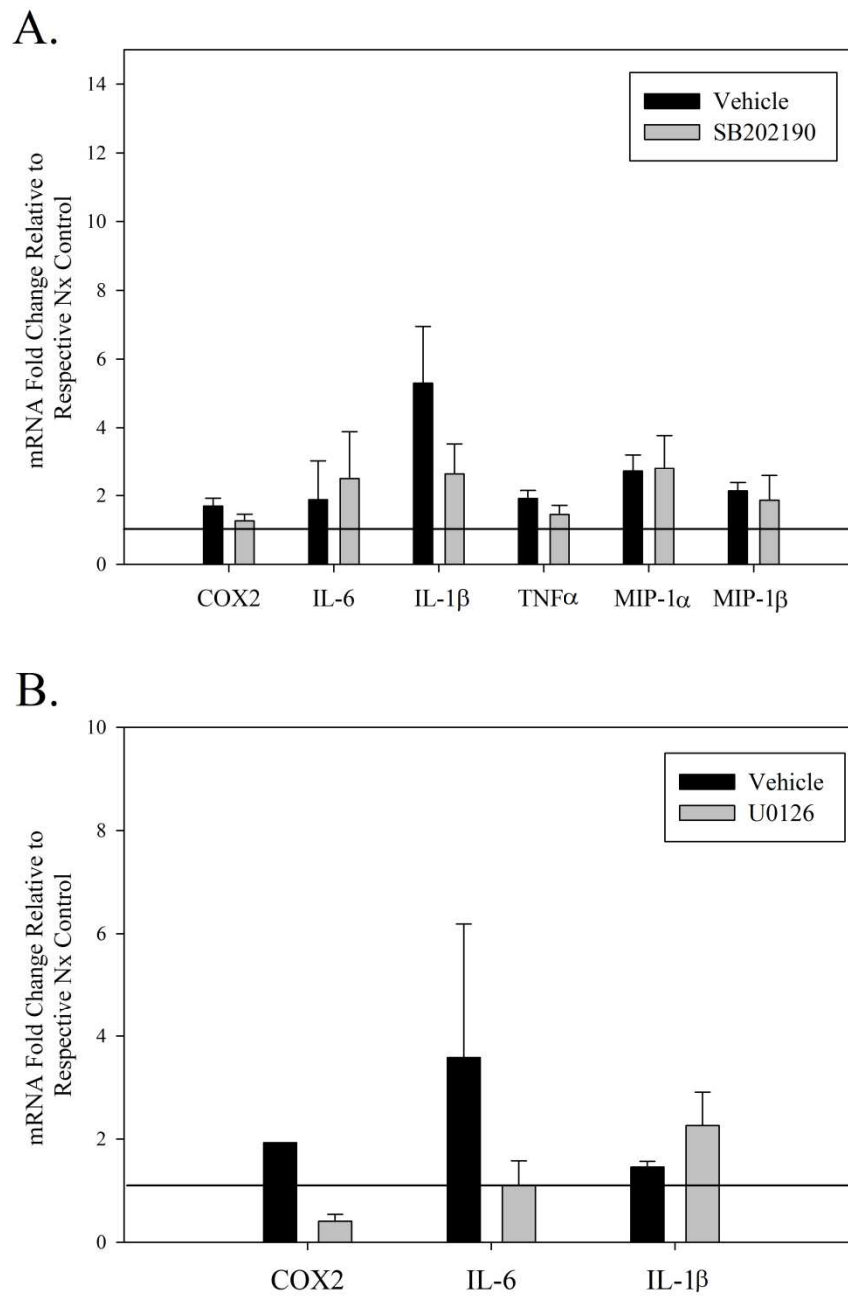
SUPPLEMENTARY FIGURE 10



Supplementary Figure Legend 10**IH increases the percentage of hippocampal neurons expressing caspase-3.**

Mice were exposed to Nx, 1, 4, 7, 14, or 28 days of IH. 14 hours following the last hypoxic exposure, microglia were harvested for analysis by flow cytometry. Singlet/DAPI+/CD11b-/NeuN+ cells were identified based on FSC/SSC and staining properties and will hereby be referred to as neurons. See Supp. Fig. 1 for the detailed gating strategy. (A) Representative dot plots of NeuN vs. caspase-3 from hippocampal tissue for all IH-timepoints. (B) Hippocampal, graphed average data of the percentage of neurons expressing caspase-3 at each IH time point analyzed. Respective tissues from 2 animals were pooled to create 1 sample. Data are representative of the means \pm 1 SEM of at least 4 individual samples. Statistical significance was determined by a One-Way ANOVA, and a Holm-Sidak post hoc test. * symbol represents statistically significant differences from normoxia. * $p < 0.05$; ** $p < 0.01$; *** $p < 0.001$

SUPPLEMENTARY FIGURE 11

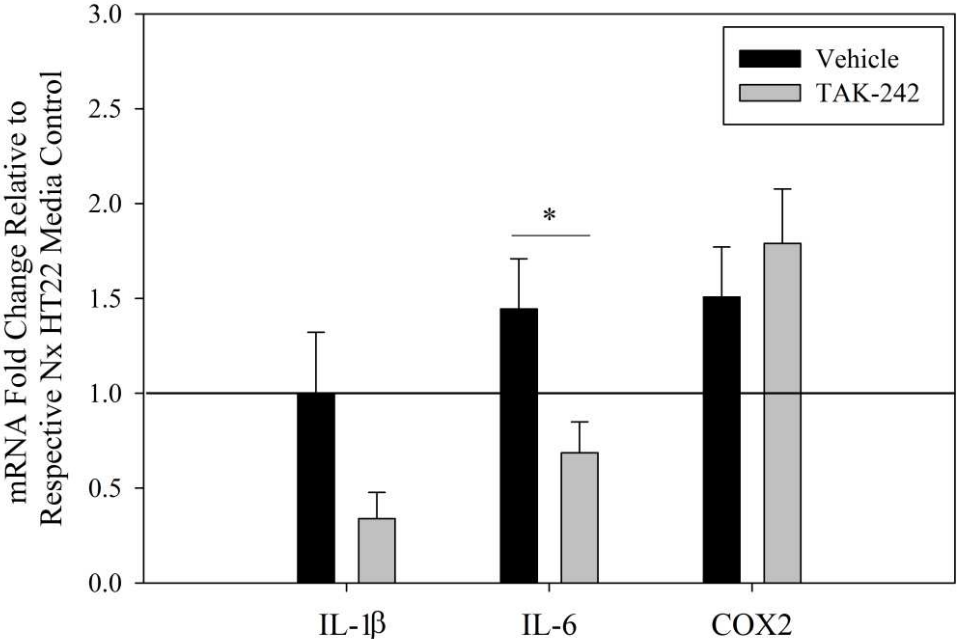


Supplementary Figure Legend 11

***In vitro* IH-treatment increases microglial pro-inflammatory gene expression which may be mediated in part by MAPK pathways.**

BV2 microglia were exposed to IH or Nx *in vitro* in the presence/absence of MAPK inhibitors and were subsequently harvested for mRNA gene expression analysis. (A) IH-treated BV2 microglia in the presence of the p38 MAPK inhibitor (SB202190, 10 μ M) with COX2, IL-1 β , IL-6, TNF α , MIP-1 α and MIP-1 β . P38 may regulate IH-induced IL-1 β expression (n=4-7). (B) IH-treated BV2 microglia in the presence of the MEK1/2 (ERK1/2) inhibitor (U0126, 10 μ M) with COX2, IL-6, and IL-1 β . ERK1/2 may regulate IH-induced IL-6 and COX2 expression (n=2-3). Fold change means \pm 1 SEM are presented relative to respective normoxic controls. Black line represents respective normoxic controls. Students T-test was performed on IH fold changes normalized to respective normoxic control. Data did not reach statistical significance, P-value >0.05 .

SUPPLEMENTARY FIGURE 12



Supplementary Figure Legend 12**Conditioned medium from HT22 neurons exposed to IH may induce microglial inflammation through pathway that is in part mediated by TLR4.**

Murine HT22 neuronal cells (kindly provided by Dr. Daniel Dorsa, Oregon Health and Sciences University, Portland OR) were plated on agar permeable membrane in specialized 50mm tissue culture plates (Starstedt, Newton, NC) at a density of 2.5×10^5 . The following day, they were treated with IH of Nx *in vitro* for 18 hours, as previously described in the methods section.

Following treatment, the neuron-conditioned media was collected. BV2 microglia were treated with the conditioned medium from Nx or IH-treated HT22s in the presence/absence of the TLR4 inhibitor (TAK-242, 1 μ M) for 18 hours and subsequently harvested for qRT-PCR analysis. Conditioned medium from IH-treated neurons appears to increase IL-6 and COX2 mRNA expression. However, this did not reach statistical significance for either gene ($p > 0.05$). Inhibition of TLR4 with TAK-242 selectively reduced IL-6 gene expression, while COX2 expression was unaffected (N=6-8). The mean fold change \pm 1 SEM are presented relative to respective normoxic HT22 media controls. The black line represents respective normoxic HT22 media controls. Student's T-test was performed on fold changes. * symbol represents statistically significant differences from vehicle control. * $p < 0.05$; ** $p < 0.01$; *** $p < 0.001$.

REFERENCES

1. Peppard, P. E., Young, T., Barnet, J. H., Palta, M., Hagen, E. W. & Hla, K. M. Increased prevalence of sleep-disordered breathing in adults. *American journal of epidemiology* **177**, 1006–1014 (2013).
2. Peppard, P. E., Szklo-Coxe, M., Hla, K. M. & Young, T. Longitudinal association of sleep-related breathing disorder and depression. *Archives of internal medicine* **166**, 1709–1715 (2006).
3. Naismith, S., Winter, V., Gotsopoulos, H., Hickie, I. & Cistulli, P. Neurobehavioral functioning in obstructive sleep apnea: differential effects of sleep quality, hypoxemia and subjective sleepiness. *Journal of clinical and experimental neuropsychology* **26**, 43–54 (2004).
4. El-Ad, B. & Lavie, P. Effect of sleep apnea on cognition and mood. *International Review of Psychiatry* **17**, 277–282 (2005).
5. Sawyer, A. M., Gooneratne, N. S., Marcus, C. L., Ofer, D., Richards, K. C. & Weaver, T. E. A systematic review of CPAP adherence across age groups: clinical and empiric insights for developing CPAP adherence interventions. *Sleep medicine reviews* **15**, 343–356 (2011).
6. Bucks, R. S., Olaithe, M. & Eastwood, P. Neurocognitive function in obstructive sleep apnoea: A meta-review. *Respirology* **18**, 61–70 (2013).
7. Saunamäki, T. & Jehkonen, M. A review of executive functions in obstructive sleep apnea syndrome. *Acta neurologica scandinavica* **115**, 1–11 (2007).
8. Kasai, T., Floras, J. S. & Bradley, T. D. Sleep Apnea and Cardiovascular Disease A Bidirectional Relationship. *Circulation* **126**, 1495–1510 (2012).
9. Go, A. S., Mozaffarian, D., Roger, V. L., Benjamin, E. J., Berry, J. D., Blaha, M. J., Dai, S., Ford, E. S., Fox, C. S., Franco, S., Fullerton, H. J., Gillespie, C., Hailpern, S. M., Heit, J. A., Howard, V. J., Huffman, M. D., Judd, S. E., ... Turner, M. B. Heart disease and stroke statistics-2014 update: a report from the American Heart Association. *Circulation* **129**, e28–e292 (2014).
10. Row, B. W., Liu, R., Xu, W., Kheirandish, L. & Gozal, D. Intermittent hypoxia is associated with oxidative stress and spatial learning deficits in the rat. *American journal of respiratory and critical care medicine* **167**, 1548–1553 (2003).
11. Row, B. W. in *Hypoxia and the Circulation* 51–67 (Springer, 2007).
12. Gozal, D., Daniel, J. M. & Dohanich, G. P. Behavioral and anatomical correlates of chronic episodic hypoxia during sleep in the rat. *The Journal of Neuroscience* **21**, 2442 (2001).

13. Li, R. C., Row, B. W., Gozal, E., Kheirandish, L., Fan, Q., Brittan, K. R., Guo, S. Z., Sachleben Jr, L. R. & Gozal, D. Cyclooxygenase 2 and intermittent hypoxia-induced spatial deficits in the rat. *American journal of respiratory and critical care medicine* **168**, 469 (2003).
14. Zhan, G., Fenik, P., Pratico, D. & Veasey, S. C. Inducible nitric oxide synthase in long-term intermittent hypoxia: hypersomnolence and brain injury. *American journal of respiratory and critical care medicine* **171**, 1414 (2005).
15. Hui-guo, L., Kui, L., Yan-ning, Z. & Yong-jian, X. Apocynin attenuate spatial learning deficits and oxidative responses to intermittent hypoxia. *Sleep medicine* **11**, 205–212 (2010).
16. Burckhardt, I. C., Gozal, D., Dayyat, E., Cheng, Y., Li, R. C., Goldbart, A. D. & Row, B. W. Green tea catechin polyphenols attenuate behavioral and oxidative responses to intermittent hypoxia. *American journal of respiratory and critical care medicine* **177**, 1135 (2008).
17. Nair, D., Dayyat, E. A., Zhang, S. X., Wang, Y. & Gozal, D. Intermittent hypoxia-induced cognitive deficits are mediated by NADPH oxidase activity in a murine model of sleep apnea. *PLoS One* **6**, e19847 (2011).
18. Smith, S. M., Friedle, S. A. & Watters, J. J. Chronic Intermittent Hypoxia Exerts CNS Region-Specific Effects on Rat Microglial Inflammatory and TLR4 Gene Expression. *PloS one* **8**, e81584 (2013).
19. Tremblay, M. È. & Majewska, A. K. A role for microglia in synaptic plasticity? *Communicative & integrative biology* **4**, 220 (2011).
20. Tremblay, M. È., Stevens, B., Sierra, A., Wake, H., Bessis, A. & Nimmerjahn, A. The role of microglia in the healthy brain. *The Journal of Neuroscience* **31**, 16064–16069 (2011).
21. Fetler, L. & Amigorena, S. Brain under surveillance: the microglia patrol. *Science* **309**, 392–393 (2005).
22. Hanisch, U. K. & Kettenmann, H. Microglia: active sensor and versatile effector cells in the normal and pathologic brain. *Nature neuroscience* **10**, 1387–1394 (2007).
23. Kettenmann, H., Hanisch, U.-K., Noda, M. & Verkhratsky, A. Physiology of microglia. *Physiological reviews* **91**, 461–553 (2011).
24. Ransohoff, R. M. & Perry, V. H. Microglial physiology: unique stimuli, specialized responses. *Annual review of immunology* **27**, 119–145 (2009).
25. Whitney, N. P., Eidem, T. M., Peng, H., Huang, Y. & Zheng, J. C. Inflammation mediates varying effects in neurogenesis: relevance to the pathogenesis of brain injury and

- neurodegenerative disorders. *Journal of neurochemistry* **108**, 1343–1359 (2009).
26. Glass, C. K., Saijo, K., Winner, B., Marchetto, M. C. & Gage, F. H. Mechanisms underlying inflammation in neurodegeneration. *Cell* **140**, 918–934 (2010).
 27. Pickering, M. & O'Connor, J. J. Pro-inflammatory cytokines and their effects in the dentate gyrus. *Progress in brain research* **163**, 339–354 (2007).
 28. Goshen, I. & Yirmiya, R. The role of pro-inflammatory cytokines in memory processes and neural plasticity. *Psychoneuroimmunology. 4th ed: Elsevier* (2007).
 29. Labrousse, V. F., Costes, L., Aubert, A., Darnaudéry, M., Ferreira, G., Amédée, T. & Layé, S. Impaired Interleukin-1 β and c-Fos Expression in the Hippocampus Is Associated with a Spatial Memory Deficit in P2X7 Receptor-Deficient Mice. *PloS one* **4**, e6006 (2009).
 30. Avital, A., Goshen, I., Kamsler, A., Segal, M., Iverfeldt, K., Richter-Levin, G. & Yirmiya, R. Impaired interleukin-1 signaling is associated with deficits in hippocampal memory processes and neural plasticity. *Hippocampus* **13**, 826–834 (2003).
 31. März, P., Heese, K., Dimitriades-Schmutz, B., Rose-John, S. & Otten, U. Role of interleukin-6 and soluble IL-6 receptor in region-specific induction of astrocytic differentiation and neurotrophin expression. *Glia* **26**, 191–200 (1999).
 32. Thier, M., März, P., Otten, U., Weis, J. & Rose-John, S. Interleukin-6 (IL-6) and its soluble receptor support survival of sensory neurons. *Journal of neuroscience research* **55**, 411–422 (1999).
 33. Broytman, O., Baertsch, N. A. & Baker-Herman, T. L. Spinal TNF is necessary for inactivity-induced phrenic motor facilitation. *J. Physiol. (Lond.)* **591**, 5585–98 (2013).
 34. McCoy, M. K. & Tansey, M. G. TNF signaling inhibition in the CNS: implications for normal brain function and neurodegenerative disease. *J Neuroinflammation* **5**, 45 (2008).
 35. Olson, J. K. & Miller, S. D. Microglia initiate central nervous system innate and adaptive immune responses through multiple TLRs. *The Journal of Immunology* **173**, 3916–3924 (2004).
 36. Jack, C. S., Arbour, N., Manusow, J., Montgrain, V., Blain, M., McCrea, E., Shapiro, A. & Antel, J. P. TLR signaling tailors innate immune responses in human microglia and astrocytes. *The Journal of Immunology* **175**, 4320–4330 (2005).
 37. Lehnardt, S. Innate immunity and neuroinflammation in the CNS: The role of microglia in Toll-like receptor-mediated neuronal injury. *Glia* **58**, 253–263 (2010).

38. Carty, M. & Bowie, A. G. Evaluating the role of Toll-like receptors in diseases of the central nervous system. *Biochemical pharmacology* **81**, 825–837 (2011).
39. Kawai, T. & Akira, S. The role of pattern-recognition receptors in innate immunity: update on Toll-like receptors. *Nature immunology* **11**, 373–384 (2010).
40. Beg, A. A. Endogenous ligands of Toll-like receptors: implications for regulating inflammatory and immune responses. *Trends in immunology* **23**, 509–512 (2002).
41. Takeuchi, O. & Akira, S. Pattern recognition receptors and inflammation. *Cell* **140**, 805–820 (2010).
42. Akinnusi, M., Jaoude, P., Kufel, T. & El-Solh, A. A. Toll-like receptor activity in patients with obstructive sleep apnea. *Sleep and Breathing* **17**, 1009–1016 (2013).
43. Yao, L., Kan, E. M., Lu, J., Hao, A., Dheen, S. T., Kaur, C. & Ling, E.-A. Toll-like receptor 4 mediates microglial activation and production of inflammatory mediators in neonatal rat brain following hypoxia: role of TLR4 in hypoxic microglia. *J Neuroinflammation* **10**, 23 (2013).
44. Ock, J., Jeong, J., Choi, W. S., Lee, W. H., Kim, S. H., Kim, I. K. & Suk, K. Regulation of Toll-like receptor 4 expression and its signaling by hypoxia in cultured microglia. *Journal of neuroscience research* **85**, 1989–1995 (2007).
45. Tsan, M. F. & Gao, B. Endogenous ligands of Toll-like receptors. *Journal of leukocyte biology* **76**, 514–519 (2004).
46. Cholidou, K. G., Kostakis, I. D., Manali, E. D., Perrea, D., Margeli, A., Vougas, K., Markozannes, E., Koulouris, N. & Alchanatis, M. Calprotectin: A protein related to cardiovascular risk in adult patients with obstructive sleep apnea. *Cytokine* **61**, 917–923 (2013).
47. Kim, J., Bhattacharjee, R., Snow, A., Capdevila, O., Kheirandish-Gozal, L. & Gozal, D. Myeloid-related protein 8/14 levels in children with obstructive sleep apnoea. *European Respiratory Journal* **35**, 843–850 (2010).
48. Wu, K.-M., Lin, C.-C., Chiu, C.-H. & Liaw, S.-F. Effect of treatment by nasal continuous positive airway pressure on serum high mobility group box-1 protein in obstructive sleep apnea. *CHEST Journal* **137**, 303–309 (2010).
49. Lavie, L., Dyugovskaya, L., GOLAN-SHANY, O. & Lavie, P. Heat-shock protein 70: expression in monocytes of patients with sleep apnoea and association with oxidative stress and tumour necrosis factor- α . *Journal of sleep research* **19**, 139–147 (2010).
50. Wessendorf, T. E., Thilmann, A. F., Wang, Y.-M., Schreiber, A., Konietzko, N. & Teschler, H. Fibrinogen levels and obstructive sleep apnea in ischemic stroke. *American*

- journal of respiratory and critical care medicine* **162**, 2039–2042 (2000).
51. Chin, K., Ohi, M., Kita, H., Noguchi, T., Otsuka, N., Tsuboi, T., Mishima, M. & Kuno, K. Effects of NCPAP therapy on fibrinogen levels in obstructive sleep apnea syndrome. *American journal of respiratory and critical care medicine* **153**, 1972–1976 (1996).
 52. Saletu, M., Nosiska, D., Kapfhammer, G., Lalouschek, W., Saletu, B., Benesch, T. & Zeitlhofer, J. Structural and serum surrogate markers of cerebrovascular disease in obstructive sleep apnea (OSA). *Journal of neurology* **253**, 746–752 (2006).
 53. Kizawa, T., Nakamura, Y., Takahashi, S., Sakurai, S., Yamauchi, K. & Inoue, H. Pathogenic role of angiotensin II and oxidised LDL in obstructive sleep apnoea. *European Respiratory Journal* **34**, 1390–1398 (2009).
 54. Mancuso, M., Bonanni, E., LoGerfo, A., Orsucci, D., Maestri, M., Chico, L., DiCoscio, E., Fabbrini, M., Siciliano, G. & Murri, L. Oxidative stress biomarkers in patients with untreated obstructive sleep apnea syndrome. *Sleep medicine* **13**, 632–636 (2012).
 55. Gao, H. M., Zhou, H., Zhang, F., Wilson, B. C., Kam, W. & Hong, J. S. HMGB1 acts on microglia Mac1 to mediate chronic neuroinflammation that drives progressive neurodegeneration. *The Journal of Neuroscience* **31**, 1081–1092 (2011).
 56. Lehnardt, S., Schott, E., Trimbuch, T., Laubisch, D., Krueger, C., Wulczyn, G., Nitsch, R. & Weber, J. R. A vicious cycle involving release of heat shock protein 60 from injured cells and activation of toll-like receptor 4 mediates neurodegeneration in the CNS. *The Journal of Neuroscience* **28**, 2320 (2008).
 57. Gozal, E., Gozal, D., Pierce, W. M., Thongboonkerd, V., Scherzer, J. A., R Sachleben Jr, L., Brittan, K. R., Guo, S. Z., Cai, J. & Klein, J. B. Proteomic analysis of CA1 and CA3 regions of rat hippocampus and differential susceptibility to intermittent hypoxia. *Journal of neurochemistry* **83**, 331–345 (2002).
 58. Kheirandish, L., Row, B. W., Li, R. C., Brittan, K. R. & Gozal, D. Apolipoprotein E-deficient mice exhibit increased vulnerability to intermittent hypoxia-induced spatial learning deficits. *SLEEP-NEW YORK THEN WESTCHESTER* **28**, 1412 (2005).
 59. Tagaito, Y., Polotsky, V., Campen, M., Wilson, J., Balbir, A., Smith, P., Schwartz, A. & O'donnell, C. A model of sleep-disordered breathing in the C57BL/6J mouse. *Journal of applied physiology* **91**, 2758–2766 (2001).
 60. Smith, S. M. C., Kimyon, R. S. & Watters, J. J. Cell-Type Specific Jumonji Histone Demethylase Gene Expression in the Healthy Rat CNS: Detection By A Novel Flow Cytometry Method. *ASN Neuro* (2014). doi:10.1042/AN20130050
 61. Lykidis, D., Van Noorden, S., Armstrong, A., Spencer-Dene, B., Li, J., Zhuang, Z. & Stamp, G. W. H. Novel zinc-based fixative for high quality DNA, RNA and protein

- analysis. *Nucleic acids research* **35**, e85 (2007).
62. Jensen, U. B., Owens, D. M., Pedersen, S. & Christensen, R. Zinc fixation preserves flow cytometry scatter and fluorescence parameters and allows simultaneous analysis of DNA content and synthesis, and intracellular and surface epitopes. *Cytometry Part A* **77**, 798–804 (2010).
 63. Fujiwara, T., Oda, K., Yokota, S., Takatsuki, A. & Ikehara, Y. Brefeldin A causes disassembly of the Golgi complex and accumulation of secretory proteins in the endoplasmic reticulum. *Journal of Biological Chemistry* **263**, 18545–18552 (1988).
 64. Blasi, E., Barluzzi, R., Bocchini, V., Mazzolla, R. & Bistoni, F. Immortalization of murine microglial cells by a v-raf/v-myc carrying retrovirus. *J. Neuroimmunol.* **27**, 229–37 (1990).
 65. Nikodemova, M., Duncan, I. D. & Watters, J. J. Minocycline exerts inhibitory effects on multiple mitogen-activated protein kinases and IkappaBalpha degradation in a stimulus-specific manner in microglia. *J. Neurochem.* **96**, 314–23 (2006).
 66. Nikodemova, M. & Watters, J. J. Efficient isolation of live microglia with preserved phenotypes from adult mouse brain. *Journal of Neuroinflammation* **9**, 147 (2012).
 67. Potucek, Y. D., Crain, J. M. & Watters, J. J. Purinergic receptors modulate MAP kinases and transcription factors that control microglial inflammatory gene expression. *Neurochemistry international* **49**, 204–214 (2006).
 68. Livak, K. J. & Schmittgen, T. D. Analysis of relative gene expression data using real-time quantitative PCR and the 2(-Delta Delta C(T)) Method. *Methods* **25**, 402–8 (2001).
 69. Poltorak, A., He, X., Smirnova, I., Liu, M. Y., Van Huffel, C., Du, X., Birdwell, D., Alejos, E., Silva, M., Galanos, C., Freudenberg, M., Ricciardi-Castagnoli, P., Layton, B. & Beutler, B. Defective LPS signaling in C3H/HeJ and C57BL/10ScCr mice: mutations in Tlr4 gene. *Science* **282**, 2085–8 (1998).
 70. Gozal, E., Row, B. W., Schurr, A. & Gozal, D. Developmental differences in cortical and hippocampal vulnerability to intermittent hypoxia in the rat. *Neuroscience letters* **305**, 197–201 (2001).
 71. Schwartz, M., Butovsky, O., Brück, W. & Hanisch, U. K. Microglial phenotype: is the commitment reversible? *Trends in neurosciences* **29**, 68–74 (2006).
 72. Kim, J.-B., Choi, J. S., Yu, Y.-M., Nam, K., Piao, C.-S., Kim, S.-W., Lee, M.-H., Han, P.-L., Park, J. & Lee, J.-K. HMGB1, a novel cytokine-like mediator linking acute neuronal death and delayed neuroinflammation in the postischemic brain. *The Journal of neuroscience* **26**, 6413–6421 (2006).

73. Faraco, G., Fossati, S., Bianchi, M., Patrone, M., Pedrazzi, M., Sparatore, B., Moroni, F. & Chiarugi, A. High mobility group box 1 protein is released by neural cells upon different stresses and worsens ischemic neurodegeneration in vitro and in vivo. *Journal of neurochemistry* **103**, 590–603 (2007).
74. Matsunaga, N., Tsuchimori, N., Matsumoto, T. & Ii, M. TAK-242 (resatorvid), a small-molecule inhibitor of Toll-like receptor (TLR) 4 signaling, binds selectively to TLR4 and interferes with interactions between TLR4 and its adaptor molecules. *Molecular Pharmacology* **79**, 34–41 (2011).
75. Ii, M., Matsunaga, N., Hazeki, K., Nakamura, K., Takashima, K., Seya, T., Hazeki, O., Kitazaki, T. & Iizawa, Y. A novel cyclohexene derivative, TAK-242, selectively inhibits Toll-like receptor 4-mediated cytokine production through suppression of intracellular signaling. *Molecular Pharmacology* (2005).
76. Yu, M., Wang, H., Ding, A., Golenbock, D. T., Latz, E., Czura, C. J., Fenton, M. J., Tracey, K. J. & Yang, H. HMGB1 signals through toll-like receptor (TLR) 4 and TLR2. *Shock* **26**, 174 (2006).
77. Vogl, T., Tenbrock, K., Ludwig, S., Leukert, N., Ehrhardt, C., van Zoelen, M. A. D., Nacken, W., Foell, D., van der Poll, T., Sorg, C. & Roth, J. Mrp8 and Mrp14 are endogenous activators of Toll-like receptor 4, promoting lethal, endotoxin-induced shock. *Nat. Med.* **13**, 1042–9 (2007).
78. Ziegler, G., Prinz, V., Albrecht, M. W., Harhausen, D., Khojasteh, U., Nacken, W., Endres, M., Dirnagl, U., Nietfeld, W. & Trendelenburg, G. Mrp-8 and -14 mediate CNS injury in focal cerebral ischemia. *Biochimica et Biophysica Acta (BBA)-Molecular Basis of Disease* **1792**, 1198–1204 (2009).
79. O'Neill, L. A. J. The interleukin-1 receptor/Toll-like receptor superfamily: 10 years of progress. *Immunological reviews* **226**, 10–18 (2008).

CHAPTER 6

**MICROGLIAL INFLAMMATORY RESPONSES TO CHRONIC INTERMITTENT
HYPOXIA ARE SUBJECT TO EPIGENETIC MODIFICATION THROUGH JMJD3
ACTIVITY**

Stephanie M.C. Smith and Jyoti J. Watters

In preparation for publication

ABSTRACT

Microglia exhibit astounding phenotypic plasticity that enables them to sense and respond to a variety of stimuli. We have previously shown that intermittent hypoxia (IH), a hallmark of sleep apnea, induces microglial inflammation *in vivo*. However, the mechanisms underlying IH-induced microglial activation are not well understood. We utilized *in vivo* and *in vitro* models to investigate the induction of IH-induced inflammation, and the role played by JMJD3, a hypoxia-sensitive jumonji histone demethylase that has recently been shown to regulate macrophage inflammatory processes. In the rat, we found that IH upregulated JMJD3 mRNA in immuno-magnetically isolated microglia from the hippocampus, in a time course that correlates with that of inflammatory gene expression. To test the requirement of JMJD3 in IH-induced microglial gene expression, we exposed microglial cell cultures to IH *in vitro*, in the presence and absence of the small molecule JMJD3 inhibitor, GSK-J4 (7.5 μ M). IH exposure increased JMJD3 mRNA levels in microglia *in vitro*, and IH-induced IL-1 β and IL-6 pro-inflammatory gene expression was blocked in the presence of GSK-J4, suggesting a critical role of JMJD3 in IH-induced cytokine expression. This is the first study to investigate jumonji demethylase activity in the context of IH in any system, and the first to link IH-induced microglial inflammation to JMJD3 activities or any epigenetic modulator.

INTRODUCTION

Microglia display significant phenotypic plasticity, which enables them to adapt to their environment, maintain a healthy CNS, and respond to a variety of pathologies. In the healthy CNS, microglia continuously survey the brain, monitor synaptic activity, and mediate synaptic remodeling¹⁻⁷. When disturbances in cellular homeostasis are detected, microglia respond by altering their phenotype^{8,9}. While these responses vary according to the stimulus, they often include the production of pro-inflammatory and/or anti-inflammatory/trophic molecules. The microglial pro-inflammatory phenotype is a major contributor to neuroinflammation in most neurodegenerative disorders, and their pro-inflammatory activities are thought cause a majority of the associated neuronal toxicity¹⁰⁻¹². Although most microglial plasticity is transcriptionally regulated and therefore highly susceptible to epigenetic modification, the epigenetic mechanisms underlying these activities are largely unknown in microglia. We have recently reported that microglia transition to a pro-inflammatory phenotype in response to intermittent hypoxia¹³, a hallmark feature of sleep apnea that causes significant hippocampal and frontal cortical neuronal death and cognitive impairments in animal models¹⁴⁻¹⁶. However, little is known about the mechanisms regulating IH-induced pro-inflammatory gene transcription.

Jumonji histone demethylases are highly conserved proteins that target specific lysine or arginine residues on histone 3 (H3) or histone 4 (H4) resulting in either the induction or repression of transcription depending on the target residue and/or specific gene¹⁷. Jumonji proteins are transcriptionally regulated, and interestingly, 17 of 22 characterized proteins are hypoxia sensitive (4 are identified as direct HIF-1 targets)¹⁸. Even more interesting is that jumonji proteins are dioxygenases and thereby catalyze histone demethylation via a reaction requiring Fe (II), α -ketoglutarate, and molecular oxygen^{17,19-21}. Therefore, in hypoxia, when

oxygen tension is low, these enzymes have reduced catalytic activity, and upon re-oxygenation, their catalytic activity would be increased. It is thought that jumonji expression is increased during hypoxia to compensate for their decreased catalytic activity, to prevent global histone methylation (and genome-wide gene silencing)¹⁹⁻²². However, the vast majority of research investigating the hypoxia sensitivity of jumonji proteins comes from the embryogenesis and tumor literature with sustained hypoxia^{18,23-25}, and no studies have evaluated the activities of these enzymes in intermittent hypoxia when there is oscillating low oxygen and reoxygenation.

The jumonji histone 3 (H3) lysine 27 (K27) demethylase, JMJD3, has recently been identified as an important modulator of macrophage and microglial pro- and anti- inflammatory phenotypes²⁶⁻²⁹. Therefore, we tested the hypothesis that JMJD3 would be transcriptionally upregulated in microglia during IH, and that its enzymatic activities were necessary for IH-induced microglial pro-inflammatory gene expression. We found that IH increased JMJD3 expression in microglia in a time course that corresponded with peak pro-inflammatory gene expression *in vivo and in vitro*. Additionally, IH-induced microglial pro-inflammatory cytokine upregulation *in vitro* was attenuated in the presence of the JMJD3 inhibitor GSK-J4, suggesting that JMJD3 may be an important regulator of microglial responses to IH in the CNS.

METHODS

Materials:

Hank's Buffered Salt Solution (HBSS) was purchased from Cellgro (Herndon, VA). Glycoblue reagent was purchased from Ambion (Austin, TX). Oligo dT, Random Primers, and RNase inhibitor were purchased from Promega (Madison, WI). Power SYBR green was purchased from Applied Biosystems (Foster City, CA). TRI reagent was purchased from Sigma Aldrich (St. Louis, MO). Percoll was purchased from GE Healthcare (Waukesha, WI). Gas permeable 24-well tissue culture plates were purchased from Coy Laboratories (Great Lake, Michigan). MMLV reverse transcriptase, RNase AWAY, and DAPI were purchased from Invitrogen (Carlsbad, CA). GSK-J4 was purchased from Tocris Biosciences (Minneapolis, MN). TAK-242 was purchased from Invivogen (San Diego, CA). H3K27me3 ELISA assay and histone isolation kit were purchased from Abcam (San Francisco, CA). Neural Tissue Dissociation Kit, anti-PE magnetic beads, and MS columns were purchased from Miltenyi Biotech (Germany). PE-Mouse anti-rat CD11b was purchased from BD Biosciences (San Jose, CA).

Animals:

Adult, male, Sprague-Dawley rats and C57BL6 mice were obtained from Harlan Laboratories (Indianapolis, IN). Rats weighing 150 ± 20 g were randomly assigned to intermittent hypoxia or normoxia groups. Animals were housed in clear polycarbonate cages under standard conditions conditions, with a 12 hour light/dark cycle (6:00am-6:00pm) with food and water *ad libitum*. All animals were maintained in an AAALAC-accredited animal facility, and protocols were approved by the University of Wisconsin Institutional Animal Care and Use Committee.

All efforts were made to minimize animal distress and reduce the number of animals used while permitting the formation of statistically reliable conclusions.

***In Vivo* Intermittent Hypoxia (IH) Exposure:**

Intermittent hypoxia exposures were performed as previously described¹³. Briefly, rats were placed in custom-manufactured chambers. O₂ and CO₂ concentrations were continuously monitored with a custom controlled computer system and brought to desired concentrations with a flow rate of 4L/min to enable rapid gas exchange and minimal CO₂ accumulation. IH exposures consisted of 2 minute episodes of hypoxia (10.5% inspired O₂) and normoxia (21% inspired O₂) for 8 h/day during their respective night cycle for 1, or 3 days. The control, normoxic, groups underwent identical handling, and were placed into chambers continuously flushed with 4L/min of room air. Following IH exposures, rats were returned to their cages.

Immunomagnetic Microglia (CD11b+) Cell Isolation:

Rats were harvested 16 hours following the last hypoxic exposure. CD11b+ cells were isolated using previously described methods^{30,31}. Briefly, rats were euthanized with an overdose of isoflurane and perfused with cold 0.1M PBS. The hippocampus was dissected out and dissociated into a single cell suspension using the papain-based, neural tissue dissociation kit (Miltenyi), per manufacturer's protocol. Myelin was removed by high speed centrifugation at 850g in a 30% solution of Percoll in 1X PBS. CD11b+ cells were tagged with an PE conjugate anti-CD11b antibody followed by a secondary anti-PE antibody conjugated to a magnetic bead. Magnetically-tagged CD11b+ cells were isolated using MS columns according to the Miltenyi MACS protocol. Reagents were kept chilled at 4°C and cells were kept on ice whenever possible to preserve microglial phenotypes. We have previously shown, this method results in a

>97% pure CD11b⁺/CD45^{low} cell population^{30,31}, and thus, this population will subsequently be referred to as “microglia.”

Cell Culture:

Murine N9³² and BV2³³ microglial cells were routinely cultured in Dulbecco's modified Eagle's medium (DMEM; Cellgro, Herndon, VA) supplemented with 10% fetal bovine growth serum (FBS, Hyclone, Logan, UT) in 100 mm BD Falcon plates. Cells were grown to ~90% confluency and passaged every 1-3 days. Cells were seeded at a density of 2.5×10^4 on specialized 24-well plates with gas-permeable base (Coy labs) to facilitate rapid gas exchange at the cellular level. The following day, cells were pre-treated with the selective H3K27 demethylase inhibitor, GSK-J4 ($7.5 \mu\text{M}$)²⁹, or the TLR4 inhibitor, TAK-242 ($1 \mu\text{M}$)³⁴, for 45 min prior to start of the IH protocol.

Primary microglial cultures were prepared as previously described³⁵. Briefly, mixed glial cultures were prepared from C57/BL6 mice (postnatal days 3-7) and cultured in DMEM supplemented with 10% fetal bovine serum and 100 U mL^{-1} penicillin/streptomycin. Primary microglia were shaken from the mixed glial cultures and were seeded at a density of 150,000 cells/well in a 24-well gas permeable tissue culture plates, and IH exposures started the following day.

***In vitro* intermittent hypoxia exposure:**

Intermittent hypoxia exposures were performed using a commercially-designed cell culture system (BioSpherix, Redfield, NY). Cells were maintained in a specialized incubator chamber at 37°C. O₂ and CO₂ concentrations were continuously measured with O₂ and CO₂ analyzers, and were changed with a computerized system controlling gas outlets (Oxycycler model C42, Biospherix, Redfield, NY). Cells were exposed to normoxia (Nx: 21% O₂, 5% CO₂,

balance N₂), or intermittent hypoxia (IH: 10min cycles of 1% and 21% O₂ held at a constant 5% CO₂, balance N₂) for 18 hours.

RNA extraction/ reverse transcription:

RNA was extracted from N9, BV2, primary, and immunomagnetically-isolated microglia according to the TriReagent protocol, with the addition of Glycoblue during the isopropanol incubation. First-strand cDNA was synthesized from total RNA using MMLV Reverse Transcriptase, and an oligo(dT)/random hexamer cocktail. cDNA was used for qRT-PCR analysis.

Quantitative-Real Time PCR:

cDNA was used in real-time quantitative PCR with Power SYBR Green using either the ABI StepOne or ABI 7500 Fast system (Applied Biosystems/Life Technologies). Primers (Table 1) were designed using Primer 3 software and the specificity was assessed through NCBI BLAST. Primer efficiency was tested through the use of serial dilutions. Verification that the dissociation curve had a single peak with an observed T_m consistent with the amplicon length was performed for every PCR reaction. CT values from duplicate measurements were averaged and normalized to levels of the ribosomal RNA, 18s. Relative gene expression was determined using the $\Delta\Delta$ CT method³⁶.

Statistical analyses:

When comparing two population means, statistical inferences were made using a Student's t-test or a paired Student's t-test, where applicable. When three or more groups were compared across 2 parameters, comparisons were made using a two-way ANOVA or two-way RM ANOVA where applicable. The Holm-Sidak post hoc test was used to assess statistical significance in individual comparisons. All statistical analyses were performed in SigmaPlot

(Sigma Stat version 11(Systat Software, San Jose, CA). Statistical significance was set at $p < 0.05$. Mean data are expressed ± 1 SEM.

RESULTS

IH increases the expression of inflammatory genes in hippocampal microglia.

We assessed changes in inflammatory gene expression (compared to normoxic controls) in hippocampal microglia following 1 and 3 days of IH, time points which correspond with peak, IH-induced neuronal death in the hippocampus^{14,16}. Consistent with the notion that inflammation contributes to IH-induced neuronal death, we observed significant increases in IL-1 β , IL-6, and COX-2 mRNA levels in hippocampal microglia following IH exposure (Fig. 1A). At 1 day of IH, only IL-1 β expression was significantly increased (~2.0 fold; $p=0.039$); however, at 3 days of IH, the expression of IL-1 β was increased by ~3-fold ($p=0.014$), COX-2 by ~2.5 fold ($p=0.003$), and IL-6 by ~3.5 fold ($p=0.005$). TNF α mRNA levels did not change at either time point with IH-treatment, as assessed by ANOVA ($p=0.896$).

IH-induced JMJD3 expression correlates with increased pro-inflammatory gene expression in hippocampal microglia.

We next sought to examine whether exposure to IH regulates JMJD3 expression in hippocampal microglia. We observed a ~5.5 fold increase in JMJD3 mRNA levels ($p=0.004$) following 3 days of IH (Fig. 1B), the time point coinciding with peak microglial pro-inflammatory gene expression (Fig. 1A). Although there appeared to be an ~2- fold increase in JMJD3 mRNA levels at 1 day of IH, this did not reach statistical significance ($p=0.098$).

JMJD3 expression is increased in N9 and primary microglial cultures in response to IH exposure *in vitro*.

Since we observed IH-induced JMJD3 expression in microglia *in vivo*, we next tested whether microglia exposed to IH *in vitro* exhibit similar responses. N9 and primary microglia were exposed to IH or Nx for 18 hours and JMJD3 gene expression was analyzed. As observed

in vivo, IH significantly increased JMJD3 mRNA levels by ~4.5- fold in N9 (p=0.027) and 6.8-fold in primary microglia (p=0.002) (Fig. 2). Since the UTX jumonji protein is structurally and functionally similar to JMJD3, we assessed whether IH-induced similar changes in UTX expression. We did not observe any changes in UTX expression in either N9 (p=0.440) or primary microglia (p=0.343) exposed to IH.

JMJD3 inhibition attenuates IH-induced cytokine but not COX-2 gene upregulation *in vitro*.

IH significantly increased the expression of IL-1 β by ~6 fold (p=0.003), IL-6 by ~3-fold (p=0.038), and TNF α by 1.5-fold (p=0.005) in N9 microglia, although it did not effect COX-2 expression (p=0.183) (Fig. 3A). These observations are consistent with our previous reports in BV2 and primary microglia (Chapter 4). To test whether JMJD3 activity is necessary for IH-induced inflammatory gene expression, N9 microglia were exposed to IH in the presence and absence of the JMJD3 inhibitor GSK-J4²⁹. We found that GSK-J4 attenuated IH-induced expression by ~65% for both IL-1 β (p=0.022) and IL-6 (p=0.046), although it did not effect the expression of COX-2 (p=0.416) or TNF α (p=0.475), suggesting gene-specific regulation by JMJD3 potentially through selective gene targets associated with the H3K27 histone mark.

IH regulates microglial expression of JMJD3 via TLR4 independent mechanisms.

We previously reported that microglial TLR4 expression is increased by IH¹³. It is also an important regulator of microglial pro-inflammatory responses to IH (Chapter 4 & 5). As, JMJD3 expression is increased in macrophages following TLR4 activation^{37,38}, we tested the hypothesis that TLR4 signaling underlies microglial up-regulation of JMJD3 by IH. N9 microglia were exposed to IH *in vitro* in the presence/absence of the selective TLR4 inhibitor, TAK-242³⁴. We found that IH-mediated increases in JMJD3 expression were regulated independently of TLR4 activation, as IH-induced JMJD3 expression was similar among vehicle

(~6 fold increase, $p=0.020$) and TAK-242 (~8 fold increase, $p=0.002$) treated microglia.

Surprisingly, IH-induced JMJD3 expression appeared to be elevated in the presence of TAK-242, but this did not reach statistical significance ($p=0.126$) (Fig. 4A). These results indicate that TLR4-independent mechanisms underlie IH-induced microglial up-regulation of JMJD3.

Conversely, we tested whether IH-induced up-regulation of TLR4 was dependent of JMJD3 activity. We found that IH-mediated increases in microglial TLR4 expression was similar between vehicle and GSK-J4 treated microglia ($p=0.557$), indicating that IH regulation of TLR4 occurs through JMJD3-independent pathways (Fig. 4B).

Preliminary findings suggest JMJD3 may promote H3K27me3 demethylation in response to IH.

JMJD3 is reported to exert biological effects through H3K27 demethylase dependent and independent activities^{28,37-39}. Preliminary studies performed in N9 and BV2 microglia indicate that IH exposure *in vitro* decreases global H3K27me3 levels in microglia by ~10% (Fig. 5). Therefore, JMJD3 may regulate microglial responses to IH through its histone H3K27 demethylase activities.

DISCUSSION

In this study, we sought to delineate the role of JMJD3 in the regulation IH-induced microglial inflammatory responses to IH. We found that hippocampal microglia up-regulated the expression of pro-inflammatory cytokines following 1 and 3 days of IH, and similar results were observed *in vitro*. Interestingly, IH also increased JMJD3 mRNA expression in microglia both *in vivo* and *in vitro*, in a time course corresponding with increased pro-inflammatory gene expression. Additionally, GSK-J4 inhibition of JMJD3 demethylase activity attenuated IH-induced pro-inflammatory gene expression *in vitro*. Together, these results suggest that JMJD3 may be an important regulator of microglial activities in response to IH, and warrant further investigation.

Previous work out of our laboratory, found that IH-induced pro-inflammatory gene expression in cortex, brain stem, and spinal cord microglia, and that the profile of microglial activation varied regionally and temporally with chronic IH exposure¹³. Here, we demonstrate that IH increases pro-inflammatory gene expression in hippocampal microglia isolated from rats exposed to 1 and 3 days of IH. These time point were specifically chosen, as they correspond with the induction of (1 day) and peak (3 day) IH-induced hippocampal neuronal death in the rat model^{14,16}. Of the genes examined, IL-1 β was the only gene whose expression was increased at the 1 day time point, whereas COX-2 and IL-6 mRNA levels were not increased until 3 days of IH, suggesting that IL-1 β may be an early response gene contributing to early IH-induced neuropathology in the hippocampus. The upregulation of COX-2 after 3 days of IH in hippocampal microglia is in line with its previous role in IH-induced neuropathology in the cortex, where COX-2 expression was increased as early as 1 day following IH in cortical homogenates, and its enzymatic inhibition protected rats from IH-induced neuronal death⁴⁰. In

the hippocampus, microglial production of COX-2 may similarly contribute to IH-induced neuronal loss.

The role of jumonji histone demethylases in the regulation of gene expression during conditions of IH was particularly intriguing due to the unique molecular properties of these enzymes that may make them particularly susceptible to this type of stimulus. Their expression is up-regulated during periods of hypoxia¹⁸ and they require molecular oxygen for catalytic activity⁴¹ suggesting that intermittent bouts of hypoxia and reoxygenation may increase both their expression and catalytic activity. Our previous studies identified JMJD3 as one of the most highly expressed jumonji demethylases in microglial cells compared to other CNS cell types⁴² (chapter 3), and JMJD3 regulates macrophage inflammatory responses^{37,38,43}. Thus, we assessed whether JMJD3 played a role in IH-induced microglial pro-inflammatory gene expression. We found that IH increased the microglial expression of JMJD3 in hippocampal microglia isolated from IH- treated animals as well as in cultured microglia exposed to IH *in vitro*. Additionally, enzymatic inhibition of JMJD3 with the small-molecule inhibitor GSK-J4²⁹ significantly decreased IH-induced expression of IL-1 β and IL-6 *in vitro*. Together these findings suggest that JMJD3 may play an important role in the regulation of microglial responses to IH.

We recently identified the TLR4 cascade as an important signaling pathway mediating microglial inflammatory responses to IH¹³ *in vitro* (see chapter 4). Interestingly, JMJD3 activity is necessary for TLR4-mediated pro-inflammatory gene production^{28,29,37}. While TLR4 activation by lipopolysaccharide (LPS) has previously been shown to increase JMJD3 expression through NF κ B-dependent³⁸ and STAT1/3- dependent mechanisms⁴⁴, we found that IH-induced increases in JMJD3 and TLR4 microglial gene expression were regulated independently of each other. The mechanisms by which JMJD3 induces pro-inflammatory gene expression are not well

understood, and JMJD3 mediated-inflammation has been reported to occur through histone demethylase dependent²⁹ and independent mechanisms^{37,38,44}. We have preliminary evidence that IH results in a ~10% reduction of global H3K27me3 levels in microglia, thus IH may promote JMJD3 demethylase activity. However, the biological significance of this histone demethylation, and the molecular mechanisms regulating the decrease are currently unknown. JMJD3 was recently shown to have transcription factor-like properties that are independent of its H3K27 demethylase activity, and that synergize with STAT1/3 signaling to enhance pro-inflammatory gene expression in LPS-stimulated microglial cells. The mechanistic and functional properties of JMJD3 are poorly understood, but recent evidence supports JMJD3 as having multiple functional roles within the cell beyond demethylase activity. Here, we have demonstrated that IH is an important regulator JMJD3 activity in microglial cells, and that JMJD3 activity contributes to the regulation of microglial pro-inflammatory responses to acute IH. However, the mechanisms by which JMJD3 exert these effects, and how these functions change with chronic exposure to IH are unknown.

ACKNOWLEDGEMENTS

We would like to thank Rebecca Kimyon and Scott Ray for their technical support on this project. This work is supported by the National Institutes of Health [NS049033, HL111598 and T32HL007654] and the BD Biosciences Research Innovation Award in Immunology.

FIGURE 1

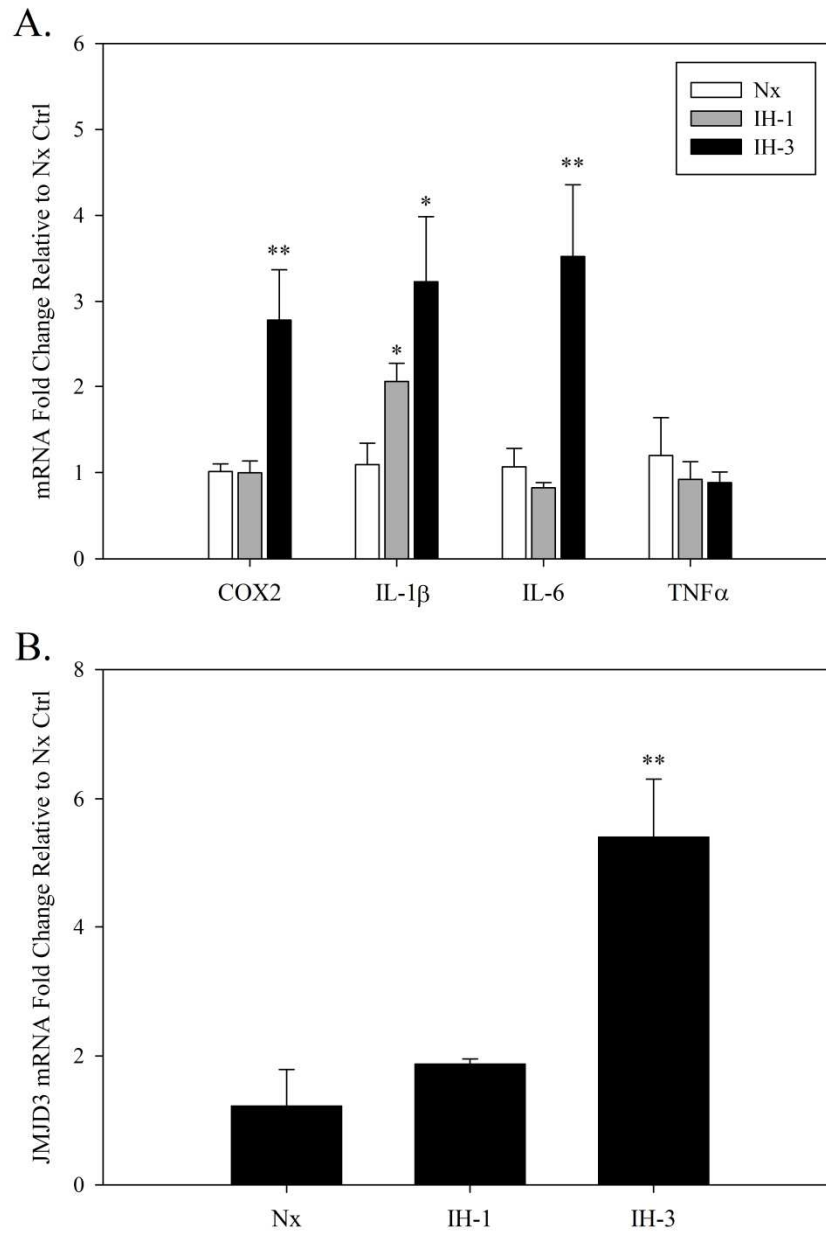


Figure Legend 1***Microglia isolated from the cortex of rats exposed to 1 and 3 days of IH increase pro-inflammatory and JMJD3 gene expression***

Microglia (CD11b+ cells) were immunomagnetically isolated from the hippocampus of rats exposed to Normoxia (Nx), 1, or 3 days of IH (IH-1, IH-3) and processed for gene expression analysis. (A) Fold-induction of hippocampal microglial pro-inflammatory gene expression following 1 and 3 days of IH relative to normoxia. (B) Fold-induction of hippocampal microglial JMJD3 mRNA expression following 1 and 3 days of IH relative to normoxia. Mean fold changes \pm 1 SEM are presented relative to the normoxic (Nx) control. Statistical significance was determined by a 1-Way ANOVA with the Holm-Sidak *pos hoc* test. N=3-4 for each group. * symbol represents a statistically significant difference relative to Nx control. * p <0.05; ** p <0.01; *** p <0.001

FIGURE 2

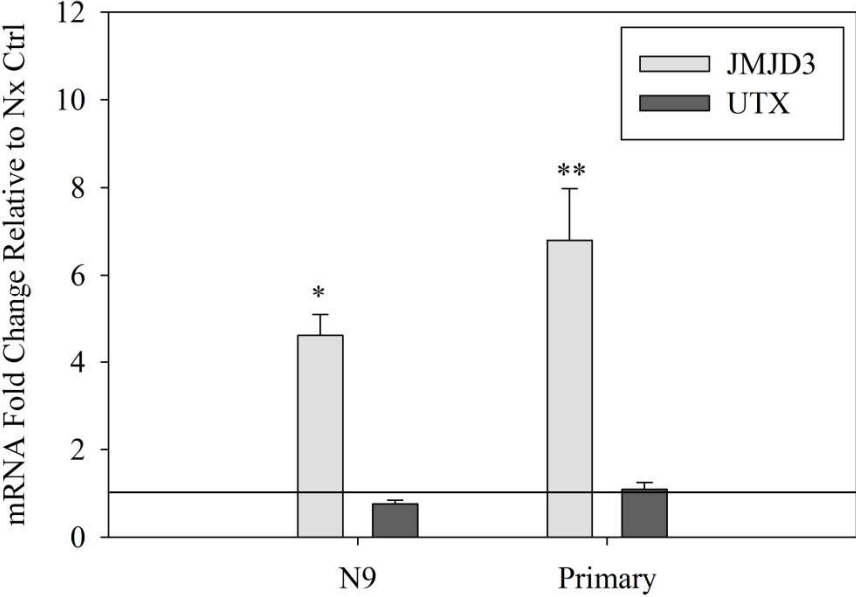


Figure Legend 2***IH induces JMJD3 but not UTX gene expression N9 and Primary microglia***

N9 microglial cell line or BL6 primary microglia were exposed to IH or Nx *in vitro* for 18 hours and were subsequently harvested for mRNA gene expression analysis. Data represent the fold-induction of JMJD3 and UTX in microglial cultures exposed to IH relative to Nx. N=4-6. Mean fold change \pm 1 SEM are presented relative to normoxic controls. Black line represents respective Nx controls. Statistical significance was determined by a paired T-test on Δ CT. * symbol represents a statistically significant difference relative to Nx control. * p <0.05; ** p <0.01; *** p <0.001

FIGURE 3

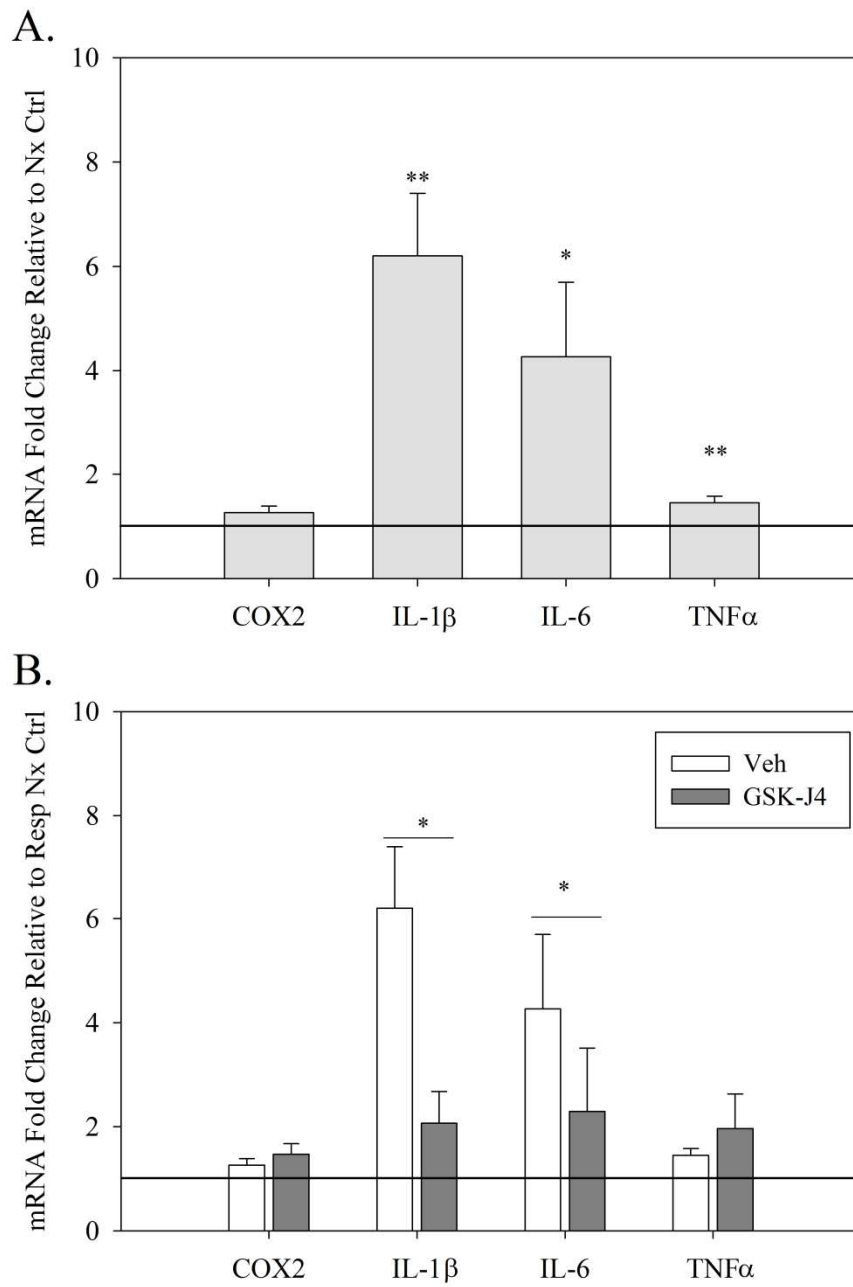


Figure Legend 3

IH induces pro-inflammatory gene expression in N9 microglia, and this induction is partially blocked by the JMJD3 inhibitor, GSK-J4

N9 microglial cultures were exposed to IH or Nx *in vitro* for 18 hours ± the JMJD3 inhibitor, GSK-J4 (7.5 μM), and were subsequently harvested for mRNA gene expression analysis. (A) Fold induction of COX2, IL-1β, IL-6, and TNFα in N9 microglia exposed to IH relative to Nx. (B) GSK-J4 partially blocks IH-induced microglial expression of pro-inflammatory genes *in vitro*. N=4. Mean fold change ± SEM are presented relative to respective treatment normoxic control. Black line represents respective Nx controls. Statistical significance was determined by a paired T-test on ΔCT values for graph (A). Student's T-test was performed on IH fold changes normalized to respective treatment normoxic controls for graph (B). * symbol represents a statistically significant difference relative to Nx control (A) or IH Vehicle (B). *p<0.05; **p<0.01; ***p<0.001

FIGURE 4

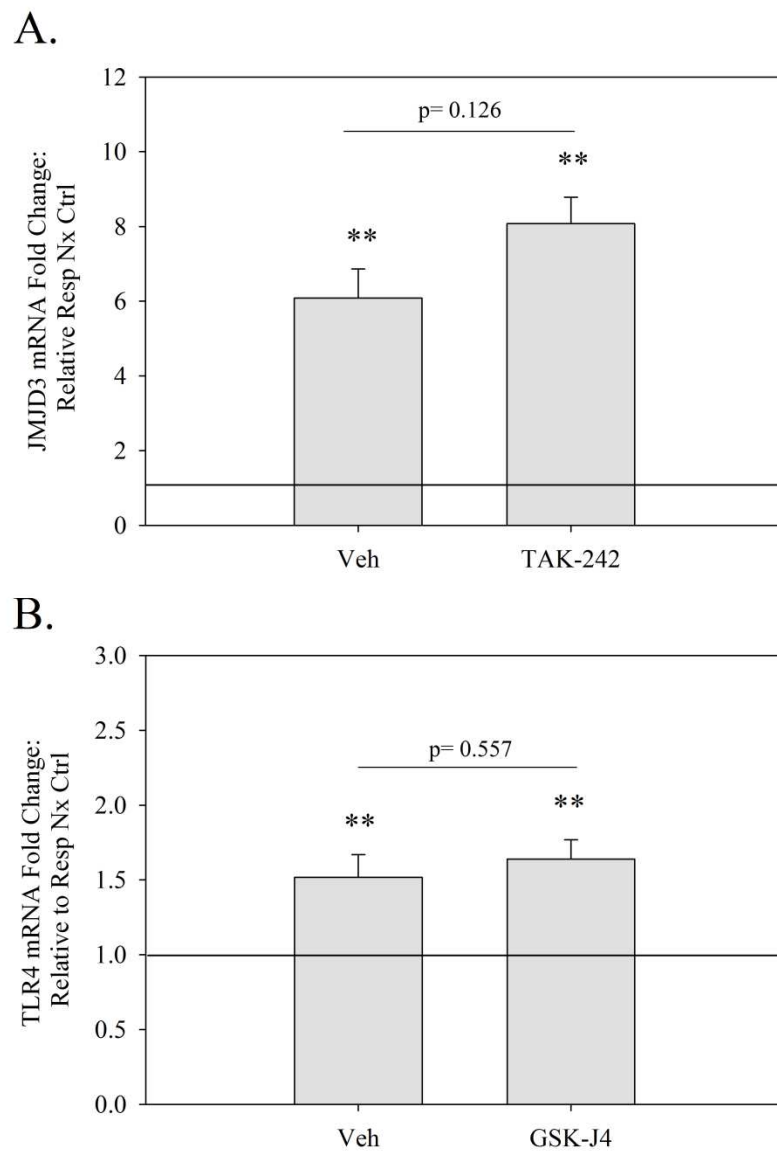


Figure Legend 4

IH-induced microglial expression of JMJD3 is independent of TLR4 activation, and conversely, increased expression of TLR4 expression by IH is independent of JMJD3 activity.

N9 microglial cultures were exposed to IH or Nx *in vitro* for 18 hours ± the JMJD3 inhibitor, GSK-J4 (7.5µM), or the TLR4 inhibitor, TAK-242 (1µM), and were subsequently harvested for mRNA gene expression analysis. (A) Fold-induction of JMJD3 in microglia exposed to IH relative to Nx is not changed in the presence of the TLR4 inhibitor, TAK-242. (B) Fold-induction of TLR4 in microglia exposed to IH relative to Nx is not changed in the presence of the JMJD3 inhibitor, GSK-J4. N=4. Mean fold change ± SEM are presented relative to respective treatment normoxic control. Black line represents respective Nx controls. Statistical significance of IH-induced gene induction relative to Nx was determined by a paired T-test on Δ CT values (denoted by a * symbol). Treatment interactions were assessed with a Student's T-test was performed on fold changes normalized to respective normoxic controls (denoted by a line over the respective bars with the associated p-value). *p<0.05; **p<0.01; ***p<0.001

FIGURE 5

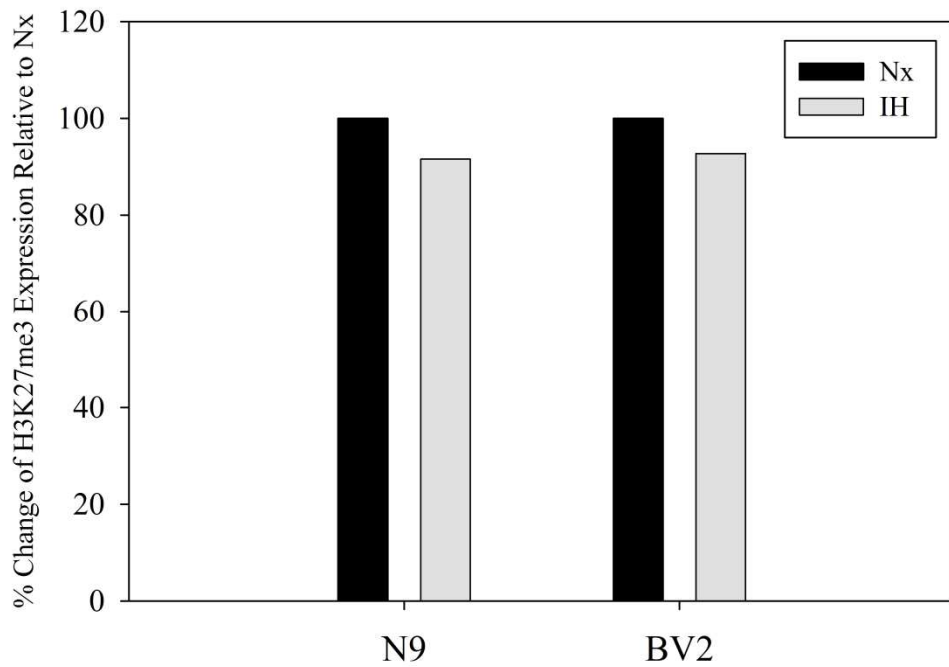


Figure Legend 5

Preliminary studies indicate that microglial cultures exhibit a mild reduction in H3K27me3 expression following in vitro exposure to IH.

N9 or BV2 microglial cultures were exposed to IH or Nx *in vitro* for 18 hours, and were subsequently harvested for histone isolation. H3K27me3 levels were measured with an ELISA based assay and results were graphed relative to the Nx control. Preliminary studies indicate that there is a reduction in H3K27me3 levels (~10% decrease) in N9 and BV2 microglial cultures exposed to IH *in vitro*. N=1.

TABLE 1

Gene	Forward Primer (5'→ 3')	Reverse Primer (5'→ 3')
18S (mouse/rat)	CGGGTGCTCTTAGCTGAGTGTCCCG	CTCGGGCCTGCTTTGAACAC
COX2 (mouse/rat)	TGTTCCAACCCATGTCAAAA	CGTAGAATCCAGTCCGGGTA
TNF α (rat)	TCCATGGCCCAGACCCTCACAC	TCCGCTTGGTGGTTTGCTACG
IL-1 β (rat)	CTGCAGATGCAATGGAAAGA	TTGCTTCCAAGGCAGACTTT
IL-6 (rat)	GTGGCTAAGGACCAAGACCA	GGTTTGCCGAGTAGACCTCA
JMJD3 (rat)	CAAACCCCCGCTTTTCTGTG	ATTTGGGTGGCAGGAGGAGG
IL-6 (mouse)	ACTTCCATCCAGTTGCCTTC	GTCTCCTCTCCGGACTTGTG
IL-1 β (mouse)	TGTGCAAGTGTCTGAAGCAGC	TGGAAGCAGCCCTTCATCTT
TNF α (mouse)	TGTAGCCCACGTCGTAGCAA	AGGTACAACCCATCGGCTGG
TLR4 (mouse)	GAGGCAGCAGGTGGAATTGTAT	TTCGAGGCTTTTCCATCCAA
JMJD3 (mouse)	CGCTGGAGGACCAGTTTGAA	CTTCATGATGTTTGCCAGCCC
UTX (mouse)	CACCACCTCCAGTAGAACAACA	GCTGTTCCAAGTGCTGTAATTTCT

REFERENCES

1. Tremblay, M. È., Stevens, B., Sierra, A., Wake, H., Bessis, A. & Nimmerjahn, A. The role of microglia in the healthy brain. *The Journal of Neuroscience* **31**, 16064–16069 (2011).
2. Olah, M., Biber, K., Vinet, J. & WGM Boddeke, H. Microglia phenotype diversity. *Cns+ Neurological Disorders-Drug Targets* **10**, 108 (2011).
3. Nimmerjahn, A., Kirchhoff, F. & Helmchen, F. Resting microglial cells are highly dynamic surveillants of brain parenchyma in vivo. *Science* **308**, 1314–1318 (2005).
4. Fetler, L. & Amigorena, S. Brain under surveillance: the microglia patrol. *Science* **309**, 392–393 (2005).
5. Wake, H., Moorhouse, A. J., Jinno, S., Kohsaka, S. & Nabekura, J. Resting microglia directly monitor the functional state of synapses in vivo and determine the fate of ischemic terminals. *The Journal of Neuroscience* **29**, 3974–3980 (2009).
6. Raivich, G. Like cops on the beat: the active role of resting microglia. *Trends in neurosciences* **28**, 571–573 (2005).
7. Paolicelli, R. C., Bolasco, G., Pagani, F., Maggi, L., Scianni, M., Panzanelli, P., Giustetto, M., Ferreira, T. A., Guiducci, E., Dumas, L., Ragozzino, D. & Gross, C. T. Synaptic pruning by microglia is necessary for normal brain development. *Science* **333**, 1456–8 (2011).
8. Bessis, A., Béchade, C., Bernard, D. & Roumier, A. Microglial control of neuronal death and synaptic properties. *Glia* **55**, 233–238 (2007).
9. Hanisch, U. K. & Kettenmann, H. Microglia: active sensor and versatile effector cells in the normal and pathologic brain. *Nature neuroscience* **10**, 1387–1394 (2007).
10. Banati, R. B., Gehrmann, J., Schubert, P. & Kreutzberg, G. W. Cytotoxicity of microglia. *Glia* **7**, 111–118 (1993).
11. Pickering, M. & O'Connor, J. J. Pro-inflammatory cytokines and their effects in the dentate gyrus. *Progress in brain research* **163**, 339–354 (2007).
12. Lehnardt, S., Massillon, L., Follett, P., Jensen, F. E., Ratan, R., Rosenberg, P. A., Volpe, J. J. & Vartanian, T. Activation of innate immunity in the CNS triggers neurodegeneration through a Toll-like receptor 4-dependent pathway. *Proceedings of the National Academy of Sciences* **100**, 8514–8519 (2003).
13. Smith, S. M., Friedle, S. A. & Watters, J. J. Chronic Intermittent Hypoxia Exerts CNS Region-Specific Effects on Rat Microglial Inflammatory and TLR4 Gene Expression. *PLoS*

one **8**, e81584 (2013).

14. Row, B. W., Liu, R., Xu, W., Kheirandish, L. & Gozal, D. Intermittent hypoxia is associated with oxidative stress and spatial learning deficits in the rat. *American journal of respiratory and critical care medicine* **167**, 1548–1553 (2003).
15. Xu, W., Chi, L., Row, B., Xu, R., Ke, Y., Xu, B., Luo, C., Kheirandish, L., Gozal, D. & Liu, R. Increased oxidative stress is associated with chronic intermittent hypoxia-mediated brain cortical neuronal cell apoptosis in a mouse model of sleep apnea. *Neuroscience* **126**, 313–323 (2004).
16. Gozal, D., Daniel, J. M. & Dohanich, G. P. Behavioral and anatomical correlates of chronic episodic hypoxia during sleep in the rat. *The Journal of Neuroscience* **21**, 2442 (2001).
17. Tamaru, H. Confining euchromatin/heterochromatin territory: jumonji crosses the line. *Genes & development* **24**, 1465–1478 (2010).
18. Yang, J., Ledaki, I., Turley, H., Gatter, K. C., Montero, J. C. M., Li, J. L. & Harris, A. L. Role of Hypoxia-Inducible Factors in Epigenetic Regulation via Histone Demethylases. *Annals of the New York Academy of Sciences* **1177**, 185–197 (2009).
19. Mosammamaparast, N. & Shi, Y. Reversal of histone methylation: biochemical and molecular mechanisms of histone demethylases. *Annual review of biochemistry* **79**, 155–179 (2010).
20. Beyer, S., Kristensen, M. M., Jensen, K. S., Johansen, J. V. & Staller, P. The histone demethylases JMJD1A and JMJD2B are transcriptional targets of hypoxia-inducible factor HIF. *Journal of Biological Chemistry* **283**, 36542–36552 (2008).
21. Tausendschön, M., Dehne, N. & Brüne, B. Hypoxia causes epigenetic gene regulation in macrophages by attenuating Jumonji histone demethylase activity. *Cytokine* **53**, 256–262 (2011).
22. Tian, X. & Fang, J. Current perspectives on histone demethylases. *Acta biochimica et biophysica Sinica* **39**, 81–88 (2007).
23. Watson, J. A., Watson, C. J., McCann, A. & Baugh, J. Epigenetics: The epicenter of the hypoxic response. *Epigenetics* **5**, 293–296 (2010).
24. Perez-Perri, J. I., Acevedo, J. M. & Wappner, P. Epigenetics: new questions on the response to hypoxia. *International Journal of Molecular Sciences* **12**, 4705–4721 (2011).
25. Takeuchi, T., Watanabe, Y., Takano-Shimizu, T. & Kondo, S. Roles of jumonji and jumonji family genes in chromatin regulation and development. *Developmental dynamics* **235**, 2449–2459 (2006).

26. Tang, Y., Li, T., Li, J., Yang, J., Liu, H., Zhang, X. & Le, W. Jmjd3 is essential for the epigenetic modulation of microglia phenotypes in the immune pathogenesis of Parkinson's disease. *Cell Death & Differentiation* (2013).
27. Lee, H. T., Kim, S. K., Kim, S. H., Kim, K., Lim, C. H., Park, J., Roh, T.-Y., Kim, N. & Chai, Y. G. Transcription-related element gene expression pattern differs between microglia and macrophages during inflammation. *Inflammation Research* 1–9 (2014).
28. Przanowski, P., Dabrowski, M., Ellert-Miklaszewska, A., Kloss, M., Mieczkowski, J., Kaza, B., Ronowicz, A., Hu, F., Piotrowski, A., Kettenmann, H., Komorowski, J. & Kaminska, B. The signal transducers Stat1 and Stat3 and their novel target Jmjd3 drive the expression of inflammatory genes in microglia. *J. Mol. Med.* **92**, 239–54 (2014).
29. Kruidenier, L., Chung, C., Cheng, Z., Liddle, J., Che, K., Joberty, G., Bantscheff, M., Bountra, C., Bridges, A., Diallo, H., Eberhard, D., Hutchinson, S., Jones, E., Katso, R., Leveridge, M., Mander, P. K., Mosley, J., ... Wilson, D. M. A selective jumonji H3K27 demethylase inhibitor modulates the proinflammatory macrophage response. *Nature* **488**, 404–8 (2012).
30. Nikodemova, M. & Watters, J. J. Efficient isolation of live microglia with preserved phenotypes from adult mouse brain. *Journal of Neuroinflammation* **9**, 147 (2012).
31. Potucek, Y. D., Crain, J. M. & Watters, J. J. Purinergic receptors modulate MAP kinases and transcription factors that control microglial inflammatory gene expression. *Neurochemistry international* **49**, 204–214 (2006).
32. Righi, M., Mori, L., Libero, G. D., Sironi, M., Biondi, A., Mantovani, A., Donini, S. D. & Ricciardi-Castagnoli, P. Monokine production by microglial cell clones. *European journal of immunology* **19**, 1443–1448 (1989).
33. Blasi, E., Barluzzi, R., Bocchini, V., Mazzolla, R. & Bistoni, F. Immortalization of murine microglial cells by a v-raf/v-myc carrying retrovirus. *J. Neuroimmunol.* **27**, 229–37 (1990).
34. Ii, M., Matsunaga, N., Hazeki, K., Nakamura, K., Takashima, K., Seya, T., Hazeki, O., Kitazaki, T. & Iizawa, Y. A novel cyclohexene derivative, TAK-242, selectively inhibits Toll-like receptor 4-mediated cytokine production through suppression of intracellular signaling. *Molecular Pharmacology* (2005).
35. Nikodemova, M., Duncan, I. D. & Watters, J. J. Minocycline exerts inhibitory effects on multiple mitogen-activated protein kinases and I κ B α degradation in a stimulus-specific manner in microglia. *Journal of neurochemistry* **96**, 314–323 (2005).
36. Livak, K. J. & Schmittgen, T. D. Analysis of Relative Gene Expression Data Using Real-Time Quantitative PCR and the $2^{-\Delta\Delta CT}$ Method. *methods* **25**, 402–408 (2001).

37. De Santa, F., Narang, V., Yap, Z. H., Tusi, B. K., Burgold, T., Austenaa, L., Bucci, G., Caganova, M., Notarbartolo, S., Casola, S., Testa, G., Sung, W.-K., Wei, C.-L. & Natoli, G. Jmjd3 contributes to the control of gene expression in LPS-activated macrophages. *EMBO J.* **28**, 3341–52 (2009).
38. De Santa, F., Totaro, M. G., Prosperini, E., Notarbartolo, S., Testa, G. & Natoli, G. The histone H3 lysine-27 demethylase Jmjd3 links inflammation to inhibition of polycomb-mediated gene silencing. *Cell* **130**, 1083–94 (2007).
39. Xiang, Y., Zhu, Z., Han, G., Lin, H., Xu, L. & Chen, C. D. JMJD3 is a histone H3K27 demethylase. *Cell research* **17**, 850–857 (2007).
40. Li, R. C., Row, B. W., Gozal, E., Kheirandish, L., Fan, Q., Brittan, K. R., Guo, S. Z., Sachleben Jr, L. R. & Gozal, D. Cyclooxygenase 2 and intermittent hypoxia-induced spatial deficits in the rat. *American journal of respiratory and critical care medicine* **168**, 469 (2003).
41. Kooistra, S. M. & Helin, K. Molecular mechanisms and potential functions of histone demethylases. *Nature reviews Molecular cell biology* **13**, 297–311 (2012).
42. Smith, S. M. C., Kimyon, R. S. & Watters, J. J. Cell-Type Specific Jumonji Histone Demethylase Gene Expression in the Healthy Rat CNS: Detection By A Novel Flow Cytometry Method. *ASN Neuro* (2014). doi:10.1042/AN20130050
43. Luo, X., Liu, Y., Kubicek, S., Myllyharju, J., Tumber, A., Ng, S., Che, K. H., Podoll, J., Heightman, T. D., Oppermann, U., Schreiber, S. L. & Wang, X. A selective inhibitor and probe of the cellular functions of Jumonji C domain-containing histone demethylases. *J. Am. Chem. Soc.* **133**, 9451–6 (2011).
44. Hanisch, U.-K. Linking STAT and TLR signaling in microglia: a new role for the histone demethylase Jmjd3. *Journal of Molecular Medicine* **92**, 197–200 (2014).

CHAPTER 7

DISCUSSION AND CONCLUSIONS

Stephanie M.C. Smith

INTRODUCTION

In Osler's 1892 book *The Principles and Practice of Medicine*, he reported that children with "loud and snorting" respirations coupled with prolonged pauses during sleep were often "stupid looking" and slow to respond to questions, becoming the first documented report of cognitive deficits associated with SDB¹. However, this observation went largely unnoticed and unstudied for close to a century, until a 1978 paper by Guilleminault *et al.* brought renewed attention to SDB and the associated cognitive deficits². Since then, steady research efforts have consistently reported the detrimental impact of SDB on cognitive function. However, despite this concentrated research effort that has spanned several decades, there remains very little known about the cellular mechanisms underlying SDB-associated cognitive deficits.

Intermittent hypoxia (IH), a hallmark feature of SDB, induces neuronal death and cognitive impairments in animal models, which is largely attributed to increased oxidative stress³⁻⁶ and inflammation^{7,8} in the CNS. While this is a significant advance in our understanding of IH-induced CNS injury, there is still surprisingly little known about the cellular source(s) and regulatory pathways underlying IH-induced neuroinflammation. Microglia, the only resident CNS immune cells, have been widely speculated as a primary source of inflammation following IH exposure^{3,9-11}. Indeed, microglial pro-inflammatory activities are a common feature among practically all neuropathologies¹² and they are a potential target for therapeutic intervention. However, until now, the impact of IH on microglial cells had not been directly studied.

SUMMARY OF FINDINGS

The studies detailed in this thesis primarily focused on profiling the microglial inflammatory response to IH, and investigating the molecular mechanisms regulating microglial

responses to chronic IH. We found that IH does indeed increase microglial pro-inflammatory gene expression (Chapter 4), and that these inflammatory responses are mediated in part, through toll-like receptor 4 (TLR4) activation (Chapter 5) and the Jumonji histone demethylase, JMJD3 (Chapter 6). Additionally, we show that microglial hypoxia –induced inflammatory gene expression is subject to purinergic receptor modulation by P2X4 and P2X7 (Chapter 2).

Guided by our previous work demonstrating the important regulatory role of extracellular nucleotides on microglial inflammatory activities^{13–17}, our initial studies investigated the impact of a single hypoxia/reoxygenation (HRO) event on microglial activation, and how purinergic receptor regulation of microglial-associated inflammation was altered under these conditions. Previous studies demonstrated that ATP is released into the extracellular space following hypoxia in the ventral medulla¹⁸, and high concentrations of nucleotides in the extracellular space, where concentrations are typically low, can act as ‘alarmins’ or danger signals to microglia and initiate inflammatory pathways^{19,20}. In chapter 2, we demonstrated that a single sustained hypoxic event followed by reoxygenation (HRO) was sufficient to induce microglial pro-inflammatory gene expression in the medulla, and this inflammatory response was susceptible to purinergic receptor modulation. Interestingly, intracisternal administration of BzATP, a potent P2X receptor agonist, up-regulated medullary microglial pro-inflammatory gene expression under normoxic conditions but had opposite effects during HRO. Indeed, BzATP attenuated HRO-induced microglial pro-inflammatory gene expression. Correlation analyses between pro-inflammatory gene expression and P2XR expression identified P2X4 and P2X7 potential regulators of microglial inflammatory responses to BzATP. This is consistent with previous studies that P2X4 and P2X7 work together to regulate microglial immune responses^{21,22}. Additionally, the down regulation of purinergic receptor-mediated microglial

inflammation following HRO may serve as a protective measure to prevent over-expression of pro-inflammatory molecules in a system already vulnerable due to hypoxic challenge.

In the remaining studies, we turned our attention away from the effects of a single hypoxic challenge, to focus on the mechanisms underlying microglial responses to chronic IH, a protocol designed to simulate aspects of SDB²³. In immuno-magnetically isolated microglia (CD11b+ cells) from the cortex, medulla, and spinal cord, we found that: 1) microglia increased pro-inflammatory gene expression in response to IH, 2) the profile of gene expression changed over time, and 3) the microglial inflammatory gene profiles were regionally distinct (Chapter 4)²⁴. Interestingly, microglia exhibited an acute and transient increase in pro-inflammatory gene expression at 1 and 3 days in spinal microglia, where levels were back down to baseline by 14 days of IH. Conversely, cortical and medullary microglia exhibited a slower inflammatory response to IH that remained elevated after 14 days of exposure to IH. This was the first direct demonstration that IH promoted microglial pro-inflammatory gene expression and that there was regional heterogeneity in these microglial responses.

Toll-like receptor (TLR)-4 gene expression was up-regulated by IH in rat cortical and medullary microglia in a time course that largely corresponded with increased inflammatory gene expression (Chapter 4). Similarly, in the mouse, TLR4 surface protein expression increased following 14 days of IH in frontal cortical and hippocampal microglia, and remained elevated at the 28 day time point when other markers of microglial activation including IL-1 β , CD11b, and CD45 had returned back to normoxic, baseline levels (Chapter 5). Since TLR4-mediated inflammation is known to play an important role in the progression of numerous neuropathologies²⁵, we hypothesized that TLR4 may also be involved in IH-induced microglial inflammation. We tested this hypothesis *in vitro* in Chapter 5, where IH increased pro-

inflammatory gene expression as well TLR4 expression. Additionally, this IH-induced increase in pro-inflammatory gene expression was partially blocked in microglia lacking TLR4, suggesting that TLR4 is an important signaling mechanism by which IH-induces microglial inflammation. Interestingly, the effects of TLR4 deletion only affected a sub-set of IH-induced pro-inflammatory genes; where the induction of cyclooxygenase-2 (COX2), interleukin (IL)-1 β , and IL-6 was sensitive to TLR4 deletion, the induction of tumor necrosis factor (TNF)- α , macrophage inflammatory protein (MIP)-1 α , and MIP-1 β was not. These results indicate that IH-induced inflammation is mediated through both TLR4-dependent and -independent pathways, and these pathways exert differential regulation of pro-inflammatory gene expression.

Having identified TLR4 as an important regulator of microglial inflammatory processes, we hypothesized that the IH-induced TLR4 up-regulation would translate into a “priming” effect on microglia. In other words, we predicted that microglia would have a more pronounced inflammatory response than what would normally be expected when challenged by an additional inflammatory stimulus. Consistent with this hypothesis, microglia pre-treated with IH *in vitro* had an exaggerated inflammatory response to the TLR4 agonist, lipopolysaccharide (LPS), when compared to normoxic controls. Surprisingly, when tested *in vivo*, we found the opposite effect. Microglia treated with 14 days of IH prior to intraperitoneal administration of LPS, exhibited a decreased inflammatory response to LPS when compared to normoxic controls (Chapter 5). Additionally, microglial expression of the neuroprotective cytokine IFN β and the trophic factor BDNF were increased following 14 days of IH. This increase in IFN β and BDNF following 14 days of IH may represent a protective/adaptive response that protects CNS cells from chronic IH exposure.

While developing the flow cytometry method (Chapter 3) utilized in Chapter 5, we identified the JMJD3 Jumonji H3K27 histone demethylase as being highly enriched in microglial cells when compared to neurons and astrocytes. JMJD3 is a known regulator of macrophage phenotypes²⁶⁻³⁰, findings that have recently shown to be true in microglia as well^{31,32}, and JMJD3 is necessary for LPS-induced induction of pro-inflammatory genes in macrophages^{26,30}. Additionally, JMJD3 is part of a class of enzymes that are up-regulated under periods of hypoxia, yet require molecular oxygen for catalytic activity. It is hypothesized that these enzymes are up-regulated during hypoxic to counteract the reduced catalytic activity resulting from low O₂ concentrations³³. Surprisingly, until now, no Jumonji protein has been studied in the context of IH where both hypoxic signals and abundant molecular oxygen are present, which in theory, could increase their activity due to increased protein expression while maintaining conditions for optimal catalytic activity. We found that microglial expression of JMJD3 is increased by IH *in vivo* in a time course similar to IH-induced pro-inflammatory gene expression (Chapter 6). This was the first indication that JMJD3 may be involved in microglial responses to IH. *In vitro*, IH increased the expression of JMJD3. Additionally, inhibition of JMJD3 by the selective inhibitor GSK-J4³⁰ partially blocked IH-induced pro-inflammatory gene expression. Since we previously found TLR4 to be important for IH-induced inflammation, and TLR4 activation can increase JMJD3 expression²⁷, we tested whether the IH-induced increase in JMJD3 is dependent on TLR4 activation. IH-induced JMJD3 expression was not changed in the presence of the selective TLR4 inhibitor, TAK-242^{34,35}, and conversely, IH-induced TLR4 expression was not affected by inhibition of JMJD3, suggesting that microglial induction of JMJD3 and TLR4 gene expression by IH are regulated independently. Overall, we identified

JMJD3 as a putative regulator of microglial pro-inflammatory responses to IH *in vitro*, however the molecular mechanisms by which JMJD3 regulates microglial responses are not yet known.

INTEGRATIVE MODEL FOR IH-INDUCED MICROGLIAL ACTIVATION

We utilized *in vitro* and *in vivo* models of IH to delineate the effects of IH on microglial pro-inflammatory processes, and identify key pathways regulating these responses. We found that: IH promoted microglial inflammation *in vivo* and *in vitro*, IH-induced inflammatory gene expression correlated with increased expression of TLR4 and JMJD3 *in vivo* and *in vitro*, and TLR4 and JMJD3 are necessary for full induction of the microglial inflammatory response to IH *in vitro*. By integrating our findings with those of previously published works, we have developed a schema depicting our working hypothesis for mechanisms by which IH induces microglial activation (Fig. 1). This working model is divided into two parts: an *in vitro* model and an *in vivo* model.

In vitro Model of IH-Induced Microglial Inflammation

Based on our *in vitro* findings, we have identified 3 pathways by which IH induces microglial inflammation: 1) TLR4-dependent, 2) JMJD3-dependent, and 3) TLR4/JMJD3-independent (Summarized in Figure 1). We hypothesize the TLR4- and JMJD3- independent pathway is mediated by an increase in reactive oxygen species (ROS). A single hypoxic/reoxygenation (HRO) event increases microglial production of ROS³⁶ which is sufficient to induce the production of pro-inflammatory cytokines³⁷⁻³⁹. As demonstrated in Figure 1, there are multiple sites where these pathways may converge on common signaling molecules, thus facilitating the possibility for cross-talk between these signaling pathways.

A particularly interesting and surprising finding from these studies is that microglial responses to IH *in vitro* were partially blocked in cells devoid of TLR4, suggesting that IH-

induces microglial inflammation through TLR4 in the absence of other CNS cells and exogenously added TLR4 ligand. This raises the possibility that IH-induced microglial pro-inflammatory gene expression is self-regulated through the release of endogenous TLR4 ligands acting in an autocrine/paracrine fashion to induce microglial activation (Fig. 1). Thus far, the putative endogenous TLR4 ligand(s) have not been identified, but the monocyte responsive protein (MRP)8/14 and high-mobility group box 1 (HMGB1) are two known endogenous TLR4 ligands that are likely candidates. Both MRP8/14 and HMGB1 can be released from immune cells following activation by an inflammatory stimulus and/or by cellular stressors, and they subsequently can induce/enhance pro-inflammatory responses through TLR4 activation^{40,41}. HMGB1 is known to be released from macrophages and monocytes in response to oxidative stress⁴², and MRP8/14 and HMGB1 levels are elevated in the serum of patients with obstructive sleep apnea (OSA), the most common form of SDB, suggesting that they may be released in response to IH⁴³⁻⁴⁵. We hypothesized that the TLR4- and JMJD3- independent pathway is mediated by increased ROS-production. Thus, IH-induced ROS production may facilitate endogenous TLR4 ligand release from microglia, and may be one point where these two pathways converge (Fig. 1).

Another point where the putative ROS and TLR4-dependent pathways may converge is on mitogen-activated protein kinase (MAPK) activation. TLR4 signaling and HRO both increase activation of the p38 MAPK⁴⁶⁻⁴⁸ which can activate multiple transcription factors involved in inflammatory processes including nuclear factor kappa-light-chain-enhancer of activated B cells (NF- κ B). In cultured microglia, HRO-induced p38 MAPK activation is necessary for production of pro-inflammatory gene expression⁴⁷. Consistent with this, monocytes exposed to IH in culture increased p38 MAPK and subsequent NF- κ B activity⁴⁹

Additionally, ROS is produced following TLR4 activation, and this ROS production is necessary for TLR4-mediated induction of p38 MAPK^{48,50}, further supporting the close relationship between TLR4, ROS, and p38 MAPK activation.

NF- κ B is the central regulator of pro-inflammatory gene expression. In the context of IH, NF- κ B is preferentially activated by IH over the prototypical hypoxia-responsive transcription factor, hypoxia inducible factor-1 α (HIF-1 α) in the vasculature, while HIF-1 α is preferentially increased by sustained hypoxia⁴⁹. Additionally, cultured monocytes from OSA patients exhibit increased NF- κ B activity and pro-inflammatory gene expression^{51,52}, supporting the notion that NF- κ B activity is an important regulator of inflammation in response to IH. Interestingly, JMJD3 is a direct NF- κ B target gene²⁷. While we found that the increased JMJD3 expression by IH was independent of TLR4 activation, ROS-induced MAPK induction may increase NF- κ B activity and facilitate JMJD3 expression, creating another potential site for cross-talk between these pathways.

In vivo Model of IH-Induced Microglial Inflammation

IH promoted microglial inflammation in a time course that correlated with increased expression of JMJD3 and TLR4 *in vivo*. While the direct role of TLR4 and JMJD3 in IH-induced activation is unknown, based on our *in vitro* studies, we hypothesize that they have an important role in the regulation of microglial responses to IH *in vivo* as well (Fig. 1). Microglia are master surveyors of their environment. As discussed in detail in Chapter 1, there are many potential triggers of microglial activation by IH including: peripheral inflammation, sensing cellular stress/damage in the surrounding CNS cells, and direct effects of IH on microglial physiology (Fig. 1). Peripheral inflammation can induce central inflammation through multiple pathways including direct cytokine entry into the CNS across the blood brain barrier (BBB)

through active transport mechanisms⁵³ or regions where the BBB is lacking⁵⁴, breakdown of the BBB, or through vagal nerve transmission^{55,56}. While the link between systemic inflammation and IH/OSA is well established, the impact of IH-induced systemic inflammation on microglial activation is unclear.

TLR4-mediated inflammation is implicated in the progression of numerous neuropathologies, where it is hypothesized that DAMPs (damage associated molecular patterns) are released from stressed/dying CNS cells that act on microglia through TLR4 to induce neuroinflammation⁵⁷⁻⁵⁹. Thus, we hypothesize that TLR4 signaling may be an important determinant of microglial inflammatory responses to IH, and DAMPs released from dying/stressed cells may be the trigger. To this end, the profile of cortical microglial gene expression supported this hypothesis, as IH-induced neuronal death (occurring after just 1 day of IH exposure⁶⁰) precedes induction of microglial pro-inflammatory expression profiles. Thus, DAMPs released from injured CNS cells following acute exposure to IH may promote the transition of microglia to the pro-inflammatory phenotype observed following 3 days of IH exposure (Chapter 4).

CLINICAL IMPLICATIONS

By recent estimates, the prevalence of moderate to severe sleep disordered breathing (SDB) has increased in the United States by ~45% over the past 2 decades^{61,62}. SDB is associated with significant neurological²¹ and cognitive⁶³ deficits which can only be partially reversed by continuous positive airway pressure (CPAP) treatment^{21,63}. Similarly, rodent models of intermittent hypoxia (IH), a hallmark feature of SDB, display increased hippocampal-frontal cortical neuronal death and cognitive impairments⁶⁰. The increased prevalence of SDB and

incomplete treatment options necessitates the development of new, more effective treatments for this pervasive public health problem.

When developing new therapies designed to target microglial activities, the extensive cellular and biochemical heterogeneity within the CNS must be considered, as they are likely to greatly affect microglial properties. Recent evidence demonstrates that microglia are not a homogeneous cell population and that microglial heterogeneity extends beyond regional differences^{64–68}. This is consistent with our findings that microglial responses to IH are regionally heterogeneous²⁴ (Chapter 4). Additionally, within the frontal cortex and hippocampus we found that only a subset of microglia increased expression of IL-1 β in response to IH (Chapter 5), and this population was distinct from those that basally expressed IL-6 or TNF α (data not shown). Together, these observations support the hypothesis that microglial heterogeneity is at least two-fold: constitutive heterogeneity creates sub-populations of microglia that perform different functions within a given region, and inducible heterogeneity occurs upon stimulation to alter these normal functions^{12,69}. Because of this heterogeneity, microglial responses to treatment are likely to vary regionally or even within a specific CNS region, and therefore, treatments may induce beneficial effects in one region but have deleterious effects in others. Microglial heterogeneity is complex and poorly understood. In response to IH, a multitude of factors could underlie the observed microglial heterogeneity including: constitutive heterogeneity, regional differences in the normal microenvironment, regional differences in the susceptibility of neuronal and other glial populations to IH, and proximity to vasculature. Greater appreciation for and understanding of microglial heterogeneity is essential if we are to safely manipulate these cells for therapeutic purposes.

We identified TLR4 as an important regulator of the microglial inflammatory responses to IH *in vitro* (Chapter 5). TLR4 activation is known to cause neurodegeneration and undermine many forms of neuro-plasticity^{25,58,70-74}, making it a potential target for therapeutic intervention. TLR4 levels were increased following 14 days of IH exposure, and we hypothesized that this up-regulation would potentiate microglial responses to IH. Surprisingly, microglial expression of the neuro-protective cytokine interferon (IFN)- β and the neurotrophin brain derived neurotrophic factor (BDNF) were increased following 14 days of IH. Additionally, microglial pro-inflammatory responses to systemic LPS were blunted in mice exposed to 14 days of IH, suggesting that chronic IH may shift microglial activities towards the anti-inflammatory/protective phenotype (Chapter 5). We hypothesize that IH-induced expression of IFN β and BDNF is neuroprotective, and prevents chronic long-term IH-induced neurological deficits, as BDNF has been shown to prevent and rescue IH-induced impairment of hippocampal synaptic plasticity⁷⁵. Thus, the microglial phenotype may shift with chronic IH exposure from pro-inflammatory to a more supportive phenotype (Figure 2). This is consistent with previous reports that despite early neuronal death following IH⁶⁰, chronic exposure to IH may promote neurogenesis⁷⁶.

Mechanistically, increased IFN β expression is downstream of the TRIF-dependent side of the TLR signaling pathway⁷⁷. TLR3 and TLR4 are the only two TLRs that signal through the TRIF pathway. TLR3 uses the TRIF pathway exclusively, while TLR4 can signal through the MYD88 or TRIF pathway^{77,78} (Chapter 1, Fig. 2). We hypothesize the increased IFN β expression is due to a shift in TLR4 signaling away from a MYD88 (pro-inflammatory)-dominant cascade to a more TRIF- dominant signaling cascade. However, we cannot rule out the possibility of TLR3 involvement in the induction of IFN β . More work needs to be performed

to assess the individual contribution of these receptors and their signaling pathways to the differential phenotype exhibited by microglia following chronic exposure to IH, and to understand the importance of this phenotypic switch in CNS health/injury during chronic IH exposures. Indeed, the inhibition of TLR4 has been proposed for the treatment of various neuropathologies²⁵, however this may have detrimental consequences if microglia are indeed exerting beneficial effects through TLR4 receptor activation. This is particularly important when considering microglial regional heterogeneity.

The functional significance of enhanced microglial expression of BDNF and IFN β following chronic IH exposures are currently unknown and should be the focus of future investigations. If these activities are indeed neuroprotective, increased importance should be placed on determining the mechanisms that underlie this transition, as it could lead to the development of novel therapeutics that harness and promote the innate neuroprotective/regenerative properties of microglia which could have widespread utility in the treatment of a host of neuropathologies.

While we have primarily focused on the severe/pathologic forms of IH, it is important to note that milder IH protocols exert beneficial effects on the CNS and induce forms of spinal neuro-respiratory plasticity in rodent models (reviewed in Reference 79 80). Additionally, similar IH protocols are yielding promising results in clinical trials where, chronic spinal cord injury patients exhibit enhanced functional motor recovery following IH treatment⁸¹. It is plausible that these therapeutic forms of IH promote microglial production of neurotrophic/protective molecules without inducing the inflammatory phenotype observed with severe/pathologic forms of IH. However, at this time, this is purely speculative and

investigations into microglial responses to therapeutic forms of IH are currently underway in our laboratory.

FUTURE DIRECTIONS

The studies presented in this thesis are the first to demonstrate IH-effects on microglial cells, and identify potential mechanisms mediating these responses, setting the foundation for all future studies into microglial regulation by IH. This is a completely novel avenue of research, and the potential future directions for these studies are numerous. As such, we will focus this section to three future directions that expand on our studies, and address critical gaps in our understanding of microglial responses to IH including: 1) microglial responses to IH when coupled with neurodegenerative diseases, 2) microglial responses to IH during development, and 3) the role of Jumonji proteins in the cellular responses to IH.

An underappreciated fact is that over 50% of patients with ischemic (e.g. stroke)/traumatic injury (e.g. spinal cord and traumatic brain injury), neurodegenerative diseases (e.g. Alzheimer's and Parkinson's), and genetic neural disorders (e.g. Down's syndrome and Fragile X) experience sleep disordered breathing⁸²⁻⁸⁵. Microglial-mediated inflammation is a hallmark feature of all of these conditions, and it is believed to contribute to increased neurotoxicity and progression of these pathologies^{86,87}. Conceivably, IH coupled with an already compromised and inflamed system may accelerate or exacerbate pathology in a number of seemingly unrelated neural disorders. To this end, stroke patients with preceding OSA have increased functional deficits and longer hospital stays; following the ischemic injury, untreated OSA increased morbidity/mortality rates and incidence of a subsequent ischemic event⁸⁸. Additionally, CPAP therapy improved cognitive functioning in Alzheimer's patients with OSA, suggesting that OSA exacerbates cognitive decline in Alzheimer's patients⁸⁹. We identified

TLR4 as an important molecule by which IH induces microglial inflammation *in vitro*, and similarly, TLR4-mediated inflammation has been implicated in the progression of many of these OSA-associated neuropathologies^{57,58,70}. Increased accumulation/release of known endogenous TLR4 ligands are associated with several of these pathologies including β -amyloid (Alzheimer's disease⁷³), α -synuclein (Parkinson's disease)⁹⁰, HMGB1 (Stroke)⁹¹ and MRP8/14 (Stroke)⁹². We hypothesize that IH-induced increases in microglial TLR4 expression will exacerbate microglial inflammatory responses in these conditions where endogenous TLR4 ligands are abundant, resulting in increased neurotoxicity and disease severity. Future studies should investigate the effects of IH on microglia in the context of a neuropathological condition, and investigate the impact of IH and microglial responses on the progression of these associated neuropathologies.

Approximately 2-3% of school-aged children experience SDB⁹³, resulting in learning and attention deficits that persist into adulthood^{44,93,94}. The importance of microglia in the proper development of the CNS is becoming increasingly appreciated⁹⁵⁻⁹⁹. As such, disruptions in microglial functions by IH early in life may underlie some of the long-lasting negative consequences associated with SDB in childhood. However, nothing is known about the impact of IH on microglial activities in the juvenile brain, or the potential long-term consequences of disrupting normal microglial functions during this critical development period. We hypothesize that the cognitive deficits induced by IH early in life are due, at least in part, to disruption in microglial normal behavior, and microglial responses to IH are likely different in the developing compared to the adult brain, and possibly even during different stages of development. We have previously demonstrated that the basal microglial receptor profiles change throughout development, likely reflecting the changing role of microglia throughout this process^{17,100}, thus

developmental microglial heterogeneity may influence their IH-induced responses. Finally, the mechanisms driving the constitutive inter- and intra- regional heterogeneity of microglia found within the adult brain are unknown, but it is plausible that this heterogeneity results from programmed maturation that begins early in life. Thus, early life exposure to IH may disrupt this process and cause long-lasting changes in the microglial phenotype that persist into adulthood, potentially altering how microglia respond to future insults/injuries.

A particularly exciting finding from this thesis is the important regulatory role of the Jumonji histone demethylase, JMJD3, in microglial responses to IH. JMJD3 is necessary for the induction of the macrophage and microglial pro-inflammatory responses^{26,27,29,31}, and the transition to a trophic/protective phenotype^{28,32,101}. Therefore, JMJD3 plays an important role in both the inflammatory and trophic responses of macrophages, but the mechanisms that mediate the dual-functionality of JMJD3 are poorly understood. We hypothesize that JMJD3 activity contributes to the spectrum of microglial activation by IH. JMJD3 may contribute to both the initial increase in pro-inflammatory gene expression, as well as the transition to the trophic phenotype; future research efforts should investigate this further. In addition to JMJD3, other Jumonji histone demethylase proteins may play an important role in the pathophysiology of IH. Jumonjis are a hypoxia-sensitive family of proteins that are up-regulated under hypoxic conditions, yet they require molecular oxygen for catalytic activity¹⁰². Therefore, the relationship between IH (where both hypoxic signals and molecular oxygen are abundant) and Jumonji proteins is a completely unexplored, yet potentially very biologically important avenue of study, and would be an interesting direction for future research efforts.

FIGURE 1

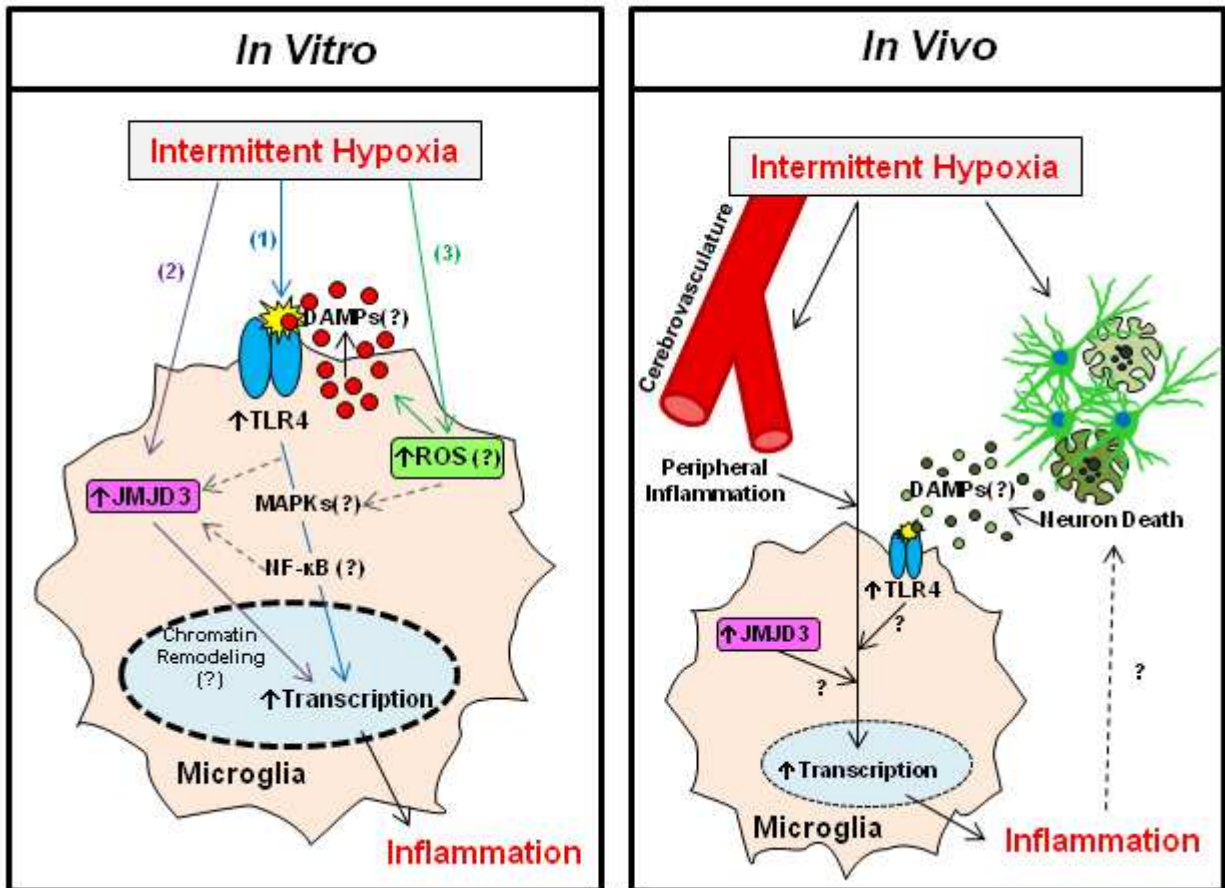


Figure Legend 1

Working models of intermittent hypoxia-induced microglial activation. *In Vitro*: we propose that IH induces microglial inflammation through 3 different but connected pathways: 1) TLR4-dependent (Blue), 2) JMJD3-dependent (Purple), and 3) TLR4/JMJD3- independent pathway (Green). Question marks denote aspects of the model that are hypothesized based on the literature, but remain to be tested with regard to IH effects in microglia. Gray dashed lines indicate potential points of cross-talk between the pathways. *In Vivo*: we propose that microglial responses to IH *in vivo* are regulated by multiple factors including: IH-induced systemic inflammation, CNS cell injury, and direct activation by IH. We hypothesize TLR4 and JMJD3 are involved in microglial response to IH *in vivo*.

FIGURE 2

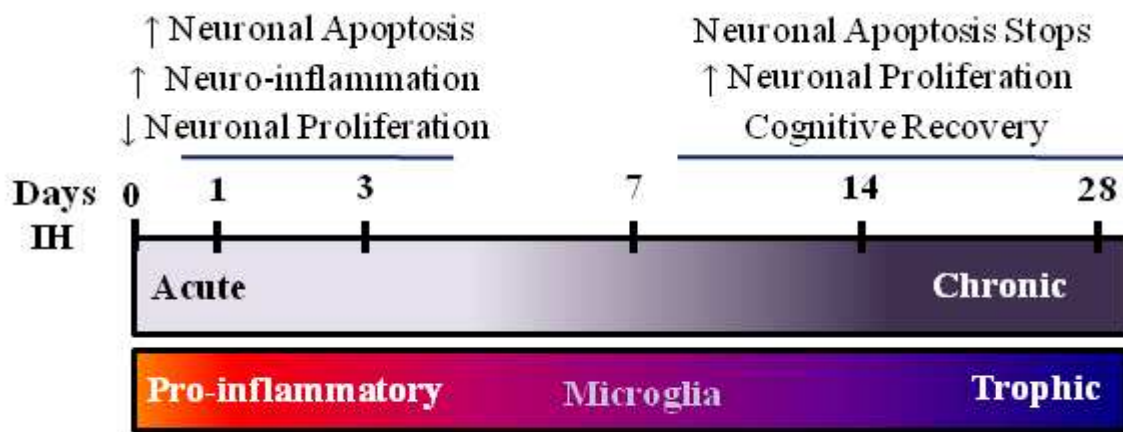


Figure Legend 2

Microglial pro-inflammatory responses to acute IH (1-4 days) may promote frontal cortical and hippocampal neuronal death and neuroinflammation observed in animal models. Chronic exposure to IH (14+ days) promotes microglial expression of trophic factors which may have neuroprotective effects and promote neuronal survival and cognitive recovery.

REFERENCES

1. Osler, W. *The principles and practice of medicine*. (D. Appleton and Company, 1893).
2. Guilleminault, C. & Dement, W. C. *Sleep apnea syndromes*. **11**, (AR Liss, 1978).
3. Burckhardt, I. C., Gozal, D., Dayyat, E., Cheng, Y., Li, R. C., Goldbart, A. D. & Row, B. W. Green tea catechin polyphenols attenuate behavioral and oxidative responses to intermittent hypoxia. *American journal of respiratory and critical care medicine* **177**, 1135 (2008).
4. Nair, D., Dayyat, E. A., Zhang, S. X., Wang, Y. & Gozal, D. Intermittent hypoxia-induced cognitive deficits are mediated by NADPH oxidase activity in a murine model of sleep apnea. *PLoS One* **6**, e19847 (2011).
5. Hui-guo, L., Kui, L., Yan-ning, Z. & Yong-jian, X. Apocynin attenuate spatial learning deficits and oxidative responses to intermittent hypoxia. *Sleep medicine* **11**, 205–212 (2010).
6. Row, B. W., Liu, R., Xu, W., Kheirandish, L. & Gozal, D. Intermittent hypoxia is associated with oxidative stress and spatial learning deficits in the rat. *American journal of respiratory and critical care medicine* **167**, 1548–1553 (2003).
7. Li, R. C., Row, B. W., Gozal, E., Kheirandish, L., Fan, Q., Brittan, K. R., Guo, S. Z., Sachleben Jr, L. R. & Gozal, D. Cyclooxygenase 2 and intermittent hypoxia-induced spatial deficits in the rat. *American journal of respiratory and critical care medicine* **168**, 469 (2003).
8. Li, R. C., Row, B. W., Kheirandish, L., Brittan, K. R., Gozal, E., Guo, S. Z., Sachleben, L. R. & Gozal, D. Nitric oxide synthase and intermittent hypoxia-induced spatial learning deficits in the rat. *Neurobiol. Dis.* **17**, 44–53 (2004).
9. Yang, Q., Wang, Y., Feng, J., Cao, J. & Chen, B. Intermittent hypoxia from obstructive sleep apnea may cause neuronal impairment and dysfunction in central nervous system: the potential roles played by microglia. *Neuropsychiatric disease and treatment* **9**, 1077 (2013).
10. Row, B. W. in *Hypoxia and the Circulation* 51–67 (Springer, 2007).
11. Zhan, G., Serrano, F., Fenik, P., Hsu, R., Kong, L., Pratico, D., Klann, E. & Veasey, S. C. NADPH oxidase mediates hypersomnolence and brain oxidative injury in a murine model of sleep apnea. *American journal of respiratory and critical care medicine* **172**, 921–929 (2005).
12. Hanisch, U. K. & Kettenmann, H. Microglia: active sensor and versatile effector cells in the normal and pathologic brain. *Nature neuroscience* **10**, 1387–1394 (2007).

13. Friedle, S., Brautigam, V., Nikodemova, M., Wright, M. & Watters, J. The P2X7-Egr pathway regulates nucleotide-dependent inflammatory gene expression in microglia. *Glia* **59**, 1–13 (2011).
14. Potucek, Y. D., Crain, J. M. & Watters, J. J. Purinergic receptors modulate MAP kinases and transcription factors that control microglial inflammatory gene expression. *Neurochemistry international* **49**, 204–214 (2006).
15. Brautigam, V. M., Frasier, C., Nikodemova, M. & Watters, J. J. Purinergic receptor modulation of BV-2 microglial cell activity: potential involvement of p38 MAP kinase and CREB. *Journal of neuroimmunology* **166**, 113–125 (2005).
16. Aga, M., Watters, J. J., Pfeiffer, Z. A., Wiepz, G. J., Sommer, J. A. & Bertics, P. J. Evidence for nucleotide receptor modulation of cross talk between MAP kinase and NF- κ B signaling pathways in murine RAW 264.7 macrophages. *American Journal of Physiology-Cell Physiology* **286**, C923–C930 (2004).
17. Crain, J. M., Nikodemova, M. & Watters, J. J. Expression of P2 nucleotide receptors varies with age and sex in murine brain microglia. *J Neuroinflammation* **6**, 24 (2009).
18. Gourine, A. V., Llaudet, E., Dale, N. & Spyer, K. M. Release of ATP in the ventral medulla during hypoxia in rats: role in hypoxic ventilatory response. *The Journal of neuroscience* **25**, 1211–1218 (2005).
19. Takeuchi, O. & Akira, S. Pattern recognition receptors and inflammation. *Cell* **140**, 805–820 (2010).
20. Jeannin, P., Jaillon, S. & Delneste, Y. Pattern recognition receptors in the immune response against dying cells. *Current opinion in immunology* **20**, 530–537 (2008).
21. Raouf, R., Chabot-Doré, A. J., Ase, A. R., Blais, D. & Séguéla, P. Differential regulation of microglial P2X4 and P2X7 ATP receptors following LPS-induced activation. *Neuropharmacology* **53**, 496–504 (2007).
22. Boumechache, M., Masin, M., Edwardson, J. M., Górecki, D. C. & Murrell-Lagnado, R. Analysis of assembly and trafficking of native P2X4 and P2X7 receptor complexes in rodent immune cells. *Journal of Biological Chemistry* **284**, 13446 (2009).
23. Tagaito, Y., Polotsky, V., Campen, M., Wilson, J., Balbir, A., Smith, P., Schwartz, A. & O'donnell, C. A model of sleep-disordered breathing in the C57BL/6J mouse. *Journal of applied physiology* **91**, 2758–2766 (2001).
24. Smith, S. M., Friedle, S. A. & Watters, J. J. Chronic Intermittent Hypoxia Exerts CNS Region-Specific Effects on Rat Microglial Inflammatory and TLR4 Gene Expression. *PloS one* **8**, e81584 (2013).

25. Buchanan, M. M., Hutchinson, M., Watkins, L. R. & Yin, H. Toll-like receptor 4 in CNS pathologies. *Journal of neurochemistry* **114**, 13–27 (2010).
26. De Santa, F., Narang, V., Yap, Z. H., Tusi, B. K., Burgold, T., Austenaa, L., Bucci, G., Caganova, M., Notarbartolo, S., Casola, S., Testa, G., Sung, W.-K., Wei, C.-L. & Natoli, G. Jmjd3 contributes to the control of gene expression in LPS-activated macrophages. *EMBO J.* **28**, 3341–52 (2009).
27. De Santa, F., Totaro, M. G., Prosperini, E., Notarbartolo, S., Testa, G. & Natoli, G. The histone H3 lysine-27 demethylase Jmjd3 links inflammation to inhibition of polycomb-mediated gene silencing. *Cell* **130**, 1083–94 (2007).
28. Satoh, T., Takeuchi, O., Vandenberg, A., Yasuda, K., Tanaka, Y., Kumagai, Y., Miyake, T., Matsushita, K., Okazaki, T., Saitoh, T., Honma, K., Matsuyama, T., Yui, K., Tsujimura, T., Standley, D. M., Nakanishi, K., Nakai, K. & Akira, S. The Jmjd3-Irf4 axis regulates M2 macrophage polarization and host responses against helminth infection. *Nat. Immunol.* **11**, 936–44 (2010).
29. Das, N. D., Jung, K. H. & Chai, Y. G. The role of NF- κ B and H3K27me3 demethylase, Jmjd3, on the anthrax lethal toxin tolerance of RAW 264.7 cells. *PloS one* **5**, e9913 (2010).
30. Kruidenier, L., Chung, C., Cheng, Z., Liddle, J., Che, K., Joberty, G., Bantscheff, M., Bountra, C., Bridges, A., Diallo, H., Eberhard, D., Hutchinson, S., Jones, E., Katso, R., Leveridge, M., Mander, P. K., Mosley, J., ... Wilson, D. M. A selective jumonji H3K27 demethylase inhibitor modulates the proinflammatory macrophage response. *Nature* **488**, 404–8 (2012).
31. Przanowski, P., Dabrowski, M., Ellert-Miklaszewska, A., Kloss, M., Mieczkowski, J., Kaza, B., Ronowicz, A., Hu, F., Piotrowski, A., Kettenmann, H., Komorowski, J. & Kaminska, B. The signal transducers Stat1 and Stat3 and their novel target Jmjd3 drive the expression of inflammatory genes in microglia. *J. Mol. Med.* **92**, 239–54 (2014).
32. Tang, Y., Li, T., Li, J., Yang, J., Liu, H., Zhang, X. & Le, W. Jmjd3 is essential for the epigenetic modulation of microglia phenotypes in the immune pathogenesis of Parkinson's disease. *Cell Death & Differentiation* (2013).
33. Klose, R. J., Kallin, E. M. & Zhang, Y. Jmjd3-domain-containing proteins and histone demethylation. *Nature Reviews Genetics* **7**, 715–727 (2006).
34. Ii, M., Matsunaga, N., Hazeki, K., Nakamura, K., Takashima, K., Seya, T., Hazeki, O., Kitazaki, T. & Iizawa, Y. A novel cyclohexene derivative, TAK-242, selectively inhibits Toll-like receptor 4-mediated cytokine production through suppression of intracellular signaling. *Molecular Pharmacology* (2005).

35. Matsunaga, N., Tsuchimori, N., Matsumoto, T. & Ii, M. TAK-242 (resatorvid), a small-molecule inhibitor of Toll-like receptor (TLR) 4 signaling, binds selectively to TLR4 and interferes with interactions between TLR4 and its adaptor molecules. *Molecular Pharmacology* **79**, 34–41 (2011).
36. Li, C. & Jackson, R. M. Reactive species mechanisms of cellular hypoxia-reoxygenation injury. *American Journal of Physiology-Cell Physiology* **282**, C227–C241 (2002).
37. Vogt, M., Bauer, M. K., Ferrari, D. & Schulze-Osthoff, K. Oxidative stress and hypoxia/reoxygenation trigger CD95 (APO-1/Fas) ligand expression in microglial cells. *FEBS letters* **429**, 67–72 (1998).
38. Spranger, M., Kiprianova, I., Krempien, S. & Schwab, S. Reoxygenation increases the release of reactive oxygen intermediates in murine microglia. *Journal of Cerebral Blood Flow & Metabolism* **18**, 670–674 (1998).
39. Hwang, K. Y., Oh, Y. T., Yoon, H., Lee, J., Kim, H., Choe, W. & Kang, I. Baicalein suppresses hypoxia-induced HIF-1 [alpha] protein accumulation and activation through inhibition of reactive oxygen species and PI 3-kinase/Akt pathway in BV2 murine microglial cells. *Neuroscience letters* **444**, 264–269 (2008).
40. Vogl, T., Tenbrock, K., Ludwig, S., Leukert, N., Ehrhardt, C., van Zoelen, M. A. D., Nacken, W., Foell, D., van der Poll, T., Sorg, C. & Roth, J. Mrp8 and Mrp14 are endogenous activators of Toll-like receptor 4, promoting lethal, endotoxin-induced shock. *Nat. Med.* **13**, 1042–9 (2007).
41. Lamkanfi, M., Sarkar, A., Walle, L. V., Vitari, A. C., Amer, A. O., Wewers, M. D., Tracey, K. J., Kanneganti, T.-D. & Dixit, V. M. Inflammasome-dependent release of the alarmin HMGB1 in endotoxemia. *The Journal of Immunology* **185**, 4385–4392 (2010).
42. Tang, D., Shi, Y., Kang, R., Li, T., Xiao, W., Wang, H. & Xiao, X. Hydrogen peroxide stimulates macrophages and monocytes to actively release HMGB1. *J. Leukoc. Biol.* **81**, 741–7 (2007).
43. Kim, J., Bhattacharjee, R., Snow, A., Capdevila, O., Kheirandish-Gozal, L. & Gozal, D. Myeloid-related protein 8/14 levels in children with obstructive sleep apnoea. *European Respiratory Journal* **35**, 843–850 (2010).
44. Cholidou, K. G., Kostakis, I. D., Manali, E. D., Perrea, D., Margeli, A., Vougas, K., Markozannes, E., Koulouris, N. & Alchanatis, M. Calprotectin: A protein related to cardiovascular risk in adult patients with obstructive sleep apnea. *Cytokine* **61**, 917–923 (2013).
45. Wu, K.-M., Lin, C.-C., Chiu, C.-H. & Liaw, S.-F. Effect of treatment by nasal continuous positive airway pressure on serum high mobility group box-1 protein in obstructive sleep

- apnea. *CHEST Journal* **137**, 303–309 (2010).
46. Suk, K. Minocycline suppresses hypoxic activation of rodent microglia in culture. *Neuroscience letters* **366**, 167–171 (2004).
 47. Park, S. Y., Lee, H., Hur, J., Kim, S. Y., Kim, H., Park, J.-H., Cha, S., Kang, S. S., Cho, G. J., Choi, W. S. & Suk, K. Hypoxia induces nitric oxide production in mouse microglia via p38 mitogen-activated protein kinase pathway. *Brain Res. Mol. Brain Res.* **107**, 9–16 (2002).
 48. Koistinaho, M. & Koistinaho, J. Role of p38 and p44/42 mitogen-activated protein kinases in microglia. *Glia* **40**, 175–183 (2002).
 49. Ryan, S., McNicholas, W. T. & Taylor, C. T. A critical role for p38 map kinase in NF- κ B signaling during intermittent hypoxia/reoxygenation. *Biochemical and biophysical research communications* **355**, 728–733 (2007).
 50. Matsuzawa, A., Saegusa, K., Noguchi, T., Sadamitsu, C., Nishitoh, H., Nagai, S., Koyasu, S., Matsumoto, K., Takeda, K. & Ichijo, H. ROS-dependent activation of the TRAF6-ASK1-p38 pathway is selectively required for TLR4-mediated innate immunity. *Nature immunology* **6**, 587–592 (2005).
 51. Greenberg, H., Ye, X., Wilson, D., Htoo, A. K., Hendersen, T. & Liu, S. F. Chronic intermittent hypoxia activates nuclear factor- κ B in cardiovascular tissues in vivo. *Biochemical and biophysical research communications* **343**, 591–596 (2006).
 52. Htoo, A. K., Greenberg, H., Tongia, S., Chen, G., Henderson, T., Wilson, D. & Liu, S. F. Activation of nuclear factor κ B in obstructive sleep apnea: a pathway leading to systemic inflammation. *Sleep and Breathing* **10**, 43–50 (2006).
 53. Wilson, C. J., Finch, C. E. & Cohen, H. J. Cytokines and cognition—the case for a head-to-toe inflammatory paradigm. *Journal of the American Geriatrics Society* **50**, 2041–2056 (2002).
 54. Konsman, J. P., Parnet, P. & Dantzer, R. Cytokine-induced sickness behaviour: mechanisms and implications. *Trends in neurosciences* **25**, 154–159 (2002).
 55. Goehler, L. E., Gaykema, R. P., Nguyen, K. T., Lee, J. E., Tilders, F. J., Maier, S. F. & Watkins, L. R. Interleukin-1 β in immune cells of the abdominal vagus nerve: a link between the immune and nervous systems? *The Journal of neuroscience* **19**, 2799–2806 (1999).
 56. Laye, S., Bluthé, R.-M., Kent, S., Combe, C., Medina, C., Parnet, P., Kelley, K. & Dantzer, R. Subdiaphragmatic vagotomy blocks induction of IL-1 beta mRNA in mice brain in response to peripheral LPS. *American Journal of Physiology-Regulatory, Integrative and*

Comparative Physiology **268**, R1327–R1331 (1995).

57. Lehnardt, S. Innate immunity and neuroinflammation in the CNS: The role of microglia in Toll-like receptor-mediated neuronal injury. *Glia* **58**, 253–263 (2010).
58. Lehnardt, S., Massillon, L., Follett, P., Jensen, F. E., Ratan, R., Rosenberg, P. A., Volpe, J. J. & Vartanian, T. Activation of innate immunity in the CNS triggers neurodegeneration through a Toll-like receptor 4-dependent pathway. *Proceedings of the National Academy of Sciences* **100**, 8514–8519 (2003).
59. Pineau, I. & Lacroix, S. Endogenous signals initiating inflammation in the injured nervous system. *Glia* **57**, 351–361 (2009).
60. Gozal, D., Daniel, J. M. & Dohanich, G. P. Behavioral and anatomical correlates of chronic episodic hypoxia during sleep in the rat. *The Journal of Neuroscience* **21**, 2442 (2001).
61. Peppard, P. E., Young, T., Barnet, J. H., Palta, M., Hagen, E. W. & Hla, K. M. Increased prevalence of sleep-disordered breathing in adults. *American journal of epidemiology* **177**, 1006–1014 (2013).
62. Young, T., Palta, M., Dempsey, J., Skatrud, J., Weber, S. & Badr, S. The occurrence of sleep-disordered breathing among middle-aged adults. *New England Journal of Medicine* **328**, 1230–1235 (1993).
63. Jackson, M. L., Howard, M. E. & Barnes, M. Cognition and daytime functioning in sleep-related breathing disorders. *Progress in brain research* **190**, 53–68 (2011).
64. de Haas, A. H., Boddeke, H. W. G. M. & Biber, K. Region-specific expression of immunoregulatory proteins on microglia in the healthy CNS. *Glia* **56**, 888–894 (2008).
65. Schmid, C. D., Sautkulis, L. N., Danielson, P. E., Cooper, J., Hasel, K. W., Hilbush, B. S., Sutcliffe, J. G. & Carson, M. J. Heterogeneous expression of the triggering receptor expressed on myeloid cells-2 on adult murine microglia. *J. Neurochem.* **83**, 1309–20 (2002).
66. Schmid, C. D., Melchior, B., Masek, K., Puntambekar, S. S., Danielson, P. E., Lo, D. D., Sutcliffe, J. G. & Carson, M. J. Differential gene expression in LPS/IFN γ activated microglia and macrophages: in vitro versus in vivo. *J. Neurochem.* **109 Suppl 1**, 117–25 (2009).
67. van Weering, H. R. J., Boddeke, H. W. G. M., Vinet, J., Brouwer, N., de Haas, A. H., van Rooijen, N., Thomsen, A. R. & Biber, K. P. H. CXCL10/CXCR3 signaling in glia cells differentially affects NMDA-induced cell death in CA and DG neurons of the mouse hippocampus. *Hippocampus* **21**, 220–32 (2011).

68. Elkabes, S., DiCicco-Bloom, E. M. & Black, I. B. Brain microglia/macrophages express neurotrophins that selectively regulate microglial proliferation and function. *The journal of neuroscience* **16**, 2508–2521 (1996).
69. Kettenmann, H., Hanisch, U.-K., Noda, M. & Verkhratsky, A. Physiology of microglia. *Physiological reviews* **91**, 461–553 (2011).
70. Okun, E., Griffioen, K. J. & Mattson, M. P. Toll-like receptor signaling in neural plasticity and disease. *Trends in neurosciences* (2011).
71. Vinit, S., Windelborn, J. A. & Mitchell, G. S. Lipopolysaccharide attenuates phrenic long-term facilitation following acute intermittent hypoxia. *Respiratory physiology & neurobiology* (2011).
72. Caso, J. R., Pradillo, J. M., Hurtado, O., Lorenzo, P., Moro, M. A. & Lizasoain, I. Toll-like receptor 4 is involved in brain damage and inflammation after experimental stroke. *Circulation* **115**, 1599–1608 (2007).
73. Walter, S., Letiembre, M., Liu, Y., Heine, H., Penke, B., Hao, W., Bode, B., Manietta, N., Walter, J., Schulz-Schuffer, W. & Fassbender, K. Role of the toll-like receptor 4 in neuroinflammation in Alzheimer's disease. *Cell. Physiol. Biochem.* **20**, 947–56 (2007).
74. Jin, J.-J., Kim, H.-D., Maxwell, J. A., Li, L. & Fukuchi, K.-I. Toll-like receptor 4-dependent upregulation of cytokines in a transgenic mouse model of Alzheimer's disease. *J Neuroinflammation* **5**, 23 (2008).
75. Xie, H., Leung, K. L., Chen, L., Chan, Y. S., Ng, P. C., Fok, T. F., Wing, Y. K., Ke, Y., Li, A. M. & Yung, W. H. Brain-derived neurotrophic factor rescues and prevents chronic intermittent hypoxia-induced impairment of hippocampal long-term synaptic plasticity. *Neurobiology of disease* **40**, 155–162 (2010).
76. Gozal, D., Row, B. W., Gozal, E., Kheirandish, L., Neville, J. J., Brittan, K. R., Sachleben, L. R. & Guo, S. Z. Temporal aspects of spatial task performance during intermittent hypoxia in the rat: evidence for neurogenesis. *European Journal of Neuroscience* **18**, 2335–2342 (2003).
77. O'Neill, L. A. J. The interleukin-1 receptor/Toll-like receptor superfamily: 10 years of progress. *Immunological reviews* **226**, 10–18 (2008).
78. Akira, S. & Takeda, K. Toll-like receptor signalling. *Nature Reviews Immunology* **4**, 499–511 (2004).
79. Fuller, D. D., Bach, K. B., Baker, T. L., Kinkead, R. & Mitchell, G. S. Long term facilitation of phrenic motor output. *Respir Physiol* **121**, 135–46 (2000).

80. Mitchell, G. S., Baker, T. L., Nanda, S. A., Fuller, D. D., Zabka, A. G., Hodgeman, B. A., Bavis, R. W., Mack, K. J. & Olson, E. Invited review: Intermittent hypoxia and respiratory plasticity. *Journal of Applied Physiology* **90**, 2466–2475 (2001).
81. Trumbower, R. D., Jayaraman, A., Mitchell, G. S. & Rymer, W. Z. Exposure to acute intermittent hypoxia augments somatic motor function in humans with incomplete spinal cord injury. *Neurorehabilitation and neural repair* **26**, 163–172 (2012).
82. Yaggi, H. K., Concato, J., Kernan, W. N., Lichtman, J. H., Brass, L. M. & Mohsenin, V. Obstructive sleep apnea as a risk factor for stroke and death. *New England Journal of Medicine* **353**, 2034–2041 (2005).
83. Go, A. S., Mozaffarian, D., Roger, V. L., Benjamin, E. J., Berry, J. D., Blaha, M. J., Dai, S., Ford, E. S., Fox, C. S., Franco, S., Fullerton, H. J., Gillespie, C., Hailpern, S. M., Heit, J. A., Howard, V. J., Huffman, M. D., Judd, S. E., ... Turner, M. B. Heart disease and stroke statistics-2014 update: a report from the American Heart Association. *Circulation* **129**, e28–e292 (2014).
84. Bliwise, D. L. Sleep disorders in Alzheimer's disease and other dementias. *Clinical Cornerstone* **6**, S16–S28 (2004).
85. Marcus, C. L., Keens, T. G., Bautista, D. B., von Pechmann, W. S. & Ward, S. L. D. Obstructive sleep apnea in children with Down syndrome. *Pediatrics* **88**, 132–139 (1991).
86. Amor, S., Puentes, F., Baker, D. & Van Der Valk, P. Inflammation in neurodegenerative diseases. *Immunology* **129**, 154–169 (2010).
87. Block, M. L., Zecca, L. & Hong, J.-S. Microglia-mediated neurotoxicity: uncovering the molecular mechanisms. *Nature Reviews Neuroscience* **8**, 57–69 (2007).
88. Morcos, Z. & Phadke, J. Re: Kaneko Y, Hajek VE, Zivanovic V et al. Relationship of sleep apnea to functional capacity and length of hospitalization following stroke. *SLEEP* 2003;26(3):293-7. *Sleep* **26**, 761; author reply 762 (2003).
89. Ancoli-Israel, S., Palmer, B. W., Cooke, J. R., Corey-Bloom, J., Fiorentino, L., Natarajan, L., Liu, L., Ayalon, L., He, F. & Loreda, J. S. Cognitive effects of treating obstructive sleep apnea in Alzheimer's disease: a randomized controlled study. *Journal of the American Geriatrics Society* **56**, 2076–2081 (2008).
90. Carty, M. & Bowie, A. G. Evaluating the role of Toll-like receptors in diseases of the central nervous system. *Biochemical pharmacology* **81**, 825–837 (2011).
91. Faraco, G., Fossati, S., Bianchi, M., Patrone, M., Pedrazzi, M., Sparatore, B., Moroni, F. & Chiarugi, A. High mobility group box 1 protein is released by neural cells upon different stresses and worsens ischemic neurodegeneration in vitro and in vivo. *Journal of*

- neurochemistry* **103**, 590–603 (2007).
92. Ziegler, G., Prinz, V., Albrecht, M. W., Harhausen, D., Khojasteh, U., Nacken, W., Endres, M., Dirnagl, U., Nietfeld, W. & Trendelenburg, G. Mrp-8 and-14 mediate CNS injury in focal cerebral ischemia. *Biochimica et Biophysica Acta (BBA)-Molecular Basis of Disease* **1792**, 1198–1204 (2009).
 93. Young, T., Peppard, P. E. & Gottlieb, D. J. Epidemiology of obstructive sleep apnea: a population health perspective. *American journal of respiratory and critical care medicine* **165**, 1217–1239 (2002).
 94. Yang, I. V. Sleep, Immunology, and Epigenetics: Tip of an Iceberg. *American journal of respiratory and critical care medicine* **185**, 243–245 (2012).
 95. Paolicelli, R. C., Bolasco, G., Pagani, F., Maggi, L., Scianni, M., Panzanelli, P., Giustetto, M., Ferreira, T. A., Guiducci, E., Dumas, L., Ragozzino, D. & Gross, C. T. Synaptic pruning by microglia is necessary for normal brain development. *Science* **333**, 1456–8 (2011).
 96. Tremblay, M. È., Stevens, B., Sierra, A., Wake, H., Bessis, A. & Nimmerjahn, A. The role of microglia in the healthy brain. *The Journal of Neuroscience* **31**, 16064–16069 (2011).
 97. Lenz, K. M., Nugent, B. M., Haliyur, R. & McCarthy, M. M. Microglia are essential to masculinization of brain and behavior. *J. Neurosci.* **33**, 2761–72 (2013).
 98. Schwarz, J. M., Sholar, P. W. & Bilbo, S. D. Sex differences in microglial colonization of the developing rat brain. *J. Neurochem.* **120**, 948–63 (2012).
 99. Schafer, D. P., Lehrman, E. K., Kautzman, A. G., Koyama, R., Mardinly, A. R., Yamasaki, R., Ransohoff, R. M., Greenberg, M. E., Barres, B. A. & Stevens, B. Microglia sculpt postnatal neural circuits in an activity and complement-dependent manner. *Neuron* **74**, 691–705 (2012).
 100. Crain, J. M., Nikodemova, M. & Watters, J. J. Microglia express distinct M1 and M2 phenotypic markers in the postnatal and adult central nervous system in male and female mice. *Journal of neuroscience research* **91**, 1143–1151 (2013).
 101. Biswas, S. K., Chittechath, M., Shalova, I. N. & Lim, J. Y. Macrophage polarization and plasticity in health and disease. *Immunologic research* 1–14 (2012).
 102. Kooistra, S. M. & Helin, K. Molecular mechanisms and potential functions of histone demethylases. *Nature reviews Molecular cell biology* **13**, 297–311 (2012).

APPENDIX 1**SYSTEMIC LPS INDUCES SPINAL INFLAMMATORY GENE EXPRESSION AND
IMPAIRS PHRENIC LONG-TERM FACILITATION FOLLOWING ACUTE
INTERMITTENT HYPOXIA**

Adrienne G. Huxtable, Stephanie M.C. Smith, Stephane Vinit, Jyoti J. Watters, and Gordon S.
Mitchell

The work from this appendix was published in the

Journal of Applied Physiology. 2013, Vol. 114, no. 7 (879-887)

Systemic LPS induces spinal inflammatory gene expression and impairs phrenic long-term
facilitation following acute intermittent hypoxia. Adrienne G. Huxtable, Stephanie M.C. Smith,
Stephane Vinit, Jyoti J. Watters, and Gordon S. Mitchell

ABSTRACT

Although systemic inflammation occurs in most pathological conditions that challenge the neural control of breathing, little is known concerning the impact of inflammation on respiratory motor plasticity. Here, we tested the hypothesis that low-grade systemic inflammation induced by lipopolysaccharide (LPS, 100 $\mu\text{g}/\text{kg}$ ip; 3 and 24 h postinjection) elicits spinal inflammatory gene expression and attenuates a form of spinal, respiratory motor plasticity: phrenic long-term facilitation (pLTF) induced by acute intermittent hypoxia (AIH; 3, 5 min hypoxic episodes, 5 min intervals). pLTF was abolished 3 h (vehicle control: $67.1 \pm 27.9\%$ baseline; LPS: $3.7 \pm 4.2\%$) and 24 h post-LPS injection (vehicle: $58.3 \pm 17.1\%$ baseline; LPS: $3.5 \pm 4.3\%$). Pretreatment with the nonsteroidal anti-inflammatory drug ketoprofen (12.5 mg/kg ip) restored pLTF 24 h post-LPS ($55.1 \pm 12.3\%$). LPS increased inflammatory gene expression in the spleen and cervical spinal cord (homogenates and isolated microglia) 3 h postinjection; however, all molecules assessed had returned to baseline by 24 h postinjection. At 3 h post-LPS, cervical spinal iNOS and COX-2 mRNA were differentially increased in microglia and homogenates, suggesting differential contributions from spinal cells. Thus LPS-induced systemic inflammation impairs AIH-induced pLTF, even after measured inflammatory genes returned to normal. Since ketoprofen restores pLTF even without detectable inflammatory gene expression, “downstream” inflammatory molecules most likely impair pLTF. These findings have important implications for many disease states where acute systemic inflammation may undermine the capacity for compensatory respiratory plasticity.

INTRODUCTION

Systemic inflammation occurs in most clinical disorders that challenge the neural control of breathing, including chronic obstructive lung disease (6, 60, 70); traumatic, ischemic, and degenerative neural disorders (e.g., spinal injury, motor neuron disease) (1, 46, 63); and sleep-disordered breathing (7, 24, 33). Although inflammation affects many neural functions (18), the impact of inflammation on the neural system controlling breathing has seldom been studied. Because of the importance of ventilatory control in many clinical disorders, it is essential to understand connections between inflammation and essential processes of ventilatory control, including rhythm generation, chemoreception, and plasticity (19, 41). In this study we focus on the impact of inflammation on an important model of respiratory plasticity, phrenic long-term facilitation following acute intermittent hypoxia (AIH).

Neuroinflammation involves complex spatial and temporal patterns of inflammatory gene expression (reviewed in 40). In the central nervous system (CNS), resident microglia are major contributors to the inflammatory response and are activated by many pathological stimuli. Upon activation, microglia change shape from stellate, ramified cells to an amoeboid shape (35) and begin to release proinflammatory and anti-inflammatory molecules (e.g., cytokines, nitric oxide, prostaglandins, and growth/trophic factors) (25). The influence of microglial inflammation on respiratory plasticity is the focus of the present study.

Systemic administration of the bacterial endotoxin lipopolysaccharide (LPS) decreases baseline ventilation and ventilatory responses to chemoreceptor stimulation in unanesthetized rats (29). These effects are reversed by pretreatment with the nonsteroidal anti-inflammatory drug ketoprofen, (29). LPS is a toll-like receptor ligand frequently used to study systemic inflammation (48). Although LPS does not cross the blood-brain barrier (49, 58), it elicits CNS

inflammation via systemic release of cytokines (which do cross the blood-brain barrier) or vagal transmission (9, 23, 36, 39, 52, 55). Systemic LPS administration impairs hippocampal synaptic plasticity, as well as learning and memory (18). Similarly, systemic LPS impairs an important model of spinal respiratory plasticity: AIH-induced phrenic long-term facilitation (pLTF) (29, 67). In the earlier study of Vinit et al. (67), 1) spinal inflammation was not confirmed, 2) only high LPS doses (3 mg/kg) and a short time interval (3 h) were studied, and 3) causality between LPS-induced inflammation and pLTF impairment was not investigated. Here, we extend the results of Vinit et al. (67) by testing the hypotheses that 1) low LPS doses impair pLTF at longer intervals postadministration (24 h), 2) systemic LPS increases inflammatory gene expression in isolated microglia and homogenates from the cervical spinal cord (a critical region for pLTF), and 3) the nonsteroidal anti-inflammatory drug ketoprofen restores pLTF following LPS administration. Our results support the hypothesis that systemic inflammation impairs spinal respiratory plasticity and demonstrate that systemic inflammation associated with many clinical disorders is of considerable relevance to the central neural control of breathing.

METHODS

All experiments were approved by the Animal Care and Use Committee in the School of Veterinary Medicine, University of Wisconsin, and conformed to policies laid out by the National Institutes of Health in the *Guide for the Care and Use of Laboratory Animals*. Experiments were performed on 3- to 4-mo-old Harlan male Sprague-Dawley rats (colony 218a). Rats were housed under standard conditions, with a 12:12-h light/dark cycle with food and water ad libitum.

Drugs and Materials

LPS (*E. coli* 0111:B4), (S)-(+)-ketoprofen, and Tri Reagent were purchased from Sigma Chemical (St. Louis, MO). M-MLV Reverse Transcriptase was purchased from Invitrogen (Carlsbad, CA). Oligo(dT), Random hexamer, and RNAsin were purchased from Promega (Madison, WI). SYBR Green PCR Master Mix was purchased from Applied Biosystems (Carlsbad, CA).

Experimental Groups

To investigate the effects of systemic inflammation, rats received an intraperitoneal (ip) injection of LPS (100 µg/kg) or vehicle (saline) 3 or 24 h prior to beginning an experiment. Rats were either used for electrophysiological experiments to study AIH-induced pLTF or for measurements of inflammatory gene expression. In the latter groups, intra-aortic saline perfusions were used to remove circulating myeloid cells before cervical spinal tissues were harvested. Prior to perfusions, the spleen was harvested for analysis.

In 24 h LPS or 24 h vehicle rats, the nonsteroidal anti-inflammatory drug ketoprofen (12.5 mg/kg ip) or vehicle (50% ethanol in saline) was injected 3 h prior to a pLTF experiment. Ketoprofen is a potent inhibitor of inflammatory activities since it directly inhibits cyclooxygenase (31, 65, 68)

and the transcription factor nuclear factor kappa B (NF- κ B) (65), a key regulator of multiple inflammatory genes (42, 51).

In specific, rats used for electrophysiology experiments after 3 h of LPS fell into one of three groups: 1) time control (includes both vehicle and LPS injected), 2) vehicle + AIH, or 3) LPS (3 h) + AIH. A separate set of rats was used to examine the effects of 24 h of LPS and fell into one of five groups: 1) time control (includes vehicle, LPS, ketoprofen, or LPS + ketoprofen injected); 2) LPS (24 h), ketoprofen + AIH; 3) LPS (24 h), vehicle + AIH; 4) vehicle (24 h), ketoprofen + AIH; and 5) vehicle + AIH.

For gene expression, rats were in comparable groups as those above for the electrophysiology. Rats were in either LPS (3 h), vehicle (3 h), LPS (24 h) + ketoprofen, LPS (24 h) + vehicle, vehicle (24 h) + ketoprofen, or vehicle groups. The rats used for gene expression analysis were not given AIH, neglecting the need for a time control group.

Electrophysiological Experiments

The protocol used in electrophysiological experiments has been described in detail previously (2, 5). In brief, rats were anesthetized with isoflurane, tracheotomized, and pump ventilated (Small Animal Ventilator 683, Harvard Apparatus, Holliston, MA). Rats were maintained with isoflurane for the remainder of the surgical preparation; after surgical preparations were complete, the rats were slowly converted to urethane anesthesia (1.8 g/kg iv, Sigma-Aldrich). During the 1-h stabilization period after conversion to urethane, pancuronium bromide (1 mg iv), was given to paralyze the rats. The rats were tracheotomized and ventilated. Anesthetic level was assessed throughout experiments by monitoring blood pressure and phrenic nerve responses to toe pinch. Approximately 1 h after beginning surgical procedures, an intravenous infusion of 1.5–2 ml/h began with a solution consisting of Hetastarch (0.3%) and

sodium bicarbonate (0.84%) in lactated Ringer's. The infusion rate was adjusted to maintain blood volume, pressure, and acid-base balance.

Surgical preparation.

Both vagi were isolated and cut, and a catheter was inserted into the right femoral artery to enable blood pressure measurements and arterial blood samples. Blood samples were analyzed for PO₂, PCO₂, pH, and base excess using a blood gas analyzer (ABL 800, Radiometer, Copenhagen, Denmark). Blood samples (62.5 µl in heparinized plastic catheter) were drawn before (baseline), during the first hypoxic episode, and 15, 30 and 60 min post-AIH. A rectal temperature probe was used to monitor and regulate body temperature throughout an experiment. The left phrenic nerve was isolated with a dorsal approach, cut caudally, desheathed, and placed on a bipolar silver recording electrode submerged in mineral oil. Nerve activity was amplified (gain X10K), bandpass filtered (300 Hz to 20 kHz) (A-M Systems, Carlsberg, WA), and integrated (absolute value, Powerlabs 830, AD Instruments, Colorado Springs, CO, time constant 100 ms). The signal was digitized, recorded, and analyzed using Powerlabs 830 (version 7.2.2, AD Instruments).

Protocol.

Baseline nerve activity was established with FIO₂ ~0.56 (PaO₂ > 300 mmHg) and CO₂ added to the inspired gas (balance nitrogen). The CO₂ apneic threshold was determined by progressively lowering inspired CO₂ until phrenic nerve activity ceased. Inspired CO₂ was slowly increased until phrenic nerve activity resumed (recruitment threshold). End-tidal CO₂ was then set 3 mmHg above the recruitment threshold to establish baseline nerve activity. End-tidal CO₂ was monitored and maintained throughout an experiment using a flow-through capnograph (Respironics, Andover, MA).

Once phrenic nerve activity was stable, an arterial blood sample was taken to establish baseline conditions; these conditions were maintained throughout the experiment. After baseline conditions, an AIH protocol began consisting of three hypoxic episodes (5 min duration, 10.5% O₂), separated by 5 min of normoxia. Blood samples were taken during the first hypoxic episode and 15, 30, and 60 min post-AIH. Data were included in analysis only if they complied with the following criteria: 1) PaO₂ during baseline and post-AIH was >180 mmHg; 2) PaO₂ during hypoxic episodes was between 35 and 45 mmHg; 3) PaCO₂ remained within 1.5 mmHg of baseline throughout the post-AIH period. Phrenic nerve amplitude and frequency were evaluated for 1 min before each blood sample. Upon completion of the experiment, rats were euthanized with an overdose of urethane.

Inflammatory Gene Expression

Sample preparation.

Tissue from cervical spinal cords was homogenized and used for quantitative PCR analysis (hereafter referred to as “homogenates”). Cervical spinal tissue was also used to isolate microglia by using antibodies for the microglial marker CD11b⁺ conjugated to magnetic beads, as previously reported (15). To isolate microglia, these labeled cells were passed through MS columns according to a modified Miltenyi MACS protocol (43). The average purity of cells with microglia-like characteristics was >95% as determined by flow cytometry FSC/SSC scatter analysis and CD11b⁺/CD45^{low} staining (43). These results are consistent with previous findings (15, 56). From here on, CD11b⁺ cells isolated with this method are referred to as “microglia.”

Reverse transcription.

Total RNA was isolated from cervical spinal cord microglia or homogenates using the TRI-reagent according to the manufacturer's instructions. First-strand cDNA was synthesized

from 1 μ g of total RNA using M-MLV Reverse Transcriptase and an oligo(dT)/random hexamer cocktail. The cDNA was then used for quantitative RT-PCR using SYBR Green PCR Master Mix.

Quantitative PCR.

Amplified cDNA was measured by fluorescence in real time using the StepOnePlus Real-Time PCR System (Applied Biosystems). The following primer sequences were used for quantitative PCR: iNOS, 5'-AGG GAG TGT TGT TCC AGG TG and 5'-TCT GCA GGA TGT CTT GAA CG; COX-2, 5'-TGT TCC AAC CCA TGT CAA AA and 5'-CGT AGA ATC CAG TCC GGG TA; IL-1 β , 5'-CTG CAG ATG CAA TGG AAA GA and 5'-TTG CTT CCA AGG CAG ACT TT; TNF- α , 5'-TCC ATG GCC CAG ACC CTC ACA C and 5'-TCC GCT TGG TGG TTT GCT ACG; IL-6, 5'-GTG GCT AAG GAC CAA GAC CA and 5'-GGT TTG CCG AGT AGA CCT CA; and 18s, 5'-CGG GTG CTC TTA GCT GAG TGT CCC G and 5'-CTC GGG CCT GCT TTG AAC AC.

All primers were designed to span introns whenever possible. Primer specificity was assessed through NCBI BLAST analysis prior to use, and all dissociation curves had a single peak with an observed melting temperature consistent with the intended amplicon sequences. Primer efficiency was calculated through the use of serial dilutions and construction of a standard curve.

Data Analysis

Electrophysiology

Peak amplitude and frequency (bursts/min) of integrated phrenic nerve activity were averaged for 30 bursts at each recorded point. Changes in phrenic nerve burst amplitude were normalized to baseline values (i.e., percent change from baseline), and burst frequency was

reported as a change from baseline frequency (bursts/min). In this study, physiological variables and phrenic amplitude are reported for baseline, during the short-term hypoxic response, and the 60 min time point only.

Statistical comparisons for the hypoxic responses were made from data at *minute 2* of the 5 min during the first hypoxic episode using a *t*-test (3 h LPS data) or one-way ANOVAs on ranks (24 h LPS data). Owing to the addition of two ketoprofen groups, an ANOVA on ranks was used for the 24 LPS hypoxic data to permit appropriate statistical comparisons.

Nonparametric analyses were used when data failed normality or equal variance.

Statistical comparisons for changes in phrenic burst amplitude after AIH were made using a repeated-measures two-way ANOVA with Tukey post hoc test to identify individual differences (Sigma Stat version 11, Systat Software, San Jose, CA). Differences were considered significant if $P < 0.05$. All values are expressed as means \pm SE.

Gene expression.

Gene expression data were analyzed based on a relative standard curve method, as specified by Applied Biosystems. In brief, all samples were run in duplicate, averaged, and interpolated onto previously run standard curves for each primer set to account for differences in primer efficiency. Values were then normalized to 18S for each sample and expressed relative to vehicle controls for each gene, reflecting the fold change for each gene. If the normalized gene expression data for an individual sample is greater than 2 standard deviations from the mean, the sample was excluded as an outlier. Statistical analysis for TNF α and IL-1 β were run on the fold change data. Statistical analysis on iNOS, COX-2, and IL-6 failed equal variance and/or normality tests; therefore data were transformed logarithmically before statistical analysis, but data are still reported as fold changes (see Fig. 4). Statistical significance was determined for

each inflammatory gene examined in the spleen by a one-way ANOVA with Tukey post hoc test for individual comparisons. For cervical spinal data, statistical significance was determined using a two-way ANOVA with Tukey post hoc test (Sigma Stat version 11, Systat Software, San Jose, CA). Differences were considered significant if $P < 0.05$. All values are expressed as means \pm SE.

RESULTS

Impaired pLTF 3 h post-LPS.

Acute LPS (3 h; 100 $\mu\text{g}/\text{kg}$ ip) had only minor effects on physiological variables measured (Table 1). Rats treated with LPS had no significant differences in temperature, PaCO_2 , or pH within or between groups. However, LPS rats had significantly lower PaO_2 and mean arterial pressure (MAP) after AIH vs. time controls but were not different from their respective baseline values. LPS-treated rats were not significantly different from vehicle-treated rats in any variable examined. In LPS- and vehicle-treated rats subjected to AIH, PaO_2 significantly decreased during hypoxic episodes, with a concurrent decrease in MAP; no similar changes were noted in time control rats without AIH.

LPS did not reduce phrenic nerve burst amplitude during hypoxia, nor did it change frequency at any time during experiments. The short-term hypoxic phrenic response (the immediate increase in phrenic nerve amplitude in response to decreased oxygen) was not significantly affected by LPS (vehicle: $147 \pm 46\%$ baseline; LPS-treated: $83 \pm 15\%$; $P = 0.261$; t -test, Fig. 1B). Baseline phrenic burst frequency was 39 ± 2 bursts/min in the vehicle group, 43 ± 3 bursts/min in the LPS group, and 43 ± 2 bursts/min in the time control group. Similarly, there were no significant changes in frequency responses during hypoxia (vehicle: 10.0 ± 2.0 burst/min; LPS: 12.8 ± 2.8 bursts/min; $P = 0.453$; t -test) or following AIH (vehicle: 1.0 ± 2.0 bursts/min at 60 min post-AIH, LPS: 5.5 ± 2.4 bursts/min; time control: -1.9 ± 1.6 bursts/min; data not shown).

Acute LPS significantly diminished pLTF magnitude vs. vehicle controls (vehicle: $67.1 \pm 27.9\%$ baseline, $n = 5$; LPS: $3.7 \pm 4.2\%$ baseline, $n = 5$; Fig. 1C; $P < 0.001$; repeated-measures two-way ANOVA, Tukey post hoc test). There was no significant difference between LPS-

treated and time control rats ($5.1 \pm 4.3\%$, $n = 5$). Thus this low LPS dose (100 $\mu\text{g}/\text{kg}$) abolishes pLTF shortly after administration (3 h), similar to previous findings with a higher LPS dose (3 mg/kg) (67). Neither this dose (3 mg/kg) nor that of Vinit et al. (67) caused overt sickness behaviors in rats (increased temperature, lethargy). Higher LPS doses are used to simulate sepsis, and overt sickness behaviors can be observed (37, 45).

pLTF remains impaired 24 h post-LPS.

Because inflammation initiates complex signaling cascades that can persist well beyond 3 h, we examined pLTF 24 h post-LPS injection. Since no significant differences were found in pLTF among the various time control groups (vehicle, LPS, ketoprofen, or LPS + ketoprofen), we combined these groups for further analysis. Further, rats treated with LPS + ketoprofen vehicle were combined with the LPS alone group since ketoprofen vehicle had no significant effects and are referred to as 24 h LPS.

Similar to 3 h post-LPS, only minor differences were observed in physiological variables 24 h post-LPS (Table 2). There were no significant differences within or between groups for temperature, PaCO₂, or pH. LPS-injected rats had higher MAP levels vs. vehicle-injected rats at baseline, during hypoxia, and after AIH, although neither group differed significantly from time control rats at baseline or post-AIH. LPS-treated rats also had higher MAP compared with rats treated with ketoprofen (without LPS) post-AIH. All treatment groups showed a significant drop in PaO₂ and MAP during hypoxia, as expected.

The short-term hypoxic phrenic response was not significantly altered 24 h post-LPS (Fig. 2, A and B). There were no significant differences in phrenic nerve burst amplitude during hypoxia in the vehicle group ($104 \pm 19\%$), ketoprofen ($71 \pm 3\%$), 24 h LPS ($66 \pm 8\%$), or 24 h LPS + ketoprofen ($97 \pm 9\%$) ($P > 0.05$, one-way ANOVA on ranks). Baseline phrenic burst

frequency was 44 ± 2 bursts/min for time controls, 42 ± 1 bursts/min for 24 h vehicle, 43 ± 2 bursts/min for ketoprofen, 47 ± 2 bursts/min for 24 h LPS, 46 ± 2 bursts/min for 24 h LPS + ketoprofen, and 46 ± 1 bursts/min for 24 h LPS + ketoprofen vehicle. There was a modest effect on phrenic burst frequency at 60 min post-AIH 24 h post-LPS (data not shown). The change in phrenic burst frequency post-AIH in vehicle-treated rats was 5.9 ± 2.3 bursts/min ($n = 5$), whereas the 24 h LPS group was -1.8 ± 1.6 bursts/min ($n = 9$) and time controls were -0.9 ± 1.2 bursts/min ($n = 15$). The change in the vehicle group was significantly different vs. LPS ($P = 0.005$) and time control ($P = 0.010$) groups but not vs. ketoprofen (2.6 ± 2.1 bursts/min, $n = 5$, $P = 0.687$) or 24 h LPS + ketoprofen (0.4 ± 1.4 bursts/min, $n = 6$, $P = 0.149$) groups (repeated-measures two-way ANOVA, Tukey post hoc test).

Impaired pLTF persisted 24 h post-LPS, and this effect was reversed by pretreatment with ketoprofen (Fig. 2C). In vehicle-injected rats ($58.3 \pm 17.1\%$; $n = 5$) and in rats treated with ketoprofen ($48.1 \pm 19.0\%$, $n = 5$), AIH elicited similar pLTF ($P = 0.948$, repeated-measures two-way ANOVA, Tukey post hoc test). pLTF was significantly reduced 24 h post-LPS ($3.5 \pm 4.3\%$, $n = 9$, $P < 0.001$ vs. vehicle, $P = 0.004$ vs. ketoprofen) and this effect was reversed by ketoprofen ($55.1 \pm 12.3\%$, $n = 6$; $P = 0.999$ vs. vehicle; $P = 0.985$ vs. ketoprofen; $P < 0.001$ vs. LPS) (repeated-measures two-way ANOVA, Tukey post hoc test).

Peripheral inflammatory gene expression.

Since LPS does not cross the blood-brain barrier, peripheral LPS-induced inflammation indirectly triggers CNS inflammatory responses (9, 23, 36, 39, 53,55). Thus we assessed splenic inflammatory gene expression as a marker for systemic inflammation; the same genes were assessed in the cervical spinal cord 3 and 24 h post-LPS. Ketoprofen effects on LPS-induced changes were evaluated only at 24 h post-LPS.

A transient increase in all inflammatory genes examined was evident in the spleen (Fig. 3). Three hours post-LPS ($n = 3$), TNF α (7.5 ± 0.2 fold, $P < 0.001$), iNOS (72.6 ± 12.3 fold, $P < 0.001$), COX-2 (4.4 ± 0.2 fold, $P = 0.013$), IL-1 β (4.6 ± 0.1 fold, $P < 0.001$), and IL-6 (19.2 ± 3.5 fold, $P < 0.001$) expressions all significantly increased vs. respective vehicle controls. However, by 24 h post-LPS, mRNA levels for all splenic genes had returned toward baseline values (TNF α : 1.0 ± 0.1 fold, $P = 0.995$; iNOS: 3.4 ± 1.6 fold, $P = 0.083$; COX-2: 1.1 ± 0.1 fold, $P = 0.844$; IL-1 β : 1.6 ± 0.4 fold, $P = 0.943$; IL-6: 2.2 ± 0.8 fold, $P = 0.640$). Gene expression 24 h post-LPS was not significantly altered by ketoprofen (TNF α 1.2 ± 0.01 fold, $P = 0.829$; iNOS 1.8 ± 0.6 fold, $P = 0.233$; COX-2 0.8 ± 0.1 fold, $P = 0.981$; IL-1 β 1.1 ± 0.1 fold, $P = 0.939$; IL-6 1.1 ± 0.02 fold, $P = 0.956$), despite the ability of ketoprofen to restore pLTF.

Cervical spinal gene expression (3 h).

Inflammatory genes were examined in cervical spinal microglia and homogenates post-LPS (Fig. 4). Only two inflammatory genes exhibited significant increases within microglia or homogenates after LPS: iNOS (microglia 16.7 ± 4.4 , $P < 0.001$, $n = 8$; homogenate 8.9 ± 1.9 , $P < 0.001$, $n = 8$) and COX-2 (microglia 2.8 ± 0.6 , $P = 0.019$, $n = 7$; homogenate 5.1 ± 1.2 , $P < 0.001$, $n = 8$) vs. vehicle controls (iNOS: microglia $n = 15$, homogenate $n = 14$; COX-2: microglia $n = 15$, homogenate $n = 15$). There were no significant differences in gene expression between sample type (microglia vs. homogenate) for iNOS or COX-2 (iNOS $P = 0.172$, COX-2 $P = 0.087$). There were no differences in either sample type vs. vehicle controls after LPS ($n = 14$) for IL-1 β (microglia 0.7 ± 0.1 fold, $P = 0.562$, $n = 8$; homogenate 0.8 ± 0.3 fold, $P = 0.884$, $n = 7$) or TNF α (microglia 0.9 ± 0.2 , $P > 0.05$, $n = 7$; homogenates 1.7 ± 0.3 , $P > 0.05$, $n = 7$).

Cervical spinal gene expression (24 h).

LPS (24 h) had no significant effects on iNOS (microglia: 2.4 ± 0.8 $P = 0.368$, $n = 7$; homogenates 1.5 ± 0.3 $P = 0.557$, $n = 6$), COX-2 (microglia: 1.0 ± 0.3 , $P = 0.978$, $n = 7$; homogenates: 2.1 ± 0.8 , $P = 0.473$, $n = 6$), IL-1 β (microglia: 0.6 ± 0.2 , $P = 0.464$, $n = 7$; homogenates: 0.5 ± 0.2 , $P = 0.390$, $n = 5$), or TNF α (microglia: 1.6 ± 0.4 , $P > 0.05$, $n = 7$; homogenates 1.7 ± 0.5 , $P > 0.05$, $n = 6$) in either sample type vs. vehicle controls (Fig. 4). However, mRNA for iNOS (microglia $P < 0.001$, homogenates $P < 0.001$; Fig. 4A) and COX-2 (microglia $P = 0.024$, homogenates $P = 0.013$; Fig. 4B) was significantly reduced vs. 3 h LPS within each sample type, suggesting that inflammatory gene expression was returning to baseline values.

Ketoprofen did not significantly alter gene expression in 24 h post-LPS rats ($P > 0.05$) in either sample type for any gene examined (Fig. 4). Nor did ketoprofen alter gene expression vs. vehicle controls for iNOS (microglia: 2.1 ± 0.6 , $P = 0.257$, $n = 8$; homogenates: 0.8 ± 0.1 , $P = 0.964$, $n = 7$), COX-2 (microglia: 0.9 ± 0.1 , $P = 0.892$, $n = 8$; homogenates: 2.2 ± 0.5 , $P = 0.066$, $n = 7$), IL-1 β (microglia: 0.5 ± 0.1 , $P = 0.302$, $n = 8$; homogenates: 0.4 ± 0.1 , $P = 0.172$, $n = 5$), or TNF α (microglia: 1.9 ± 0.8 , $P > 0.05$, $n = 8$; homogenates: 2.2 ± 1.1 , $P > 0.05$, $n = 7$).

Ketoprofen pretreatment did, however, highlight differences between sample types (microglia vs. homogenate) (Fig. 4). Microglia had greater iNOS gene expression vs. homogenates ($P = 0.037$), whereas microglia had less COX-2 mRNA vs. homogenates ($P = 0.011$). Thus microglia may not be the sole contributors to inflammatory molecules in some conditions.

DISCUSSION

Here, we demonstrate that systemic administration of a low dose of LPS impairs AIH-induced pLTF as early as 3 h post LPS injection, an effect that lasts for at least 24 h. However, pLTF impairment is accompanied by only transient (3 h) increases in inflammatory gene expression in the cervical spinal cord. Despite a lack of detectable inflammatory gene expression 24 h post-LPS, systemic administration of the nonsteroidal anti-inflammatory drug ketoprofen (at 21 h) reverses pLTF impairment. We do not yet know the basis for persistent impairment of pLTF without increases in measured inflammatory molecules. Several possibilities are discussed below.

LPS as a model of inflammation.

At low doses, LPS activates TLR4/2 receptors, triggering levels of inflammation frequently experienced by humans (62). Since many clinical disorders are associated with low-grade systemic inflammation, low LPS doses may better represent low-grade infections or inflammation and their impact on respiratory plasticity.

In the literature, LPS has been used at a variety of dosages and time points to stimulate systemic inflammation. LPS doses vary from nanograms to milligrams per kilogram (26, 28). LPS effects include behaviors indicative of illness (10, 14,22), microglial activation, impaired memory, and motor function (32, 57, 61, 64,66), and changes in neurotrophic factor expression (55). The concentration used here is in the low range reported for rats (16) and elicits reliable systemic and CNS inflammation in mice (62, 72). Higher LPS doses (500 $\mu\text{g}/\text{kg}$ or more) typically cause severe systemic inflammation, septic shock, and fever (34, 59, 71), none of which were observed in this study.

Although LPS is often administered systemically to induce CNS inflammation, it does not cross the blood-brain barrier (49, 58). CNS inflammation arises from indirect effects, such as circulating or vascular endothelial cytokines (or other inflammatory molecules) that do cross the blood-brain barrier (49, 58) or neural transmission to the CNS via the vagus nerves (8, 21, 54, 69). Potential molecules crossing the blood-brain barrier to trigger CNS inflammatory activities include the cytokines we assessed in the spleen (e.g., IL-1 β and TNF- α) or prostaglandins produced by perivascular macrophages and/or endothelial cells that line the blood-brain barrier (9, 23, 36, 39, 53, 55). However, the precise mechanism(s) of CNS inflammation following LPS injection was not a focus of this study.

We confirmed both systemic and CNS inflammation by examining mRNA levels of selected proinflammatory molecules (iNOS, COX-2, TNF α , and IL-1 β). In general, mRNA changes were similar in the spleen and cervical spinal cord. Spleen inflammatory gene expression was greatest 3 h post-LPS (up to 150-fold increase) but had largely returned to baseline expression levels by 24 h post-LPS. We assessed CNS inflammation in cervical spinal segments associated with the phrenic motor nucleus, since cellular mechanisms of pLTF are localized in this region (3, 5, 27, 38). Cervical spinal inflammation was evident in both isolated microglia and homogenates.

Although microglia comprise only a small component of the CNS by volume, they are the predominant immune cells in the CNS (25). To assess microglial LPS responses in the cervical spinal cord, we compared mRNA in spinal homogenates and isolated microglia. Overall, similar trends to the spleen were observed, where iNOS and COX-2 mRNA increased 3- to 15-fold in microglia and homogenates 3 h post-LPS. Although mRNA levels returned nearly to baseline by 24 h post-LPS, we do not have information concerning protein levels for any of the

molecules assessed. Collectively, our data suggest that microglia are major contributors to overall changes in inflammatory gene expression in the cervical spinal cord after LPS; however, we cannot rule out important contributions from other cells types, such as astrocytes or neurons.

The time course for increased inflammatory gene expression was shorter than pLTF impairment. Potential explanations include long-lasting changes in the expression of unmeasured molecules that undermine pLTF. Candidate molecules include unmeasured cytokines, interleukins, interferons, chemokines, or other enzymes that initiate distinct signaling cascades. Another possibility is that protein levels of a key molecule outlast mRNA changes (e.g., iNOS or COX-2). A third possibility is that small, persistent elevations in measured molecules were critical in the mechanism undermining pLTF, although not statistically detectable. For example, a critical molecule may need to change very little to undermine pLTF or, more likely, multiple small but undetectable increases (1–2 fold) may act in a cumulative manner, activating a common downstream target molecule that more directly impairs pLTF. All of these possibilities are consistent with ketoprofen restoration of pLTF.

Unlike our previous study using a high LPS dose (67), we observed no change in short-term hypoxic ventilatory response after the low LPS dose used here (either 3 or 24 h post-LPS). Since the magnitude of pLTF correlates with the magnitude of the hypoxic phrenic response in rats (4, 20), there was some concern that the depressed hypoxic phrenic response indirectly impaired pLTF in Vinit et al. (67). Since the hypoxic phrenic response was not affected here, yet pLTF was nevertheless abolished, potential indirect effects are ruled out. Collectively, the data presented here are consistent with the conclusion that a low-grade systemic inflammation suppresses pLTF in rats.

Ketoprofen is a general anti-inflammatory drug used here to confirm that LPS undermines pLTF by inducing inflammation. *S*-enantiomers of ketoprofen inhibit COX-1 and COX-2 at low doses and NFκB at higher doses (13, 73). Ketoprofen inhibits both cyclooxygenase and lipoxygenase pathways for arachidonic acid metabolism, thereby inhibiting synthesis of prostaglandins and leukotrienes (11). Ketoprofen has been given at doses ranging from 100 μg/kg to 50 mg/kg via multiple routes of administration (11, 12, 44, 47). The ketoprofen dose used here was moderately high, making it unclear if its effects were on COX-2 or NFκB. Ketoprofen did not reduce expression of any inflammatory molecules examined; however, we cannot rule out effects of ketoprofen on proteins or other inflammatory molecules not examined. Regardless, our results suggest that a long-lasting, ketoprofen-sensitive molecule significantly impacts AIH-induced pLTF.

The rapid effects of ketoprofen (3 h) in restoring pLTF may implicate COX-2 and prostaglandin synthesis in the impairment of pLTF. These rapid effects are more easily explained by inhibition of COX-2 enzymatic activity (vs. inhibition of NF-κB regulated gene expression). Other studies demonstrate that CNS effects of low-grade systemic inflammation can be dependent on prostaglandins and COX activity (62). Additional studies are necessary to test this idea.

In conclusion, we are only beginning to understand the profound impact of inflammation on respiratory plasticity. The present study highlights the impact of even low-grade systemic inflammation on an important model of respiratory plasticity, AIH-induced pLTF. Further, we provide evidence that microglia, and perhaps other CNS cells, may generate the (as yet unknown) inflammatory molecules that undermine pLTF.

GRANTS

This study was supported by National Institutes of Health Grants HL-80209, HL-69064, HL-111598, T32-HL-007654 (S. M. Smith), and NS-049033 (J. J. Watters), and the Craig H. Neilsen foundation (S. Vinit).

AUTHOR CONTRIBUTIONS

Author contributions: A.G.H., S.M.S., J.J.W., and G.S.M. conception and design of research; A.G.H., S.M.S., and S.V. performed experiments; A.G.H., S.M.S., and S.V. analyzed data; A.G.H., S.M.S., J.J.W., and G.S.M. interpreted results of experiments; A.G.H. and S.M.S. prepared figures; A.G.H. drafted manuscript; A.G.H., S.M.S., S.V., J.J.W., and G.S.M. edited and revised manuscript; A.G.H., S.M.S., J.J.W., and G.S.M. approved final version of manuscript.

FIGURE 1

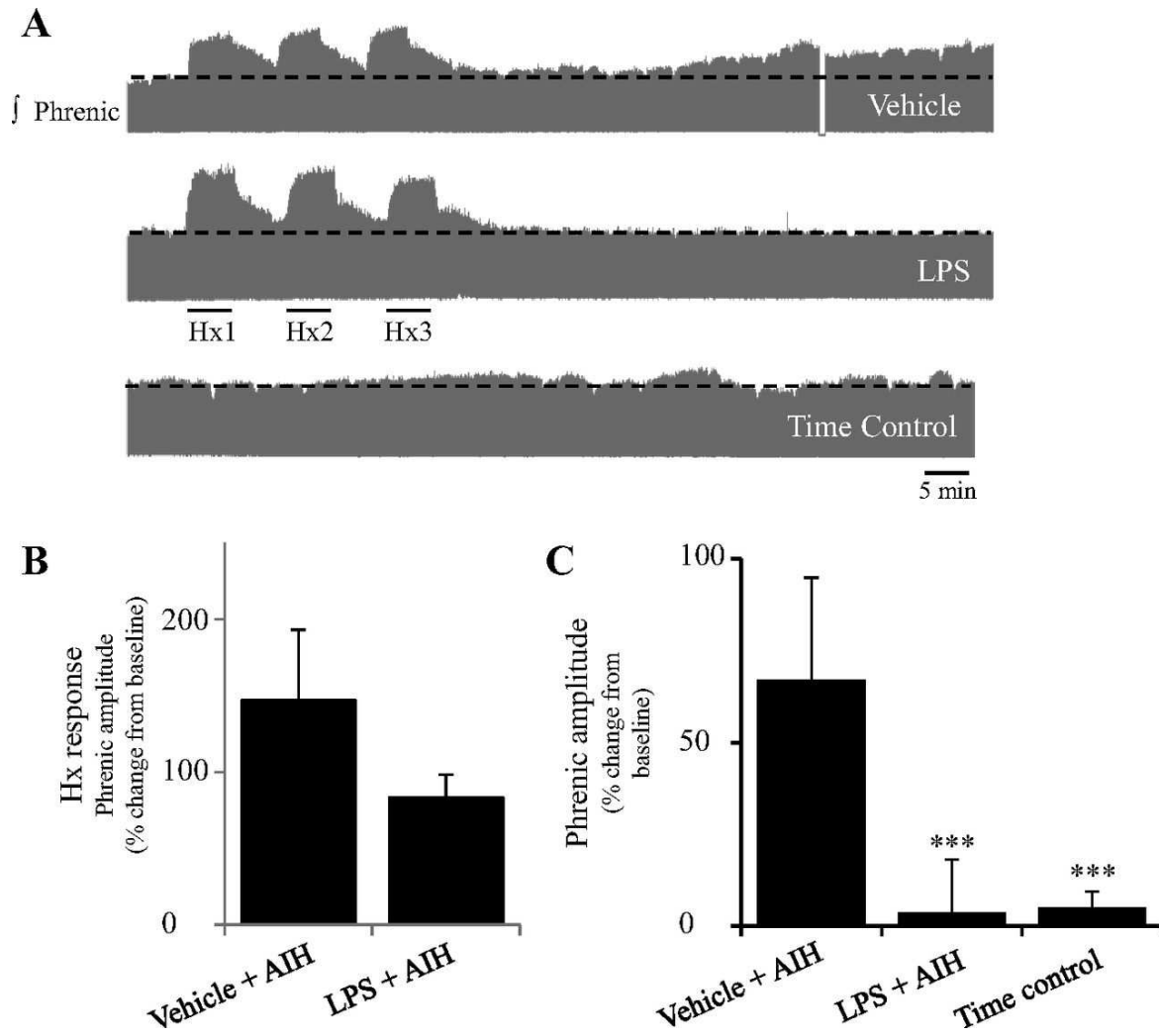


Figure Legend 1

Systemic inflammation (3 h) induced by LPS (100 µg/kg ip) significantly reduced acute intermittent hypoxia (AIH)-induced phrenic long-term facilitation (pLTF). *A*: representative integrated phrenic neurograms from anesthetized rats during the AIH (3 × 5 min hypoxia: Hx1, Hx2, Hx3) protocol for a vehicle-injected (saline, top trace), or LPS-injected (middle trace), or time control (no AIH, bottom trace) rats. Black dashed line indicates baseline phrenic amplitude in each trace. Development of pLTF is evident as a progressive increase in phrenic nerve amplitude over 60 min in the vehicle-injected animal. *B*: no change in the short-term hypoxia response was evident. *C*: group data for vehicle-injected AIH ($n = 5$), LPS-injected AIH ($n = 5$), and time control ($n = 5$) demonstrating a significant reduction in the magnitude of pLTF 60 min post-AIH in LPS treated and time control rats ($***P < 0.001$ repeated-measures two-way ANOVA, Tukey post hoc test).

FIGURE 2

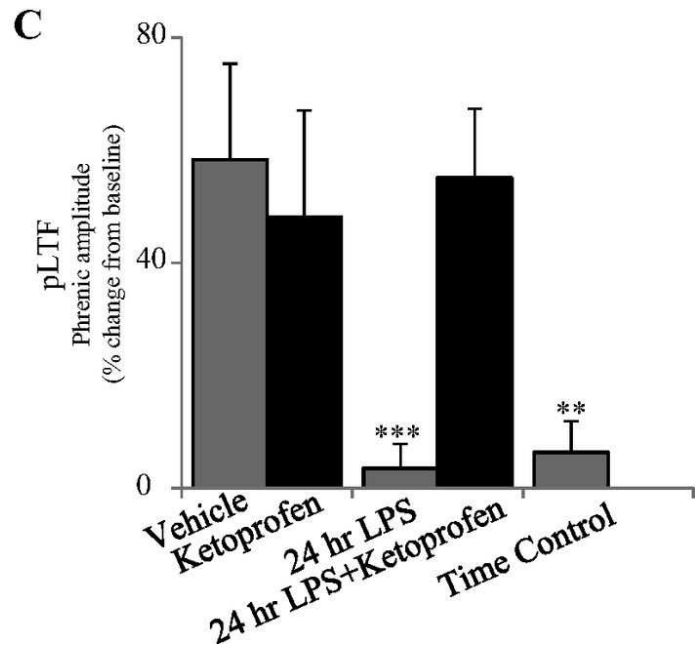
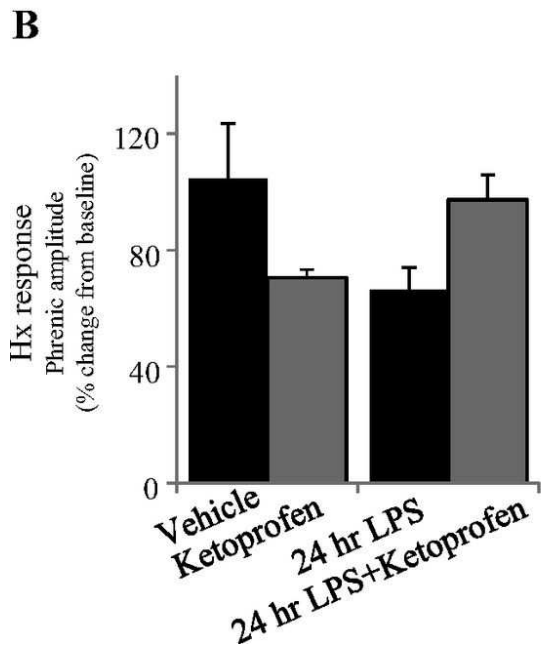
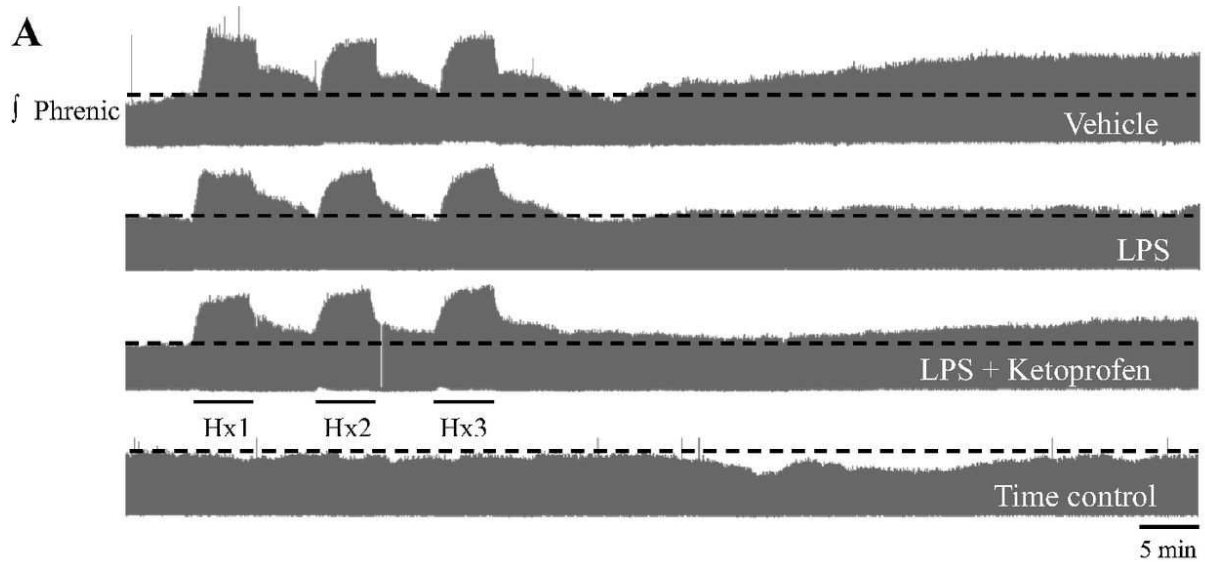


Figure Legend 2

Systemic inflammation (24 h) induced by LPS (100 µg/kg ip) did not alter the short-term hypoxia response, significantly reduced AIH-induced pLTF, but pLTF was restored with the anti-inflammatory drug ketoprofen (12.5 mg/kg ip, 3 h). *A*: representative integrated phrenic neurograms from anesthetized rats during the AIH (3 × 5 min hypoxia) protocol for vehicle-injected (saline, top trace), LPS-injected (second trace), LPS + ketoprofen-injected (third trace), and time control (no AIH, bottom trace) rats. Black dashed line indicates baseline phrenic amplitude in each trace. Development of pLTF was evident as a progressive increase in phrenic nerve amplitude over 60 min. *B*: no change in the short-term hypoxia response was evident. *C*: group data showing pLTF for vehicle-injected ($n = 5$) and ketoprofen-injected ($n = 6$) rats with AIH, and a reduction in pLTF in rats injected with LPS ($n = 9$). The appearance of pLTF was restored in rats injected with LPS and after treatment with ketoprofen ($n = 6$). There was no increase in phrenic nerve amplitude in time control rats ($n = 15$). (*** $P < 0.001$, ** $P < 0.01$ indicates significant difference from vehicle, ketoprofen, and 24 h LPS + ketoprofen).

FIGURE 3

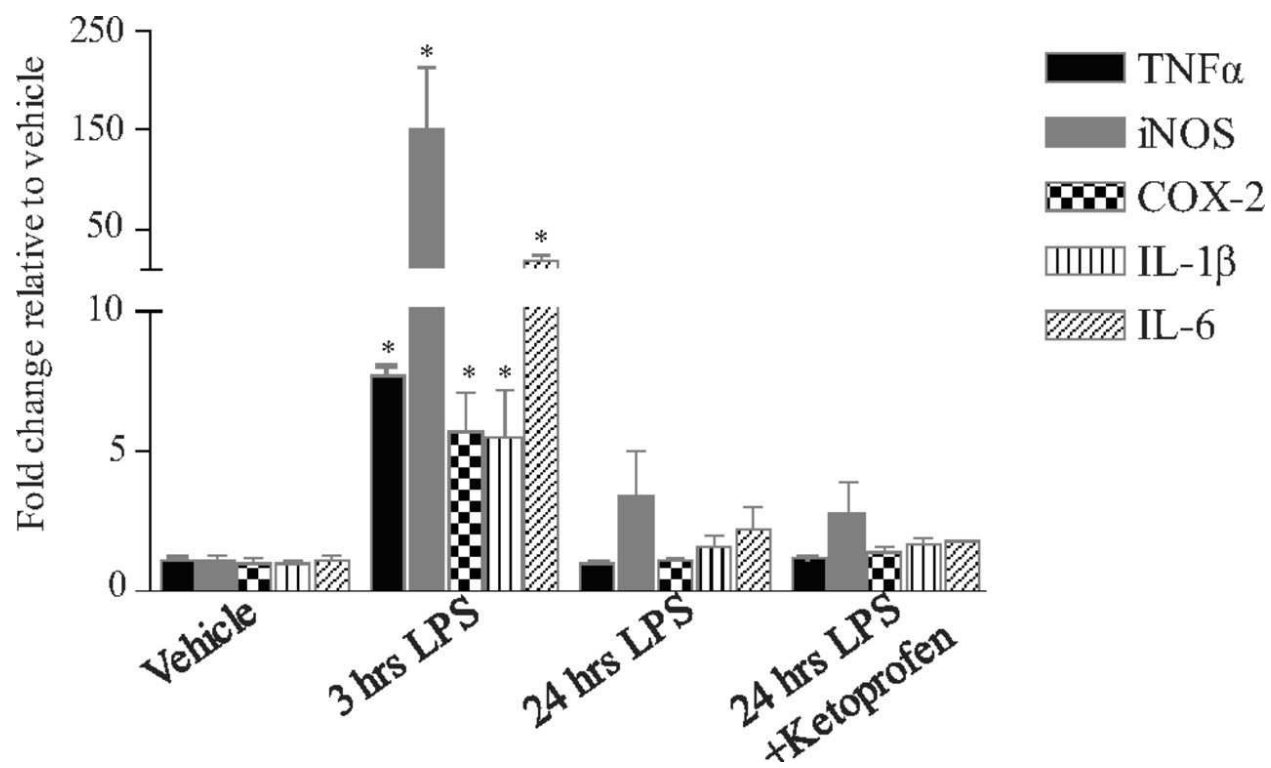


Figure Legend 3

Systemic inflammation induced by LPS (100 µg/kg ip) caused a transient increase in inflammatory gene expression in the spleen. LPS (3 h) caused a significant increase in all inflammatory genes ($n = 3$) examined compared with the respective vehicle control ($n = 4$) but returned to baseline levels by 24 h ($n = 3$) and was not altered with ketoprofen ($n = 2$) ($*P \leq 0.001$ different from all other treatment groups).

FIGURE 4

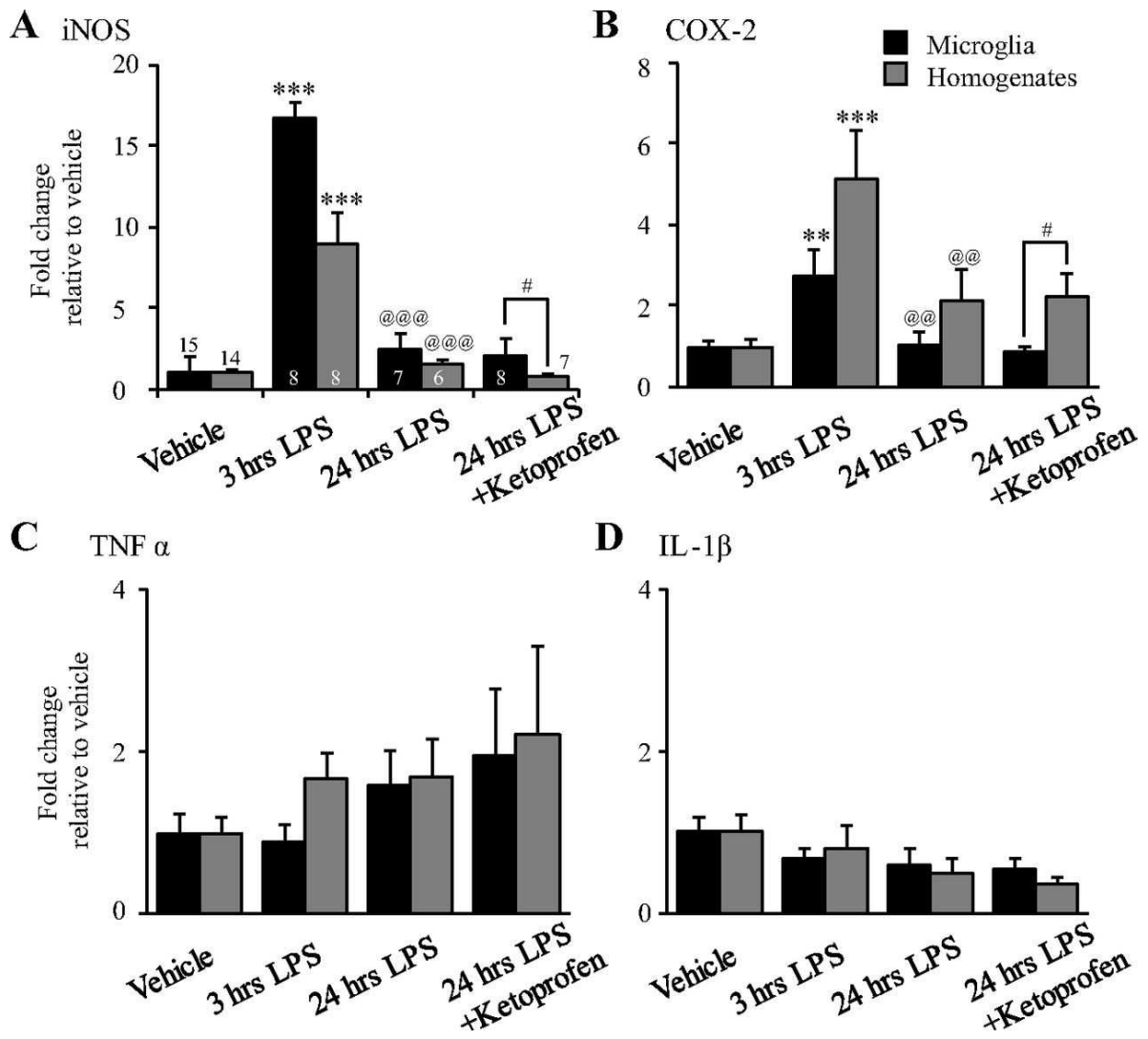


Figure Legend 4

Systemic inflammation evoked by LPS (100 µg/kg ip) caused transient and differential changes in inflammatory gene expression in isolated microglia (black bars) and homogenates (gray bars) from the cervical spinal cord. *A*: treatment with LPS (3 h) increased mRNA for iNOS compared with vehicle (microglia $n = 15$, homogenates $n = 14$) in both microglia ($n = 8$) and homogenate ($n = 8$) samples. Expression of iNOS was reduced 24 h post-LPS (microglia $n = 7$, homogenates $n = 6$) compared with 3 h post-LPS in both sample types but was not changed relative to vehicle. After ketoprofen (12.5 mg/kg ip, 3 h), microglia had greater iNOS gene expression ($n = 8$) compared with homogenates ($n = 7$). *B*: treatment with LPS (3 h) increased COX-2 mRNA in both microglia ($n = 7$) and homogenate ($n = 8$) compared with vehicle (microglia $n = 15$, homogenates $n = 15$), but was reduced 24 h post-LPS. LPS (24 h) alone (microglia $n = 7$, homogenates $n = 6$) or with ketoprofen (microglia $n = 8$, homogenates $n = 7$) did not alter COX-2 mRNA in either microglia or homogenates compared with vehicle. After ketoprofen treatment, microglia had less COX-2 mRNA compared with homogenates. LPS treatment (3 or 24 h) had no effect on gene expression for TNF α (*C*) or IL-1 β (*D*). ** $P < 0.01$, *** $P < 0.001$, significant difference from vehicle; @@ $P < 0.01$, @@@ $P < 0.001$, significant difference from 3 h LPS; # $P < 0.05$, significant difference between microglia and homogenate samples.

TABLE 1

Time	Treatment Group	Temperature		PaO ₂		PaCO ₂		pH		MAP	
		Mean	SE	Mean	SE	Mean	SE	Mean	SE	Mean	SE
Baseline	3 h Time control	37.5	0.1	351.8	6.7	45.8	1.3	7.362	0.008	132.5	3.9
	3 h Vehicle	37.7	0.1	331.25	14.1	47.6	1.4	7.356	0.006	128.2	2.8
	3 h LPS	37.5	0.3	351.2	3.7	47.0	0.7	7.353	0.013	125.4	3.9
Hx	3 h Time control	37.5	0.1	349.4	7.4 ^a	45.8	1.8	7.360	0.008	137.6	3.8 ^d
	3 h Vehicle	37.4	0.1	38.5	2.7 ^c	48.5	1.0	7.338	0.008	87.3	5.1 ^c
	3 h LPS	37.3	0.2	41.5	2.6 ^c	48.9	1.0	7.336	0.010	75.6	9.1 ^c
60 min	3 h Time control	37.7	0.02	347.4	3.7	45.4	1.7	7.375	0.008	130.1	2.8 ^e
	3 h Vehicle	37.8	0.1	312.8	20.4 ^{bb}	48.4	1.3	7.365	0.015	117.6	6.2
	3 h LPS	37.8	0.1	317.6	6.9 ^b	47.1	0.9	7.364	0.022	111.9	3.7

- Temperatures are in °C; PaO₂, PaCO₂, and MAP are in mmHg. There were no significant differences within or between groups in temperature, PaCO₂, or pH.
- a $P < 0.001$, significant difference from all other hypoxia (Hx) groups.
- b $P < 0.05$, significant difference from time control within 60 min.
- bb $P < 0.01$, significant difference from time control within 60 min.
- c $P < 0.001$, significant difference from all other within group.
- d $P < 0.001$, significant difference from all other groups in Hx.
- e $P < 0.05$, significant difference from LPS.

Table Legend 1

Physiological parameters for Sprague-Dawley rats during electrophysiological experiments after 3 h of LPS

TABLE 2

Time	Treatment Group	Temperature		PaO ₂		PaCO ₂		pH		MAP	
		Mean	SE	Mean	SE	Mean	SE	Mean	SE	Mean	SE
Baseline	24 h Time control	37.5	0.2	335.7	7.4	45.0	0.9	7.334	0.011	130.6	6.0
	24 h Vehicle	37.4	0.3	327.4	12.2	47.4	1.6	7.351	0.014	115.5	8.5 ^d
	Ketoprofen	37.7	0.1	328.4	11.4	44.0	1.1	7.365	0.015	130.6	4.0
	24 h LPS	37.6	0.2	325	11.3	45.9	0.4	7.334	0.007	149.8	9.8
	24 h LPS + ketoprofen	37.4	0.2	326	8.5	46.4	1.3	7.3165	0.012	143.4	8.9
	24 h LPS + ketoprofen vehicle	37.6	0.2	342.5	7.6	46.3	2.0	7.324	0.022	140.9	10.9
Hx	24 h Time control	37.5	0.2	336.7	6.8 ^a	45.7	1.0	7.334	0.012	129.6	6.2 ^a
	24 h Vehicle	37.4	0.3	37.9	2.9 ^b	47.8	1.3	7.351	0.014	75.3	20.6 ^{c,d}
	Ketoprofen	37.6	0.1	39.6	1.7 ^b	45.8	2.0	7.365	0.015	57.7	8.2 ^{b,d}
	24 h LPS	37.6	0.2	39.7	2.1 ^b	47.8	0.3	7.334	0.008	111.0	18.0 ^b
	24 h LPS + ketoprofen	37.4	0.2	39.3	1.7 ^b	47.9	1.6	7.317	0.012	88.1	10.6 ^b
	24 h LPS + ketoprofen vehicle	37.4	0.1	42.8	0.7 ^b	44.8	2.0	7.324	0.022	82.8	21.7 ^b
60 min	24 h Time control	37.4	0.2	334.3	6.3	45.8	0.8	7.372	0.011	126.5	6.2
	24 h Vehicle	37.2	0.3	326.0	9.0	48.8	1.0	7.351	0.017	105.6	7.7 ^d
	Ketoprofen	37.7	0.1	322.2	6.1	44.3	1.4	7.380	0.022	112.9	8.3 ^d
	24 h LPS	37.6	0.2	319.6	8.0	45.8	0.6	7.361	0.012	145.2	9.7
	24 h LPS + ketoprofen	37.4	0.1	319.2	11.1	46.5	1.4	7.360	0.011	134.2	10.2
	24 h LPS + ketoprofen vehicle	37.6	0.1	310.5	8.9	46.1	1.8	7.375	0.017	133.8	10.1

Table Legend 2

Physiological parameters for Sprague-Dawley rats during electrophysiological experiments 24 h after LPS

- Temperatures are in °C; PaO₂, PaCO₂, and MAP are in mmHg. There were no significant differences in temperature, PaCO₂, or pH.
- a $P < 0.001$, significant difference from all other Hx groups.
- b $P < 0.001$, significant difference from other time points within group.
- c $P < 0.05$, significant difference from baseline within group.
- d $P < 0.05$, significant difference from 24 h LPS.

REFERENCES

1. Amor S, Puentes F, Baker D, van der Valk P. Inflammation in neuro- degenerative diseases. *Immunology* 129: 154–169, 2010.
2. Bach KB, Mitchell GS. Hypoxia-induced long-term facilitation of respi- ratory activity is serotonin dependent. *Respir Physiol* 104: 251–260, 1996.
3. Baker-Herman TL, Fuller DD, Bavis RW, Zabka AG, Golder FJ, Doperalski NJ, Johnson RA, Watters JJ, Mitchell GS. BDNF is necessary and sufficient for spinal respiratory plasticity following inter- mittent hypoxia. *Nat Neurosci* 7: 48–55, 2004.
4. Baker-Herman TL, Mitchell GS. Determinants of frequency long-term facilitation following acute intermittent hypoxia in vagotomized rats. *Respir Physiol Neurobiol* 162: 8–17, 2008.
5. Baker-Herman TL, Mitchell GS. Phrenic long-term facilitation requires spinal serotonin receptor activation and protein synthesis. *J Neurosci* 22: 6239–6246, 2002.
6. Balan KV, Kc P, Hoxha Z, Mayer CA, Wilson CG, Martin RJ. Vagal afferents modulate cytokine-mediated respiratory control at the neonatal medulla oblongata. *Respir Physiol Neurobiol* 178: 458–464, 2011.
7. Bhattacharjee R, Kim J, Kheirandish-Gozal L, Gozal D. Obesity and obstructive sleep apnea syndrome in children: A tale of inflammatory cascades. *Pediatr Pulmonol* 46: 313–323, 2010.
8. Blatteis CM. The onset of fever: new insights into its mechanism. *Prog Brain Res* 162: 3–14, 2007.
9. Blatteis CM, Li S. Pyrogenic signaling via vagal afferents: what stimu- lates their receptors? *Auton Neurosci* 85: 66–71, 2000.
10. Broad A, Jones DE, Kirby JA. Toll-like receptor (TLR) response tolerance: a key physiological “damage limitation” effect and an important potential opportunity for therapy. *Curr Med Chem* 13: 2487–2502, 2006.
11. Buritova J, Honore P, Besson JM. Ketoprofen produces profound inhibition of spinal c-Fos protein expression resulting from an inflamma- tory stimulus but not from noxious heat. *Pain* 67: 379–389, 1996.
12. Cabre F, Fernandez MF, Calvo L, Ferrer X, Garcia ML, Mauleon D. Analgesic, antiinflammatory, and antipyretic effects of S(?) -ketoprofen in vivo. *J Clin Pharmacol* 38: 3S–10S, 1998.
13. Cashman JN. The mechanisms of action of NSAIDs in analgesia. *Drugs* 5: 13–23, 1996.

14. Conrad A, Bull DF, King MG, Husband AJ. The effects of lipopolysaccharide (LPS) on the fever response in rats at different ambient temperatures. *Physiol Behav* 62: 1197–1201, 1997.
15. Crain JM, Nikodemova M, Watters JJ. Expression of P2 nucleotide receptors varies with age and sex in murine brain microglia. *J Neuroinflammation* 6: 24, 2009.
16. Cunningham C, Campion S, Lunnon K, Murray CL, Woods JF, Deacon RM, Rawlins JN, Perry VH. Systemic inflammation induces acute behavioral and cognitive changes and accelerates neurodegenerative disease. *Biol Psychiatry* 65: 304–312, 2009.
17. Deakin AM, Payne AN, Whittle BJ, Moncada S. The modulation of IL-6 and TNF- α release by nitric oxide following stimulation of J774 cells with LPS and IFN- γ . *Cytokine* 7: 408–416, 1995.
18. Di Filippo M, Sarchielli P, Picconi B, Calabresi P. Neuroinflammation and synaptic plasticity: theoretical basis for a novel, immune-centred, therapeutic approach to neurological disorders. *Trends Pharmacol Sci* 29: 402–412, 2008.
19. Feldman JL, Mitchell GS, Nattie EE. Breathing: rhythmicity, plasticity, chemosensitivity. *Annu Rev Neurosci* 26: 239–266, 2003.
20. Fuller DD, Bach KB, Baker TL, Kinkead R, Mitchell GS. Long term facilitation of phrenic motor output. *Respir Physiol* 121: 135–146, 2000.
21. Ge X, Yang Z, Duan L, Rao Z. Evidence for involvement of the neural pathway containing the peripheral vagus nerve, medullary visceral zone and central amygdaloid nucleus in neuroimmunomodulation. *Brain Res* 914: 149–158, 2001.
22. Godbout JP, Berg BM, Kelley KW, Johnson RW. α -Tocopherol reduces lipopolysaccharide-induced peroxide radical formation and interleukin-6 secretion in primary murine microglia and in brain. *J Neuroimmunol* 149: 101–109, 2004.
23. Goehler LE, Gaykema RPA, Nguyen KT, Lee JE, Tilders FJH, Maier SF, Watkins LR. Interleukin-1 β in immune cells of the abdominal vagus nerve: a link between the immune and nervous systems? *J Neurosci* 19: 2799–2806, 1999.
24. Gozal D. Sleep, sleep disorders and inflammation in children. *Sleep Med* 1: S12–S16, 2009.
25. Graeber MB. Changing face of microglia. *Science* 330: 783–788, 2010.
26. Hashimoto M, Nitta A, Fukumitsu H, Nomoto H, Shen L, Furukawa S. Inflammation-induced GDNF improves locomotor function after spinal cord injury. *Neuroreport* 16: 99–102, 2005.

27. Hoffman MS, Nichols NL, Macfarlane PM, Mitchell GS. Phrenic long-term facilitation after acute intermittent hypoxia requires spinal ERK activation but not TrkB synthesis. *J Appl Physiol* 113: 1184–1193, 2012.
28. Holden JM, Meyers-Manor JE, Overmier JB, Gahtan E, Sweeney W, Miller H. Lipopolysaccharide-induced immune activation impairs attention but has little effect on short-term working memory. *Behav Brain Res* 194: 138–145, 2008.
29. Huxtable AG, Vinit S, Windelborn JA, Crader SM, Guenther CH, Watters JJ, Mitchell GS. Systemic inflammation impairs respiratory chemoreflexes and plasticity. *Respir Physiol Neurobiol* 178: 482–489, 2011.
30. Kaminska B, Gozdz A, Zawadzka M, Ellert-Miklaszewska A, Lipko M. MAPK signal transduction underlying brain inflammation and gliosis as therapeutic target. *Anat Rec (Hoboken)* 292: 1902–1913, 2009.
31. Kaufmann WE, Andreasson KI, Isakson PC, Worley PF. Cyclooxygenases and the central nervous system. *Prostaglandins* 54: 601–624, 1997.
32. Kelly A, Laroche S, Davis S. Activation of mitogen-activated protein kinase/extracellular signal-regulated kinase in hippocampal circuitry is required for consolidation and reconsolidation of recognition memory. *J Neurosci* 23: 5354–5360, 2003.
33. Kimoff RJ, Hamid Q, Divangahi M, Hussain S, Bao W, Naor N, Payne RJ, Ariyaratnam A, Mulrain K, Petrof BJ. Increased upper airway cytokines and oxidative stress in severe obstructive sleep apnoea. *Eur Respir J* 38: 89–97, 2010.
34. Kozak W, Soszynski D, Rudolph K, Conn CA, Kluger MJ. Dietary n-3 fatty acids differentially affect sickness behavior in mice during local and systemic inflammation. *Am J Physiol Regul Integr Comp Physiol* 272: R1298–R1307, 1997.
35. Kreutzberg GW. Microglia: a sensor for pathological events in the CNS. *Trends Neurosci* 19: 312–318, 1996.
36. Laflamme N, Lacroix S, Rivest S. An essential role of interleukin-1beta in mediating NF-kappa B activity and COX-2 transcription in cells of the blood-brain barrier in response to a systemic and localized inflammation but not during endotoxemia. *J Neurosci* 19: 10923–10930, 1999.
37. Leon CG, Tory R, Jia J, Sivak O, Wasan KM. Discovery and development of toll-like receptor 4 (TLR4) antagonists: a new paradigm for treating sepsis and other diseases. *Pharm Res* 25: 1751–1761, 2008.
38. MacFarlane PM, Mitchell GS. Episodic spinal serotonin receptor activation elicits long-lasting phrenic motor facilitation by an NADPH oxidase-dependent mechanism. *J Physiol* 587: 5469–5481, 2009.

39. Maier SF, Goehler LE, Fleshner M, Watkins LR. The role of the vagus nerve in cytokine-to-brain communication. *Ann NY Acad Sci* 840: 289–300, 1998.
40. McColl BW, Allan SM, Rothwell NJ. Systemic infection, inflammation and acute ischemic stroke. *Neuroscience* 158: 1049–1061, 2009.
41. Mitchell GS, Johnson SM. Neuroplasticity in respiratory motor control. *J Appl Physiol* 94: 358–374, 2003.
42. Nam NH. Naturally occurring NF-kappaB inhibitors. *Mini Rev Med Chem* 6: 945–951, 2006.
43. Nikodemova M, Watters JJ. Efficient isolation of live microglia with preserved phenotypes from adult mouse brain. *J Neuroinflammation* 9: 147, 2012.
44. Ossipov MH, Jerussi TP, Ren K, Sun H, Porreca F. Differential effects of spinal (R)-ketoprofen and (S)-ketoprofen against signs of neuropathic pain and tonic nociception: evidence for a novel mechanism of action of (R)-ketoprofen against tactile allodynia. *Pain* 87: 193–199, 2000.
45. Parrillo JE, Parker MM, Natanson C, Suffredini AF, Danner RL, Cunnion RE, Ognibene FP. Septic shock in humans: Advances in the understanding of pathogenesis, cardiovascular dysfunction, and therapy. *Ann Intern Med* 113: 227–242, 1990.
46. Perry VH. Contribution of systemic inflammation to chronic neurodegeneration. *Acta Neuropathol (Berl)* 120: 277–286, 2010.
47. Pinardi G, Sierralta F, Miranda HF. Atropine reverses the antinociception of nonsteroidal anti-inflammatory drugs in the tail-flick test of mice. *Pharmacol Biochem Behav* 74: 603–608, 2003.
48. Poltorak A, He X, Smirnova I, Liu MY, Huffel CV, Du X, Birdwell D, Alejos E, Silva M, Galanos C, Freudenberg M, Ricciardi-Castagnoli P, Layton B, Beutler B. Defective LPS signaling in C3H/HeJ and C57BL/10ScCr mice: Mutations in Tlr4 gene. *Science* 282: 2085–2088, 1998.
49. Qin L, Wu X, Block ML, Liu Y, Breese GR, Hong JS, Knapp DJ, Crews FT. Systemic LPS causes chronic neuroinflammation and progressive neurodegeneration. *Glia* 55: 453–462, 2007.
50. Renz H, Gong JH, Schmidt A, Nain M, Gems D. Release of tumor necrosis factor-alpha from macrophages: Enhancement and suppression are dose-dependently regulated by prostaglandin E2 and cyclic nucleotides. *J Immunol* 141: 2388–2393, 1988.

51. Ricciardolo FL, Sterk PJ, Gaston B, Folkerts G. Nitric oxide in health and disease of the respiratory system. *Physiol Rev* 84: 731–765, 2004.
52. Rivest S. How circulating cytokines trigger the neural circuits that control the hypothalamic-pituitary-adrenal axis. *Psychoneuroendocrinology* 26: 761–788, 2001.
53. Rivest S. Regulation of innate immune responses in the brain. *Nat Rev Immunol* 9: 429–439, 2009.
54. Roth J, De Souza GE. Fever induction pathways: evidence from responses to systemic or local cytokine formation. *Braz J Med Biol Res* 34: 301–314, 2001.
55. Schnydrig S, Korner L, Landweer S, Ernst B, Walker G, Otten U, Kunz D. Peripheral lipopolysaccharide administration transiently affects expression of brain-derived neurotrophic factor, corticotropin and pro-opiomelanocortin in mouse brain. *Neurosci Lett* 429: 69–73, 2007.
56. Sedgwick JD, Schwender S, Imrich H, Dorries R, Butcher GW, ter Meulen V. Isolation and direct characterization of resident microglial cells from the normal and inflamed central nervous system. *Proc Natl Acad Sci USA* 88: 7438–7442, 1991.
57. Shaw KN, Commins S, O'Mara SM. Lipopolysaccharide causes deficits in spatial learning in the watermaze but not in BDNF expression in the rat dentate gyrus. *Behav Brain Res* 124: 47–54, 2001.
58. Singh AK, Jiang Y. How does peripheral lipopolysaccharide induce gene expression in the brain of rats? *Toxicology* 201: 197–207, 2004.
59. Sparkman NL, Buchanan JB, Heyen JR, Chen J, Beverly JL, Johnson RW. Interleukin-6 facilitates lipopolysaccharide-induced disruption in working memory and expression of other proinflammatory cytokines in hippocampal neuronal cell layers. *J Neurosci* 26: 10709–10716, 2006.
60. Stockley RA. Progression of chronic obstructive pulmonary disease: impact of inflammation, comorbidities and therapeutic intervention. *Curr Med Res Opin* 25: 1235–1245, 2009.
61. Swiergiel AH, Dunn AJ. Effects of interleukin-1beta and lipopolysaccharide on behavior of mice in the elevated plus-maze and open field tests. *Pharmacol Biochem Behav* 86: 651–659, 2007.
62. Teeling JL, Felton LM, Deacon RM, Cunningham C, Rawlins JN, Perry VH. Sub-pyrogenic systemic inflammation impacts on brain and behavior, independent of cytokines. *Brain Behav Immun* 21: 836–850, 2007.
63. Teeling JL, Perry VH. Systemic infection and inflammation in acute CNS injury and chronic neurodegeneration: underlying mechanisms. *Neuroscience* 158: 1062–1073, 2009.

64. Thomson LM, Sutherland RJ. Systemic administration of lipopolysaccharide and interleukin-1beta have different effects on memory consolidation. *Brain Res Bull* 67: 24–29, 2005.
65. Vane JR. Inhibition of prostaglandin synthesis as a mechanism of action for aspirin-like drugs. *Nat New Biol* 231: 232–235, 1971.
66. Vereker E, Campbell V, Roche E, McEntee E, Lynch MA. Lipopolysaccharide inhibits long term potentiation in the rat dentate gyrus by activating caspase-1. *J Biol Chem* 275: 26,252–26,258, 2000.
67. Vinit S, Windelborn JA, Mitchell GS. Lipopolysaccharide attenuates phrenic long-term facilitation following acute intermittent hypoxia. *Respir Physiol Neurobiol* 176: 130–135, 2011.
68. Walker JS. NSAID: an update on their analgesic effects. *Clin Exp Pharmacol Physiol* 22: 855–860, 1995.
69. Wiczorek M, Swiergiel AH, Pournajafi-Nazarloo H, Dunn AJ. Physiological and behavioral responses to interleukin-1beta and LPS in vagotomized mice. *Physiol Behav* 85: 500–511, 2005.
70. Wills-Karp M. Immunologic basis of antigen-induced airway hyperresponsiveness. *Annu Rev Immunol* 17: 255–281, 1999.
71. Wong ML, Bongiorno PB, Rettori V, McCann SM, Licinio J. Interleukin (IL) 1beta, IL-1 receptor antagonist, IL-10, and IL-13 gene expression in the central nervous system and anterior pituitary during systemic inflammation: pathophysiological implications. *Proc Natl Acad Sci USA* 94: 227–232, 1997.
72. Yamawaki Y, Kimura H, Hosoi T, Ozawa K. MyD88 plays a key role in LPS-induced Stat3 activation in the hypothalamus. *Am J Physiol Regul Integr Comp Physiol* 298: R403–R410, 2010.
73. Yin MJ, Yamamoto Y, Gaynor RB. The anti-inflammatory agents aspirin and salicylate inhibit the activity of I(kappa)B kinase-beta. *Nature* 396: 77–80, 1998.

APPENDIX 2

**INTERMITTENT HYPOXIA-INDUCED SPINAL INFLAMMATION IMPAIRS
RESPIRATORY MOTOR PLASTICITY BY A SPINAL P38 MAP KINASE-
DEPENDENT MECHANISM**

A.G. Huxtable, S.M.C. Smith, T.J. Peterson, J.J. Watters and G. S. Mitchell

In preparation for publication

ABSTRACT

Rationale: Inflammation is present in almost every disorder challenging the respiratory system and may compromise respiratory motor plasticity conferring adaptability to the system. One frequently studied model of spinal, respiratory motor plasticity is phrenic long-term facilitation (pLTF), a long-lasting increase in phrenic motor output following acute intermittent hypoxia (AIH; 3, 5 min hypoxic episodes).

Objectives: To determine the effect of one night of intermittent hypoxia on pLTF and spinal inflammation.

Methods: Rats were exposed to intermittent hypoxia (2 min hypoxia, 2 min normoxia; 8 hours) or normoxia and allowed 16 hours recovery (IH-1).

Measurements and Main Results: IH-1 abolished pLTF (IH-1: $-1\pm 5\%$; normoxic controls: $56\pm 10\%$; $n=6$, $p<0.001$) and transiently increased IL-6 (1.5 ± 0.2 fold change, $n=5$, $p=0.017$) and iNOS (2.4 ± 0.4 fold change, $n=6$, $p=0.010$) mRNA in cervical spinal homogenates, demonstrating spinal inflammation. IH-1 also elicited a sustained increase in IL-1 β mRNA (2.4 ± 0.2 fold change, $n=5$, $p<0.001$) in immunomagnetically isolated cervical spinal microglia. After IH-1, pLTF was restored by systemic administration of the non-steroidal anti-inflammatory drug ketoprofen ($55\pm 9\%$ baseline, $n=6$, $p<0.001$) or spinal p38 MAPK inhibition ($58\pm 2\%$, $n=7$, $p<0.001$). Increased immunofluorescent labeling of phosphorylated (activated) p38 MAPK was evident in identified phrenic motoneurons and adjacent microglia.

Conclusions: IH-1 induces spinal inflammation and impairs pLTF by a spinal p38 MAP kinase-dependent mechanism and this kinase is likely a key orchestrator impairing pLTF. By targeting inflammation, we may develop strategies to manipulate respiratory motor plasticity for

therapeutic advantage in conditions where the respiratory system is compromised (e.g. obstructive sleep apnea, apnea of prematurity, spinal cord injury).

INTRODUCTION

Inflammation is prevalent in many clinical disorders that challenge ventilatory control, including obstructive sleep apnea (OSA), apnea of prematurity, neurodegenerative disorders (e.g. Amyotrophic Lateral Sclerosis), and spinal cord injury. Nevertheless, we know little concerning interactions between inflammation and any aspect of the neural control of breathing (1).

Systemic inflammation has a major impact on central nervous system (CNS) function, including neuroplasticity (1-3). However, the impact of inflammation on neuroplasticity is complex. In some instances, inflammation initiates plasticity, such as in the spinal dorsal horn where it elicits allodynia (4) and involves complex cell-cell interactions between microglia and sensory neurons (5). Similarly, chronic sustained hypoxia elicits inflammation and sensory plasticity in carotid chemoreceptors, enhancing hypoxic sensitivity (6). In contrast, inflammation inhibits plasticity in other regions of the CNS, including activity-dependent hippocampal synaptic plasticity (7) and spinal instrumental learning (8). We know comparatively little about the impact of systemic inflammation on CNS mechanisms of ventilatory control (1, 9, 10).

We previously demonstrated that systemic inflammation induced by a low dose of lipopolysaccharide (LPS) profoundly inhibits phrenic long-term facilitation (pLTF), a form of spinal respiratory motor plasticity elicited by acute intermittent hypoxia (AIH), and causes transient cervical spinal inflammation (10). The non-steroidal anti-inflammatory drug ketoprofen restored pLTF (10), highlighting the critical impact of low level inflammation on respiratory plasticity. Here, we study a unique model of inflammation caused by short, repetitive bouts of nocturnal intermittent hypoxia (8 hours, 16 hours recovery, IH-1). This IH-1 protocol mimics some aspects of the intermittent hypoxia experienced in a single night of OSA, but without

comorbidities (e.g. obesity, cardiovascular problems) (11) and the severity of hypoxic episodes are tightly controlled. A similar 12 hour IH exposure caused inflammation in the cortex and hippocampus (12, 13). Our goal was to determine if IH-1 elicits spinal inflammation and if this inflammation impairs AIH-induced pLTF.

Respiratory plasticity has potential to both stabilize (14), and destabilize breathing (15). The specific impact of respiratory plasticity may depend on the duration of intermittent hypoxia, the site of respiratory plasticity and the extent of intermittent hypoxia-induced inflammation. It is not yet known whether inflammation acts to stabilize or destabilize breathing through its impact on respiratory plasticity. The present study is a key first step towards understanding the impact of inflammation on respiratory plasticity, and its potential consequences in clinical disorders that compromise breathing capacity or stability (e.g. cervical spinal injury, ALS, OSA, and others).

METHODS

All experiments were approved by the Animal Care and Use Committee at the School of Veterinary Medicine, University of Wisconsin – Madison and conformed to policies laid out by the National Institutes of Health in the *Guide for the Care and Use of Laboratory Animals*. Experiments were performed on 3-4 month old Harlan male Sprague Dawley rats (colony 211, 300-450 g). Rats were housed under standard conditions, with food and water *ad libitum* and a 12-hour light/dark cycle.

Experimental Groups

Rats were individually placed in cylindrical, Plexiglas exposure chambers for 8 hours with ClearH₂O® hydrogel (Portland, ME) for nutrition and hydration during exposures. Gas flow through the chambers was maintained at 4 L/min, was regulated by mass flow controllers (Teledyne, Hastings Instruments, Hampton, VA) with a customized computer program (National Instruments, LabVIEW™ 2009, Service Pack 1, version 9.0.1, Austin, TX; customized by B. Wathen) and was continuously measured with respiratory gas analyzers (Gemini, CWE, Inc., Ardmore, PA). Rats were exposed to either intermittent hypoxia (2 min of 10.5% O₂, 2 min normoxic intervals) or continuous normoxia (21% O₂). Exposures occurred the day prior to electrophysiology experiments, mRNA analysis or immunohistochemistry (see below). In some cases, they were sacrificed and taken immediately for mRNA analysis (as indicated).

In the first study investigating IH-1 effects on pLTF, rats were assigned to three groups: 1) Normoxia (Nx, n=6); 2) IH-1 (n=6); and 3) Time controls (4 Nx, 2 IH-1; total n=6). In subsequent neurophysiological studies, rats received intraperitoneal injections of the non-steroidal anti-inflammatory drug, ketoprofen ((S)-(+)-Ketoprofen, keto, 12.5 mg/kg; Sigma Chemical Company, St. Louis, MO) or vehicle (veh, 50% ethanol and saline, 100 µl/kg) and

were divided among three groups: 1) Nx + keto (n=7); 2) IH-1 + keto (n=6); or 3) Time control + keto (3 Nx, 3 IH-1, total n=6). In the final experimental series, rats were instrumented with intrathecal catheters at spinal segment C₄ for delivery of a p38 MAP kinase inhibitor (SB 202190, 1 mM, p38 inhib; Tocris Bioscience, Minneapolis, MN) as described previously (16, 17). SB 202190 or vehicle (artificial cerebrospinal fluid) was given 2 µl/30 sec to a total of 12 µl, 15 min prior to AIH. These rats were divided into 6 groups: 1) Nx + veh (n=9); 2) IH-1+ veh (n=6); 3) Time control + veh (6 Nx, 2 IH-1; total n=8); 4) Nx + p38 inhib (n=7); 5) IH-1 + p38 inhib (n=7); 6) Time control + p38 inhib (3 Nx, 3 IH-1; total n=5).

pLTF Measurement

The experimental protocol to assess pLTF has been described in detail previously (10, 16, 18). In anesthetized, paralyzed, vagotomized and pump-ventilated rats, integrated phrenic nerve activity was recorded. Stable baseline activity was obtained (>30min) and an arterial blood sample was taken to assess PO₂, PCO₂, pH and base excess using a blood gas analyzer (ABL 800, Radiometer, Copenhagen, Denmark). After baseline conditions were established, AIH consisting of 3 hypoxic episodes (5 min duration, 9-10.5% O₂) separated by 5 min of normoxia was initiated. Blood samples were taken during the first hypoxic episode, and 15, 30, 60 and 90 min post-AIH. Data were included in analyses only if they complied with the following criteria: 1) PaO₂ during baseline and post-AIH was >180 mmHg; 2) PaO₂ during hypoxic episodes was between 35 to 45 mmHg; 3) PaCO₂ remained within 1.5 mmHg of baseline throughout the post-AIH period. Integrated phrenic nerve amplitude was evaluated for 1 min before each blood sample. Upon completion of experiments, rats were euthanized with an overdose of urethane.

Inflammatory Gene Expression

Sample preparation. Rats were anesthetized with isoflurane and transcardially perfused with ice-cold phosphate-buffered saline (PBS). Tissue from cervical spinal cords (C₃-C₆) was removed, homogenized, and used for quantitative PCR analysis (hereafter referred to as “homogenates”). Microglial isolations were performed as previously described (10, 19, 20). CD11b⁺ cells isolated with this method are referred to as “microglia.” Neural Tissue Dissociation Kit, anti-PE magnetic beads, and MS columns were purchased from Miltenyi Biotec (Germany).

Reverse Transcription. Total RNA was isolated using the TRI-reagent (Sigma Chemical Company, St. Louis, MO) and first-strand cDNA was synthesized from 1 µg of total RNA using M-MLV Reverse Transcriptase (Invitrogen, Carlsbad, CA) and an oligo(dT)/random hexamer cocktail (Promega, Madison, WI). The cDNA was then used for quantitative RT-PCR using SYBR Green PCR Master Mix (Applied Biosystems, Carlsbad, CA).

Quantitative PCR. Amplified cDNA was measured by fluorescence in real-time using the ABI 7500 Fast Real-Time PCR System (Applied Biosystems). The following primer sequences were used for quantitative PCR:

IL-1 β - 5' CTG CAG ATG CAA TGG AAA GA; 5' TTG CTT CCA AGG CAG ACT TT

IL-6 - 5' GTG GCT AAG GAC CAA GAC CA; 5' GGT TTG CCG AGT AGA CCT CA

TNF- α - 5' TCC ATG GCC CAG ACC CTC ACA C; 5' TCC GCT TGG TGG TTT GCT ACG

iNOS- 5' AGG GAG TGT TGT TCC AGG TG; 5' TCT GCA GGA TGT CTT GAA CG

COX-2- 5' TGT TCC AAC CCA TGT CAA AA; 5' CGT AGA ATC CAG TCC GGG TA

18s- 5' CGG GTG CTC TTA GCT GAG TGT CCC G; 3' CTC GGG CCT GCT TTG AAC AC

All primers were designed (using Primer3 software) to span introns where possible and specificity was assessed through NCBI BLAST. Dissociation curves had a single peak with an

observed T_m consistent with the intended amplicon sequences. Primer efficiency was calculated through serial dilutions and construction of a standard curve.

Phrenic motoneuron back-labeling and tissue collection

A separate group of rats were bilaterally, intrapleurally injected with cholera toxin b-subunit (25 μ g/side, Calbiochem, Billerica, MA) to retrogradely label phrenic motoneurons as described previously (21-26). Three days later, rats were exposed to IH-1 (n=6) or normoxia (n=6) and 20 hours later were transcardially perfused with cold phosphate buffered saline (PBS, 0.01 M, pH 7.4, Thermo Fisher Scientific, Waltham, MA) followed by 4% paraformaldehyde (PFA, Thermo Fisher Scientific, Waltham, MA). After perfusion, brains and spinal cords were immersion-fixed in 4% PFA in 0.01 M PBS overnight at 4° C, then saturated in 20% and 30% sucrose at 4°C.

Immunofluorescence

The cervical spinal cord (C₃-C₆) was cut into 40 μ m sections using a freezing microtome (Leica, SM 2000 R). Free-floating sections were washed and non-specific binding sites were blocked (1 hr) with 1% bovine serum albumin (BSA, Research Products International Corporation, Mount Prospect, IL). Tissue sections were incubated in the following antibodies (16 hrs, room temperature, 0.1% BSA): phospho-p38 MAPK antibody (rabbit, 1:250, Cell Signaling, Danvers, MA), anti-cholera toxin B (goat, 1:5000, Calbiochem, Billerica, MA) and CD11b (mouse, 1:200, AbD Serotec, Raleigh, NC). The following day, tissues were washed and incubated in the respective secondary antibodies (2 hrs, room temperature): AlexaFluor 488 donkey anti-rabbit (DAR, 1:500, Invitrogen, Grand Island, NY), AlexaFluor 647 donkey anti-goat (DAG, 1:1000, Invitrogen, Grand Island, NY), and AlexaFluor 594 donkey anti-mouse (DAM, 1:1000, Invitrogen, Grand Island, NY). Sections were washed and mounted with anti-

fade solution (ProLong Gold anti-fade reagent, Invitrogen, Grand Island, NY). Negative controls were run concurrently to ensure specific labeling. No staining was evident in any of the control tissue sections.

Image processing. All immunofluorescent images (1024 x 1024 pixels) were viewed using a Nikon C1 laser scanning confocal microscope with lambda strobing in the Nikon EZ-C1 Gold (Version 3.80) confocal imaging software (2 μm step increments for z stacks). All image pairs (IH-1 vs. Nx sections) were adjusted identically for contrast and brightness in the Nikon EZ-C1 FreeViewer Gold software.

Data Analysis

Electrophysiology. Physiological variables and peak amplitude of integrated phrenic nerve activity was averaged for 30 bursts for baseline, during the short-term hypoxic response (within a hypoxic episode), and at 60 and/or 90 min post-AIH. Changes in phrenic nerve burst amplitude were normalized to baseline values and expressed as a percent change from baseline.

Statistical comparisons for short-term hypoxic responses were made for minute two of the first hypoxic episode with a t-test or One-Way ANOVA on Ranks (p38 MAPK data). An ANOVA on Ranks was used for the p38 MAPK data since these data failed normality/equal variance.

Statistical comparisons for changes in phrenic burst amplitude post-AIH were made using a Two-Way ANOVA with a repeated measures design and Fisher LSD *post-hoc* tests (Sigma Stat version 11, Systat Software, San Jose, CA). Differences were considered significant if $p < 0.05$. All values are expressed as means \pm 1 SEM.

Gene Expression. Gene expression data were analyzed based on a relative standard curve method, as previously described (10, 27). Statistical significance was determined for each gene by a One-Way ANOVA with Fisher LSD *post-hoc* test for individual comparisons (Sigma Stat version 11, Systat Software, San Jose, CA). Differences were considered significant if $p < 0.05$. All values are expressed as the mean \pm 1 SEM.

RESULTS

IH-1 abolishes AIH-induced pLTF

IH-1 pretreatment had no significant effect on blood pressure, body temperature, or blood gases (Table 1). As expected, decreased inspired oxygen significantly decreased PaO₂, pH, and mean arterial pressure in both normoxic and IH-1 pre-treated groups versus time controls. However, time controls did have a slightly lower pH at 60 min versus the IH-1 and normoxia groups. IH-1 also had no effect on the magnitude of the short-term hypoxic phrenic response (Fig 1A, B, D).

Normoxia pre-treated rats exhibited normal pLTF 60 min post-AIH ($p < 0.001$, Fig 1A), whereas pLTF was not evident IH-1 pre-treatment ($p = 0.866$, Fig 1B). Further, there was no apparent pLTF in time control rats (no AIH) pre-treated with IH-1 or normoxia ($p = 0.320$, Fig 1C). At 60 min, phrenic nerve amplitudes in Nx + AIH treated rats were significantly greater than IH-1 + AIH treated rats ($p < 0.001$) and time control rats ($p < 0.001$), while there was no significant difference between IH-1 + AIH and time control rats ($p = 0.336$).

IH-1 elicits cervical spinal inflammation

To examine whether IH-1 induced spinal inflammation, inflammatory gene expression was assessed in cervical spinal cord homogenates and immunomagnetically isolated microglia. In homogenates, IH-1 increased iNOS mRNA above normoxic controls ($p = 0.010$; Fig 2A). In microglia, IL-1 β mRNA was increased ($p < 0.001$) versus normoxic controls (Fig 2B). No other genes examined (IL-6, TNF α , and COX-2) were significantly changed in either homogenates or microglia ($p > 0.05$, Fig 2).

Since the inflammatory response is dynamic, inflammatory gene expression was also examined in homogenates and microglia immediately following the 8 hour IH exposure. At this

earlier time point in homogenates, IL-6 mRNA was significantly greater than IL-6 gene expression the next day (i.e. IH-1; $p=0.017$), but it was not significantly different from normoxic controls ($p=0.07$). Thus, there is a transient, early increase in IL-6 mRNA that returned to control levels the next day (Fig 2A). In microglia, IL-1 β gene expression was significantly increased after 8 hours of IH ($p<0.001$) versus normoxic controls and was maintained until the next day. There was no significant difference between IL-1 β mRNA immediately following 8 hours of IH and IH-1 ($p=0.753$). Homogenate iNOS gene expression was not significantly different from normoxic controls ($p=0.624$) at this early time point, but there was a small, yet significant reduction in iNOS gene expression versus IH-1 ($p=0.008$), suggesting small, dynamic changes in iNOS gene expression after 8 hours of IH.

Ketoprofen restores pLTF after IH-1

We hypothesized that systemic administration of the non-steroidal anti-inflammatory drug, ketoprofen, would restore pLTF by reducing systemic inflammation. Rats were divided into three groups where they were exposed to normoxia or IH-1, and ketoprofen was administered 3 hours prior to beginning AIH protocols. Two groups received AIH: Nx + keto and IH-1 + keto. The third group was a time control and did not receive AIH (time control + keto; 3 Nx, 3 IH-1). There was no significant difference between these three groups for body temperature ($p=0.514$). As expected, AIH caused significant reductions in PaO₂ and mean arterial pressure during hypoxic episodes versus baseline ($p<0.001$). There was also a significant reduction in arterial pH in the IH-1 + keto group during hypoxia versus 60 min post-AIH ($p=0.001$). PaO₂ in the Nx + keto group did not fully recover to baseline levels 60 min post-AIH ($p=0.002$); it was significantly different from IH-1 + keto ($p=0.004$) and time control + keto ($p=0.001$) at 60 min post-AIH. However, since PaO₂ was >180 mmHg at all times, we do not

believe this PaO₂ fluctuation affected our results. PaCO₂ was also significantly higher at 60 min post-AIH for the IH-1 + keto group versus baseline (p=0.038), and during hypoxia (p=0.002), but it was not different from the other groups at this same time point, reflecting higher group variability and remained within acceptable levels (see Methods).

Ketoprofen (12.5 mg/kg, i.p., 3 hours prior to AIH) restored pLTF (Fig 3) and had no significant effects on the short-term hypoxic phrenic response between Nx + keto and IH-1 + keto treated animals (p=0.215, t-test, Fig 3D). Nx + keto treated rats exhibited normal pLTF (Fig 3A, E: p<0.001) that was significantly greater than the time control + keto group (p=0.003), which did not exhibit significant changes in phrenic burst amplitude over the course of an experiment (Fig 3E). IH-1 + keto rats exhibited significant AIH-induced pLTF (p<0.001), and this effect was not different from the Nx + keto group (p=0.221). pLTF in the IH-1 + keto group was significantly greater than the time control + keto group (p<0.001; Fig 3E).

Spinal p38 MAPK inhibition restores pLTF after IH-1

We next tested the role of spinal p38 MAPK in pLTF impairment following IH-1. We targeted p38 MAPK since it is an enzyme activated by multiple pro-inflammatory molecules that can subsequently trigger additional inflammation. Intrathecal application of the p38 MAPK inhibitor (SB 202190, 1 mM) caused no immediate alteration in phrenic burst amplitude or other physiological variables.

As expected, PaO₂, pH and mean arterial pressure were affected by hypoxia during AIH (p<0.001). Body temperature in the Nx + veh (p<0.05) and IH-1 + veh (p<0.01) groups significantly decreased during hypoxia, but returned to baseline values by the end of the experiments. Small PaO₂ variations beyond those hypoxic episodes occurred, but PaO₂ remained >180 mmHg in all cases. Differences in pH and mean arterial pressure were also evident in some

groups, but remained above acceptable levels (see Methods). These changes were observed in all treatment groups and likely reflect time-dependent changes in this experimental preparation.

Spinal p38 MAPK inhibition did not affect the short-term hypoxic phrenic response, but restored pLTF in IH-1 pre-treated rats (Fig 4). The hypoxic response magnitude was not different between any AIH treated groups ($p=0.948$; Fig 4D). Spinal p38 inhibition did not affect pLTF in normoxia pre-treated rats (Fig 4A, E). Nx + veh and Nx + p38 inhib treated rats both exhibited significant pLTF ($p<0.001$) 60 min (data not shown) and 90 min post-AIH (Fig 4E) and were not different from each other at either time point (60 min: $p=0.382$ and 90 min: $p=0.266$). Spinal p38 MAPK inhibition significantly enhanced pLTF in IH-1 pre-treated rats (both $p<0.001$, Fig 4B, E). This pLTF was significantly greater than time control + veh (60 min: $p=0.029$; 90 min: $p=0.008$) and time control + p38 inhib rats (60 min: $p=0.003$, 90 min: $p<0.001$). With IH-1 + p38 MAPK inhibition, AIH-induced pLTF was significantly greater than in IH-1 + veh at 60 min ($p=0.046$) and 90 min ($p=0.018$) post-AIH, but was not significantly greater than in Nx + veh (60 min: $p=0.890$; 90 min; $p=0.289$) or Nx + p38 pre-treated rats (60 min: $p=0.487$, 90 min: $p=0.289$). In contrast, IH-1 + veh rats did not express significant pLTF at 60 min or 90 min.

Increased phosphorylated p38 MAPK protein levels in motoneurons and microglia

Since spinal p38 MAPK inhibition restores pLTF after IH-1, we evaluated dually phosphorylated (activated) p38 MAPK expression after IH-1 via immunofluorescence. At low magnification (20X), some phospho-p38 MAPK positive cells were appreciated in normoxia treated rats that co-localized with both Cholera Toxin B labeled phrenic motoneurons and CD11b (used to identify microglia) of the C₃-C₆ ventral horn (Fig 5A, top). After IH-1, qualitatively more phrenic motoneurons and adjacent microglia were visibly positive for phospho-p38 MAPK, and the intensity of staining within individual cells appeared increased (Fig

5A, bottom). This difference between normoxia and IH-1 is more evident in higher magnification images of the phrenic motor nucleus region (100X, Fig 5B; from boxed region in Fig 5A). This immunofluorescence analysis suggests that IH-1 increased activated p38 MAPK in both microglia and identified phrenic motoneurons.

DISCUSSION

Although inflammation is prominent in nearly all clinical disorders, little is known concerning how inflammation alters the neural control of breathing. Here, we studied a novel inflammatory stimulus induced by 8 hours of nocturnal intermittent hypoxia. We demonstrate that even one “night” of intermittent hypoxia elicits spinal inflammation that undermines AIH-induced pLTF. One key molecule in pLTF impairment is p38 MAPK. This is the first demonstration of a physiologically relevant stimulus (IH-1) impairing respiratory motor plasticity because of spinal inflammation. Further, this is the first demonstration that spinal p38 MAPK is a critical link between inflammation and pLTF impairment. Thus, p38 MAPK is a molecule of considerable interest as modest protocols of intermittent hypoxia have considerable promise as a treatment for diverse clinical disorders that impair movement (e.g. spinal injury and ALS; (28)).

The surprising results presented here have profound implications concerning the potential impact of even one night of sleep apnea, particularly in individuals with sub-clinical OSA. In such individuals, exacerbating factors such as alcohol consumption or acute respiratory infection may tip the balance, leading to a night of obstructions and sleep apnea. Based on our results, even transient OSA may trigger inflammation, undermining mechanisms of compensation (e.g. pLTF or LTF in upper airway motor pools). The result may be a positive feedback loop, where one night of OSA leads to the next. This concept is worthy of additional investigation.

The IH-1 protocol used here differs from other protocols of chronic intermittent hypoxia (CIH). CIH enhances carotid body hypoxic sensitivity (29-32), but these CIH protocols were considerably longer in duration than IH-1. Although the extent of carotid body inflammation is not known in either the earlier studies using CIH or in our study after IH-1, it is possible that

CIH elicits qualitatively different or greater systemic inflammation than IH-1, thereby increasing carotid body sensitivity and increasing the hypoxic ventilatory response. The lack of change in the short-term hypoxic response following IH-1 is consistent with the hypothesis that IH-1 is not sufficient to elicit such profound carotid body plasticity.

Differences in the type or magnitude of inflammation induced by CIH versus IH-1 may also account for differences in the effect of intermittent hypoxia pre-conditioning on AIH-induced pLTF. Longer CIH protocols (5 min hypoxic episodes, 5 min intervals, 12 hours/day, 7 days, during the active period) that enhance pLTF (33) and ventilatory LTF (34, 35) may be due to differences in inflammatory signaling molecules or increased expression of trophic factors known to promote respiratory plasticity (22, 25, 36). After IH-1, the negative effects of inflammation may predominate, disturbing critical features of the respiratory control system, including respiratory motor plasticity. The presence or absence of respiratory plasticity after prolonged intermittent hypoxia may be determined by the duration of intermittent hypoxia exposure, diurnal variation of episodes, state of the inflammatory cascade, expression of pro-plasticity molecules (e.g. growth/trophic factors), or other as yet undetermined factors (15).

A fundamental understanding of the mechanisms that undermine AIH-induced motor plasticity is of considerable interest to many clinical disorders. For example, repetitive (low dose) intermittent hypoxia has been therapeutically used to restore respiratory motor function in rodent models of cervical spinal injury (23) and ALS (37), as well as in humans with chronic, incomplete spinal injuries (38). Similarly, therapeutic intermittent hypoxia is restorative for non-respiratory motor functions, such as leg strength (39) and walking (23, 40) in both rodent models and humans with chronic, incomplete, spinal injuries. Since patients with spinal injury and ALS are prone to systemic infections and inflammation, inflammation may undermine the therapeutic

efficacy of low dose intermittent hypoxia. Here, we have begun to elucidate the means of counter-acting inflammation and its impact on AIH-induced motor plasticity. This knowledge may be of considerable benefit in using low dose intermittent hypoxia as a therapeutic intervention in the future.

Systemic treatment with ketoprofen restores pLTF, demonstrating that systemic inflammation is the essential feature of IH-1 undermining pLTF. Ketoprofen is a potent anti-inflammatory and analgesic agent used in many species, including humans (41) and rats (42, 43). Ketoprofen inhibits prostaglandin and leukotriene synthesis peripherally (44) and centrally (45, 46). Restoration of pLTF by ketoprofen after IH-1 most likely results from 1) diminished CNS inflammation, 2) indirect effects resulting from decreased transduction of inflammatory signals via the vagus nerve (47), 3) decreased systemic expression of cytokines that do cross the blood-brain barrier (48), and/or 4) preventing disruption of the blood-brain barrier which can lead to inhibition of synaptic plasticity (49). Whereas the systemic ketoprofen data support the hypothesis that inflammation specifically undermines pLTF, a targeted inflammatory treatment would be more beneficial since chronic use of anti-inflammatory drugs is associated with gastrointestinal problems. Additionally, systemic NSAID treatment does not identify where the relevant inflammation occurs.

Spinal administration of the p38 MAPK inhibitor provides information concerning the site of inflammation relevant to impairment of pLTF. Because inflammatory responses are complex in their temporal dynamics and the diversity of inflammatory molecules involved, we targeted p38 MAPK, which often acts as a convergent, downstream molecule activated by many pro-inflammatory molecules, stress, and apoptosis (50). Additionally, p38 MAPK also increases posttranslational modification and subsequently transcription of inflammatory molecules (51,

52). Data presented here are the first to demonstrate that p38 MAPK is critical in IH-1 impairment of pLTF. Specifically, activated (phosphorylated) p38 MAPK increases within phrenic motoneurons and adjacent microglia. It is not yet clear if p38 MAPK orchestrates the relevant inflammation or is a convergent, downstream molecule that directly impairs pLTF; nor whether the relevant p38 MAPK is in phrenic motoneurons, adjacent microglia or both. Previous work has demonstrated increased p38 MAPK in microglia after spinal nerve ligation (53-55), spinal cord injury (56), and is associated with other conditions that cause chronic pain (57, 58). Additional research is warranted on the cell types involved and the sequence of cellular activation.

The p38 MAPK inhibitor used here (SB 202190) is reported to be a specific inhibitor of p38 MAPK (59, 60); however, other p38 MAPK inhibitors with similar chemical structures (e.g. SB 203580) directly inhibit cyclooxygenase (COX) activity (61). Although no studies are available concerning the actions of SB 202190 on COX activity, we cannot rule out COX inhibition as a contributor to pLTF restoration after IH-1. Regardless, we clearly demonstrate that relevant inflammatory processes are localized within the cervical spinal cord after IH-1.

In conclusion, we demonstrate a profound link between systemic inflammation initiated by physiologically relevant intermittent hypoxia and impairment of respiratory motor plasticity. Even one night (8 hours) of intermittent hypoxia abolishes pLTF and initiates cervical spinal inflammation. We describe initial steps in the process of identifying mechanism(s) whereby inflammation impairs plasticity. Systemic anti-inflammatory treatment or spinal p38 MAPK inhibitors restore pLTF.

It is essential to understand the impact of inflammation on the neural control of breathing, including respiratory plasticity. In clinical conditions associated with systemic inflammation, we

postulate that the inflammation undermines respiratory plasticity, potentially explaining at least some differences in results reported in humans with CIH or OSA (15). While it is unclear whether plasticity stabilizes or destabilizes breathing, it has become clear that understanding links between inflammation and respiratory plasticity are necessary to determine functional outcomes and appropriate treatments. Understanding and targeting relevant pro-inflammatory molecules may lead to new therapeutic interventions to restore plasticity in breathing and non-respiratory motor functions in devastating disorders that compromise ventilatory capacity in the presence of continual inflammatory activity.

FIGURE 1

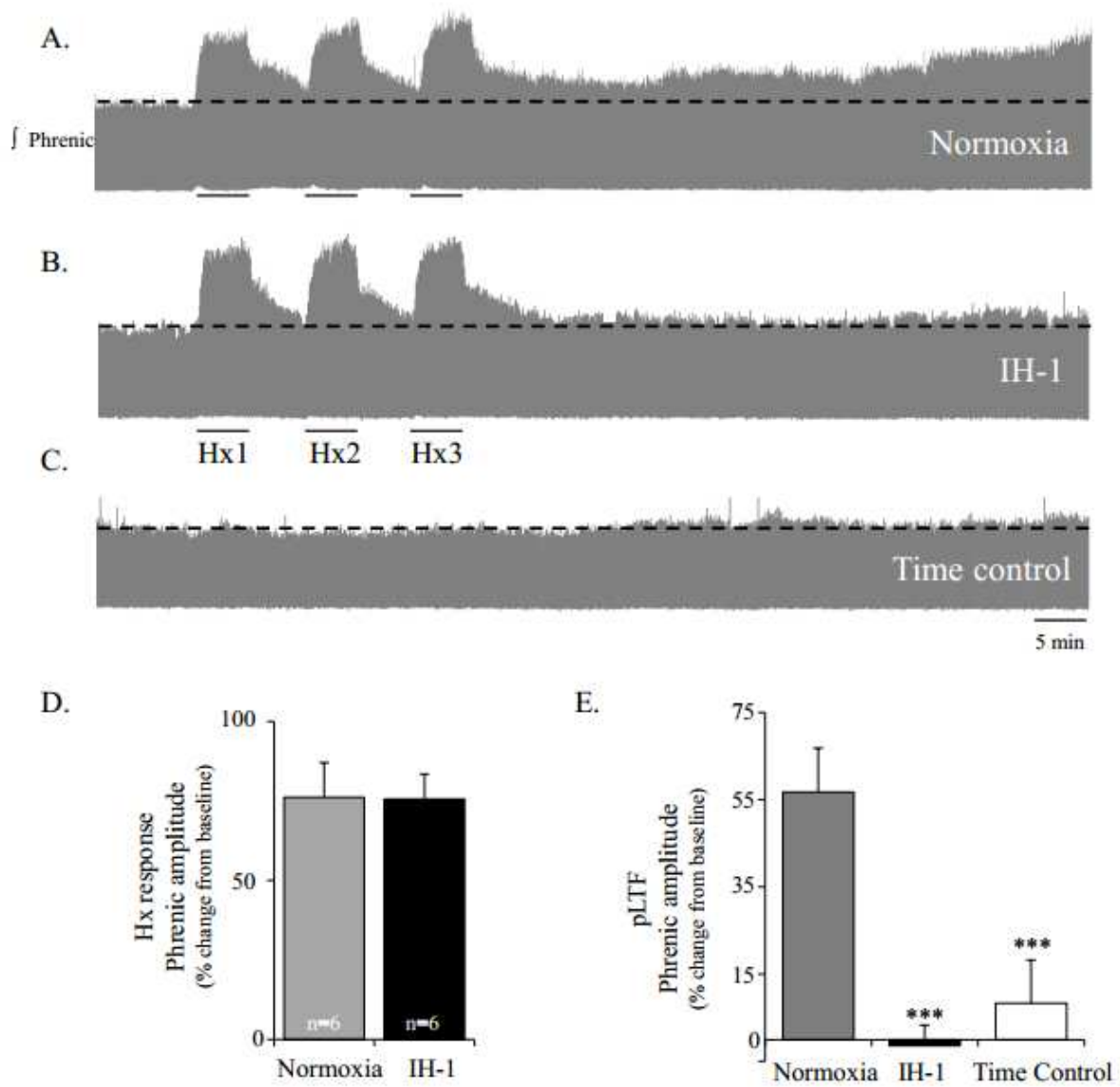


Figure Legend 1**One night of intermittent hypoxia (IH-1) significantly reduced AIH-induced pLTF.**

Representative integrated phrenic neurograms during AIH protocols for rats receiving normoxia (A), IH-1 (B), and time control (no AIH, C). Development of pLTF is evident as a progressive increase in phrenic nerve amplitude from baseline (black dashed line) over 60 min in normoxic rats, but not in IH-1-treated or time control rats. D. Previous exposure to IH-1 did not alter hypoxic responses ($76 \pm 11\%$) vs. normoxic ($76 \pm 8\%$) treated rats (t-test). E. pLTF was abolished after IH-1 ($-1 \pm 5\%$, $n=6$) compared to normoxia ($56 \pm 10\%$, $n=6$). There was no increase in phrenic nerve amplitude in time control rats ($8 \pm 10\%$, $n=6$). (***) $p < 0.001$ significant difference from normoxia, Two-Way RM ANOVA, Fisher LSD post-test).

FIGURE 2

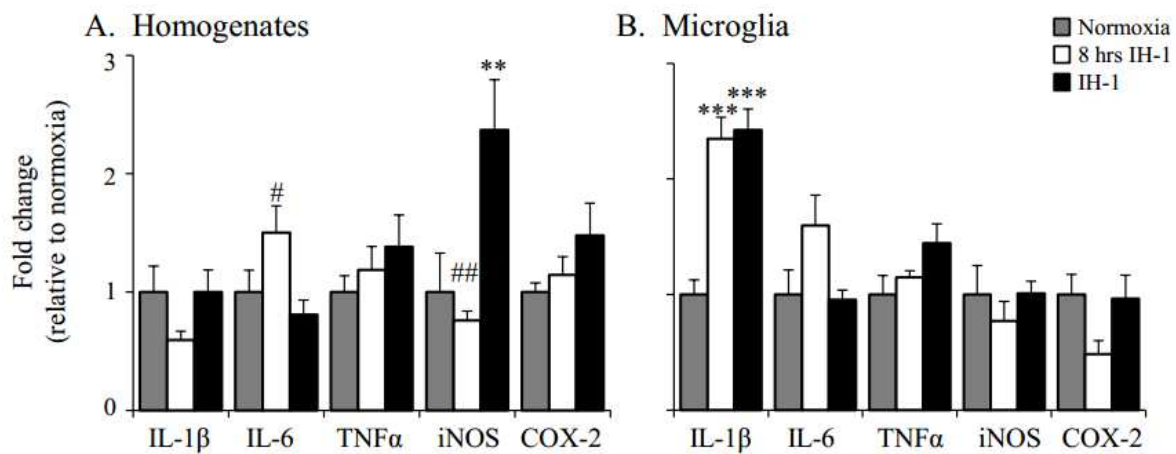


Figure Legend 2**One night of intermittent hypoxia (IH-1) increased inflammatory gene expression in the cervical spinal cord.**

A. Homogenate samples isolated from the cervical spinal cord containing neurons, astrocytes, and microglia showed an initial increase in IL-6 (1.5 ± 0.2 fold change) immediately after 8 hrs of intermittent hypoxia and an increase in iNOS (2.4 ± 0.4 fold change) mRNA after IH-1 which were significantly greater than normoxia and samples taken immediately after 8 hrs IH. B. Isolated microglia demonstrated a sustained increase in IL-1 β immediately after 8 hrs IH (2.4 ± 0.2 fold change) and IH-1 (2.4 ± 0.2 fold change) compared to normoxic controls. No other inflammatory genes in the homogenate or microglia samples changed significantly at either time point after IH. (** $p < 0.01$, *** $p < 0.001$ significant difference from normoxic controls, # $p < 0.05$, ## $p < 0.01$ significant different from IH-1, One-Way ANOVA, Fisher LSD post-test).

FIGURE 3

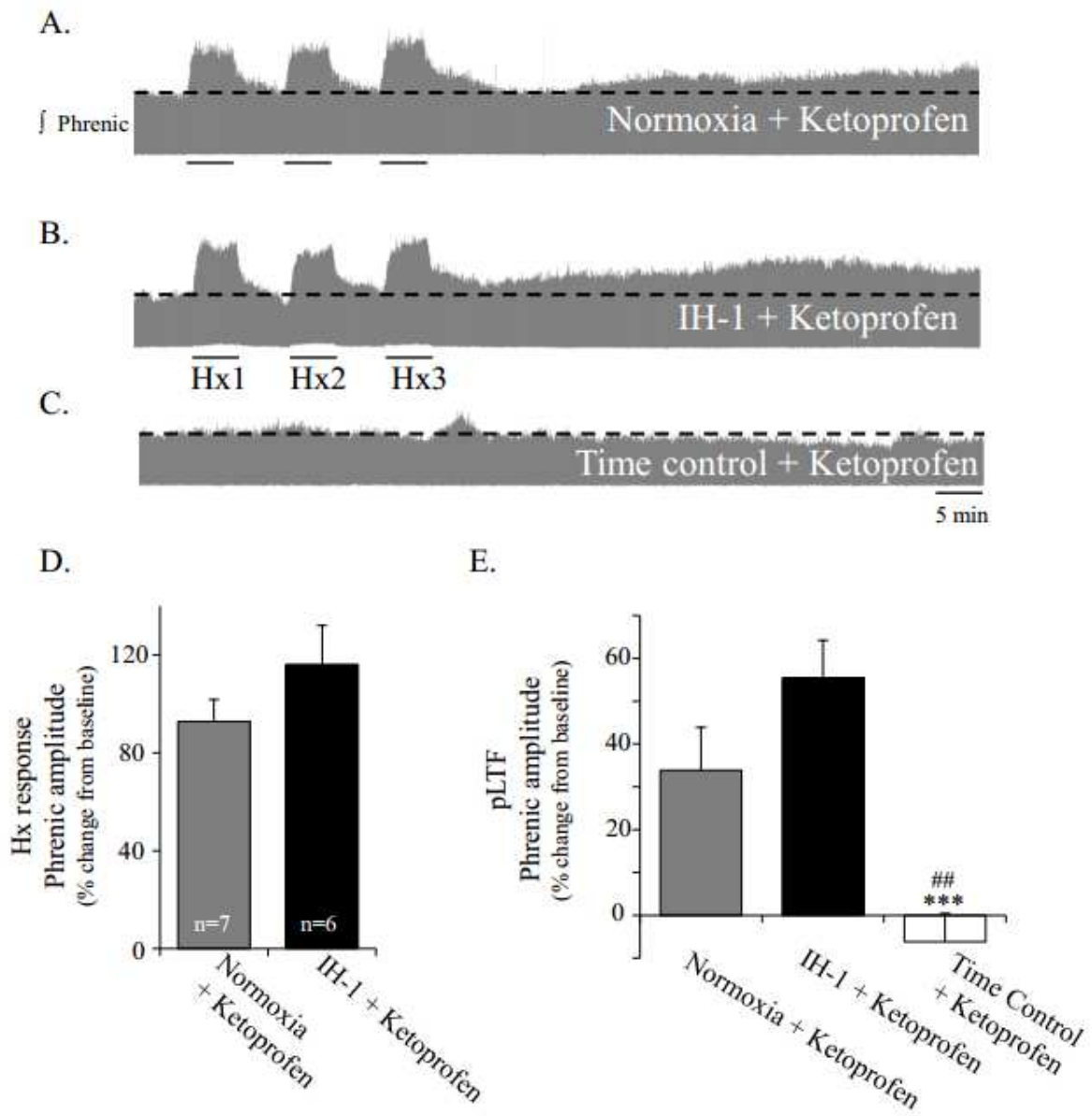


Figure Legend 3

Inflammation after one night of intermittent hypoxia (IH-1) impairs pLTF. Representative integrated phrenic neurograms during AIH protocols for rats receiving normoxia + ketoprofen (nonsteroidal anti-inflammatory, 12.5 mg/kg, i.p., A), IH-1 + ketoprofen (B), and time control + ketoprofen (no AIH, C). Development of pLTF is evident as a progressive increase in phrenic nerve amplitude from baseline (black dashed line) over 90 min in normoxic + ketoprofen and IH-1 + ketoprofen rats, but not in Time Control + ketoprofen rats. D. Ketoprofen did not alter short-term hypoxic responses between normoxic ($93\pm 9\%$) and IH-1-treated ($116\pm 16\%$) rats (t-test). E. pLTF was not different between normoxic + ketoprofen ($34\pm 10\%$, n=7) or IH-1 + ketoprofen-treated rats ($55\pm 9\%$, n=6), but was significantly greater than time controls + ketoprofen ($-6\pm 7\%$, n=6). (***) $p < 0.001$ significant difference from , Two-Way RM ANOVA, Fisher LSD post-test).

FIGURE 4

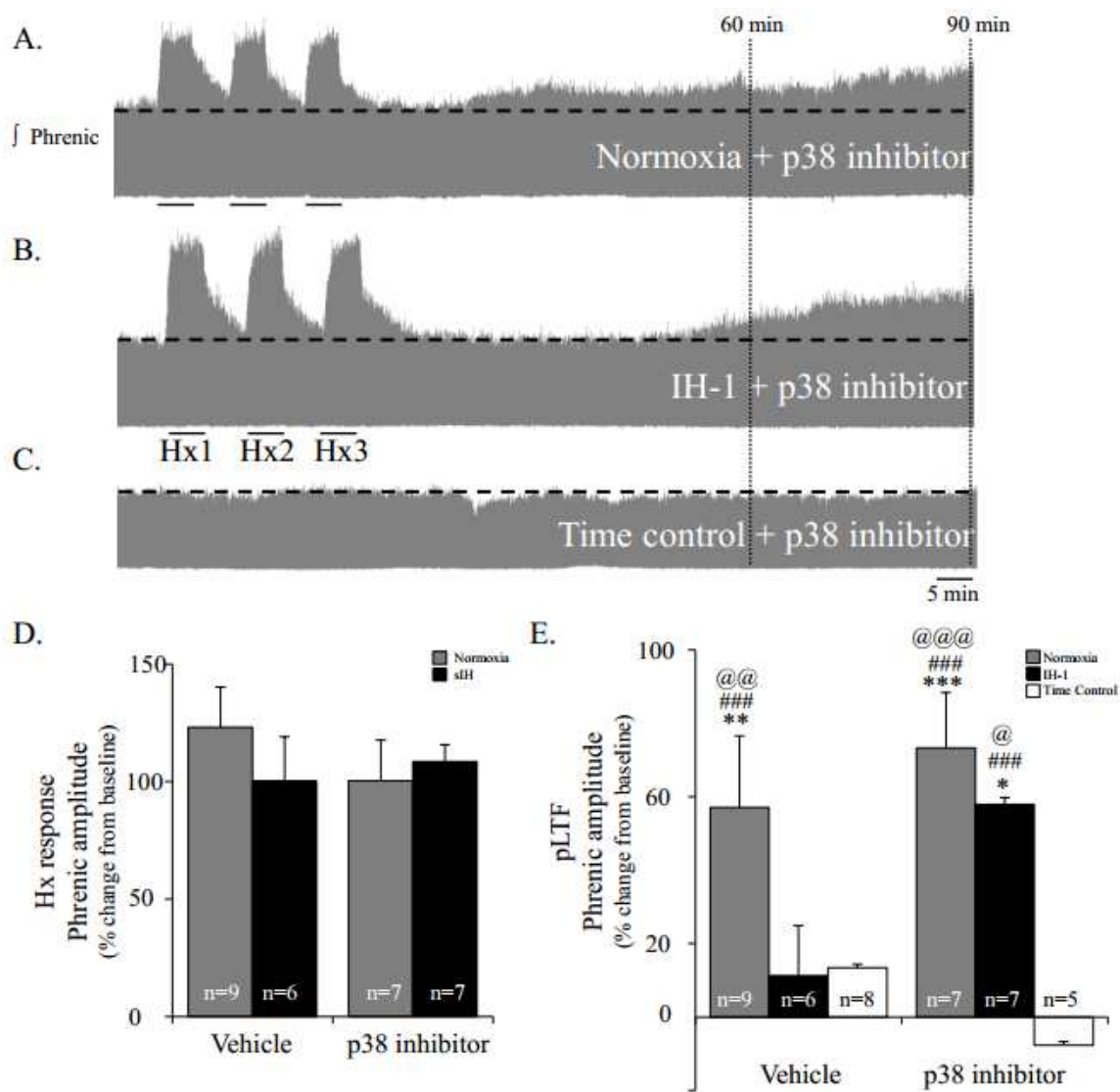


Figure Legend 4

Inhibition of p38 MAPK restored AIH-induced pLTF after IH-1, but did not alter the hypoxic responses or pLTF in normoxic controls. Representative integrated phrenic neurograms during AIH protocols for rats receiving normoxia + p38 MAPK inhibitor (SB202190, 1mM, intrathecal) (A), IH-1 + p38 MAPK inhibitor (B), and time control + p38 MAPK inhibitor (no AIH, C). Development of pLTF is evident as a progressive increase in phrenic nerve amplitude from baseline (black dashed line) over 90 min in normoxic + p38 MAPK inhibitor and IH-1 + p38 MAPK inhibitor rats, but not in Time Control + p38 MAPK inhibitor rats. D. Inhibition of p38 MAPK did not alter short-term hypoxic responses between normoxic + veh ($123\pm 17\%$), IH-1 + veh ($100\pm 19\%$), Nx + p38 inhib ($100\pm 17\%$), and IH-1 + p38 inhib ($108\pm 7\%$) rats (t-test). E. At 90 min post-AIH, IH-1 + vehicle ($11\pm 14\%$) was significantly reduced compared to normoxic + vehicle ($57\pm 19\%$), normoxic + p38 inhibitor ($73\pm 15\%$), and IH-1 + p38 inhibitor ($58\pm 2\%$), but was not different from time controls + vehicle ($13\pm 11\%$) or time controls + p38 inhibitor ($-7\pm 13\%$). After p38 inhibitor, there was no difference between rats treated with IH-1 or normoxia. (* $p < 0.05$, ** $p < 0.01$, *** $p < 0.001$ significantly different from time control + vehicle; ### $p < 0.001$ significantly different from time control + p38 inhibitor; @ $p < 0.05$, @@ $p < 0.01$, @@@ $p < 0.001$ significantly different from IH-1 + vehicle; Two-Way RM ANOVA, Fisher LSD post-test).

FIGURE 5

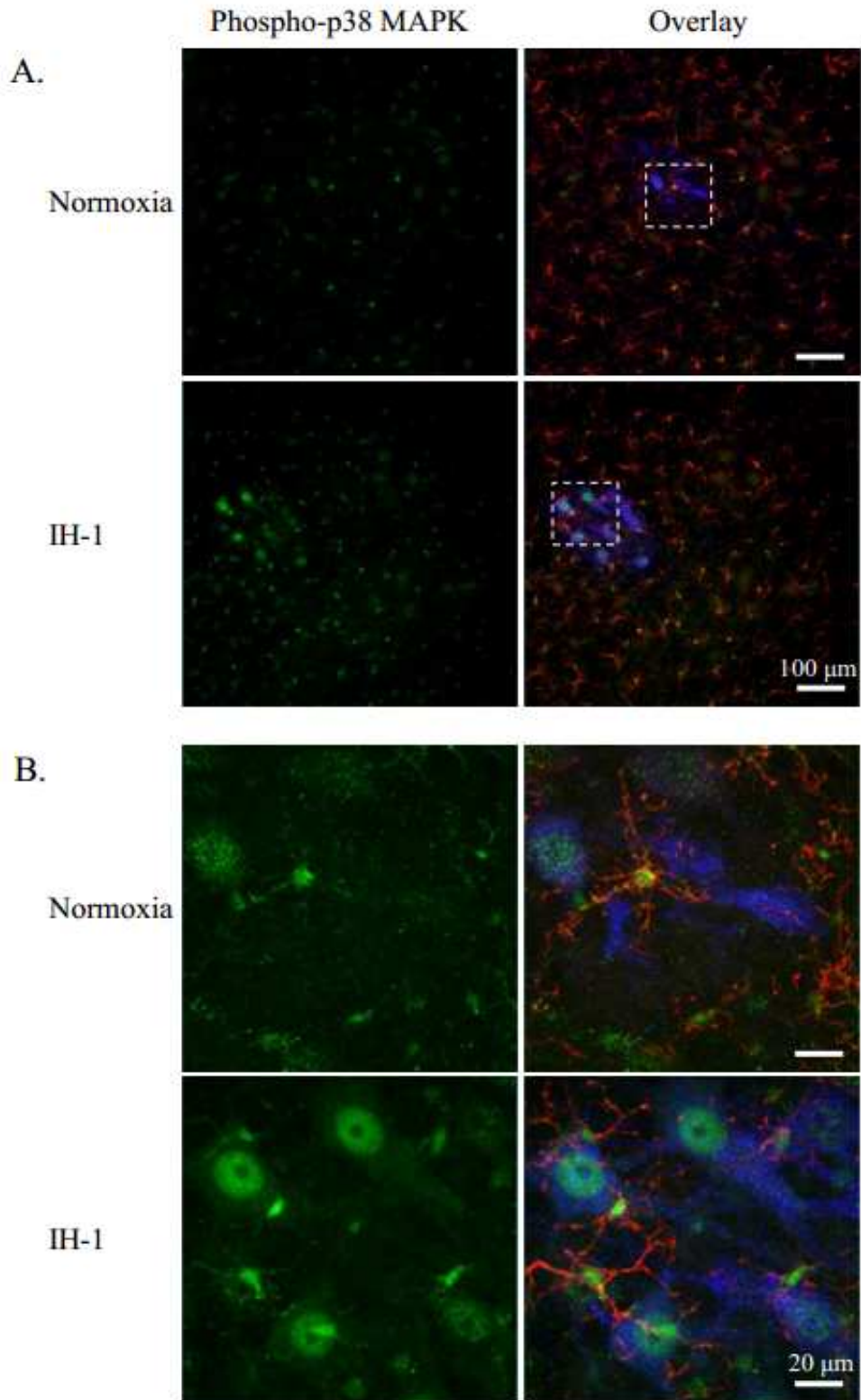


Figure Legend 5

Phospho-p38 MAPK immunofluorescence is evident in back-labeled phrenic motoneurons and microglia of the ventral cervical spinal cord after IH-1, but not after normoxia. A. Confocal images (20X) show representative phospho-p38 MAPK (green) staining in the ventral cervical spinal cord after IH-1 (n=6), which co-localized with back-labeled phrenic motoneurons (Cholera Toxin B, blue) and CD11b (microglia label, red). Minimal staining was evident after the normoxia treatment (n=6, bottom panels). B. Higher magnification (100X) from the boxed area in A. of the phrenic motor nucleus clearly shows co-localization with phrenic motoneurons and microglia after IH-1 (top panels). Less co-localization is evident after normoxia (bottom panels).

TABLE 1

Time	Treatment Group	Temperature	PaO ₂	PaCO ₂	pH	MAP
Baseline	Time Control	37.7±0.1	343±12	47±1	7.336±0.006	121±5
	IH-1 + AIH	37.7±0.1	328±17	45±1	7.364±0.008	116±7
	Nx + AIH	37.5±0.2	325±20	45±1	7.371±0.005	120±5
Hx	Time Control	37.6±0.1	346±5	46±1	7.330±0.008	118±6
	IH-1 + AIH	37.6±0.1	42±2	46±1	7.350±0.008	66±9
	Nx + AIH	37.3±0.1	36±2	45±1	7.343±0.005	64±7
60 min	Time Control	37.5±0.1	347±3	47±1	7.343±0.012	114±7
	IH-1 + AIH	37.6±0.1	347±10	45±0.5	7.391±0.010	112±7
	Nx + AIH	37.4±0.2	308±15	45±1	7.371±0.005	115±7

a= p<0.001 diff from all other

HX groups

b= p<0.05 from TC within 60
min

bb = p<0.01 from TC within 60
min

Table 1 Legend

Physiological variables for Sprague-Dawley 211 rats during electrophysiological

experiments after IH-1 and normoxia with AIH (acute intermittent hypoxia), or time control.

TABLE 2

Time	Treatment Group	Temperature	PaO ₂	PaCO ₂	pH	MAP
Baseline	Time Control	37.2±0.1	342±5	43±2	7.380±0.010	102±4 ^f
	Nx, keto + AIH	37.4±0.1	325±13	44±1	7.376±0.006	110±5
	IH-1, keto + AIH	37.4±0.1	340±5	43±1	7.365±0.009	116±3
Hx	Time Control	37.3±0.1	339±4 ^a	43±2	7.381±0.010	102±3 ^a
	Nx, keto + AIH	37.3±0.1	37±2 ^b	44±1	7.367±0.010	55±5 ^b
	IH-1, keto + AIH	37.4±0.1	37±1 ^b	42±1	7.367±0.010 ^c	54±3 ^b
60 min	Time Control	37.3±0.1	330±4	43±2	7.389±0.010	100±4
	Nx, keto + AIH	37.4±0.1	296±11 ^{a,c}	44±1	7.376±0.010	104±4
	IH-1, keto + AIH	37.4±0.2	327±8	44±1 ^d	7.376±0.006	107±6

a= p<0.001 diff from all other groups within time point

b= p<0.001 different from other time points within group

c = p<0.01 different from baseline within group

d = p<0.05 different from other time points within group

e = p<0.01 different from other time points within group

f = p<0.05 different from IH-1, keto + AIH within time point

Table 2 Legend

Physiological variables for Sprague-Dawley 211 rats during electrophysiological experiments after IH-1 and normoxia with AIH (acute intermittent hypoxia), or time control and systemic treatment with ketoprofen.

TABLE 3

Time	Treatment Group	Temperature	PaO ₂	PaCO ₂	pH	MAP
Baseline	Time Control, veh	37.6±0.2	331±9 ¹	45±1	7.364±0.005	124±2
	Nx, veh	37.3±0.1	310±12	45±1	7.355±0.011	117±5
	IH-1, veh	37.3±0.3	311±9	45±1	7.337±0.013	128±5
	Nx, p38	37.5±0.1	328±3	44±1	7.367±0.007 ⁴	124±6
	IH-1, p38	37.2±0.1	322±10	44±1	7.346±0.007	125±7
	Time control, p38	37.3±0.3	312±9.5	45±1	7.324±0.018 ³	134±3 ¹
Hx	Time Control, veh	37.6±0.1	328±5 ²	45±1	7.361±0.005	123±3 ²
	Nx, veh	37.3±0.1	38±1 ^a	45±1	7.341±0.014	62±7 ^a
	IH-1, veh	37.2±0.3	40±1 ^a	46±1	7.322±0.014 ³	71±7 ^a
	Nx, p38	37.4±0.1	35±1 ^a	44±2	7.339±0.012 ^{b,3}	63±6 ^a
	IH-1, p38	37.2±0.1	38±1 ^a	45±1	7.332±0.011	67±5 ^a
	Time Control, p38	37.2±0.2	311±10 ²	45±1	7.329±0.014	134±3 ²
60 min	Time Control, veh	37.6±0.1	315±10	44±1	7.381±0.008 ^{b,c}	118±3
	Nx, veh	37.5±0.1	297±11	45±1	7.359±0.009	107±5
	IH-1, veh	37.5±0.2	305±11	45±1	7.339±0.017 ^{c,3}	115±5
	Nx, p38	37.6±0.1	305±5 ^b	45±1	7.362±0.010 ^c	119±5
	IH-1, p38	37.5±0.1	299±8 ^b	44±1	7.348±0.005 ^c	114±4 ^b
	Time Control, p38	37.2±0.2	308±12	45±1	7.343±0.014 ³	121±5 ^a
90 min	Time Control, veh	37.6±0.1	327±3 ¹	44±1	7.388±0.007 ^{b,c}	117±6
	Nx, veh	37.5±0.1	295±9	45±1	7.361±0.009 ^c	108±4
	IH-1, veh	37.3±0.2	300±10	46±2	7.341±0.024 ^c	113±5
	Nx, p38	37.5±0.1	308±4 ^{b,d,3}	44±2	7.367±0.011 ^c	116±6 ^b
	IH-1, p38	37.5±0.1	303±7	45±1	7.359±0.006 ^c	109±4 ^b
	Time Control, p38	37.4±0.2	307±11	45±1	7.376±0.011 ^{b,c}	123±4 ¹

Table 3 Legend

Physiological parameters for Sprague-Dawley rats during electrophysiological experiments after IH-1, normoxia, or time control and spinal inhibition of p38 MAPK (SB202190, 1mM).

a= $p < 0.001$ diff from all other time points within treatment group

b= $p < 0.05$ different from baseline within treatment group

c = $p < 0.05$ different from Hx within treatment group

1 = $p < 0.05$ different from Nx, veh within time point

2 = $p < 0.001$ different from treatment groups receiving AIH within Hx

3 = $p < 0.01$ different from Time Control, veh within time point

4 = $p < 0.05$ different from Nx, p38 and Nx, veh

REFERENCES

1. Huxtable AG, Vinit S, Windelborn JA, Crader SM, Guenther CH, Watters JJ, Mitchell GS. Systemic inflammation impairs respiratory chemoreflexes and plasticity. *Respir Physiol Neurobiol* 2011;178:482-489.
2. Teeling JL, Cunningham C, Newman TA, Perry VH. The effect of non-steroidal anti-inflammatory agents on behavioural changes and cytokine production following systemic inflammation: Implications for a role of cox-1. *Brain Behav Immun* 2010;24:409-419.
3. Di Filippo M, Sarchielli P, Picconi B, Calabresi P. Neuroinflammation and synaptic plasticity: Theoretical basis for a novel, immune-centred, therapeutic approach to neurological disorders. *Trends Pharmacol Sci* 2008;29:402-412.
4. Woolf CJ, Salter MW. Neuronal plasticity: Increasing the gain in pain. *Science* 2000;288:1765-1769.
5. Coull JA, Beggs S, Boudreau D, Boivin D, Tsuda M, Inoue K, Gravel C, Salter MW, De Koninck Y. Bdnf from microglia causes the shift in neuronal anion gradient underlying neuropathic pain. *Nature* 2005;438:1017-1021.
6. Liu X, He L, Stensaas L, Dinger B, Fidone S. Adaptation to chronic hypoxia involves immune cell invasion and increased expression of inflammatory cytokines in rat carotid body. *American journal of physiology Lung cellular and molecular physiology* 2009;296:L158-166.
7. Vereker E, Campbell V, Roche E, McEntee E, Lynch MA. Lipopolysaccharide inhibits long term potentiation in the rat dentate gyrus by activating caspase-1. *The Journal of biological chemistry* 2000;275:26252-26258.
8. Shaw KN, Commins S, O'Mara SM. Lipopolysaccharide causes deficits in spatial learning in the watermaze but not in bdnf expression in the rat dentate gyrus. *Behav Brain Res* 2001;124:47-54.
9. Vinit S, Windelborn JA, Mitchell GS. Lipopolysaccharide attenuates phrenic long-term facilitation following acute intermittent hypoxia. *Respir Physiol Neurobiol* 2011;176:130-135.
10. Huxtable AG, Smith SM, Vinit S, Watters JJ, Mitchell GS. Systemic lps induces spinal inflammatory gene expression and impairs phrenic long-term facilitation following acute intermittent hypoxia. *J Appl Physiol* 2013.

11. Gozal D, Kheirandish-Gozal L. Cardiovascular morbidity in obstructive sleep apnea: Oxidative stress, inflammation, and much more. *Am J Respir Crit Care Med* 2008;177:369-375.
12. Li RC, Row BW, Gozal E, Kheirandish L, Fan Q, Brittian KR, Guo SZ, Sachleben LR, Jr., Gozal D. Cyclooxygenase 2 and intermittent hypoxia-induced spatial deficits in the rat. *Am J Respir Crit Care Med* 2003;168:469-475.
13. Li RC, Row BW, Kheirandish L, Brittian KR, Gozal E, Guo SZ, Sachleben LR, Gozal D. Nitric oxide synthase and intermittent hypoxia-induced spatial learning deficits in the rat. *Neurobiology of Disease* 2004;17:44-53.
14. Mahamed S, Mitchell GS. Is there a link between intermittent hypoxia-induced respiratory plasticity and obstructive sleep apnoea? *Exp Physiol* 2007;92:27-37.
15. Mateika JH, Narwani G. Intermittent hypoxia and respiratory plasticity in humans and other animals: Does exposure to intermittent hypoxia promote or mitigate sleep apnoea? *Exp Physiol* 2009;94:279-296.
16. Baker-Herman TL, Mitchell GS. Phrenic long-term facilitation requires spinal serotonin receptor activation and protein synthesis. *J Neurosci* 2002;22:6239-6246.
17. MacFarlane PM, Mitchell GS. Episodic spinal serotonin receptor activation elicits long-lasting phrenic motor facilitation by an nadph oxidase-dependent mechanism. *J Physiol* 2009;587:5469-5481.
18. Bach KB, Mitchell GS. Hypoxia-induced long-term facilitation of respiratory activity is serotonin dependent. *Respir Physiol* 1996;104:251-260.
19. Crain JM, Nikodemova M, Watters JJ. Expression of p2 nucleotide receptors varies with age and sex in murine brain microglia. *J Neuroinflammation* 2009;6:24.
20. Nikodemova M, Watters JJ. Efficient isolation of live microglia with preserved phenotypes from adult mouse brain. *Journal of Neuroinflammation* 2012.
21. Mantilla CB, Zhan WZ, Sieck GC. Retrograde labeling of phrenic motoneurons by intrapleural injection. *J Neurosci Methods* 2009;182:244-249.
22. Dale EA, Satriotomo I, Mitchell GS. Cervical spinal erythropoietin induces phrenic motor facilitation via extracellular signal-regulated protein kinase and akt signaling. *J Neurosci* 2012;32:5973-5983.

23. Lovett-Barr MR, Satriotomo I, Muir GD, Wilkerson JE, Hoffman MS, Vinit S, Mitchell GS. Repetitive intermittent hypoxia induces respiratory and somatic motor recovery after chronic cervical spinal injury. *J Neurosci* 2012;32:3591-3600.
24. Golder FJ, Fuller DD, Lovett-Barr MR, Vinit S, Resnick DK, Mitchell GS. Breathing patterns after mid-cervical spinal contusion in rats. *Experimental neurology* 2011;231:97-103.
25. Dale-Nagle EA, Satriotomo I, Mitchell GS. Spinal vascular endothelial growth factor induces phrenic motor facilitation via extracellular signal-regulated kinase and akt signaling. *J Neurosci* 2011;31:7682-7690.
26. Guenther CH, Vinit S, Windelborn JA, Behan M, Mitchell GS. Atypical protein kinase c expression in phrenic motor neurons of the rat. *Neuroscience* 2010;169:787-793.
27. Rutledge RG, Cote C. Mathematics of quantitative kinetic per and the application of standard curves. *Nucleic acids research* 2003;31:e93.
28. Dale EA, Ben Mabrouk F, Mitchell GS. Unexpected benefits of intermittent hypoxia: Enhanced respiratory and nonrespiratory motor function. *Physiology* 2014;29:39-48.
29. Rey S, Del Rio R, Alcayaga J, Iturriaga R. Chronic intermittent hypoxia enhances cat chemosensory and ventilatory responses to hypoxia. *J Physiol* 2004;560:577-586.
30. Prabhakar NR, Peng YJ, Kumar GK, Pawar A. Altered carotid body function by intermittent hypoxia in neonates and adults: Relevance to recurrent apneas. *Respir Physiol Neurobiol* 2007;157:148-153.
31. Peng YJ, Overholt JL, Kline D, Kumar GK, Prabhakar NR. Induction of sensory long-term facilitation in the carotid body by intermittent hypoxia: Implications for recurrent apneas. *Proc Natl Acad Sci U S A* 2003;100:10073-10078.
32. Pawar A, Peng YJ, Jacono FJ, Prabhakar NR. Comparative analysis of neonatal and adult rat carotid body responses to chronic intermittent hypoxia. *J Appl Physiol* 2008;104:1287-1294.
33. Ling L, Fuller DD, Bach KB, Kinkead R, Olson EB, Jr., Mitchell GS. Chronic intermittent hypoxia elicits serotonin-dependent plasticity in the central neural control of breathing. *J Neurosci* 2001;21:5381-5388.
34. McGuire M, Zhang Y, White DP, Ling L. Chronic intermittent hypoxia enhances ventilatory long-term facilitation in awake rats. *J Appl Physiol* 2003;95:1499-1508.

35. McGuire M, Zhang Y, White DP, Ling L. Serotonin receptor subtypes required for ventilatory long-term facilitation and its enhancement after chronic intermittent hypoxia in awake rats. *Am J Physiol Regul Integr Comp Physiol* 2004;286:R334-341.
36. Baker-Herman TL, Fuller DD, Bavis RW, Zabka AG, Golder FJ, Doperalski NJ, Johnson RA, Watters JJ, Mitchell GS. Bdnf is necessary and sufficient for spinal respiratory plasticity following intermittent hypoxia. *Nature neuroscience* 2004;7:48-55.
37. Nichols NL, Gowing G, Satriotomo I, Nashold LJ, Dale EA, Suzuki M, Avalos P, Mulcrone PL, McHugh J, Svendsen CN, Mitchell GS. Intermittent hypoxia and stem cell implants preserve breathing capacity in a rodent model of amyotrophic lateral sclerosis. *Am J Respir Crit Care Med* 2013;187:535-542.
38. Tester NJ, Fuller DD, Fromm JS, Spiess MR, Behrman AL, Mateika JH. Long-term facilitation of ventilation in humans with chronic spinal cord injury. *Am J Respir Crit Care Med* 2014;189:57-65.
39. Trumbower RD, Jayaraman A, Mitchell GS, Rymer WZ. Exposure to acute intermittent hypoxia augments somatic motor function in humans with incomplete spinal cord injury. *Neurorehabil Neural Repair* 2012;26:163-172.
40. Hayes HB, Jayaraman A, Herrmann M, Mitchell GS, Rymer WZ, Trumbower RD. Daily intermittent hypoxia enhances walking after chronic spinal cord injury: A randomized trial. *Neurology* 2014;82:104-113.
41. Foster RT, Jamali F, Russell AS, Alballa SR. Pharmacokinetics of ketoprofen enantiomers in healthy subjects following single and multiple doses. *Journal of pharmaceutical sciences* 1988;77:70-73.
42. Foster RT, Jamali F. Stereoselective pharmacokinetics of ketoprofen in the rat. Influence of route of administration. *Drug metabolism and disposition: the biological fate of chemicals* 1988;16:623-626.
43. Carabaza A, Suesa N, Tost D, Pascual J, Gomez M, Gutierrez M, Ortega E, Montserrat X, Garcia AM, Mis R, Cabre F, Mauleon D, Carganico G. Stereoselective metabolic pathways of ketoprofen in the rat: Incorporation into triacylglycerols and enantiomeric inversion. *Chirality* 1996;8:163-172.
44. Cabre F, Fernandez MF, Calvo L, Ferrer X, Garcia ML, Mauleon D. Analgesic, antiinflammatory, and antipyretic effects of s(+)-ketoprofen in vivo. *J Clin Pharmacol* 1998;38:3S-10S.
45. Walker JS. Nsaid: An update on their analgesic effects. *Clin Exp Pharmacol Physiol* 1995;22:855-860.

46. Netter P, Lopicque F, Bannwarth B, Tamisier JN, Thomas P, Royer RJ. Diffusion of intramuscular ketoprofen into the cerebrospinal fluid. *European journal of clinical pharmacology* 1985;29:319-321.
47. Hansen MK, Taishi P, Chen Z, Krueger JM. Vagotomy blocks the induction of interleukin-1beta (il-1beta) mrna in the brain of rats in response to systemic il-1beta. *J Neurosci* 1998;18:2247-2253.
48. Carson MJ, Doose JM, Melchior B, Schmid CD, Ploix CC. Cns immune privilege: Hiding in plain sight. *Immunological reviews* 2006;213:48-65.
49. Lim DC, Pack AI. Obstructive sleep apnea and cognitive impairment: Addressing the blood-brain barrier. *Sleep medicine reviews* 2013.
50. Widmann C, Gibson S, Jarpe MB, Johnson GL. Mitogen-activated protein kinase: Conservation of a three-kinase module from yeast to human. *Physiological reviews* 1999;79:143-180.
51. Kaminska B. Mapk signalling pathways as molecular targets for anti-inflammatory therapy--from molecular mechanisms to therapeutic benefits. *Biochimica et biophysica acta* 2005;1754:253-262.
52. Clark A, Dean J, Tudor C, Saklatvala J. Post-transcriptional gene regulation by map kinases via au-rich elements. *Frontiers in bioscience : a journal and virtual library* 2009;14:847-871.
53. Ji RR, Suter MR. P38 mapk, microglial signaling, and neuropathic pain. *Molecular pain* 2007;3:33.
54. Tsuda M, Mizokoshi A, Shigemoto-Mogami Y, Koizumi S, Inoue K. Activation of p38 mitogen-activated protein kinase in spinal hyperactive microglia contributes to pain hypersensitivity following peripheral nerve injury. *Glia* 2004;45:89-95.
55. Katsura H, Obata K, Mizushima T, Sakurai J, Kobayashi K, Yamanaka H, Dai Y, Fukuoka T, Sakagami M, Noguchi K. Activation of src-family kinases in spinal microglia contributes to mechanical hypersensitivity after nerve injury. *J Neurosci* 2006;26:8680-8690.
56. Hains BC, Waxman SG. Activated microglia contribute to the maintenance of chronic pain after spinal cord injury. *J Neurosci* 2006;26:4308-4317.
57. Cui Y, Chen Y, Zhi JL, Guo RX, Feng JQ, Chen PX. Activation of p38 mitogen-activated protein kinase in spinal microglia mediates morphine antinociceptive tolerance. *Brain Res* 2006;1069:235-243.

58. Boyle DL, Jones TL, Hammaker D, Svensson CI, Rosengren S, Albani S, Sorkin L, Firestein GS. Regulation of peripheral inflammation by spinal p38 map kinase in rats. *PLoS medicine* 2006;3:e338.
59. Lv H, Li S, Zhang J, Liang W, Mu X, Jiang Y. In vitro effects of sb202190 on echinococcus granulosus. *The Korean journal of parasitology* 2013;51:255-258.
60. Manthey CL, Wang SW, Kinney SD, Yao Z. Sb202190, a selective inhibitor of p38 mitogen-activated protein kinase, is a powerful regulator of lps-induced mrnas in monocytes. *J Leukoc Biol* 1998;64:409-417.
61. Borsch-Haubold AG, Pasquet S, Watson SP. Direct inhibition of cyclooxygenase-1 and -2 by the kinase inhibitors sb 203580 and pd 98059. Sb 203580 also inhibits thromboxane synthase. *The Journal of biological chemistry* 1998;273:28766-28772.

APPENDIX 3

**TIME COURSE OF INTERMITTENT HYPOXIA INDUCED MICROGLIAL PRO-
INFLAMMATORY GENE EXPRESSION IN THE MURINE ANIMAL MODEL.**

Stephanie M.C. Smith and Jyoti J. Watters

METHODS

Materials

Hank's Buffered Salt Solution (HBSS) was purchased from Cellgro (Herndon, VA). Glycoblue reagent was purchased from Ambion (Austin, TX). Oligo dT, Random Primers, and RNase inhibitor were purchased from Promega (Madison, WI). Power SYBR green was purchased from Applied Biosystems (Foster City, CA). DEPC and TRI reagent were purchased from Sigma Aldrich (St. Louis, MO). Percoll was purchased from GE Healthcare (Waukesha, WI). DNase was purchased from Worthington Biochemicals (Lakewood, NJ). MMLV reverse transcriptase, and RNase AWAY were purchased from Invitrogen (Carlsbad, CA).

Animals

Experiments were performed on adult, male, C57/BL6 (Harlan Laboratories, Madison, WI) mice, weighing 25-28g. Mice were randomly assigned to intermittent hypoxia or room air groups. Mice were housed in clear polycarbonate cages under standard conditions conditions, with a 12 hour light/dark cycle (6:00am-6:00pm) and *ad libitum* food and water. All protocols were approved by the University of Wisconsin Institutional Animal Care and Use Committee. All efforts were made to minimize animal distress and reduce the numbers used, while permitting the formation of statistically reliable conclusions.

Intermittent Hypoxia (IH) Exposure

All animal exposures were performed using a commercially-designed system (BioSpherix, Redfield, NY), as previously described (Chapter 5). Briefly, animals were housed in standard polycarbonate cages with access to food and water *ad libitum* and maintained in a specialized chamber (12x20x30) connected to a computer controlled system that continuously measures oxygen and carbon dioxide concentrations and changes the gas profile by controlling

gas outlets (Oxycycler model G2 and Watview software). During the sleep cycle (light-on hours), oxygen concentrations were modified to generate a cyclical pattern of either 6% or 21% oxygen every 90 seconds (intermittent hypoxia). During their awake period (lights-off), O₂ concentration was maintained at a steady 21%. During the IH exposure, the rapid airflow was sufficient to prevent CO₂ accumulation, and during the normoxia period, room air was periodically flushed through the system maintain a CO₂ concentration below 0.3%. Normoxic control animals were either housed outside of the hypoxia chamber in room air.

Immunomagnetic Microglia (CD11b⁺) Cell Isolation from IH Treated Mice ± LPS

Mice were exposed to 1, 4, 7, 14, or 28 days of IH. 13±1.5 hours after the last hypoxic exposure CD11b⁺ cells were isolated using previously described methods^{1,2}. Briefly, mice were euthanized with an overdose of isoflurane and perfused with cold 0.1M PBS. The whole brain minus (the cerebellum, medulla, and olfactory bulbs) or the frontal cortex and hippocampus were dissected out and dissociated into a single cell suspension using 0.7mg/ml Papain and 50µg/ml DNase in HBSS. Myelin was removed by high speed centrifugation at 850g in a 26% solution of Percoll in 1X PBS. CD11b⁺ cells were tagged with an anti-CD11b antibody conjugated to a magnetic bead. Magnetically-tagged CD11b⁺ cells were isolated using MS columns according to the Miltenyi MACS protocol. Reagents were kept chilled at 4°C and cells were kept on ice whenever possible to preserve microglial phenotypes. We have previously shown, this method results in a >97% pure CD11b⁺/CD45^{low} cell population^{1,2}, and thus, this population will subsequently be referred to as “microglia.”

RNA extraction/ reverse transcription

RNA was extracted from immunomagnetically isolated microglia according to the TriReagent protocol, with the addition of Glycoblue during the isopropanol incubation. First-

strand cDNA was synthesized from total RNA using MMLV Reverse Transcriptase, and an oligo(dT)/random hexamer cocktail. cDNA was used for qRT-PCR analysis.

Quantitative-Real Time PCR:

cDNA was used in real-time quantitative PCR with Power SYBR Green using either the ABI StepOne or ABI 7500 Fast system (Applied Biosystems/Life Technologies). Primers (Table 1) were designed using Primer 3 software and the specificity was assessed through NCBI BLAST. Primer efficiency was tested through the use of serial dilutions. Verification that the dissociation curve had a single peak with an observed T_m consistent with the amplicon length was performed for every PCR reaction. CT values from duplicate measurements were averaged and normalized to levels of the ribosomal RNA, 18s. Relative gene expression was determined using the $\Delta\Delta CT$ method³.

Statistical analyses:

When comparing two population means, statistical inferences were made using a Student's t-test. IH-treated animals are compared to matched normoxic controls that were harvest at the same time as the IH treated animals. All statistical analyses were performed in SigmaPlot (Sigma Stat version 11(Systat Software, San Jose, CA). Statistical significance was set at $p < 0.05$. Mean data are expressed + 1 SEM.

FIGURE 1

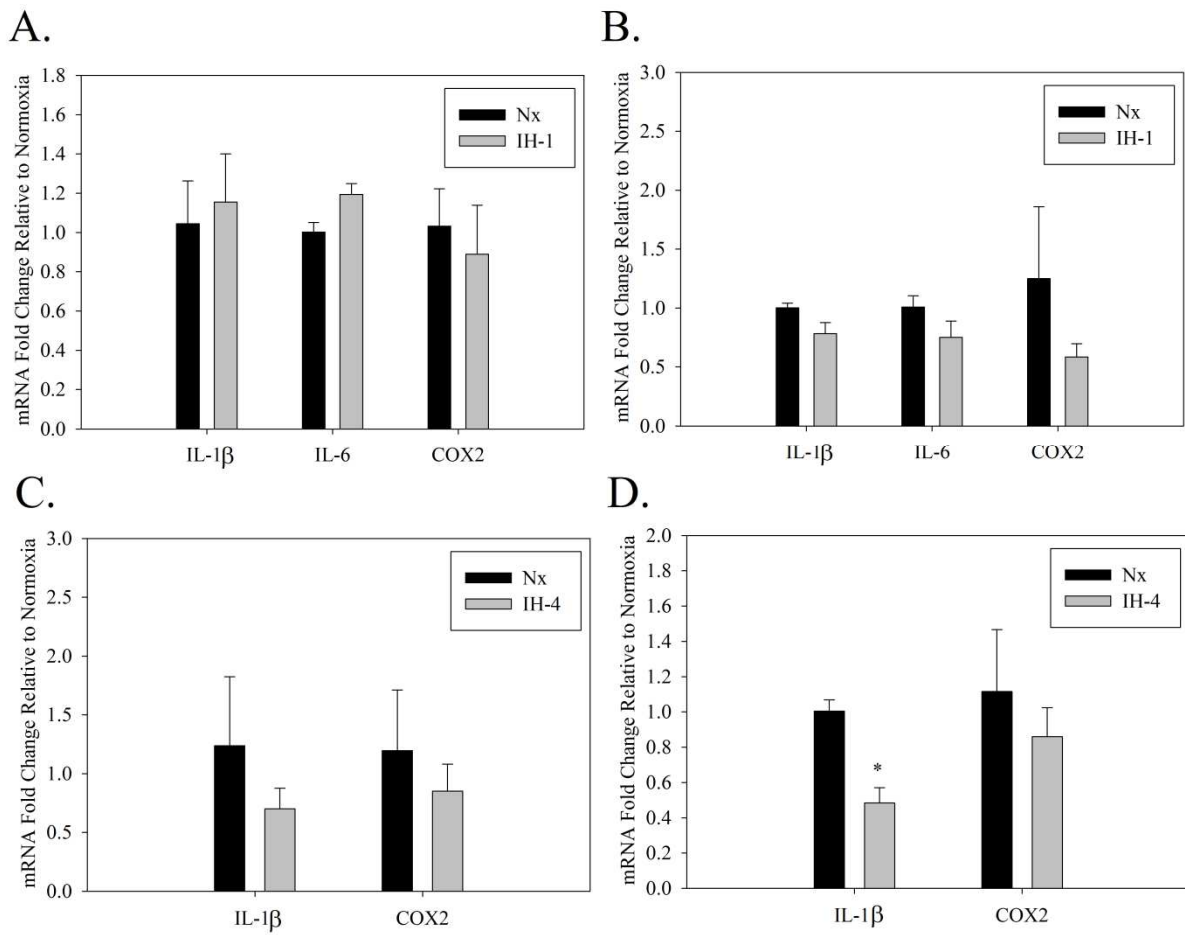


Figure Legend 1***Microglia isolated from mice exposed to 1 or 4 days of IH do not exhibit increased pro-inflammatory gene expression***

Mice were exposed to Nx, 1 or 4 days of IH. 13±1.5 hours following the last hypoxic exposure mice were sacrificed microglia for immunomagnetic microglia isolation from frontal cortical and hippocampal tissues. (A) Fold change of frontal cortical microglial pro-inflammatory gene expression following 1 day of IH relative to normoxic controls. (B) Fold change of hippocampal microglial pro-inflammatory gene expression following 1 day of IH relative to normoxic controls. (C) Fold change of frontal cortical microglial pro-inflammatory gene expression following 4 days of IH relative to normoxic controls. (D) Fold change of hippocampal microglial pro-inflammatory gene expression following 4 days of IH relative to normoxic controls. N=3-5. Mean fold changes + 1 SEM are presented relative to the normoxic control. Statistical significance was determined by a Student's T-test. * symbol represents statistically significant difference from normoxia. *p<0.05; **p<0.01; ***p<0.001

FIGURE 2

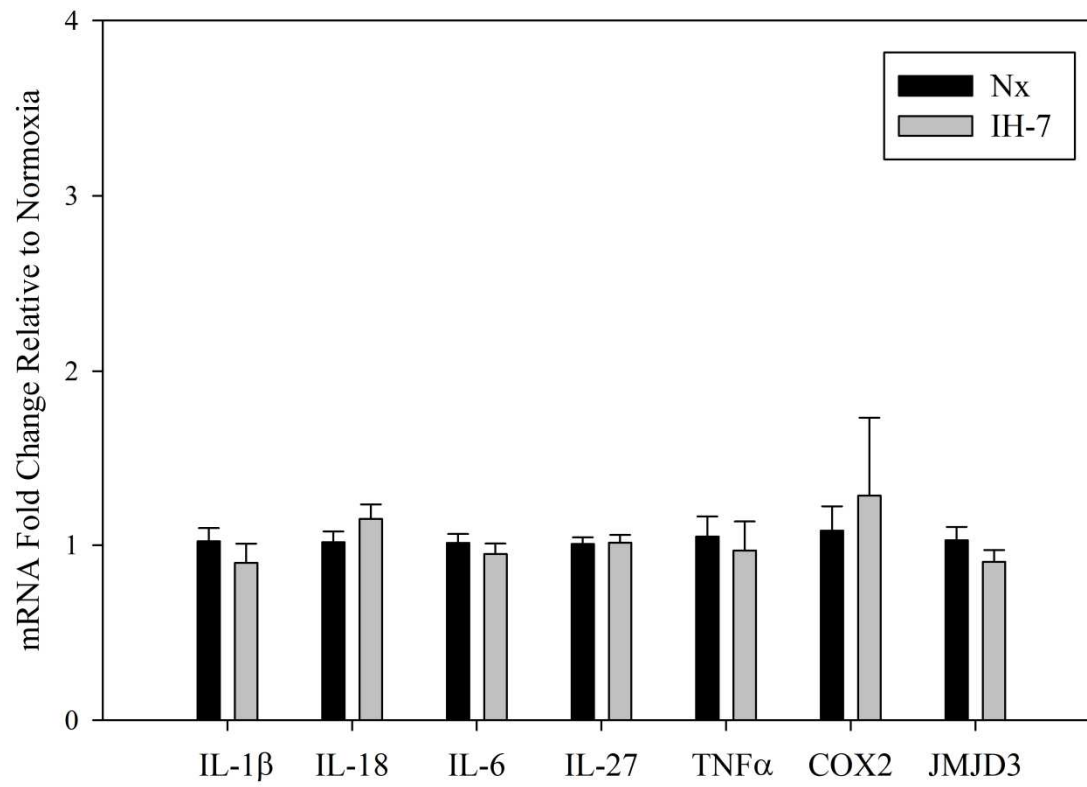


Figure Legend 2

No changes in microglial inflammatory gene expression was observed following 7 days of IH.

Mice were exposed to Nx or 7 days of IH. 13±1.5 hours following the last hypoxic exposure mice were sacrificed and the whole brain was taken for immunomagnetic microglia isolation.

Here we present the fold change of microglial pro-inflammatory gene expression relative to normoxic controls. N=8-10. Mean fold changes + 1 SEM are presented relative to the normoxic control. Statistical significance was determined by a Student's T-test.

FIGURE 3

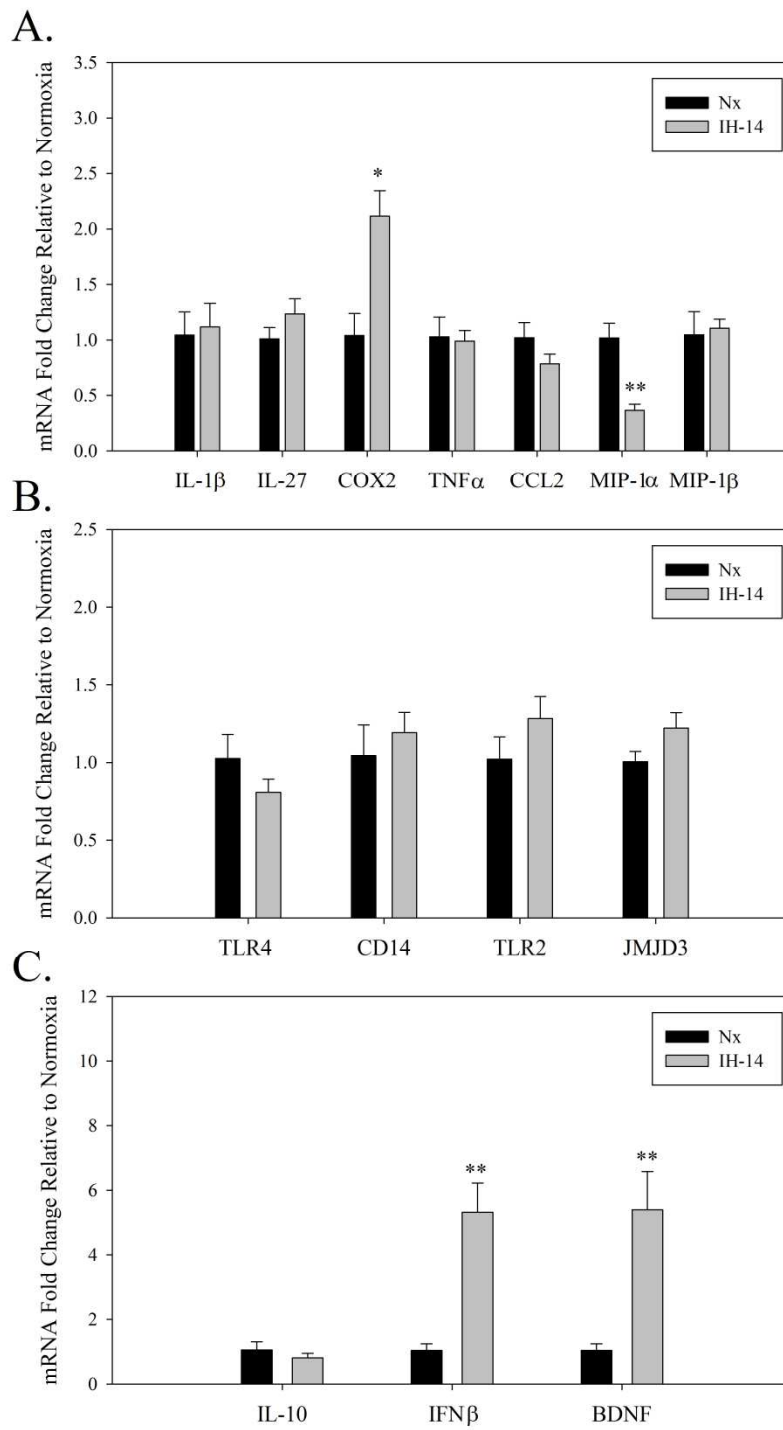


Figure Legend 3

Microglia isolated from mice exposed to IH-14 exhibit increased expression of COX2, IFN β , and BDNF.

Mice were exposed to Nx or 14 days of IH. 13 \pm 1.5 hours following the last hypoxic exposure mice were sacrificed and the whole brain was taken for immunomagnetic microglia isolation.

(A) Fold change of microglial pro-inflammatory gene expression relative to normoxic controls.

(B) Fold change of microglial expression of toll-like receptor and associated proteins. (C) Fold

change of microglial anti-inflammatory/neurotrophic. N=3-5. Mean fold changes + 1 SEM are

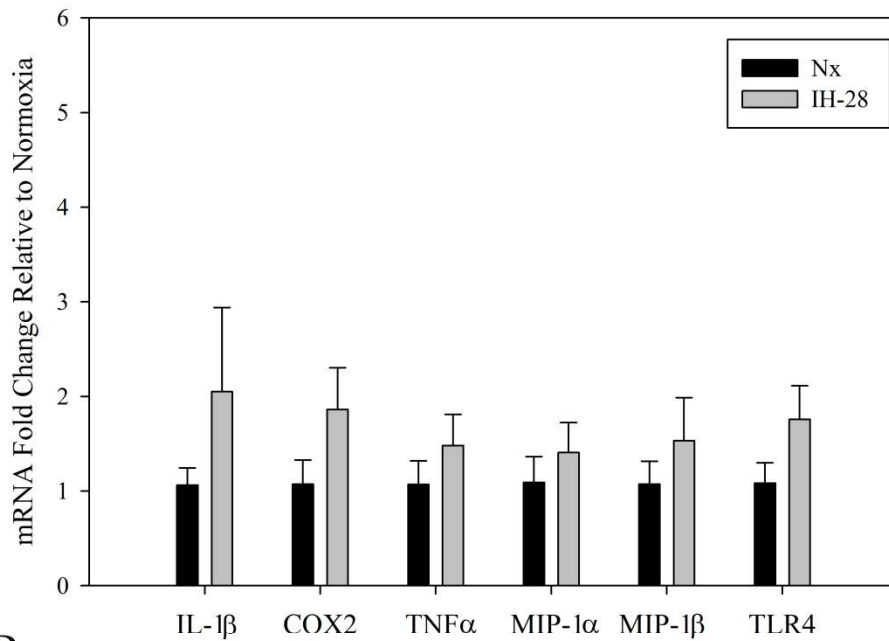
presented relative to the normoxic control. Statistical significance was determined by a Student's

T-test. * symbol represents statistically significant difference from normoxia. *p<0.05;

p<0.01; *p<0.001

FIGURE 4

A.



B.

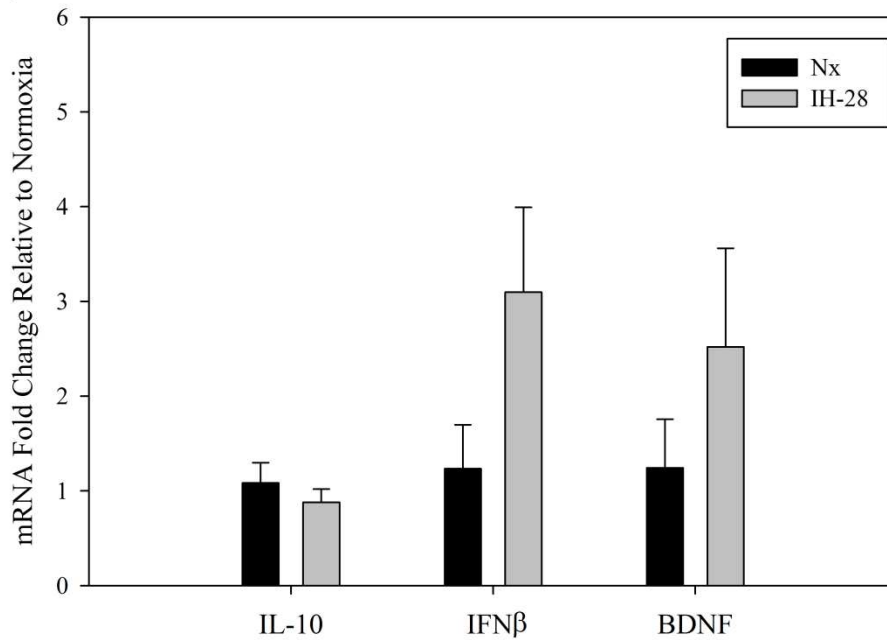


Figure Legend 4

Microglia isolated from mice exposed to IH-28 trend towards increased trophic/neuroprotective gene expression.

Mice were exposed to Nx or 28 days of IH. 13±1.5 hours following the last hypoxic exposure mice were sacrificed and the whole brain was taken for immunomagnetic microglia isolation.

(A) Fold change of microglial pro-inflammatory gene expression relative to normoxic controls.

(B) Fold change of microglial anti-inflammatory/neurotrophic gene expression relative to normoxic controls. N=3-4. Mean fold changes + 1 SEM are presented relative to the normoxic control. Statistical significance was determined by a Student's T-test.

TABLE 1

Gene	Forward Primer (5'→3')	Reverse Primer (5'→3')
18S	CGGGTGCTCTTAGCTGAGTGTC	CTCGGGCCTGCTTTGAACAC
COX2	TGTTCCAACCCATGTCAAAA	CGTAGAATCCAGTCCGGGTA
IL-6	ACTTCCATCCAGTTGCCTTC	GTCTCCTCTCCGGACTTGTG
IL-1 β	TCAAAGTGCCAGTGAACCCC	GGTCACAGCCAGTCCTCTTAC
TNF α	TGTAGCCCACGTCGTAGCAA	AGGTACAACCCATCGGCTGG
MIP-1 α (CCL3)	TACAGCCGGAAGATTCCACG	TCAGGAAAATGACACCTGGCT
MIP-1 β (CCL4)	TGTGATGGATTACTATGAGACCAGC	GCCTCTTTTGGTCAGGAATACCA
TLR4	GAGGCAGCAGGTGGAATTGTAT	TTCGAGGCTTTTCCATCCAA
CD14	GCCAAATTGGTCGAACAAGC	CCATGGTCGGTAGATTCTGAAAGT
TLR2	CGAGTGGTGCAAGTACGAACTG	TGGTGTTCATTATCTTGCGCAG
IL-10	GCCTTATCGGAAATGATCCA	TCTCACCCAGGGAATTCAAA
IFN β	TCTCCATCGACTACAAGCAG	GTCTCATTCCACCCAGTGCT
BDNF	TGCTTTACTGGCGTAAGGGAC	TCCATCCCTACTCCGGGTG

REFERENCES

1. Nikodemova, M. & Watters, J. J. Efficient isolation of live microglia with preserved phenotypes from adult mouse brain. *Journal of Neuroinflammation* **9**, 147 (2012).
2. Potucek, Y. D., Crain, J. M. & Watters, J. J. Purinergic receptors modulate MAP kinases and transcription factors that control microglial inflammatory gene expression. *Neurochemistry international* **49**, 204–214 (2006).
3. Livak, K. J. & Schmittgen, T. D. Analysis of relative gene expression data using real-time quantitative PCR and the 2(-Delta Delta C(T)) Method. *Methods* **25**, 402–8 (2001).